



Nerurkar, Louis (2017) Neuro-immune responses to distal immune stimulus. PhD thesis.

<http://theses.gla.ac.uk/8529/>

Copyright and moral rights for this work are retained by the author

A copy can be downloaded for personal non-commercial research or study, without prior permission or charge

This work cannot be reproduced or quoted extensively from without first obtaining permission in writing from the author

The content must not be changed in any way or sold commercially in any format or medium without the formal permission of the author

When referring to this work, full bibliographic details including the author, title, awarding institution and date of the thesis must be given

Enlighten:Theses
<http://theses.gla.ac.uk/>
theses@gla.ac.uk

Neuro-immune responses to distal immune stimulus

**Louis Nerurkar
BSc (Hons)**

Submitted in fulfilment of the requirements for the degree
of Doctor of Philosophy

Institute of Infection, Immunity and Inflammation
College of Medical, Veterinary and Life Sciences
University of Glasgow

June 2017

Abstract

Depression is a major disease burden worldwide and, despite its prevalence and socioeconomic costs, around 30% of patients do not respond to currently available treatments. Inflammation is increasingly associated with, not only depressive illness but also resistance to existing therapies. This highlights the need for investigation of the mechanisms of neuro-inflammation, particularly in the context of peripheral inflammatory stimuli. Specifically, the chemokine molecular family is increasingly associated with human depressive illness, and neuro-inflammation and behavioural change in rodent models, making this an attractive molecular family for study. This thesis describes research aimed at investigating the association of these molecules with human depression and analysis of their role in an animal model of peripherally stimulated neuro-inflammation, the Aldara model of psoriasis-like inflammation.

Systematic review and meta-analysis of the human biomarker literature using a random effects, inverse variance model revealed that a number of chemokines (CCL2, CCL3, CCL4, CCL11, CXCL4, CXCL7, CXCL8) are significantly associated with depressive illness in a human population. However this work revealed that there are a number of limitations of the human literature primarily associated with the methodological challenges of studies in human populations and confounding factors.

Alongside this work, the Aldara model, which utilises the toll-like receptor 7 (TLR7) ligand imiquimod (IMQ), was investigated as a tool for studying neuroinflammation. Initial time-course investigation revealed that significant chemokine and cytokine transcriptional alterations occur within four hours at the local site of cutaneous treatment, the peripheral tissues and the brain. In addition, protein quantification in the brain confirmed that many of these transcriptional responses are translated to protein. Interestingly, it was shown that the brain response was temporally distinct from that of the peripheral tissues, and that in general brain responses were induced slightly more slowly and persisted for a longer period of time than those in the periphery. Investigation of Iba1⁺ (microglia/monocytes), GFAP⁺ (astrocytes) and CD3⁺ (T-cells) cells within the brain revealed significant changes in the microglial and T-cell populations, which were consistent with microgliosis and T-cell recruitment

to the brain parenchyma. Changes in astrocyte populations were more equivocal although there was evidence of astrogliosis.

Mechanistic investigations into responses to the Aldara model in inflammatory chemokine receptor (iCCR) KO mice did not reveal significant alterations in chemokine and cytokine transcription or in microglial responses to cutaneous Aldara treatment in the absence of the iCCRs (CCR1, CCR2, CCR3 and CCR5), but there did appear to be evidence of reduced CD3⁺ T-cell recruitment. In contrast, investigations in type I interferon receptor (IFNAR) KO mice identified a clear role for type I IFN signalling through IFNAR in the induction of chemokine and cytokine gene expression in the brain, and associated changes in Iba1⁺ microglial and CD3⁺ T-cell populations in response to cutaneous Aldara treatment. Mass spectrometric analysis of IMQ, the main active ingredient of Aldara, revealed that within four hours it enters both the circulation and the brain. The finding of IMQ within the brain parenchyma suggests that, while it is not an appropriate tool for studying peripheral-central immune crosstalk, it is a useful non-invasive model of TLR7 mediated neuroinflammation.

These data provide compelling evidence of a role for chemokines in human depression and in neuro-inflammation, although the precise actions of this family of molecules remain unclear. In addition, building on previous work, the Aldara model appears to be a suitable tool for the study of neuro-inflammation, particularly interferon-driven immune responses, but is less appropriate for studying peripherally driven CNS immune reactions. Further work into the specific role of chemokines and associated cellular populations will hopefully provide additional insight into how CNS immune reactions are co-ordinated.

Table of Contents

Abstract	2
Table of Contents	4
List of Tables.....	9
List of Figures	10
List of Accompanying Material.....	14
Acknowledgements.....	15
Author’s Declaration	17
Definitions/Abbreviations	18
Chapter 1 Introduction	23
1.1 Overview.....	23
1.2 Immune System	25
1.2.1 Overview.....	25
1.2.2 Innate Immunity and TLRs.....	26
1.2.3 Adaptive Immunity	29
1.2.4 Inflammatory regulation and resolution.....	30
1.2.5 Cytokines	32
1.2.6 Chemokines.....	34
1.2.7 Cellular functions of the immune system	37
1.2.8 Summary	39
1.3 Central Nervous System Immunity	40
1.3.1 CNS Overview	40
1.3.2 Cells of the CNS.....	41
1.3.3 Immune “Privilege” in the CNS.....	44
1.3.4 Immune Responses to Central Inflammatory Stimuli	46
1.3.5 CNS Immune Responses to Peripheral Inflammatory Stimuli	50
1.3.6 Peripheral-Central Immune Communication.....	53
1.3.7 Aldara Model of Psoriasis-like Inflammation.....	58
1.3.8 Functional Consequences of CNS Immune Responses	60
1.3.9 Summary	63
1.4 Human Depression and the Immune System	64
1.4.1 Overview	64
1.4.2 Human Biomarker Studies	65
1.4.3 Other Studies of Inflammation and Depression	72
1.4.4 Summary	75
1.5 Justification and Thesis Aims	76
Chapter 2 Materials and Methods	80

2.1	Companies	80
2.2	Systematic Review and Meta-Analysis	80
2.2.1	Search Strategy	80
2.2.2	Study Selection	80
2.2.3	Data Extraction	81
2.2.4	Quality Assessment	82
2.2.5	Statistical Analysis.....	83
2.3	General Materials.....	84
2.3.1	Plastics	84
2.3.2	Buffers and solutions.....	84
2.4	Animals.....	87
2.5	Aldara Model of Inflammation	88
2.5.1	Aldara Model of Psoriasiform Inflammation Overview	88
2.5.2	Three Day Aldara Model	88
2.5.3	Time-course Aldara Models of Inflammation	89
2.5.4	Single Treatment Time-course Model of Inflammation	89
2.5.5	Knockout Models of Inflammation.....	89
2.6	Tissue Collection following Animal Models	90
2.6.1	Peripheral blood leukocytes (PBL) collection for RNA	90
2.6.2	Tissue collection for RNA.....	90
2.6.3	Tissue collection for Protein Analysis.....	90
2.6.4	Tissue collection for formalin-fixed paraffin embedded (FFPE) sections.....	91
2.6.5	Tissue collection for Mass Spectrometry	91
2.7	Tissue Processing	91
2.7.1	RNA Extraction.....	91
2.7.2	RNA to complementary DNA (cDNA) conversion.....	92
2.7.3	Protein Extraction	92
2.7.4	Tissue processing and paraffin embedding for FFPE sections.....	93
2.7.5	FFPE sectioning	93
2.8	Gene Expression Analysis	93
2.8.1	Primer Design	93
2.8.2	Standard Curve Generation	96
2.8.3	Primer Validation PCR	97
2.8.4	Gel Electrophoresis.....	97
2.8.5	Quantitative Real-time Polymerase Chain Reaction qRT-PCR.....	98
2.8.6	Analysis.....	99
2.9	LegendPlex Protein Assay	99
2.9.1	LegendPlex Protein Assay	99

2.10	Immunohistochemistry	100
2.10.1	Haematoxylin and eosin staining	100
2.10.2	Chromogenic Immunohistochemistry.....	100
1.5.1	Image Analysis and Quantification	101
2.11	Mass Spectrometry Analysis	102
2.11.1	Mass Spectrometry Analysis.....	102
2.12	Statistical Analysis	102
2.12.1	Between group comparisons.....	102
2.12.2	Linear regression analysis.....	103
2.12.3	Power calculation	103
Chapter 3	A Systematic Review and Meta-Analysis of Chemokines in Human Depression	105
3.1	Introduction	105
3.2	Results	106
3.2.1	Search Results and Study Inclusion	106
3.2.2	Study Quality	107
3.2.3	CCL2	109
3.2.4	CCL3	111
3.2.5	CCL4	113
3.2.6	CCL5	115
3.2.7	CCL11.....	117
3.2.8	CXCL4.....	119
3.2.9	CXCL7.....	121
3.2.10	CXCL8	124
3.2.11	CXCL10.....	125
3.2.12	CXCL12.....	125
3.2.13	Other chemokines.....	125
3.3	Discussion	127
3.3.1	Summary of results and concordance with existing literature.....	127
3.3.2	Biological relevance.....	129
3.3.3	Limitations and Strengths of Study	131
3.3.4	Conclusion	132
Chapter 4	Initial characterisation of the Aldara Model.....	135
4.1	Introduction	135
4.2	Results	137
4.2.1	The effect of repeated cutaneous treatment with Aldara on mouse weight and skin thickness after 3 days	137
4.2.2	The effect of repeated cutaneous treatment with Aldara on systemic chemokine and cytokine transcription after 3 days.....	137

4.2.3	The effect of repeated cutaneous treatment with Aldara on mouse weight and skin thickness over a 5-day timecourse.....	141
4.2.4	The effect of repeated cutaneous treatment with Aldara on chemokine and cytokine transcription in the brain over a 5-day timecourse.. ..	143
4.2.5	The effect of repeated cutaneous treatment with Aldara on chemokine and cytokine transcription in the periphery over a 5-day timecourse	146
4.2.6	Comparison of the response between 1- and 3-days in the brain and periphery	159
4.2.7	The effect of repeated cutaneous treatment on chemokine and cytokine protein levels in the brain over a 5-day time-course	160
4.2.8	The effect of repeated cutaneous treatment with Aldara on cellular populations within the brain parenchyma.....	167
4.3	Discussion	172
4.3.1	Summary of results	172
4.3.2	Transcriptional responses to cutaneous Aldara treatment	174
4.3.3	Protein responses in the CNS	175
4.3.4	Cellular changes in the CNS.....	176
4.3.5	Other findings of note	177
4.3.6	Summary	178
Chapter 5	Exploring mechanisms of Aldara-induced brain inflammation	180
5.1	Introduction	180
5.2	Results	182
5.2.1	The effect of iCCRKO on brain chemokine and cytokine transcriptional responses to repeated cutaneous Aldara treatment	182
5.2.2	The effect of iCCRKO on brain cellular responses to repeated cutaneous Aldara treatment.....	186
5.2.3	The effect of IFNARKO on chemokine and cytokine transcriptional responses to repeated cutaneous Aldara treatment.....	191
5.2.4	The effect of IFNARKO on cellular responses to repeated Aldara treatment	196
5.3	Discussion	202
5.3.1	Summary of results	202
5.3.2	Role of iCCRs in response to cutaneous Aldara treatment	202
5.3.3	Role of IFNAR in response to cutaneous Aldara treatment	203
5.3.4	Other findings of note	205
5.3.5	Summary	206
Chapter 6	Further characterisation of the Aldara Model ... Error! Bookmark not defined.	
6.1	Introduction	208
6.2	Results	209

6.2.1	Comparison of control levels of gene expression between tissues	209
6.2.2	The effect of a single cutaneous treatment with Aldara on chemokine and cytokine transcription in the brain	211
6.2.3	The effect of a single cutaneous treatment with Aldara on chemokine and cytokine transcription in the periphery	213
6.2.4	Mass spectrometry of plasma and brain imiquimod in the Aldara model	225
6.3	Discussion	228
6.3.1	Overview of results	228
6.3.2	Control gene expression between tissues	228
6.3.3	Relevance of findings from single treatment model	230
6.3.4	Importance of the mass spectrometry results	230
6.3.5	Summary and conclusions	231
Chapter 7	Discussion	234
7.1	Summary of Findings	234
7.2	Discussion	235
7.2.1	Human biomarker data	235
7.2.2	IMQ in the brain	236
7.2.3	Cellular responses to TLR7 Stimulus	237
7.3	Conclusions	240
7.4	Future directions	241
Appendices		244
List of References		273

List of Tables

Table 1.1: Summary of findings in meta-analysis of cytokines/chemokines in human depression	67
Table 2.1: Details of animals used in KO experiments.....	89
Table 2.2: Primers for qRT-PCR	95
Table 2.3: Primers for generation of standard curves	95
Table 2.4: Thermal cycles of qRT-PCR machines	98
Table 2.5: Primary and Secondary Antibodies used in IHC	101
Table 3.1: Risk of bias scores from studies included in meta-analysis. Higher scores indicate lower risks of bias.	109
Table 3.2: Non-significant results from chemokines with ≤ 3 studies included in meta-analysis.	125
Table 3.3: Significant results and sensitivity analysis in chemokines with >5 studies identified and a significant difference.....	127

List of Figures

Figure 1.1: Simplified TLR Signalling Overview	27
Figure 1.2: Chemokine ligand structure.....	35
Figure 1.3: CNS response to peripheral inflammatory stimuli	53
Figure 1.4: Routes of peripheral-central immune communication.....	58
Figure 1.5: Possible routes to psychological alterations and behavioural change in the context of stress and inflammation.....	62
Figure 1.6: Links between depressive disorder and inflammation in human populations	65
Figure 2.1 Image demonstrating treatment area on dorsal skin of mouse	88
Figure 3.1: PRISMA Flow Chart demonstrating study selection process for meta-analysis.....	106
Figure 3.2: (Previous page) Meta-analysis of blood CCL2 in depressed and non-depressed subjects.	111
Figure 3.3: Funnel plot of blood CCL2 studies generated in R using metafor package.	111
Figure 3.4: Meta-analysis of blood CCL3 in depressed and non-depressed subjects.	112
Figure 3.5: Funnel plot of blood CCL3 studies generated in R using metafor package.	113
Figure 3.6: Meta-analysis of blood CCL4 in depressed and non-depressed subjects.	114
Figure 3.7: Funnel plot of blood CCL4 studies generated in R using metafor package.	115
Figure 3.8: Meta-analysis of blood CCL11 in depressed and non-depressed subjects.	116
Figure 3.9: Funnel plot of blood CCL11 studies generated in R using metafor package.	117
Figure 3.10: Meta-analysis of blood CXCL4 in depressed and non-depressed subjects.	118
Figure 3.11: Funnel plot of blood CXCL4 studies generated in R using metafor package	119
Figure 3.12: Meta-analysis of blood CXCL7 in depressed and non-depressed subjects.	120
Figure 3.13: Funnel plot of blood CXCL7 studies generated in R using metafor package.	121
Figure 3.14: Meta-analysis of blood CXCL8 in depressed and non-depressed subjects.	123
Figure 3.15: Funnel plot of blood CXCL8 studies generated in R using metafor package.	124
Figure 3.16: Meta-analysis of blood CXCL12 in depressed and non-depressed subjects.	126

Figure 4.1: 3-day Aldara Model Weight Change and Skin Haematoxylin & Eosin.	138
Figure 4.2: 3-day Aldara Model CC Chemokine Transcript.	139
Figure 4.3: 3-day Aldara Model CXC Chemokine Transcript.	140
Figure 4.4: 3-day Aldara Model Cytokine Transcript.	141
Figure 4.5: Time-course Aldara Model Weight Change and Skin Haematoxylin & Eosin.	142
Figure 4.6: (Overleaf) Time-course Aldara Model Brain CC Chemokine Transcript.	143
Figure 4.7: Time-course Aldara Model Brain CXC Chemokine Transcript.	145
Figure 4.8: Time-course Aldara Model Brain Cytokine Transcript.	146
Figure 4.9: (Previous page) Time-course Aldara Model Skin CC Chemokine Transcript.	148
Figure 4.10: (Previous page) Time-course Aldara Model Skin CXC Chemokine Transcript.	149
Figure 4.11: Time-course Aldara Model Skin Cytokine Transcript.	149
Figure 4.12: Time-course Aldara Model PBL CC Chemokine Transcript.	151
Figure 4.13: Time-course Aldara Model PBL CXC Chemokine Transcript.	152
Figure 4.14: Time-course Aldara Model PBL Cytokine Transcript.	153
Figure 4.15: (Previous page) Time-course Aldara Model Liver CC Chemokine Transcript.	155
Figure 4.16: Time-course Aldara Model Liver CXC Chemokine Transcript.	155
Figure 4.17: Time-course Aldara Model Liver Cytokine Transcript.	156
Figure 4.18: Time-course Aldara Model Lungs CC Chemokine Transcript.	158
Figure 4.19: Time-course Aldara Model Lungs CXC Chemokine Transcript.	158
Figure 4.20: Time-course Aldara Model Lungs Cytokine Transcript.	159
Figure 4.21: Time-course Aldara Model 1 day to 3 day relative gene expression change.	160
Figure 4.22: Time-course Aldara Model Brain CC Chemokine Protein Expression.	161
Figure 4.23: Time-course Aldara Model Brain CXC Chemokine Protein Expression.	162
Figure 4.24: Time-course Aldara Model Brain Cytokine Protein Expression.	163
Figure 4.25: (Overleaf) Linear regression of Brain CC chemokine mRNA and protein expression values in Aldara treated mice.	164
Figure 4.26: Linear regression of Brain CXC chemokine mRNA and protein expression values in Aldara treated mice.	166
Figure 4.27: Linear regression of Brain cytokine mRNA and protein expression values in Aldara treated mice.	167
Figure 4.28: (Overleaf) Iba1 staining of brain in Aldara Model.	168
Figure 4.29: GFAP staining of brain in Aldara Model.	170
Figure 4.30: (Previous page) CD3 staining of brain in Aldara Model.	172

Figure 4.31: Heatmap of chemokine and cytokine gene expression after a repeated daily cutaneous treatments of Aldara cream.	173
Figure 5.1: CCL-CCR Overlapping Interactions	181
Figure 5.2: 4-day iCCRKO Aldara Model 1 Brain Chemokine Transcript.	183
Figure 5.3: 4-day iCCRKO Aldara Model 1 Brain Cytokine Transcript	184
Figure 5.4: 4-day iCCRKO Aldara Model 2 Brain Chemokine Transcript	185
Figure 5.5: 4-day iCCRKO Aldara Model 2 Brain Cytokine Transcript	186
Figure 5.6: Iba1 staining of brain in iCCRKO Aldara Models	187
Figure 5.7: GFAP staining of brain in iCCRKO Aldara Models.....	188
Figure 5.8: CD3 staining of brain in iCCRKO Aldara Models	190
Figure 5.9: (Overleaf) 3-day IFNARKO Aldara Model 1 Brain Chemokine and Cytokine Transcript	191
Figure 5.10: 3-day IFNARKO Aldara Model 2 Brain Chemokine Transcript	193
Figure 5.11: 3-day IFNARKO Aldara Model 2 Brain Cytokine Transcript	194
Figure 5.12: (Previous page) 3-day IFNARKO Aldara Model 1 Skin Chemokine and Cytokine Transcript	196
Figure 5.13: (Overleaf) 3-day IFNARKO Aldara Model 1 PBL Chemokine and Cytokine Transcript	196
Figure 5.14: Iba1 staining of brain in IFNARKO Aldara Models	198
Figure 5.15: GFAP staining of brain in IFNARKO Aldara Models.....	199
Figure 5.16: (Overleaf) CD3 staining of brain in IFNARKO Aldara Models	200
Figure 6.1: Chemokine transcription in control tissue	210
Figure 6.2: Cytokine transcription in control tissue.....	211
Figure 6.3: Brain chemokine transcript levels after a single Aldara treatment.	212
Figure 6.4: Brain cytokine transcript levels after a single Aldara treatment....	213
Figure 6.5: Skin chemokine transcript levels after a single Aldara treatment.	214
Figure 6.6: Skin cytokine transcript levels after a single Aldara treatment.	215
Figure 6.7: PBL chemokine transcript levels after a single Aldara treatment....	216
Figure 6.8: PBL cytokine transcript levels after a single Aldara treatment.	217
Figure 6.9: Liver chemokine transcript levels after a single Aldara treatment.	218
Figure 6.10: Liver cytokine transcript levels after a single Aldara treatment.	219
Figure 6.11: Lung chemokine transcript levels after a single Aldara treatment.	220
Figure 6.12: Lung cytokine transcript levels after a single Aldara treatment....	221
Figure 6.13: Spleen chemokine transcript levels after a single Aldara treatment.	222
Figure 6.14: Spleen cytokine transcript levels after a single Aldara treatment....	223
Figure 6.15: Colon chemokine transcript levels after a single Aldara treatment.	224
Figure 6.16: Colon cytokine transcript levels after a single Aldara treatment....	225
Figure 6.17: Mass spectrometry of imiquimod in Aldara treated mice.	227

Figure 6.18: Heatmap of chemokine and cytokine gene expression after a single cutaneous treatment of Aldara cream.229

List of Accompanying Material

Appendix 1: Companies referenced in methods	244
Appendix 2: Example search strategy used for meta-analysis of chemokines...	246
Appendix 3: Custom data extraction template used for assessment of studies in meta-analysis	251
Appendix 4: RIN Values determined by agilent bioanalyzer at Glasgow Polyomics	258

Acknowledgements

I would firstly like to thank my supervisors Prof. Jonathan Cavanagh and Prof. Gerard Graham for their support, guidance and intellectual stimulation throughout the course of this PhD. It has been a pleasure to work with you both and to experience being part of your research group. I would also like to thank the Dr. Mortimer and Theresa Sackler Foundation for the generous funding of this project.

I would also like to thank Ruairidh Taggart an undergraduate student for his assistance during the IFNARKO models and Dr. Sam Leighton for his work on the collaborative meta-analysis.

My heartfelt thanks to Dr. Alison McColl, without her this would not have been achieved. She has provided incomparable support above and beyond the call of duty during this endeavour. I will be sad to depart, and hope that even though you live on the other side of the river we will continue to be the best of friends for a long time to come. May you and your perfectly proportioned head excel in everything you do (although it might be harder without me to help). PhD-Postdoc dream team forever.

To the members of the CRG, Cavanagh Group and other level 3 groups, past and present thank you for the laughs, the drinks, the science, the eye rolls and moans, the knowledge and the “thank god it’s Friday (maybe Thursday)” pub visits. While I will inevitably miss someone out thanks especially to (in no particular order!) Doug, Laura, Chris H, Chris K, Kenny, Catherine, Paul, Robin, Maria, Jen, Kayleigh, Clive, Gill, Emma, Jenny and Sam. I would like to give a special note of thanks to Dr. Patricia Collins for her advice, support and friendship (mainly consisting of snapchats and borderline insanity) over my time in the lab.

In addition, my thanks to Prof. Christoph Kellendonk and Dr. Abby Clark for their guidance and assistance during my time at Columbia University and to Dr. Matt Bailey who showed me a passion for science and innovation I will never forget.

Thank you to all my friends who have put up with me going AWOL, being stressed, having no time for fun and being in an obsessive work zone. Special thanks to Alaa Al-Mohammad for our shared PhD catharsis sessions and the new perspectives you have brought to my work and to Sam Dance for putting up with me stressing around the flat for months on end while providing some much needed laughter to keep me sane.

Thanks to my family who have supported me wholeheartedly not just on this journey but on all the journeys that came before. To my parents Helena and Ian, without you I would not be the person I am today, and I definitely wouldn't be in the place I am. You are true role models to all that you meet, and your hard work and dedication shows that even when we think we're at our busiest, most of us aren't. To my grandparents thank you all for inspiring me to strive harder and reach further, and a special thanks to Granddad Graeme for his guidance in choosing this path! To my brother Max, you remind me of what is most important in life and make me question everything, may your life be an example to many.

Finally, I would like to thank my wonderful girlfriend Lisa Murphy for her unwavering support. You inspire me to be a better person every day and without you I definitely wouldn't have made it to this point. You've travelled at the worst of times after the worst of days to come see me. You have looked after me when I'm down and brought me higher when I'm up. You are my sunshine, you are my shining star, and you are the best. All my love, Louis xxx

Author's Declaration

I declare that all work in this thesis is the result of my own work, aside from where explicit reference has been made to the contribution of others. None of the data included in this thesis has been submitted for any other degree, either at the University of Glasgow or at any other institution.

Signature.....

Printed name: Louis Nerurkar

Definitions/Abbreviations

5		CMS	Chronic mild stress
5-HTT	5-Hydroxytryptamine (serotonin) transporter	COX-2	Cyclooxygenase-2
A		CRH	Corticotrophin- releasing hormone
ACKR	Atypical chemokine receptor	CSF	Cerebrospinal fluid
AD	Alzheimer's disease	Ct	Cycle threshold
ANOVA	Analysis of variance	CTE	Chronic traumatic encephalopathy
APC	Antigen-presenting cell	CTL	Cytotoxic T-lymphocyte
B		CVO	Circumventricular organ
BBB	Blood-brain-barrier	D	
BDI	Beck's depression inventory	DAB	3,3'-diaminobenzidine
BMI	Body mass index	DAMP	Damage-associated molecular pattern
bp	Base pair	DC	Dendritic cell
C		dd	Double distilled
cDNA	Complementary DNA	DNA	Deoxyribonucleic acid
CI	Confidence interval		
CNS	Central nervous system		

E		i.v.	Intravenous
EDTA	Ethylenediaminetetraacetic acid	Iba1	Ionised calcium binding adaptor molecule 1
EtOH	Ethanol	ICAM-1	Intercellular adhesion molecule 1
F		iCCR	Inflammatory chemokine receptor
FACS	Fluorescence-activated cell sorting	IDO	Indoleamine 2,3-dioxygenase
FFPE	Formalin fixed paraffin embedded	IFN	Interferon
G		IFN α	Interferon alpha
GFAP	Glial fibrillary acidic protein	IFNAR	Interferon alpha/beta receptor
GPCR	G-protein coupled receptor	IFN β	Interferon beta
GWAS	Genome wide association study	IFN γ	Interferon gamma
H		IHC	Immunohistochemistry
		Il-10	Interleukin-10
HPA axis	Hypothalamic pituitary axis	Il-1 β	Interleukin-1 beta
I		Il-1r	Interleukin-1 receptor
i.c.v	Intracerebroventricular	Il-1Ra	Interleukin-1 receptor antagonist
i.p.	Intraperitoneal	Il-6	Interleukin-6

IMQ	Imiquimod	NF-κB	Nuclear factor kappa-light-chain-enhancer of activated B cells
IRF factor	Interferon regulatory factor	NK	Natural killer
ISG gene	Interferon stimulated gene	NLRP3	NOD-like receptor family pyrin domain containing 3
K		N-PER	Neuronal protein extraction reagent
kDa	kiloDaltons	P	
KO	Knockout	PAMP	Pathogen-associated molecular pattern
L		PBL	Peripheral blood leukocytes
LPS	Lipopolysaccharide	PBS	Phosphate buffered saline
M		PCR	Polymerase chain reaction
MAPK	Mitogen activated protein kinase	PIC	Polyinosinic:polycytidilic acid
MHC	Major histocompatibility complex	PRR	Pattern recognition receptor
MHV	Mouse hepatitis virus	Q	
mRNA	Messenger RNA	qRT-PCR	Quantitative real-time polymerase chain reaction
MYD88	Myeloid differentiation primary response gene 88		
N			
NEB	New England Biolabs		

R

RIN RNA integrity number

RNA Ribonucleic acid

ROS Reactive oxygen species

RT Room temperature

S

SA-PE Streptavidin-phycoerythrin

SD Standard deviation

sIL-6R Soluble interleukin-6 receptor

SIRT1 Sirtuin 1

SMD Standardised mean difference

SNP Single nucleotide polymorphism

ssRNA Single stranded RNA

STAT Signal transducer and activator of transcription

STW Scott's tap water

T

Tbp TATA-binding protein

TBS Tris-buffered saline

Th T-helper

TLR Toll-like receptor

Tm Annealing temperature

TNF α Tumor necrosis factor alpha

TNFR Tumor necrosis factor receptor

TRIF TIR-domain-containing adaptor protein inducing IFN- β

V

VSV Vesicular stomatitis virus

W

WNV West Nile virus

Chapter 1

Introduction

Chapter 1 Introduction

1.1 Overview

Depressive disorders are a significant and increasing burden on health and social care systems worldwide(1). Despite considerable impact on both quality of life, morbidity and mortality, depressive disorders are not only inadequately understood(2) but the therapeutic options available are limited and often lack efficacy(3).

Ongoing research has increasingly associated inflammatory mechanisms with the pathogenesis of depression(4-8). Animal studies have identified a role for pro-inflammatory cytokines in the generation of sickness behaviours, behaviours that share many phenotypic similarities with the symptoms of depression in humans (5, 9-11). In addition, animal models looking at stress and depressive behaviours have begun to identify alterations in inflammatory status associated with behavioural changes(12).

In human studies, a number of findings provide strong evidence for the involvement of the immune system in depressive illness; (i) treatment with interferons (IFNs) in hepatitis C infection results in a depressive disorder in 25-40% of patients undergoing treatment(13, 14); (ii) alterations in both immune molecules and cells are present in depressed patients when compared to healthy controls(15-20); (iii) treatment of patients with anti-inflammatory medications can alleviate depressive symptoms(21, 22) and (iv) response to anti-depressants has been associated with reductions in inflammatory biomarkers (16, 23).

Taken together, these data provide convincing evidence that the immune system plays an important role in depressive disorders, although the mechanisms underlying this remain to be fully elucidated. The sickness behaviour hypothesis of depression proposes that sickness behaviours, manifested in response to immune alterations, may drive an underlying phenotype that predisposes to depressive disorder.

Understanding the mechanisms that underlie the behavioural alterations of depressive disorder requires an appropriate model that can investigate these

responses and relate the findings back to human physiology. While it is impossible to accurately model human depression in a rodent, it is possible to aim to emulate aspects of inflammatory and psychological biology.

Peripheral-central inflammatory models use a peripheral immune stimulus to examine the effects of peripheral inflammation on the central nervous system (CNS) and are commonly used to study the relationship between inflammation and CNS responses. One model that has been used previously to study this relationship within our laboratory is the Aldara model of psoriasiform inflammation (24, 25). This model uses Aldara cream as a topical dermatological immune stimulus that results not only in inflammatory changes within the brain but also changes in wellbeing as measured by burrowing in mice. Aldara cream generates a response through toll-like receptor (TLR) 7 agonism, a receptor that detects viral single stranded ribonucleic acids (ssRNAs), and it is being investigated as an alternative to existing models of peripheral-central inflammation.

Chemokines, or chemotactic cytokines, are known to be key regulators of immune cell infiltration and retention (26, 27). In addition, chemokines have important roles in development (28, 29) and are increasingly implicated in other CNS functions associated with behavioural change such as neurogenesis, hypothalamic-pituitary axis (HPA) function and neurotransmitter regulation (30-32). The dual function of chemokines as modulators of both CNS and immune function makes them attractive candidates for study, particularly as they are not well characterised within the CNS.

In summary, depressive disorders are a major burden on the health of populations around the globe. Ongoing research provides strong evidence for a link between the immune system and depressive illness, however the mechanisms that underlie this relationship are still incompletely understood. Given their role in co-ordinating immune responses and their increasing links to CNS biology the chemokine family of molecules provide an attractive candidate for study in the field of psychoneuroimmunology.

The work presented in this thesis initially investigates the relevance of chemokine responses in human depression through a meta-analysis of the human

literature in this area. Alongside this, the Aldara model of psoriasiform inflammation was further characterised and validated with a particular focus on chemokine responses. This involved assays of chemokine expression in the peripheral tissues and CNS. As chemokines are strongly linked to cellular migration, it also examined changes in cellular populations associated with changes in chemokine expression. An overview of relevant areas of immunology and neuroscience, alongside key findings from related research is provided in the following sections in order to place the original work presented in this thesis in context.

1.2 Immune System

1.1.1 Overview

The immune system is present throughout all organs of the body, although its precise function varies between tissues. It consists of a variety of cells that are responsible for normal immune homeostasis and response to inflammatory insults(33). In addition, many components of what is classically considered the immune system, appear to play important roles in non-inflammatory contexts, particularly within the CNS (34, 35).

Anatomically, the immune system can be subdivided into primary and secondary lymphoid organs. The primary lymphoid organs are the bone marrow, where many immune cells are generated, and the thymus, where T cells mature. The secondary lymphoid organs are the lymph nodes, where antigen can be presented to B and T cells by antigen-presenting cells (APCs) to activate them and generate an immune response, and the spleen wherein the blood can be surveilled and white cells removed from the circulation when required. Lymphoid nodules are smaller sites of immune organization and include the tonsils, mucosa-associated lymphoid tissue and bronchus-associated lymphoid tissue. Finally, a system of lymphatic ducts and vessels drain lymph from tissues to the lymph nodes prior to re-absorption into the circulation(33).

In normal physiological states the immune system is relatively quiescent, circulating white cells are minimal(36) and its primary functions are the

maintenance of immune homeostasis and surveillance of body tissues for pathological insults.

In pathological states the immune system becomes activated through a variety of mechanisms including automatic recognition of damage- or pathogen-associated molecular patterns (DAMPs or PAMPs), or recognition of previously encountered antigenic motifs by memory T cells(33). Once activated, feed-forward pathways generate massive responses that, if uncontrolled, can rapidly become pathological in themselves(33, 37, 38).

Immune responses are generally considered to be biphasic with the initial rapid and automatic activation of innate immunity being followed by a slower but more targeted adaptive response(33, 39). In addition, a final important stage of a normal immune response is resolution of the inflammatory state and a return to physiological immune homeostasis(40, 41).

1.1.2 Innate Immunity and TLRs

The innate immune system is the body's first line of defence against immune insults such as wounds, pathogens and other noxious stimuli once barrier defences such as the skin have been breached. It primarily relies on pattern recognition receptors (PRRs), which include TLRs, RIG-I like receptors, NOD-like receptors and C-type lectin receptors(42). Another important component of the innate immune system is complement. These small circulating proteins can bind to bacterial surfaces and once bound they can either opsonize the surface to allow for efficient phagocytosis or they can attack the cell directly through the formation of membrane attack complexes that perforate the cell membrane(33). As the focus of this thesis is on work with a TLR7 agonist, the focus of the next section here is on the role and function of TLRs, and more specifically TLR7, within the innate immune system.

PRRs are expressed by a variety of cells of the immune system including macrophages (resident tissue monocytes) and microglia (resident CNS immune cell). The TLR family of PRRs detects conserved molecular motifs that are associated with bacterial, viral, protozoal and fungal infection. Examples include TLR4, that detects lipopolysaccharide (LPS), a component of bacterial cell walls,

and other pathogenic proteins, TLR3 that detects double stranded ribonucleic acid (RNA) from viruses and TLR7 that detects ssRNA from viruses(42).

Once TLRs are activated a cascade of downstream signalling occurs, initiated by the adaptor proteins TIR-domain-containing adaptor protein inducing IFN- β (TRIF) and/or myeloid differentiation primary response gene 88 (MYD88) depending on the TLR. For example, TLR3 uses TRIF, TLR7 uses MYD88 and TLR4 uses both adaptor proteins. These adaptor proteins initiate protein kinase pathways that generate IFN regulatory factor (IRF) and nuclear factor kappa-light-chain-enhancer of activated B cells (NF- κ B) responses(43) (Figure 1.1).

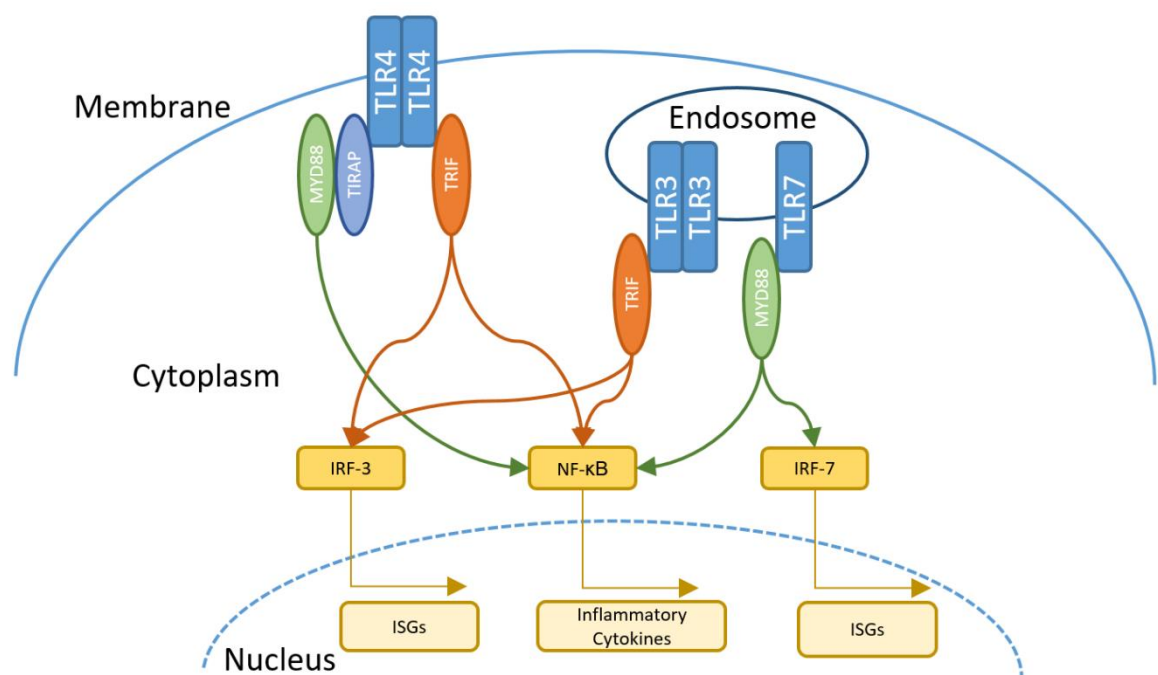


Figure 1.1: Simplified TLR Signalling Overview

Engagement of TLR receptors initiates signalling pathways from adaptor proteins TRIF and/or MYD88. Through the action of protein kinases these signalling pathways initiate IRF and NF- κ B signalling that results in the production of ISGs and inflammatory cytokines respectively.

Abbreviations: TLR – Toll-like receptor; MYD88 - Myeloid differentiation primary response gene 88; TIRAP – Toll-interleukin 1 receptor domain containing adaptor protein; TRIF – TIR-domain-containing adapter-inducing interferon- β ; IRF – Interferon regulatory factor; NF- κ B – nuclear factor kappa-light-chain-enhancer of activated B cells; ISG – Interferon stimulated gene. Adapted from (25, 44, 45)

IRF activation generates type-1/2 IFN responses(46) (Interferon-alpha (IFN α)/ Interferon-beta (IFN β)/Interferon-gamma (IFN γ)) characterised by IFN stimulated gene (ISG) induction, including several chemokines, most notably *Cxcl9*, *Cxcl10* and *Cxcl11*(47, 48). NF- κ B activation generates pro-inflammatory cytokine responses that include interleukin-1 beta (IL-1 β), interleukin-6 (IL-6) and tumor

necrosis factor alpha ($\text{TNF}\alpha$)(49). In addition, $\text{NF-}\kappa\text{B}$ can induce expression of the anti-inflammatory cytokine interleukin-10 (IL-10)(49).

Another important effect of TLR signalling is induction of the NOD-like receptor family pyrin domain containing 3 (NLRP3) inflammasome(50). Downstream of $\text{NF-}\kappa\text{B}$ signalling, there is an increase in the expression of inactive NLRP3 protein, TLR signalling activates NLRP3 through de-ubiquitination. Once active NLRP3 inflammasomes activate pro-caspase-1 to its active form caspase-1. This enzyme can then proteolytically cleave inflammatory proteins to their active form, for example cleaving pro-IL-1 β to IL-1 β (51, 52). The tight regulation of this inflammation-promoting molecule, as demonstrated through not only its low constitutive expression but its production in an inactive form, provides an example of the complex mechanisms of control used by the immune system.

Initiation of these molecular pathways leads to a variety of changes that promote cellular recruitment and immune activation. For example, upregulation of adhesion molecules and chemokines promotes cellular infiltration(26, 27, 33, 53) while pro-inflammatory cytokines can induce both local changes such as vasodilation(54) and systemic changes such as fever and fatigue(9).

Alongside resident macrophages, two other phagocytic cell types are key to innate immunity, particularly in the context of TLR activation; neutrophils and dendritic cells (DCs)(33). Neutrophils are rapidly recruited to inflamed tissues in response to TLR activation(55, 56) and can phagocytose target cells and bacteria, as well as releasing toxic granules into the surrounding tissue. DCs are APCs that migrate to draining lymph nodes. Once TLR signalling is initiated, CCR7 becomes upregulated(57), allowing DCs to respond to CCL19 and CCL21 in lymphatic vessels, interstitium and high endothelial venules (58). Subsequent CCR7 dependent migration to lymph nodes is often considered as the junction between innate and adaptive immunity as once DCs present antigen within the lymph node the adaptive immune system is engaged.

Other cells of the innate immune system include natural killer (NK) cells and gamma/delta T cells. Natural killer cells are thought to play key roles in control of cancer development and defence against viral infections. They have two primary effector functions, firstly they can employ cytotoxic activity against

virus infected or tumor cells and secondly they can produce robust cytokine responses following activation (59, 60) NK cells use complex signalling mechanisms that balance both inhibitory (e.g. major histocompatibility complex (MHC)-class I) and excitatory (e.g. natural killer NKG2D ligands) stimuli (59, 60). Evidence for NK cell activation by TLRs appears significant. However, whether this is by indirect or both direct and indirect mechanisms is unclear. Despite this, it is clear that type I interferon signalling is a key pathway in NK activation. There is now reasonable evidence that for TLR7-mediated activation, accessory cells providing additional signals, such as Il-12 or IFN α are required for full cytotoxic capabilities(61, 62). NK cells produce significant amounts of IFN γ when in the presence of Il-12(61), and have also been shown to be producers of CCL3, CCL4 and CCL5 in response to the TLR7 agonist loxiribine in conjunction with Il-12(63). In addition, mast cells, basophils and eosinophils form part of the innate immune system. However, they are generally associated with atopic reactions or parasitic infections.

Recent developments in the study of innate immunity have shown that it is not as generalizable as previously thought and there may be some elements of memory involved. Innate immune memory appears to be mediated through a variety of mechanisms but epigenetic modifications and metabolic-immunological interactions appear to be key(64). One of the simplest examples of innate memory is the process of tolerance, whereby pre-stimulation with lower doses of PAMPs can “tolerise” the immune system and ameliorate subsequent responses to larger stimuli of the same PAMP(65, 66). This process is particularly well characterised for the TLR4 agonist LPS.

1.1.3 Adaptive Immunity

The innate immune system is the primary focus of this thesis. However because of the complex nature of immune responses and the blurred line between innate and adaptive immunity it is worth also briefly reviewing the adaptive immune response. This is particularly true for early events of adaptive immunity such as the recruitment of T cells to sites of immune insult or injury.

The adaptive immune system is a second line of immune defence that aims to mobilise specific defences against antigens if the innate immune system cannot

effectively clear an insult. Once APCs of the innate immune system reach the lymph nodes, they present antigen via MHC and co-stimulatory molecules to enable the activation of B and T cells(33). TLR activation in APCs, particularly DCs, promotes delivery of antigen to MHC(67) and upregulation of co-stimulatory molecules(68, 69) that are required for full activation of adaptive immune cells.

Adaptive immunity is generally considered to be specific as, once presented with antigen, only those cells that have an ability to bind it will become activated and leave the lymph node to travel to sites of immune insult. Following activation via APCs, B cells can go on to become short-lived plasmablasts, that produce large amounts of circulating antibody, or longer-lived memory and plasma B cells. T cells can become a variety of different subclasses including CD4+ T-Helper (T_H) cells, CD8+ cytotoxic T lymphocytes (CTLs), regulatory or suppressor T cells and memory T cells. Respectively, these cells act to co-ordinate and promote immune responses, lyse and apoptose infected cells, prevent excessive immune reactions and remember foreign antigen to enable rapid immune mobilisation in the case of re-exposure(33).

Once activated, a variety of signalling and other molecules act to direct these cells to sites of immune insult. These molecules include chemokines, leukotrienes and adhesion molecules that coordinate cellular arrest within the vasculature and subsequent migration through tissue parenchyma(26, 27, 53). Upon arrival at sites of interest these cells can execute their effector functions, which aim to clear immune insults and generate resolution of the inflammatory process.

1.1.4 Inflammatory regulation and resolution

Inflammatory resolution is a critical part of any immune response. It begins the moment an inflammatory insult is encountered and the innate immune system is engaged and continues until normal immune homeostasis is restored. Ongoing equilibrium between pro- and anti-inflammatory mechanisms drive inflammatory reactions, and aims to prevent excessive tissue damage and cellular death due to uncontrolled responses(40, 41).

Release of anti-inflammatory mediators such as Il-10(70, 71), and pro-resolution factors such as lipoxins, resolvins and protectins(72), are one mechanism for the control of these responses. Another resolutive mechanism is the role of macrophages and other phagocytes in clearing apoptotic leukocytes from tissue(73), a process known as efferocytosis. A recent study in CXCR2^{-/-} mice provided strong evidence for macrophage interactions with apoptotic neutrophils as being an important step in the generation of anti-inflammatory mediators and the subsequent resolution of inflammation(74). Efferocytosis induces phenotypic switching, characterised by raised levels of mediators associated with resolution such as cyclooxygenase-2 (COX-2) and inducible nitric oxide synthase(75). Atypical chemokine receptors (ACKRs) such as ACKR2 also appear to play a role in immune regulation, with ACKR2 deficient mice displaying exaggerated inflammatory responses in a variety of contexts(76, 77). This effect appears to be due to the role of ACKRs in scavenging chemokine molecules and limiting their signalling potential(76). While not exhaustive these examples provide significant evidence for the active nature of inflammatory regulation and resolution.

Of interest, the brain appears to have challenges fully resolving some inflammatory insults. Two examples of this within the human population are Alzheimer's disease (AD) and chronic traumatic encephalopathy (CTE). In AD pathogenic proteins such as amyloid and tau are implicated in a chronic neurodegeneration that appears to be accompanied by an inflammatory pathology and an inability to clear these accumulating proteins. These proteins have the ability to trigger innate immune responses through PRRs and recent evidence suggests that the ongoing inflammation contributes to the pathology of AD(78, 79). CTE describes a condition that results from brain injury, originally described in boxers as dementia pugilistica. It has now been identified in athletes engaging in other high impact sports such as American football and those who have suffered from a traumatic brain injury. Inflammation is increasingly recognised as being associated with CTE and while some animal models have identified mechanistic links it is unclear whether it is a cause or consequence(80). In addition to these two human conditions, Qin et al. have identified altered immune responses within the CNS at up to 10 months post-endotoxin exposure in an animal model, this work will be discussed in more

detail later(81). Overall these data suggest that mechanisms of inflammatory resolution within the CNS may be different when compared to the periphery, although the reasons for this remain to be elucidated.

In summary, the innate and adaptive immune systems work together to initiate, co-ordinate and resolve inflammatory reactions and immune insults. A multitude of signalling pathways, molecules and cellular types can be rapidly engaged over time-courses spanning minutes to days to co-ordinate and fine-tune these responses. Specific relevant aspects of these pathways will be discussed below.

1.1.5 Cytokines

Cytokines are a broad class of cell signalling molecules that can act in an autocrine, juxtacrine, paracrine and/or endocrine manner and interact with their cognate receptors to alter cellular function. IFNs and interleukins are major classes of cytokines that drive many cellular responses. As the work discussed in this thesis examines the Type I/II IFN response and a limited number of other cytokines, these will be the focus of this section. Chemokines, another large class of cytokine molecules specifically associated with chemotaxis, are discussed in more detail in the subsequent section as they are a primary focus of this thesis.

Type I IFNs include, but are not limited to, IFN- α and IFN- β . These high-level signalling molecules are associated with antiviral responses but also play a role in response to bacterial infection as demonstrated by their induction in the presence of LPS, a bacterial cell wall component. Honda et al. demonstrated that IRF7, an IRF downstream of both TRIF and MYD88 is a key regulator of type-I IFN responses, and that many inflammatory gene responses are abrogated in IRF7^{-/-} mice(82). In this study a lack of IFN induction resulted in an increased mortality in IRF7^{-/-} mice exposed to viral infection, strongly supporting the theory that these responses are critical to effective immunity.

Upon induction, Type I IFNs act to sustain and promote inflammatory responses, signalling through the interferon alpha/beta receptor (IFNAR) complex (IFNAR1/IFNAR2 heterodimer) (83). IFNAR signalling results in activation of many different molecular pathways, with microarray studies and data compilations

showing upregulation of over 1000 genes in response to IFN signalling (84, 85). Despite IFN-signalling appearing to be a key pathway shared between TLRs, IFNAR is not critical to the expression of major pro-inflammatory cytokines(86). This is probably because TLR signalling pathways also induce NF- κ B responses that drive the induction of the cytokines Il-1 β , Il-6 and TNF α , independent of IFNAR signalling. In addition to type I IFNs there is a single type II IFN, IFN γ , that can also be secreted downstream of TLR signalling(87). One of the main functions of IFN γ is to potentiate the action of macrophages(88, 89).

The pro-inflammatory cytokines Il-1 β , Il-6 and TNF α have both shared and unique features. They can be produced by a wide variety of cells, primarily through activation of the NF- κ B pathway. These cytokines are pleiotropic, with their exact function dependent on the inflammatory context in which they are produced. Despite, their general designation as pro-inflammatory, both TNF α and Il-6 have immunoregulatory and anti-inflammatory properties(90, 91). Il-1 β signals through the MYD88 pathway similar to some TLRs, Il-6 signals through its own receptor linked to the gp130 signalling receptor and TNF can signal through either TNF receptor (TNFR) 1, a ubiquitous receptor, or TNFR2, whose expression is restricted to a handful of different cell types.

The full cascade of signalling events generates many downstream alterations. Both TNF and Il-1 β promote NF- κ B signalling, showing evidence of positive feedback loops. However, there is some evidence they can also induce their own negative feedback loops. Examples include degradation or internalisation of TNFRs in response to TNF(92) and induction of interleukin-1 receptor antagonist (Il-1Ra) in response to Il-1 β (93). Il6 can possibly inhibit the induction and actions of Il-1 β and TNF α (90, 94), while through production of soluble Il-6 receptor (sIl-6R) it increases its own half-life and bioavailability (90) .

Functionally these signalling events act to promote immune cell function through encouraging T and B cell activation and proliferation, induce the production of further inflammatory molecules such as chemokines, and promote the sustenance of inflammatory processes through various feedback loops.

Il-10, one of the most potent anti-inflammatory cytokines is produced by several immune cells including macrophages and DCs of the innate immune system and both B and T cells of the adaptive immune system(95). In innate immune cells, activation of extracellular signal-regulated kinases, downstream of TLR ligation, promotes Il-10 production(95). Studies have shown that absence of Il-10 during infection can result in an increased production of pro-inflammatory cytokines that is associated with a more severe immunopathology, although it can enhance bacterial and viral clearance(96).

In summary, cytokine signalling is a balance of pro- and anti-inflammatory signals mediated by a variety of highly pleiotropic and overlapping mediators. The downstream effects of this signalling aim to simultaneously promote and restrain production of inflammatory mediators, activate and inhibit immune cell function and differentiation, and exert both positive and negative feedback on the original signal. As demonstrated by the dysfunction observed in cytokine knockout (KO) models, it is evident that induction of cytokine signalling is a key step in producing a co-ordinated, effective and resolvable inflammatory response.

1.1.6 Chemokines

Chemokines, originally named for their role as chemotactic cytokines are key to cell migration and homing during homeostasis, inflammation and development. In addition, since these first functional roles were discovered they have been shown to be involved in several other systems including angiogenesis (97, 98), neuroendocrine function (99, 100), neuromodulation (32, 101-103), neurogenesis (30, 104, 105), and tumorigenesis and metastasis (106, 107). Chemokines are structurally defined by their conserved cysteine motifs and signal through a group of 7 transmembrane G-protein coupled receptors (GPCRs). Four major classes of chemokines exist CC, CXC, CX3C and XC based on the cysteine residues present at their amino terminus and any intermediate amino acids (Figure 1.2). The CX3C group has only 1 member, CX3CL1 that plays an important role in neuron-microglia crosstalk and homeostasis within the CNS (105, 108). It is one of only 2 chemokines that exists in both a transmembrane and secreted form, the other being CXCL16 (109, 110).

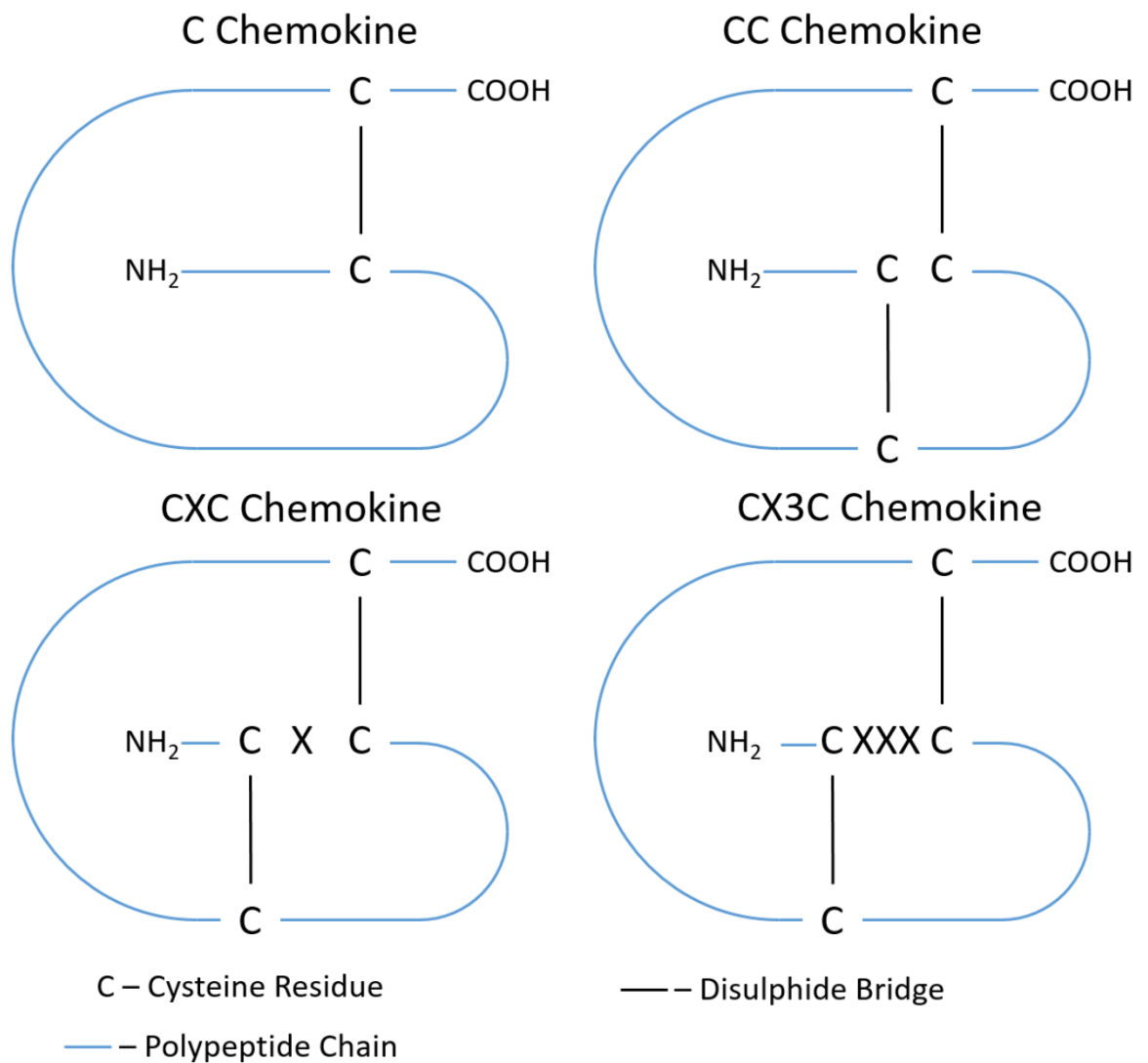


Figure 1.2: Chemokine ligand structure

Schematic detailing the basic structure of the chemokine ligands that are defined on the basis of conserved cysteine motifs present at the N-terminus of the chemokine polypeptide chain. Naming is based on both the number of cysteines and spacing between them.

As previously mentioned, apart from the classical chemokine ligands and receptors, a family of ACKRs also exist. These are ACKR1-4 and they are primarily thought to act as non-signalling scavengers that help maintain immune homeostasis and prevent excessive immune reactions by internalising inflammatory chemokine ligands (77). These receptors are classified as atypical, due to their inability to initiate classical signalling pathways through G-protein receptor signalling.

One feature of chemokines is that ligands can often bind multiple receptors, CCL5 can bind CCR1/3/5, and receptors can bind multiple ligands, CCR5 can bind CCL3/4/5/11 and other chemokine ligands(29). This promiscuity leads to a high

level of redundancy within the system. However, how much of this redundancy is true redundancy remains to be elucidated. For example, although CCL19 and CCL21 both bind CCR7 they can induce different downstream responses (111, 112). This signalling bias in chemokine receptors is a relatively novel area of research and the full extent of the bias and its functional implications remain to be determined. Multiple lines of evidence suggest that induction of inflammatory chemokine ligands occurs downstream of both NF- κ B signalling and IFN signalling (49, 84, 113-116) that are characteristic of TLR activation.

Functionally, chemokines have been implicated in multiple systems as discussed earlier and their potential roles in the CNS will be detailed later in this chapter. Here, only their role as chemotactic molecules in the context of inflammatory pathology will be discussed. Chemokines can attract a variety of different immune cells and upon receiving a chemokine signal cells undergo structural changes that aid cellular migration(117-120). These changes are linked to alterations in the cytoskeleton based on areas of higher chemokine concentration. It has been suggested through *in vitro* work that chemokine gradients are important for the migration and directionality of immune cells(58), and recent *in vivo* work by Lim et al. has suggested that neutrophil migration may be guided through trails of chemokines that are left within tissue parenchyma (121).

Generally, chemokines are associated with the attraction of specific cell types, for example CCL5 and CXCL10 are strongly associated with T-cell migration through CCR5 and CXCR3 signalling respectively (122, 123), and the CCL2-CCR2 axis is important in monocyte trafficking(124, 125). Further evidence of the promiscuity and redundancy of this system is demonstrated by the fact that CCL5 also appears to be able to attract monocytes (124, 125). As well as acting as inducers of cellular migration, chemokine ligand-receptor interactions are also responsible for homeostatic immune mechanisms. The CXCL12-CXCR4 axis is critical to the maintenance of haematopoietic stem cells within the bone marrow(126) and data suggests that down-regulation of CXCR4 allows egress of neutrophils, and possibly other leukocytes, to the circulation(127-129). The critical nature of CXCL12-CXCR4 in development is demonstrated by the perinatal lethality of CXCR4 and CXCL12 KO (130, 131).

An interesting area of development in chemokine biology is the idea of specific molecular “postcodes”. This concept suggests the need for cells of the immune system to have mechanisms for homeostatic trafficking and identification of sites of inflammation. This allows cells to both migrate to appropriate locations and to enact an appropriate response. The most compelling example of this is the CCL19/21-CCR7 axis that drives DC migration to the lymph nodes(58, 132). Alongside this, evidence also suggests that CCR4-CCL17 and CCR10-CCL27 are important in skin homing (133, 134), and CCR9-CCL25 are important for homing to the gut(135, 136). For the CNS the CCR6-CCL20 axis has been implicated in both humans(137) and mice(138, 139), and there is some evidence CXCR3-CXCL10 may also be important in homing of leukocytes to the CNS and specific areas within it(139, 140).

Overall the chemokine family is a structurally defined set of ligands that signals through GPCRs. They have diverse functions, not just in inflammatory contexts, but also in a variety of physiological and pathological states, including developmental processes.

1.1.7 Cellular functions of the immune system

Cells of the immune system are generally classified into innate immune cells; monocytes/macrophages, neutrophils, DCs, NK cells, eosinophils, basophils, mast cells and $\gamma\delta$ T cells, and adaptive immune cells; B and T cells. When looking at a conceptual overview of the immune system, it is worth considering the functions that immune cells fulfil. One primary function of all immune cells is immunological support either through cell-cell interaction or release of inflammatory mediators. The release of inflammatory mediators such as IFNs, cytokines and chemokines alters cellular functions through receptor-mediated alterations in transcriptional regulation as discussed above. Cell-cell interactions can promote activation of immune cells through antigen presentation and co-stimulatory molecules, as described for DCs and T cells of the lymph node. Cell-cell interactions can also involve engagement of Fas ligand to Fas receptor that induces apoptosis(141, 142), although this is primarily thought to be important in T cell homeostasis rather than acute inflammatory reactions. Another important example of cell-cell interactions is in immune cell-endothelial cell interactions,

where adhesion molecules expressed by vascular endothelium allow migrating immune cells to slow and adhere to endothelium before diapedesis occurs(33).

While nearly all immune cells provide immunological support in some form, T_h cells are unique in that this appears to be their primary function. Depending on the inflammatory environment T_h cells can take on different lineages, including T_h1 , T_h2 and T_h17 . In the context of TLR activation, $CD4^+$ T_h cells are thought to be driven towards the T_h1 lineage, through DC derived Il-12 (143). More recent evidence suggests that this response may be differential depending on both the TLR activated and the extent of activation(144). TLR responses and T_h1 responses also appear to be a key step in the activation of NK cells by DCs (145).

Neutrophils, monocytes/macrophages and DCs are all phagocytic cells of the immune system. Phagocytosis is a critical immune function that serves two purposes. Firstly, it allows APCs to scavenge and subsequently process antigens from the tissue environment and present them to other immune cells (146, 147). Secondly it allows for direct ingestion of bacteria followed by degradation using phagolysosomes (148). Phagocytosis occurs in DCs for the purposes of antigen presentation, neutrophils for intracellular destruction and macrophages for both antigen presentation and internal degradation. As discussed earlier macrophage phagocytosis also plays a role in inflammatory resolution through the uptake of apoptotic leukocytes.

Neutrophils and macrophages can also release reactive oxygen species (ROS) into the surrounding tissue in what is known as a respiratory burst (149). These ROS can directly kill bacteria they encounter aiding the immune response, however they can also damage host cells and tissue, highlighting the need for controlled inflammatory responses. Alongside ROS other factors can be released into the tissue to damage bacterial cells and inhibit viral replication, these include the perforins and granzymes expressed by NK cells and CTLs(150) and, neutrophils can also undergo degranulation that releases a variety of antimicrobial peptides(151).

Other cells of the immune system promote other responses; however, these are generally less related to TLR, anti-bacterial and anti-viral immunobiology. The

effector functions listed above demonstrate the diverse strategies the immune system can employ to combat foreign invaders.

1.1.8 Summary

Upregulation of cytokines, including chemokines, in response to stimuli are key early events in any immunological response and the subsequent activation and migration of diverse cell populations is critical to the resolution of inflammatory insults. The precise response to any insult is guided by molecular patterns and antigens that are encountered, and the nature of the insult itself. Co-ordinated immune responses utilise a variety of tools to combat the invader and if sustained provide immunological memory that allows for a rapid and effective response to future invasion. As discussed, in the context of TLR activation, NF- κ B and IRFs drive transcriptional changes that promote antiviral and antibacterial immune responses. In addition, lack of co-ordinated immune responses with appropriate mechanisms for both positive- and negative-feedback can potentially fail to resolve resulting in ongoing inflammatory pathology in the absence of stimulus.

The immune system is a highly complex system that has been extensively studied in a wide variety of contexts. The whole field of immunological knowledge is well beyond the scope of this Thesis. Despite this, I hope that the introduction to several key concepts and some specific aspects of immunity detailed above provides an appropriate context for approaching the work put forward in later chapters and demonstrates the functional relevance of those molecules and cells that are investigated.

1.3 Central Nervous System Immunity

1.1.9 CNS Overview

The CNS is composed of the brain and spinal cord. Its primary function is to integrate information transferred to it from the peripheral nervous system and environment, process this information and then relay responses back to the periphery. The processing of this information can be rapid and automatic such as in motor reflexes, or complex and conscious as is the case for higher brain functions such as problem solving.

Anatomically the brain itself has been the subject of many different subdivisions based on function and/or anatomical criteria. Broadly speaking there are three main areas of the brain, the cerebellum, brainstem and cerebrum. In addition, the brain has a series of ventricles through which the cerebrospinal fluid (CSF), produced at the choroid plexus, flows before being reabsorbed into the vascular and lymphatic circulation(152, 153). The CSF acts as both a mechanical and chemical buffer. Mechanically it acts to prevent pressure on the brain and provide buoyancy and chemically it acts as a system through which waste products and toxins can be removed (154, 155). The brain and spinal cord are also lined by three meningeal layers, the pia, arachnoid and dura mater and CSF flows between pia and arachnoid mater in the subarachnoid space after leaving the ventricular system of the brain.

The CNS consists of neurons, the processing units of the brain that transfer electrical and chemical signals between each other through their synaptic connections, and non-neuronal cells. The non-neuronal cell population primarily consists of microglia, astrocytes, oligodendrocytes, radial glia and ependymal cells, a group of cells collectively known as glia (156, 157). Alongside the glial cells there are also endothelial cells, pericytes, epithelial cells and small numbers of peripheral immune cells present(158, 159). The endothelial cells of the CNS, along with astrocytes and pericytes form the blood-brain-barrier (BBB) a specialized barrier that helps maintain CNS homeostasis and, which is an important part of CNS immune control(158, 160).

This thesis will focus on the inflammatory molecules that are induced, particularly chemokines, and the cells that are recruited to and activated in the brain in response to inflammatory stimuli. The following sections will provide an overview of the cells present within the CNS and the immune reactions that occur within the CNS in response to inflammation.

1.1.10 Cells of the CNS

Given the multitude of cell types present within the CNS this section will primarily focus on microglia and astrocytes, as they are involved in immune function, and neurons, as they are involved in CNS function. Microglia are the resident immune cells of the CNS and astrocytes, while long considered to be relatively inert and mainly supportive in function, have become increasingly implicated in immune responses in recent years(161, 162).

Microglia are resident immune cells that can be broadly considered as the macrophages of the brain. They are derived from the yolk sac early in embryogenesis, and there appears to be only a limited, if any, capacity for replacement through haematopoiesis (163). Activated microglia have historically been phenotypically subdivided into pro-inflammatory demyelinating ‘classically activated’ M1 microglia or pro-resolving remyelinating M2 microglia (164, 165), similar to macrophages of the peripheral tissues. Recently this dichotomisation has been challenged, and it is likely that microglia are highly plastic and exist on a continuous spectrum (166, 167).

Despite this changing perspective, TLR responses in microglia are associated with inflammatory cytokine production that would previously be considered as characteristic of an M1 response (168-170). In addition, microglia clearly react to LPS stimulation and undergo reactive changes(171). The most characteristic change seen in activated microglia is morphological. Although opinion is divided prevailing theories suggest that, at first, as microglia attempt to survey the surrounding area and react to stimuli there is an increase in the number of ramified processes, also known as “hyper-ramification”. Once fully “activated” it is thought that microglia take on an amoeboid morphology(172). However it is likely that microglia are plastic and can change both their phenotype and their morphology depending on the precise environmental context(167).

Alongside their roles in immunity microglia also play key roles in synaptic development and in maintenance of neuronal homeostasis. Complement molecules of the immune system help guide synaptic pruning by microglia throughout development and adulthood (173, 174) and CX3CL1-CX3CR1 interactions are key to neuronal survival and modulation of neurotoxicity(105, 108).

Astrocytes are key supportive cells in the CNS, they support the BBB through the encirclement of vessels with astrocytic end feet that allow for bidirectional interactions between astrocyte and endothelium(158). These interactions allow for modulation of BBB properties, including permeability and transport mechanisms, by astrocytes. In addition to their role at the BBB there is also evidence for their role at synaptic junctions. Tripartite synapses describe the three-piece suite of a pre-synaptic neuron, post-synaptic neuron and an astrocyte (175). The astrocyte acts to scavenge excess neurotransmitter and modulate synaptic properties. An example of this is the ability of astrocytes to take up glutamate from the synapse and thereby limit excitotoxicity (176).

Alongside their supportive roles, astrocytes also participate in CNS immune function, they express a variety of TLRs, the IFNAR receptor and a variety of cytokine and chemokine receptors (177-181). In response to immune stimuli they have been shown to produce inflammatory mediators (179, 182) and undergo reactive changes characterised by increased expression of glial fibrillary acidic protein (GFAP) (183, 184).

As we are interested in innate immune responses downstream of TLR signalling and particularly the chemokine response to this, it is interesting to note that there is evidence that both microglia and astrocytes express not only TLRs but a variety of chemokine receptors. *In vitro* work established that both microglia and astrocytes express CCR3-6 and CXCR1-5 at rest (177), with microglia expressing higher levels of CCR3 and CXCR3. It is interesting to note that in this study microglia, but not astrocytes, could readily migrate in response to CXCL10, probably mediated through CXCR3. Despite this, both TNF α and IFN γ significantly increased expression of CXCR3 in astrocytes, and stimulation with specific

concentrations of CXCL10 was able to promote astrocyte proliferation, implicating CXCL10-CXCR3 as having a role in astrogliosis.

Neuronal cells of the CNS communicate through both direct electrical connections and the chemical release of neurotransmitters, although, direct electrical communication is rarer within the mammalian CNS(153). Neurotransmitters are the most common form of neuron-neuron communication. Once an electrical signal has reached the axon terminal of a neuron, vesicles release neurotransmitter from the pre-synaptic neuron, into the synaptic cleft. The neurotransmitter then binds to the postsynaptic neuron, either inhibiting or promoting activation of an electrical impulse. Neurotransmitters are often associated with specific psychological functions, for example dopamine is the neurotransmitter characteristic of reward pathways whereas serotonin is associated with mood(153). Many different molecules, as well as other neurons of the brain can influence the release of neurotransmitters from neurons and alter their electrical excitability.

Neurons are generally considered to be non-replenishing cells, and death of neurons usually results in permanent loss that often causes functional deficits. While pre-natal and early life neurogenesis has clear developmental functions, there now appears to be a role for neuronal replenishment through ongoing neurogenesis in adults. However, this has been most extensively characterised for olfactory neurons in rodents (185) and, while there is strong evidence for ongoing neurogenesis in adult humans as well (186, 187), its functional purpose is equivocal. Despite this, some evidence suggests it plays a role in learning and memory (185). Despite these unknowns, reductions in hippocampal volume, thought to be due to decreased neurogenesis, are present in depressed populations (188-190) and increased neurogenesis has been implicated in the function of antidepressants (191-193).

Like microglia and astrocytes, neurons can also express TLRs and chemokine receptors. While there is a clear role for chemokine receptors, particularly CXCL12/CXCR4, during neuronal development and guidance (194, 195), their role in the adult CNS is less well defined. Recent studies have demonstrated that chemokines may be able to modulate neuronal function, for example, *in vitro* electrophysiology demonstrated alterations in serotonergic neurons modulated

by CCL2 and CXCL10(102, 103). In addition, CCL2 appears to be important during pain sensitisation in animal models (196, 197).

In summary astrocytes, microglia and neurons have overlapping functions within the CNS. Interactions between these cell types help maintain normal CNS function and allow for modulation of a variety of parameters in response to pathology. In addition, expression of TLRs and chemokine receptors by microglia, astrocytes and to some extent neurons, highlights the need for an understanding of the role they play in innate immune responses and CNS function.

1.1.11 Immune “Privilege” in the CNS

Due to the specialised barriers present in the CNS alongside the limited number of peripheral immune cells present, the CNS was previously considered to be “immune privileged” i.e. to be protected from normal immune reactions. Recent developments in CNS immunology suggest that this is not the case and that rather than being a site of “immune privilege” like the cornea, the CNS is much more likely a place of modified immune function (198-200). Despite this changing perspective, there is still a requirement to prevent parenchymal damage due to the largely non-replenishing nature of neurons. In addition, the swelling and oedema characteristic of inflammatory responses can be fatal within the enclosed compartment of the skull, and therefore several mechanisms exist to limit immunoreactivity within the CNS.

One mechanism of protection is the extensive barrier function of the BBB and unlike other tissues of the body the capillaries of the CNS have a very limited “leakiness”. There is an absence of fenestrations, and nearly complete presence of tight junctions preventing easy ingress of many molecules and cells (157, 201). In addition, while the ependymal cells of the choroid plexus have fenestrations and lack tight junctions, the choroid plexus epithelium itself does not, forming what is known as the blood-CSF barrier(201).

Modified immune function is another mechanism through which the CNS is protected, this is particularly true for T cell responses. In contrast to peripheral tissues, foreign grafts into the CNS survive for longer(202), heat treated bacillus

calmette-guérin injected directly to the CNS attracts monocytes but not T cells(203), and T cells specific against CNS antigens fail to initiate immune responses if no other stimuli are present(204). Although there is immune surveillance of the meningeal compartments lining the brain and a CD4+ T cell population in the CSF (159, 205), the parenchyma itself is subjected to very limited immune surveillance by T cells. Microglia are able to survey the brain parenchyma however they do not detect specific antigens, only conserved motifs that can be detected by their PRRs.

If antigen is introduced to the periphery as well as the CNS, as would be the case in most real-world circumstances, the CNS can mount a true response(202) probably due to peripheral antigen presentation allowing for the activation and proliferation of antigen specific T cells that can then enter the CNS. The lack of T cell responses in the CNS is probably due to the lack of DCs in the healthy CNS parenchyma (159, 206). As there are no DCs to survey the area, it is unlikely that T cells would be presented with the antigen and co-stimulatory molecules required for full activation. Whether other cells drain to lymph nodes and present antigen is currently unknown.

Another modification in the CNS, is that there is no lymphatic drainage of the parenchyma itself. Recent animal work has shown that there may be lymphatics present within the meninges (207), although whether these are present in humans as well as mice remains to be established. Despite this the CSF is reabsorbed back into the lymph and drains to the cervical lymph nodes (206). However, whether APCs can follow this route is unclear.

In summary, a combination of specialized barriers, altered immune cell residency and surveillance, an anti-inflammatory environment and a deficit of draining lymphatics appear to be the underlying mechanisms through which the CNS displays differences in immune function. One of the main challenges facing study of CNS immune responses is the fact that much immunological research into peripheral tissues and organs is not clearly translatable to the CNS because of the differences in immunity highlighted above. While previously regarded as a site of immune “privilege” it is becoming clear that it is not in fact as privileged as originally thought and more analogous to an area of modified immune function. Original animal studies demonstrating immune privilege and a lack of

responses were limited by their use of pathological models that directly introduced stimuli to the CNS without peripheral interaction, a situation that would rarely be seen in real life.

1.1.12 Immune Responses to Central Inflammatory Stimuli

Although immune responses within the CNS have been studied in a variety of contexts, the focus of this section will be on viral, bacterial and TLR responses within the brain. Generally, these models, utilise either direct injection of stimuli intracerebroventricularly (i.c.v) or encephalitic pathogens that home to the CNS, for example West Nile Virus (WNV).

After bacterial or viral invasion into the CNS, microglia can detect their presence through PRRs. Signalling through the TLRs generates distinct responses including the activation of NF- κ B and IFN as discussed earlier. One important thing to note is that in normal CNS infection, whereby inoculation occurs at a peripheral site, the immune system has already encountered the antigen and is therefore primed to respond (208). This allows the immune system to mount a more effective and prominent T cell response than if it had entered the CNS directly, as was the mechanism in some immune privilege studies.

Viral or bacterial infection of the CNS results in dramatic upregulation of a variety of cytokines and chemokines including Il-1 β , TNF α and Il-6 as well as the chemokines CCL2, CCL5, and CXCL10 (209-213). Alongside these molecular alterations there are changes in the activation state of microglia, death of neurons and an influx of peripheral immune cells. For example, in WNV there is an influx of both CD4⁺ and CD8⁺ T cells(214, 215), NK cells and monocytes(216, 217). Alongside this, astrocytes and microglia become activated in response to the infection (218, 219).

A number of studies have begun to highlight the role of CNS chemokines in coordinating immune responses. Examples include the role for astrocytic CXCL10 during viral encephalomyelitis(220), the increased susceptibility of patients with the CCR5 Δ 32 mutation to WNV (221) and the reduction in infiltrating monocytes seen in both Ccl2^{-/-} and Ccl7^{-/-} mice(222). In addition previous work within our laboratory identified upregulation of CCL2, CCL3, CCL5 and CXCL10 among other

chemokines in two models of viral encephalitis(213). This study also identified the chemokine receptors CXCR3 and CCR2 as being key to CNS inflammation and inhibition of these receptors improved host survival. Expression of CXC chemokines drives neutrophil infiltration in the JHM strain of mouse hepatitis virus (MHV) and aids neuroprotection. A further study of CNS MHV in CXCL10^{-/-} mice resulted in increased viral load at 12 days post-infection that was associated with a decreased T cell infiltrate (223). CXCL12 appears to have a role in maintaining cells in the perivascular space (224), similar to its role in maintaining haematopoietic stem cells in the bone marrow niche. This cellular retention in the perivascular space of the BBB is often cited as an example of the altered immunity in the CNS.

Alongside these findings in CNS infection, work has been done to understand innate immune responses in the CNS through direct introduction of a TLR ligand to the brain or through *in vitro* studies. TLR4 is the predominant TLR that has been studied and *in vitro* study of LPS agonism in neuronal cultures demonstrated upregulation of both chemokines, CCL5 and CXCL1, and cytokines, TNF α and Il-6 (225). Using conditioned medium from these experiments indicated that these changes were associated with increased *in vitro* neutrophil migration across endothelium.

A number of studies have demonstrated that LPS i.c.v increases expression of the pro-inflammatory cytokines Il-1 β , TNF α and Il-6(226-228). These cytokines are directly associated with parenchymal alterations and Il-1ra antagonism of Il-1 β markedly reduced ventricular dilation following i.c.v LPS (226). Of note, many of these effects appear to be age dependent, with older mice exhibiting increased cytokine responses and prolonged behavioural changes (229). While not directly relevant to the work in this thesis it is worthwhile noting the importance of age-matching animals when performing investigations into inflammatory responses.

These inflammatory responses are also associated with cellular changes characteristic of microglial reactivity and astrogliosis (226, 228, 230), suggesting that the innate immune responses of the CNS alter the phenotype of resident glial cells. Chemokine responses have been less extensively studied in this

model. One study in CCL2^{-/-} mice demonstrated that although there were no obvious alterations in microglial and astrocytic responses to LPS, there were reductions in pro-inflammatory cytokine levels (228). The authors suggested two possible mechanisms for these changes. Firstly, absence of any CCL2 might mean that glial cells were under-primed for inflammatory responses. However this is not necessarily supported by the morphological data. The second mechanism proposed is that lack of monocyte recruitment due to the absence of CCL2 reduces overall levels of inflammation. This study also demonstrated that in WT mice there is a significant upregulation of CCL2 in response to i.c.v LPS.

Because of the limited number of *in vivo* studies examining chemokine responses, consideration of *in vitro* data on glial chemokine production in response to LPS is important. An array study of microglial responses to LPS observed significant transcriptional upregulation of multiple chemokine ligands including *Ccl2*, *Ccl3*, *Ccl5*, *Cxcl2*, *Cxcl9* and *Cxcl11*(231). CCL2 and CCL5 protein were also found to be upregulated in an *in vivo* experiment to confirm these findings. The other chemokines were not studied in the *in vivo* model so confirmation of their expression is an area for further work. These chemokines have the ability to attract a wide variety of cells including monocytes, T cells and neutrophils, suggesting the ability of microglia to promote diverse immune cell infiltration in response to innate immune challenges. Similar to microglia, astrocytes have been shown to upregulate CCL2, CCL3, CCL5 and CXCL10, among other chemokines, in response to LPS (232-234).

Although TLR4 has been most extensively studied, a limited number of studies have looked at the role of TLR7 in neuroimmune responses. As this is the agonist utilised in the model of inflammation presented in this thesis it is worth briefly discussing some key findings here. Butchi et al. found that i.c.v treatment of neonatal mice with either imiquimod (IMQ) (TLR7 agonist) or LPS induced significant increases in *Ifnb1*, *Tnf*, *Ccl2* and *Cxcl10* gene expression at 12 hours post inoculation (235). For IMQ this did not persist to time-points greater than 48 hours, whereas for LPS this upregulation persisted up to 96 hours post inoculation for some transcripts. Despite this upregulation there was no significant upregulation of Cd3ε messenger RNA (mRNA), that would be indicative of T-cell infiltration, in IMQ treated brains at any time-point, although

both meningitis and ventriculitis were observed. Despite the lack of immune cell infiltration there is an upregulation of GFAP at this time-point, suggesting astrogliosis in response to IMQ inoculation. This may reflect the fact that direct introduction of inflammatory stimuli to the CNS does not allow an effective T cell response until the antigen is encountered in the periphery as discussed earlier. A later study by Butchi et al. also found a similar upregulation of chemokine and cytokine proteins in response to TLR7 agonism at 12 hours(236). In addition to *in vivo* work Butchi et al. have also demonstrated *in vitro* TLR7 expression in microglia and astrocytes using flow cytometry(237) and this has also been shown by in-situ hybridization in another study, where TLR7 expression was also observed in neurons(238). The *in vitro* study by Butchi et al. also demonstrated significant upregulation of CCL2, CCL3, CCL5, CXCL1 and CXCL10 protein in response to stimulation with IMQ (237). A limitation of this data set is that all of the findings in relation to TLR7 response are from a single research group.

Overall, CNS infection in physiological circumstances such as in viral models of encephalitis induces not only cytokine and chemokine responses within the brain parenchyma but also attraction of peripheral immune cells. In the case of direct TLR stimulation a similar pattern of upregulation is observed. While chemokines have been examined to a lesser extent than the major cytokines, there are a number of studies that demonstrate alterations in the immune response if chemokines are absent. This suggests that the chemokine family plays an important role in co-ordinating and promoting innate immune responses within the CNS.

It appears that both microglia and astrocytes have the ability to promote pro-inflammatory changes in response to TLR activation. Molecular alterations in mRNA and protein, and functional alterations demonstrated by changes in morphology and immunohistochemical staining are probably downstream of TLR activation. Alongside these alterations in glial cell function, infiltrating immune cells can contribute to the inflammatory milieu, particularly in the context of viral illness. The upregulation of chemokines that is observed in many of these models is likely to help mediate this immune cell influx.

1.1.13 CNS Immune Responses to Peripheral Inflammatory Stimuli

In recent years, there has been an increasing focus on the role of peripheral inflammatory stimuli in driving CNS immune responses. These studies have largely concentrated on the TLR4 agonist LPS, but have also utilised the TLR3 agonist polyinosinic:polycytidylic acid (PIC), other TLR agonists, and direct injection of pro-inflammatory molecules into the circulation. The majority of studies have used animal models as this allows for post-mortem tissue examination throughout a pre-determined time-course and closer investigation of the molecular and cellular response. Human studies have focused on lower doses of peripheral stimuli coupled with emotional/mood measures and imaging studies.

In animal models, LPS has been most widely utilised. It is usually delivered intraperitoneally (i.p.) and has been demonstrated to induce upregulation of pro-inflammatory molecules within the CNS, including $IL-1\beta$ and $TNF\alpha$ (81, 102, 239-242). Alongside these changes there is activation of microglia within the parenchyma itself (81, 240, 243). Studies aiming to quantify whether LPS reaches the brain itself have concluded that limited if any LPS crosses the BBB although it does associate with the endothelium (244), suggesting that its effects are not entirely mediated by direct access to the parenchyma.

Alongside LPS, another immune stimulant that has been used is PIC. PIC is a TLR3 agonist, which mimics the dsRNA present in some viruses that TLR3 would normally detect. This provides an alternative to LPS that is considered to model bacterial TLR responses. Like LPS, upregulation of pro-inflammatory cytokines and chemokines has been observed in response to PIC (245-247). For both LPS and PIC the most commonly studied chemokine is CCL2, its upregulation has been observed in several brain areas as well as at brain-periphery interfaces such as the choroid plexus, other circumventricular organs (CVOs) and cerebral blood vessels (102, 248). Upregulation of the CCL2 receptor CCR2 has also been observed in response to LPS stimulation (102), providing further evidence for a potential functional role in the CNS. A longitudinal study performed by Qin et al. identified that even at 10 months after i.p. LPS administration there were alterations in brain $TNF\alpha$ levels and alterations in substantia nigra neurons (81).

In addition, using i.p. $\text{TNF}\alpha$ they demonstrated an increase in CCL2 in the brain that was associated with an upregulation of $\text{IL-1}\beta$ and $\text{NF-}\kappa\text{B}$ transcript. Overall this suggests that single systemic inflammatory stimuli can drive long-lasting alterations in CNS function that are at least in part driven by $\text{TNF}\alpha$. The concept that individual inflammatory insults can drive long-lasting changes within the brain is reinforced by an increasing body of human post-mortem literature. The primary example of this being the profound alterations observed in CTE and AD discussed earlier.

LPS, delivered systemically, has also been shown to induce activation of astrocytes in a variety of brain areas in animal models (226, 249). In another study infiltration of neutrophils and monocytes was observed in the CNS using flow cytometry, and alterations of microglial staining were seen using ionized calcium binding adaptor molecule 1 (Iba1) antibody (102). These alterations in microglial phenotype have also been observed using *in vivo* positron emission tomography imaging in a non-human primate study, indicating that this response is not limited to rodents and is potentially translatable to humans (250). A recent study by Hao et al. found that after repeated administration of i.p. LPS there was no alteration in the number of CD3 cells present within the CNS parenchyma suggesting that peripheral T lymphocytes did not infiltrate into the brain at this point (251). Despite this NK cells and neutrophils were found to enter the CNS. Systemic NK cell depletion significantly ameliorated neutrophil entry into the CNS. Alongside this, microglia from NK depleted mice had significant reductions in some chemokine transcripts, particularly CXCL1 a key neutrophil chemoattractant. This finding highlights the interaction between resident and recruited immune cells in driving CNS immune responses.

Earlier work within our group demonstrated that i.p. LPS not only upregulated a variety of pro-inflammatory cytokines but also generated a robust IFN response within the brain (25). This IFN response was associated with increased expression of the chemokine *Cxcl10*. Another experimental model used by our group, and studied in more detail in the work reported in this thesis, is the Aldara model of peripheral inflammation. In this model, animals are treated topically with Aldara cream, containing the TLR7 agonist IMQ. Work comparing the response to Aldara with the response to LPS identified the IFN pathway as a shared response

between the two TLR agonists (25). As discussed earlier, both TLR agonists drive MyD88 dependent activation of NF- κ B. However, TLR4 drives IFN responses via IRF3 downstream of TRIF adaptor protein signalling, whereas TLR7 drives an MyD88 dependent activation of IRF7. Further work into the Aldara model demonstrated that significant upregulation of chemokine transcripts was observed in the brain in response to Aldara stimulation and that this peaked after 3 days of repeated daily treatment. The upregulated chemokines included Ccl3, Ccl5, Ccl9, Cxcl9, Cxcl10, Cxcl13, Cxcl16 and the receptor Ccr5. Flow cytometry analysis of the brain tissues, demonstrated that this transcriptional upregulation was associated with infiltration of monocytes, CD4⁺ T cells, CD8⁺ T cells, NK cells and NK T cells(24). The multiple cell types attracted is probably due to the diverse chemokine upregulation seen.

These data together provide evidence that peripheral inflammatory insults not only drive a systemic response but a CNS response that is associated with upregulation of chemokines and cytokines. Alongside these molecular alterations, cellular changes are observed in both resident CNS cells particularly astrocytes and microglia and infiltrating peripheral immune cells that include monocytes, neutrophils and T cells (Figure 1.3).

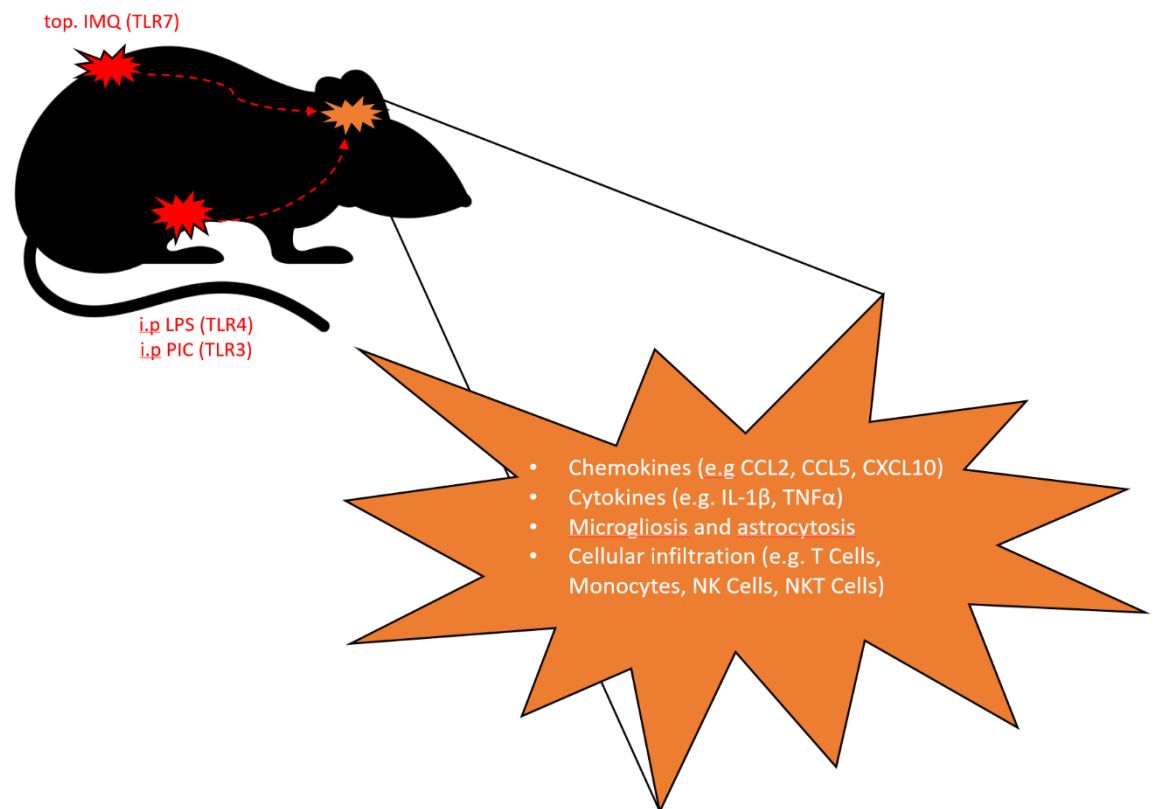


Figure 1.3: CNS response to peripheral inflammatory stimuli

A variety of peripheral inflammatory stimuli delivered both i.p. and topically have been shown to induce inflammatory responses within the CNS. These responses include the upregulation of chemokine and cytokine ligands, alongside reactive changes in microglial and astrocytic populations and infiltration of peripheral immune cells. Abbreviations: top. – topical; IMQ – imiquimod; TLR – toll-like receptor; i.p. – intraperitoneal; PIC – polyinosinic-polycytidylic acid; LPS – lipopolysaccharide; NK – natural killer

1.1.14 Peripheral-Central Immune Communication

Despite a significant number of studies demonstrating that peripheral inflammation can drive a central response, the exact mechanisms that underlie this inflammatory crosstalk remain unclear. The two primary routes that are considered are the humoral or circulatory route whereby inflammatory mediators in the circulation drive changes in CNS function, and the neural route wherein nerves directly transmit information relating to systemic immune status to the CNS.

Humoral routes drive CNS inflammation through a variety of mechanisms; (i) circulating mediators can activate BBB endothelium and/or perivascular cells transmitting signals to the CNS (181, 252, 253); (ii) the BBB can actively transport molecules into the CNS (253-256) and; (iii) mediators may activate cells of, or gain access through, the CVOs (252, 257, 258) .

Activation and alteration of the BBB by circulating mediators has been demonstrated in a variety of ways. Upregulation of adhesion molecules is a key step in inflammatory cell recruitment and i.p. LPS has been shown to increase adhesion molecule expression by brain endothelium (259). In the same study, KO of intracellular adhesion molecule 1 (ICAM-1) significantly reduced the influx of neutrophils into the brain parenchyma following peripheral LPS administration. *In vitro* studies of endothelial cells have suggested that LPS has the ability to upregulate chemokine and cytokine production by the BBB (260-262). In addition Blank et al. demonstrated increases in ISG15, an IFN response gene, in BBB endothelium after systemic infection with vesicular stomatitis virus (VSV) suggesting that IFN signalling can also drive endothelial production of inflammatory mediators(103). Alongside these mechanisms showing that systemic pathogens or PAMPs can drive changes in the BBB, work has also demonstrated the ability of $Il-1\beta$ to induce prostaglandin synthesis in brain endothelium(252). Combined with the findings that KO of COX-2 ameliorates fever responses to circulating $Il-1\beta$ (263) it is likely that these $Il-1$ responses play an important role in CNS immune function.

It has also been suggested the BBB has the ability to actively transport cytokines such as $Il-1\beta$ and $Il-6$ across the endothelium in a blood-to-brain manner(254). These cytokines would then be able to act on cells of the CNS and drive a downstream inflammatory response. These data all suggest that the BBB plays an important role in controlling CNS inflammation and allowing for information about inflammatory states to be relayed to the CNS. This probably occurs through active transport of molecular mediators, localized activation of the endothelium to promote immune cell influx and through production of inflammatory molecules at the endothelium itself.

Alongside these BBB mechanisms it has also been demonstrated that cytokines and other immune molecules can cross into the CNS at the CVOs. Following intravenous (i.v.) injection of circulating cytokines there is an accumulation of these molecules at the CVOs(264). This is likely to be due to the altered composition of the endothelium at these sites and the increased ability of circulating mediators to diffuse across a more permeable barrier that has an altered tight junction composition(265). Although there is limited diffusion of

large molecules across CVOs compared to systemic organs(266), it has been shown that dextrans of molecular weights greater than 10kiloDaltons (kDa) can cross the vascular endothelium although they do not diffuse widely(267). This suggests that molecules such as TNF α (17kDa) and proteolytically cleaved Il-1 β (17.5kDa) may be able to cross the endothelium at these sites and activate cells with the corresponding receptors.

Neural routes are less well defined than the humoral routes probably because the concept of neural inflammatory communication is newer, the increased complexity of studying neural routes using *in vitro* models, and difficulty in performing effective *in vivo* studies that can comprehensively remove neural pathways. It is generally difficult to completely remove innervation to an area and therefore much of the work has centred on the vagal nerve probably because of the relative ease with which vagotomy can be performed and its extensive innervation throughout the body. The other area in which work has primarily been done is in the study of pain where anatomical routes of nervous pathways are more clearly defined and therefore studying alterations in these pathways is an easier task (268).

The inflammatory reflex has been both described and reviewed a number of times over the past 15 years (269-272). In brief it supposes that cytokines, particularly Il-1 β activate afferent fibres of the vagus nerve that route to the brain. Descending efferent fibres can then release acetylcholine at peripheral lymphoid organs, particularly the spleen, which acts to suppress inflammatory responses. This mechanism has been demonstrated through both augmentation and abrogation of this pathway. Electrical stimulation of the efferent vagus nerve has been shown to inhibit TNF production in peripheral organs(270) and stimulation of the afferent vagus was recently shown to reduce neuroinflammation induced by LPS as measured by reductions in cytokines and microglial and astrocytic reactivity(273). Interestingly, a 2012 study by Bratton et al. did not find a neural connection between the vagus nerve and the splenic sympathetic neurons(274), suggesting that this may not be a direct reflex but that there are intermediate actors that are as yet undefined. These findings have led to a recognition of the need for reconsideration of the inflammatory reflex model(275).

The inflammatory reflex pathway is often described as anti-inflammatory(270-272). However, there can also be release of noradrenaline and adrenaline in response to inflammatory stimulation, particularly in the context of pain. While these molecules do have anti-inflammatory properties, they can also promote inflammation and therefore it appears as though neural control of inflammation, much like humoral control, is a complex process that involves a balance of both pro and anti-inflammatory signals(276-278).

Pain, while not a focus of this thesis, is an inherently inflammatory process as it is usually a response to an inflammatory insult be it trauma, infection or disease. It has been demonstrated that inflammatory mediators play an important role in sensitizing nerve fibres and promoting hyperalgesia (279, 280). In addition, increases in both cytokines and chemokines, particularly CCL2, have been found in the dorsal horn of the spinal cord in response to pain (281, 282).

A further route with crossover between the neural and humoral pathways is the HPA where inflammatory mediators such as $Il-1\beta$ can activate corticotrophin-releasing hormone (CRH) neurons of the hypothalamus and drive secretion of glucocorticoids that then act to suppress inflammatory activity (283, 284). However, this route does not provide an explanatory mechanism for the induction of CNS inflammation in response to peripheral stimuli but rather a pathway through which systemic inflammation can be influenced through top-down control. Despite this, it does provide further evidence supporting the idea that neurons can respond to inflammatory stimuli and be induced to promote effector responses.

The mechanisms of communication between the periphery and CNS have begun to be elucidated (Figure 1.4). The critical role of the BBB in CNS inflammation is demonstrated repeatedly and in a number of different contexts. Circulating cytokines and PAMPs can drive changes in endothelial function and, in the case of cytokines, be directly transferred into the CNS itself. Neural routes also appear to contribute to immune homeostasis within both the CNS and the body, the vagal nerve clearly plays an important role in peripheral-central crosstalk and studies that aim to alter the function of this pathway identified alterations in inflammation associated with this. A challenge for this field is that currently the vast majority of work has been performed using LPS in murine models of

inflammation. While useful, this model is generally viewed as a model of sepsis that would be indicative of very severe systemic inflammation and therefore is not applicable in all human contexts. In addition, because of its i.p. administration LPS and the inflammation it induces will have immediate access to the vagus nerve due to its widespread gut innervation and this may influence the outcome of some models and therefore limit the generalisability of conclusions that are drawn. A final challenge is the marked difference in LPS reactivity observed between humans and mice. *In vivo* work in mice generally utilises doses of LPS in mg/kg whereas human work will use ng/kg doses. This 100,000 fold difference in concentration may influence some of the observed effects and again limit the overall generalisability of these findings.

Many challenges remain in the study of peripheral-central crosstalk. These include; (i) identifying the most appropriate *in vivo* models for its study; (ii) the need to perform complex mechanistic studies that target specific components of the immune system, for example the endothelial specific KO of IFNAR1 used by Blank et al. and; (iii) the need for improved *in vitro* models due to the challenges of *in vivo* mechanistic work, particularly when putative mechanisms are not well understood or even known.

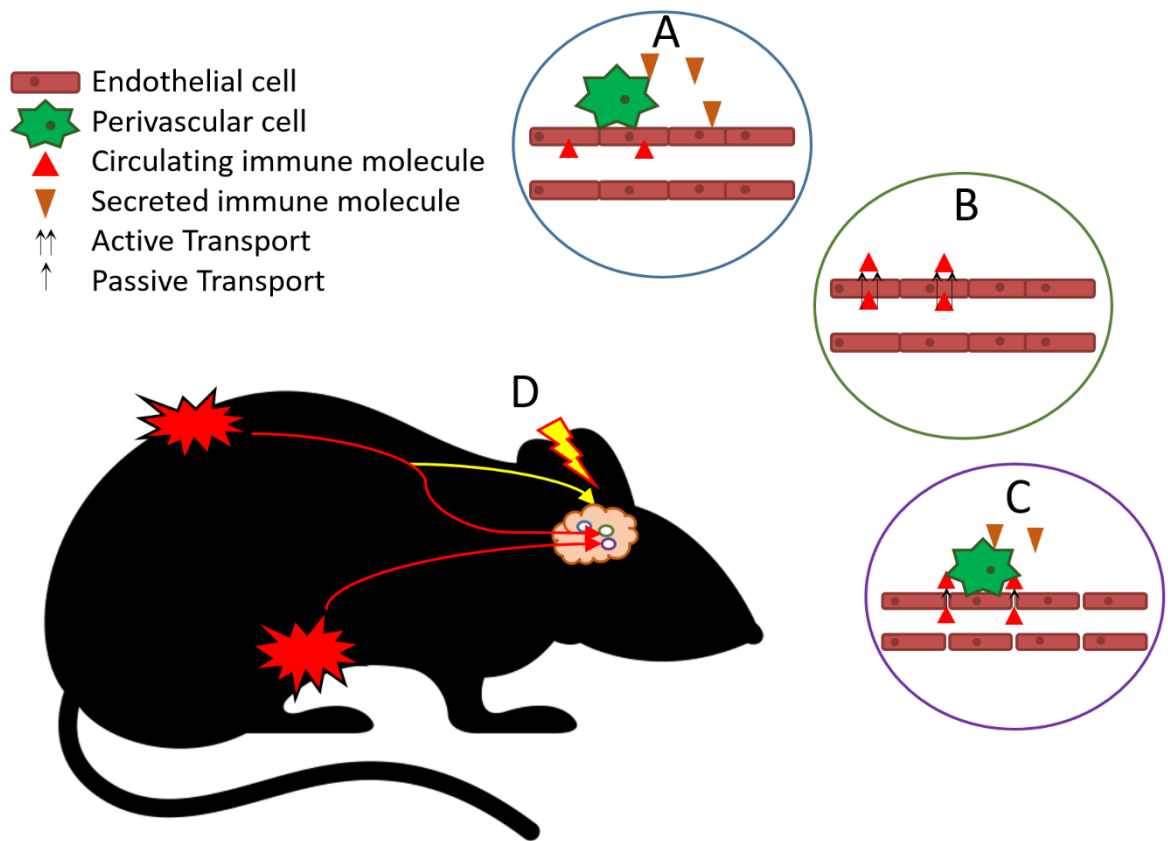


Figure 1.4: Routes of peripheral-central immune communication

Multiple routes have been identified through which peripheral immune responses can be communicated to the CNS. (A) Circulating immune molecules can activate brain endothelium or perivascular cells inducing them to secrete their own immune mediators. (B) Circulating immune molecules can be actively transported across brain endothelium. (C) Circulating immune molecules can gain access to the brain at CVOs where the blood-brain-barrier is less tightly sealed. In addition, they may also activate perivascular cells at CVOs. (D) Neural routes of communication appear to exist with the vagus nerve able to detect circulating immune molecules and subsequently communicate this to the CNS.

1.1.15 Aldara Model of Psoriasis-like Inflammation

The Aldara model of psoriasis-like inflammation that is described in this thesis uses the TLR7 agonist IMQ as its active component. Topical Aldara is applied daily where it induces psoriasiform inflammation characterised by epidermal hyperplasia and hyper-keratosis. It was originally described in 2009 by van der Fits et al. as a dermatological model for the study of psoriasis(285). Treatment of skin with Aldara cream has been shown to induce robust inflammatory responses at the local site and, as discussed earlier, IMQ has been shown to induce both cytokine and chemokine responses in the brain if injected i.c.v or applied to CNS cells *in vitro*(235-237). Alongside this other work has demonstrated the ability of IMQ to induce cytokines and chemokines *in vivo*(286).

Our own laboratory's findings with the Aldara model have been discussed earlier in this section and included the finding that topical application of the cream to the dorsal skin of mice induced an IFN response within the CNS. This response was associated with upregulation of some chemokines and an influx of peripheral immune cells into the CNS parenchyma.

The rationale for moving away from the LPS model of peripheral inflammation has been alluded to earlier. Firstly LPS is generally a severe insult that induces septicaemia-like inflammation and the Aldara model may be viable alternative to this for studying less severe peripheral immune insults and subsequent CNS responses. Secondly, LPS models generally use an i.p. route of administration that provides immediate and extensive access to vagal nerve innervation and can be rapidly disseminated into the body due to absorption through the peritoneum. Finally, although difficult to model and study, it does not appear as though differences in rodent and human responses to Aldara are of the same order of magnitude as for LPS. Aldara is routinely used in human clinical practice to treat actinic keratosis and warts. Induction of inflammation at these sites helps to promote immune responses against these benign growths. In some cases it is applied to the scalp, or large areas of the forearms. If the differences in responsiveness were similar to those observed in LPS this would almost certainly be fatal for human subjects. Overall therefore, it seems the Aldara model may be a good alternative model to the LPS model for studying peripheral-central immune responses.

Nevertheless, there are a number of limitations of this model. Firstly, it has been shown that Aldara cream has a second active component that acts to promote skin inflammation through sterile inflammatory mechanisms; isostearic acid, the solvent used in Aldara, has the ability to activate the inflammasome and promote keratinocyte death in the absence of Aldara, indicating that not all findings using this model can be attributed directly to TLR7 agonism(287). This is particularly true for observations in the skin where the acid can act locally on keratinocytes. However a major limitation of this study is that while *in vitro* isostearic acid induced keratinocyte death, *in vivo* it did not significantly induce inflammatory-associated transcripts aside from interleukin-1 alpha, which was only raised by a factor of 2 compared to a factor of 10 for Aldara cream. In

addition, there was no apparent histological study of the skin in response to isostearic acid making it difficult to draw more complete conclusions. Another recently published study also identified a further potential limitation. Grine et al. reported that many of the effects of Aldara cream observed in mice are actually reliant on ingestion of the cream and subsequent activation of the gut(288). However, this study described a significant attenuation in skin inflammation associated with prevention of ingestion which does not entirely fit with the human literature. Humans are extremely unlikely to be ingesting Aldara in clinical practice yet still go on to develop psoriasiform lesions similar to those observed in mice(287) questioning the criticality of Aldara cream ingestion for development of inflammatory responses.

Despite its potential limitations, overall the Aldara model provides a promising alternative to the LPS model of peripheral inflammation in studying peripheral-central crosstalk. Earlier work has established that it can induce central responses, and now additional work must aim to further characterise the immune responses in this model, with a particular focus on the central response, and to ensure that it is an appropriate model for study, while keeping newly identified limitations in mind.

1.1.16 Functional Consequences of CNS Immune Responses

Following on from inflammation, associated changes occur that can be attributed to alterations in CNS function. These changes include alterations in behaviour, HPA axis function, neurogenesis and chronic inflammation and neurodegeneration. Certain inflammatory stimuli are also associated with demyelination, for example, experimental autoimmune encephalitis, a commonly used animal model of human multiple sclerosis, has profound impacts on CNS myelination(289, 290). Many of these responses are associated not only with direct CNS insults, but also the peripheral inflammatory insults that can drive immune changes in the brain as discussed above.

Sickness behaviour describes a group of symptoms that are associated with response to illness and systemic inflammation. Behaviourally these changes include anhedonia or loss of pleasure, social withdrawal, fatigue and altered learning and memory. Physiological changes associated with sickness behaviour

include fever and altered HPA axis function. Examples of anhedonic sickness behaviours in animal models include reduced sucrose preference following on from LPS treatment(291, 292) and reduced burrowing, a measure of overall wellbeing, following on from Aldara treatment(24). Multiple reviews have now expanded upon the role of cytokines in generating sickness behaviours, with $Il-1\beta$ and $TNF\alpha$ appearing to be the key molecular mediators of this response (4, 8, 11, 293). These cytokines have been shown to rise in the hypothalamus and, as noted earlier, influence CRH neurons providing a mechanism through which inflammation can drive these changes.

Other mechanisms include alterations in neurogenesis and neuronal signalling. Reductions in hippocampal neurogenesis have been observed in response to peripheral LPS treatment and decreased neurogenesis has been implicated in alterations of learning, memory and mood in rodents. Furthermore, cytokines have been implicated in neurotransmitter alterations, and a recent study using CCL2 demonstrated that CCL2 treatment could alter serotonergic neuronal function(102). Alongside this, there is evidence that the enzyme indoleamine 2,3-dioxygenase (IDO) that can impact brain serotonin levels, through alterations in tryptophan catabolism, can be induced in the context of inflammation and plays a role in mediating depressive-like behaviours (294).

Goshen et al. demonstrated the potential bi-directional nature of this relationship, wherein mice exposed to chronic mild stress (CMS), a model commonly used to induce depressive symptoms, were found to have increased $Il-1\beta$ in the hippocampus(295). Using interleukin-1 receptor ($Il-1r$) KO, and transgenic $Il-1ra$ mice, they demonstrated that the behavioural alterations in CMS, reduced sucrose preference and social exploration, were mediated by $Il-1\beta$. In addition, wild type mice had decreased neurogenesis and increased corticosterone levels compared to their $Il-1r$ KO counterparts. This study drew together a number of threads in the sickness behaviour story and demonstrated the important role of $Il-1\beta$ in mediating these effects. They also provided evidence to suggest that not only can inflammation drive psychological alterations but that psychological stress can itself drive immune alterations.

Blank et al. also demonstrated that in response to VSV there was a significant upregulation of the IFN stimulated chemokine CXCL10 by endothelial cells that appeared to be in response to circulating IFN- β . When *Cxcr3*^{-/-}, the receptor for CXCL10, or *Cxcl10*^{-/-} mice were treated with VSV, depressive behaviours were significantly ameliorated compared to wild type mice(103). In addition, they demonstrated that CXCL10 could directly influence neuronal firing strongly implicating CXCL10 in psychological alterations.

As we move forward to discuss human depression and the immune system, it is important to consider the potential mechanisms through which immune alterations may be able to drive psychological changes. The section above highlights several findings that suggest mechanistic links between altered inflammatory states and altered psychological function (Figure 1.5).

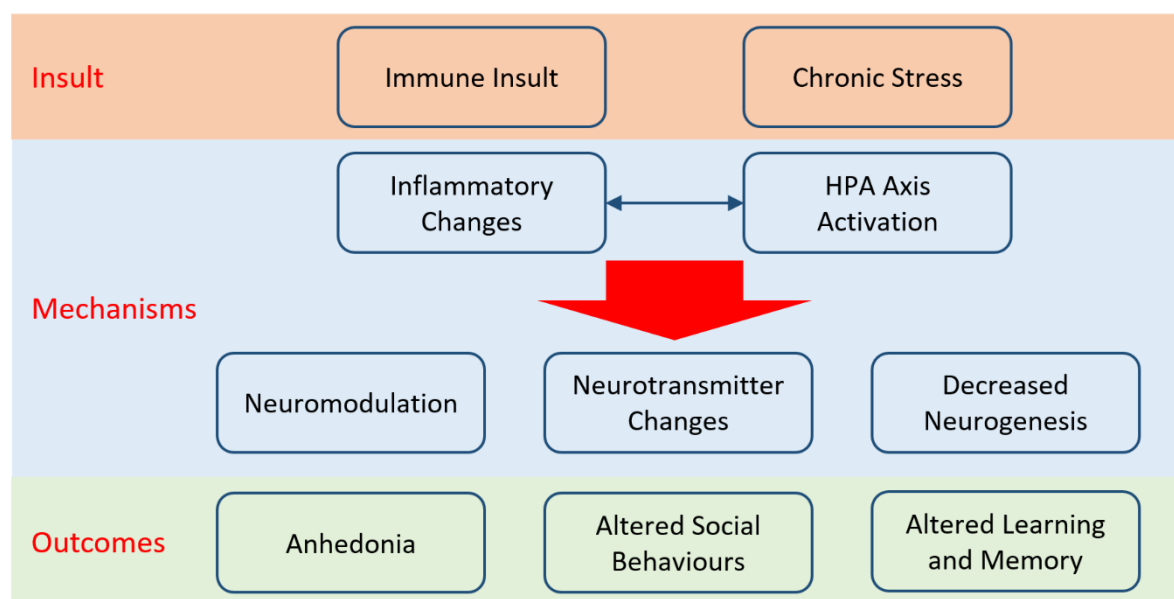


Figure 1.5: Possible routes to psychological alterations and behavioural change in the context of stress and inflammation

Immune insults or chronic stress can induce inflammatory changes and HPA axis activation within the CNS. These two systems appear to interact and there is evidence of a bidirectional relationship. Downstream of inflammation and HPA axis activation there appear to be alterations in neuromodulation, neurotransmitter levels and turnover and reductions in neurogenesis. These functional changes within the CNS have been associated with changes in behavioural phenotypes as evidenced by anhedonia, alterations in social behaviours and altered learning and memory.

It is already well established that altered HPA axis function is a prominent feature in depressive disorders, as shown by the high rate of abnormal dexamethasone suppression tests in clinical settings (296). Newer evidence is suggesting a link between pro-inflammatory cytokines and depressive disorders,

and there is considerable overlap between the symptoms of depression including anhedonia, fatigue and altered learning and memory, and sickness behaviours. Altogether this suggests that, at least within a subset of patients, depressive illness may be driven by a low level sickness behaviour due to either inflammatory illness or immune dysregulation.

1.1.17 Summary

The CNS is a complex system that appears to extensively interact with the rest of the body in states of altered immunity. While the CNS has been shown to have a modified immune function, ideas surrounding immune “privilege” are now contentious and their relation to real world physiology unclear.

Immune responses in the CNS are characterised by upregulation of a diverse range of cytokines and chemokines, particularly $IL-1\beta$ and $TNF\alpha$ and these molecular alterations are associated with reactive changes in resident cells, particularly those associated with inflammatory responses, microglia and astrocytes. Alongside resident cells, infiltrating immune cells invade the CNS, at least partly due to the upregulation of chemokines that is observed. These infiltrating immune cells are an important part of the inflammatory milieu and drive CNS inflammation while attempting to clear pathogenic insults. These immune changes appear to occur in response to both central and peripheral inflammatory stimuli, with i.p. LPS being the most commonly used model to study this peripheral-central crosstalk.

Interestingly these immune responses are also associated with altered CNS function that is collectively known as sickness behaviour. Sickness behaviour is strongly associated with pro-inflammatory cytokines, particularly $IL-1\beta$, that appear to drive the altered behavioural phenotype observed in these inflamed animals.

Despite the large body of literature and considerable work that has gone into this extensive field, the pathways through which peripheral inflammation drives central responses remain unclear, although it is likely that both humoral and neural mechanisms play a role. Research has begun to demonstrate several potential mechanisms, but to understand the whole story more work is required.

1.4 Human Depression and the Immune System

1.1.18 Overview

Depression is a significant burden on the health of society and mental illness is a major burden of disease worldwide (1). Current treatment strategies in depression focus around the monoamine hypothesis of depression, in that mood is altered due to an imbalance in neurotransmitter systems(297, 298). As such, the majority of therapeutics aim to target these systems particularly the serotonergic and noradrenergic systems. Despite being efficacious in some patient populations, up to 30% of patients will receive no benefit from these treatments (3, 299). As a result, further research has attempted to better understand the pathogenesis of depressive disorders and a number of other potential mechanisms have been identified as potential drivers of illness. These include the HPA, the immune system and hippocampal neurogenesis.

As discussed earlier, a number of strands of human research support the concept of inflammation as a potential driver of depressive disorders (13-16, 18, 21-23). While alone each of these observations is not conclusive, taken together these data provide convincing evidence for the ability of inflammation to drive alterations in mood within a human population. Research in the human population is increasingly supported by mechanistic studies in animals. As discussed earlier, inflammatory models, both peripheral and central, appear to have the ability to drive changes in CNS function that are associated with alterations in behaviour.

While cytokines, have been extensively studied in human populations, chemokines are a newer field of research in relation to psychoneuroimmunology. Chemokines are attractive research targets for a number of reasons. Firstly chemokines are thought to be key co-ordinators of the immune response particularly with regards to cellular migration. As various subsets of immune cells become increasingly implicated in depressive disorders this has some merit. Secondly, chemokines are increasingly shown to be highly pleiotropic molecules. Research has shown that they have the ability to modulate both neuronal function and neurogenesis, systems that have been implicated in depressive disorders. Thirdly, while the pro-inflammatory cytokines are potential targets

they may not be appropriate in a therapeutic environment. Antagonism of the major pro-inflammatory cytokines has profound implications for whole body inflammatory responses. In contrast, chemokines have higher levels of redundancy and promiscuity within the immune system. This is a double-edged sword, as it may make them harder to target as individual molecules but could also allow for targeting of specific chemokines that have functions within the CNS while leaving the general chemokine system intact for immune purposes.

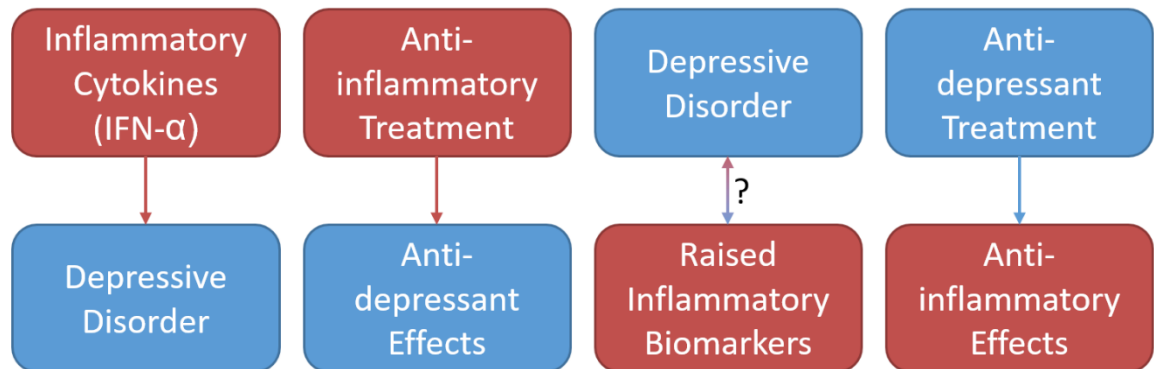


Figure 1.6: Links between depressive disorder and inflammation in human populations

Multiple associations have now been found that appear to mechanistically link inflammation and depressive disorders. Inflammatory components (red); psychiatric component (blue); Arrows (directionality); ? indicates unknown directionality. Abbreviations: IFN – Interferon.

The following sections discuss key findings from meta-analyses of human biomarker studies and other human studies of note, and then attempt to introduce and revisit some of the mechanisms through which psychological alterations may occur.

1.1.19 Human Biomarker Studies

Systematic review and meta-analysis is considered the gold-standard of evidence within clinical research. It aims to synthesise data from many different studies and to provide an estimate of the overall effect size that exists within the population. In general, systematic and structured search strategies must be used in an attempt to avoid biases in searching and then data should be extracted from all appropriate studies where possible.

During the course of the work undertaken for this thesis (2014-2017) several meta-analyses of cytokines and/or chemokines were published (15, 16, 300, 301). Earlier work had already begun to study this area (17, 302, 303) and the

newer papers build on that earlier research. The primary findings of these meta-analyses are summarised in Table 1.1.

Paper	Year	Cytokines/Chemokines Examined (N of studies)	Model
Howren et al.(302)	2009	Il-1 (N=14) Il-1ra (N=9) Il-6 (N=62)	RE; SMD
Dowlati et al.(17)	2010	IFN- γ (N=4) Il-1 β (N=9) Il-2 (N=5) Il-4 (N=5) Il-6 (N=16) Il-8/CXCL8 (N=4) Il-10 (N=6) TNF α (N=13)	RE; MD
Valkanova et al.(303)	2013	Il-6 (N=3)	ME; SMD
Haapakoski et al.(301)	2015	Il-1 β (N=14) Il-6 (N=31) TNF α (N=31)	RE; SMD
Goldsmith et al.(16)	2016	IFN- γ (N=2) Il-1 β (N=4) Il-1ra (N=2) Il-2 (N=3) Il-4 (N=2) Il-6 (N=10) Il-10 (N=4) Il-12 (N=4) sIl-2R (N=5) sIl-6R (N=3) TNF α (N=8)	FE; SMD
Eyre et al.(300)	2016	CCL2 (N=8) Il-8/CXCL8 (N=7)	RE; MD

Paper	Year	Cytokines/Chemokines Examined (N of studies)	Model
Köhler et al.(15)	2017	CCL2 (N=8) CCL3 (N=3) <i>IFN-γ</i> (N=17) IL-1B (N=22) IL-1ra (N=4) IL-2 (N=10) IL-4 (N=10) IL-5 (N=4) IL-6 (N=42) IL-8/CXCL8 (N=7) IL-10 (N=17) IL-12 (N=4) IL-13 (N=6) IL-17 (N=3) IL-18 (N=5) sIL-2R (N=10) sIL-6R (N=7) sTNFR2 (N=3) TNFα (N=42) TGFB1 (N=3)	RE; SMD

Table 1.1: Summary of findings in meta-analysis of cytokines/chemokines in human depression

Analyses in bold found the cytokines/chemokines highlighted to be significantly increased and analytes in italics were found to be significantly decreased. Abbreviations: RE – random effects; FE – fixed effects; ME – mixed effects; SMD – standardised mean difference; MD – mean difference

The findings of these meta-analyses vary but it is worth focusing on some findings of note. All of the meta-analyses examining IL-6, aside from Valkanova et al. that only included three studies, found it to be significantly positively associated with depressive disorder. For the other major pro-inflammatory cytokines discussed in this introduction, namely IL-1B and TNF α , results were more equivocal with TNF α positively associated in 3 of the 4 studies examining it. In this case the discrepant study actually included a large number of studies

suggesting that there may still be work to be done in this area to provide a more conclusive idea of the role of TNF α . Il-1 β and Il-1ra are closely related and some studies have chosen to measure Il-1ra as it can be easier to detect in the circulation. As such it is worth looking at both of these analyses in tandem. Il-1 was found to be significantly associated with depressive disorder in an early meta-analysis by Howren et al.. However, since then, no meta-analysis has found it to be significantly associated with depressive disorder. Despite this the Il-1ra receptor has consistently been found to be associated with depressive disorder, suggesting that difficulties in measuring Il-1 β may mean that it is an unsuitable biomarker for study in these generally physically healthy depressed populations.

Other cytokines of note include Il-10, Il-12 and sIl-2R all of which were found to be significantly upregulated in depressive disorder in two meta-analyses. The mechanistic role these molecules play in depressive disorder is largely unclear. Interestingly patients treated with Il-2, the ligand for sIl-2R, often experience neuropsychiatric alterations including depressed mood(304), and very high doses of Il-2 have been associated with extreme psychiatric disturbances(305). Increased Il-10 contradicts the animal literature, where Il-10^{-/-} mice were found to exhibit increased depressive behaviour that was reversible upon administration of Il-10(306). Raised Il-10 may simply be reflective of altered inflammatory status as it is usually increased in conjunction with pro-inflammatory factors due to its role in inflammatory resolution and regulation.

CCL2 one of the few chemokines examined in these meta-analyses was found to be significantly associated with depressive disorder in both the meta-analyses examining it. However, the more recent meta-analysis performed by Köhler et al. found that after removal of an outlying study this effect disappeared. In addition, there was considerable overlap between the two meta-analyses in the 8 studies examined, with 5 studies being present in both. The other chemokine CXCL8 was not found to be significantly associated in any of the three meta-analyses that included it.

This work examining biomarkers provides new insight into potential pathogenic mechanisms in depressive disorder, although the nature of these biomarker studies means they rarely provide insight into the directionality of this

relationship. It is impossible to determine in case-control studies, particularly those that are looking at single time points, whether the alteration observed is a cause or a consequence of the disease being examined. As such, work looking at alterations in immune markers following on from anti-depressant treatment, and alterations in depressive status following on from anti-inflammatory treatment, are key to providing a clearer insight into this relationship.

In their recent meta-analysis Goldsmith et al. also examined whether the biomarkers they had examined were changed following treatment. They identified Il-1 β and Il-4 as being increased following treatment, while Il-6, Il-10 and Il-12 were all decreased. This is in keeping with the data comparing acutely ill depressed patients with controls, as this demonstrates a reversal in directionality. For Il-1 β directionality is more difficult to assess as there are no significant differences between controls and depressed patients at baseline. However the increasing levels may be reflective of anti-depressant treatment. It has been shown that anti-depressants can increase Il-1 β , TNF α and Il-6 in *in vitro* studies of depressed patient's cells (307). Interestingly this same study found no effect on Il-4 production following on from whole blood stimulation with anti-depressants in contrast to the findings of Goldsmith et al. An earlier meta-analysis examining just Il-1 β , Il-6 and TNF α , found that for Il-6 there was no significant difference before, and after, treatment using a random effects model. However if a fixed effects model was used there was a small but significant decrease in the levels of Il-6(23). Interestingly they found this to be largely attributable to the effect of selective serotonin reuptake inhibitors, a specific class of anti-depressants, and the class that was examined in the *in vitro* study discussed above. In contrast, to the meta-analysis performed by Goldsmith et al., Hannestad et al. found that Il-1 β was decreased in response to anti-depressant treatment. However, in keeping with Goldsmith et al, they found no significant alterations in TNF α .

Due to the increased difficulty of assaying circulating cell populations, compared to circulating molecules, there is less research into cellular alterations in depressive illness. Despite this, links with circulating white cell populations and depressive symptoms have been identified(18-20). However, one study found that the directionality did not appear to support alterations in immune cells

driving depression but rather the other way around(19), and another study only found an association in men(18). Despite this, based on work around animal models and the limited findings available in human populations, microglia(308) and T-cells(309), both effector and regulatory, are now implicated in the immune pathogenesis of depression.

Despite being the gold standard in clinical evidence, there are large variations in how these meta-analyses were conducted, from the number of studies included to the cytokines and chemokines studied. The number of studies included will be influenced by the rigor of the search strategy employed and the stringency of inclusion and exclusion criteria. This can be particularly difficult when studying chemokines which may have upwards of five alternative names before the nomenclature was standardised. In addition, analytical techniques can increase variation. The majority of studies used standardised mean differences (SMD) to generate effect size estimates. However, both Dowlati et al. and Eyre et al. used mean difference without standardisation and that may go some way to explaining heterogeneity of results. In addition the choice of random or fixed effects models will further influence outcomes. Random effects models should be used when heterogeneity between studies is expected to be high. Random effects provide a more conservative estimate of the result, generating a larger 95% confidence interval. Finally some studies chose not to apply weighting to their studies, or applied weighting in differing ways. For example, Goldsmith et al. did not apply any weighting to their studies, while others used inverse variance, a common method for weighting studies. Inverse variance weights studies with higher variance less than those with lower variance, generally aiming to provide more weight to studies that found a more consistent effect. Inverse variance can cause issues if not using a SMD model. This is because studies that have higher assay readings, for example due to different measurement techniques, will be penalised for the greater standard deviation that generally is found with higher means, examples of this can be found in the Dowlati et al. meta-analysis(17).

In addition to meta-analytical study of human biomarkers for depressive disorder, there has been an increasing focus on genome wide association studies (GWAS) as it has become easier and more cost-effective to engage in high

throughput sequencing techniques. This has led to a number of large GWAS attempting to identify single nucleotide polymorphisms (SNPs) that are associated with depressive disorders. Disappointingly to many in the field, these GWAS have at times failed to identify significant associations with depressive illness(310). Later analysis of this “mega-analysis” did yield a significant SNP association, rs7647854, in those who had later age of onsets of depressive illness (311). Although not contained within a particular gene it is flanked by a number of genes one of which is a mitogen activated protein kinase (MAPK) gene, MAP3K13, that may play a role in NF- κ B signalling(312). A further GWAS study performed by the CONVERGE consortium in a Chinese population identified an SNP near the sirtuin 1 (SIRT1) gene that was particularly associated with a specific symptom of severe depressive illness known as melancholia(313). While not it’s only function, SIRT1 has been shown to antagonise NF- κ B activity and alter both inflammatory transcription and responsiveness(314, 315). Meta-analysis of two large multi-ethnic cohorts of GWAS, also identified a SNP in the signal transducer and activator of transcription (STAT) 1 gene as being associated with depression. This is of particular interest as STAT1 plays a role in type I and type II IFN signalling(316). A final large GWAS study, using the 23andme cohort and meta-analysis of prior GWAS, failed to replicate the findings of the CONVERGE consortium yet did identify a number of other SNPs(317) most of which were not directly associated with genes. However, they did find that many of these SNPs were either in, or near to, genes associated with brain development.

A more mechanistically-focussed study using immunoassay combined with *in vivo* imaging techniques identified a convincing link between TNF α and the serotonin transporter (5-HTT)(318). Decreased serotonin availability is a hallmark of depressive disease and the monoamine hypothesis. This can be due to reduced release or increased uptake. Krishnadas et al. studied both healthy and psoriatic patients and they found significant positive correlations between circulating TNF α and brainstem 5-HTT, suggesting that altered immunity may drive alterations in neurotransmitter states that are associated with depression. Using Beck’s depression inventory (BDI), a depression research scale, they also found a significant indirect effect of TNF on BDI, suggesting that increases in TNF α may induce depressive symptoms through effects on the 5-HTT (318).

Overall the findings presented here provide compelling evidence of an association between alterations in immunity and human depression. Although, there is variation between biomarker studies there does appear to be consistent alterations in immune status in the depressed population. GWAS studies identifying SNPs in or near to genes associated with inflammatory regulation also provide further evidence to support this, although the lack of consistency between GWAS studies does raise concerns. Despite this strong association, little work has been done to provide evidence of directionality in the human population and varying results regarding response to treatment do little to further clarify the issue. Even with more consistent results suggesting that Il-6 is raised in the depressed population, and has a tendency to be reduced following on from successful treatment of depressive disorder, it is difficult to ascertain the exact mechanism of this, particularly due to the often focused nature of biomarker studies. These alterations may be due to the fact that psychological alterations and stress can drive changes in circulating biomarkers, and that upon correction of these abnormalities immune homeostasis is restored. On the other hand, it may be that Il-6 itself drives depressive illness, and anti-depressant treatment acts to alter the regulation of this molecule in the periphery resulting in its reduction. Although this is not supported completely by the *in vitro* work, it is difficult to ascertain how drugs such as selective serotonin reuptake inhibitors that can alter the function of many different cells, will perform in more complex *in vivo* systems. Finally it is worth noting one of the main limitations of all the peripheral biomarker studies; by sampling the blood and assaying either plasma/serum you are examining a compartment that is not directly involved in the pathogenesis of psychiatric disorders. Whether plasma/serum values are an accurate marker of what is happening within the CNS remains to be ascertained, and sampling of CSF may provide a better window into the CNS.

1.1.20 Other Studies of Inflammation and Depression

To better understand the relationship between depression and inflammation, researchers have attempted to undertake more mechanistically focused studies in both human and animal populations. The challenge here is that depression is often a chronic disease that can persist for extended periods of time, whereas for practical purposes most animal models use relatively short time courses and

for ethical reasons most inflammatory human studies must be time limited and minimise risk exposure.

Depression, as an illness, cannot be modelled in an animal. It is a complex disease with multiple symptomatology that can vary from person to person. To overcome this challenge, specific aspects of depressive behaviour are often modelled or studied. These include anhedonia, altered memory and learning and social withdrawal. These behaviours demonstrate considerable overlap with sickness behaviours that have been discussed earlier. Studies will generally use one of two approaches. The first is to induce inflammation in an animal and observe downstream consequences that can be associated with depressive illness. These models have been discussed in 'the functional consequences of CNS inflammation' section, and outcomes include altered behavioural measures, changes in HPA axis function and alterations in neurogenesis. The second approach is to try to induce depressive behaviours through models of stress, a mechanism commonly implicated in human depression, and then to observe if there are changes in immune status associated with the depressive behaviours.

Animal models of stress aim to understand the outcomes of stressful stimuli on CNS function in an attempt to model depressive behaviour. While not the focus of this thesis they are worth considering when examining potential mechanisms that may drive depressive behaviours. Briefly these models use different stressors to induce a "depressive" state, these include; chronic mild stress where mice are exposed to random but mild stressors, such as isolation or altered light-dark cycles for up to 3 months, and learned helplessness where mice are exposed to unpredictable and uncontrollable stressors, such as foot shocks.

Many of the findings in these models have been highly equivocal. While some studies identify clear alterations in cytokine measures or microglial reactivity others do not find these same differences. A large review by Kubera et al. highlights this as it discusses that although alterations in $IL-1\beta$, $IL-6$ and $TNF\alpha$ have been observed in animal models of stress, other studies have failed to identify these (12). Alongside this, for papers with positive findings some papers find large differences in cytokine concentrations in specific brain regions, others

find very small but significant differences. Determining biological significance of these very small changes is difficult and further mechanistic work would be required. Despite these challenges, some studies have presented stronger evidence to suggest that inflammation is a critical part of chronic stress models. For example, the study discussed earlier by Goshen et al. strongly implicates CNS IL-1 β in the generation of depressive behaviours (295). One caveat is that they were able to mimic the effects of chronic stress through administration of corticosterone and this effect persisted in IL-1rKO mice suggesting that IL-1 β may not drive behavioural changes directly but via indirect effects on the HPA.

Other studies utilising the chronic stress model find alterations in neurogenesis, neurotransmitter systems and the HPA axis, associated with “depressive” behaviours(12, 319, 320). This aligns with findings from human depression and with data from inflammatory models studying sickness behaviours. One of the main challenges in terms of using these models for therapeutic development is that to validate a depressive behaviour many studies use reversibility upon anti-depressant treatment. In many ways, this is almost the opposite of what should be striven for. Identification of models that generate depressive-like behaviours that are not reversible upon anti-depressant treatment is key, as these may mimic those seen in treatment-resistant depression better. Currently, these models appear to be studying, and identifying, depressive behaviours that we already have efficacious therapeutics available for.

Other than animal models, human studies have also attempted to study the relationship of depression and inflammation in a more experimental manner. A common model for this is to administer endotoxin such as LPS at a low dose and then monitor changes in immune markers, mood and/or neuroimaging. Unsurprisingly administration of low doses of endotoxin induces innate immune responses in human subjects characterised by increases in IL-1 β , IL-6, TNF α and IL-10 alongside increases in cortisol (321-323). In addition to immune changes, alterations in behavioural and mood measures are observed (323-325). While these studies identify clear alterations in immune parameters and mood in response to LPS administration, identifying direct links between changes in circulating immune mediators, mood and CNS function has been more challenging. Using fMRI changes in blood oxygen level dependent signal are also

detected(324), and these have been correlated to changes in Il-6 levels. Furthermore, studies have identified correlations with Il-6 in sub-groups stratified by either sex or dosage, with females and higher dose groups showing significant correlations and male and lower dosage groups not(323, 324), suggesting either that these links may only be valid in specific circumstances or that for the weaker correlations increased sample sizes may be required.

1.1.21 Summary

The data presented above provide strong evidence for an association between inflammatory alterations and human depressive illness. While, attempts have been made to mechanistically link immune alterations this has proved challenging within human populations, and animal models have provided equivocal results, particularly for direct effects. It is likely that inflammatory changes can induce HPA alterations and possibly reductions in neurogenesis. The Goshen et al. study suggests that Il-1 β mediates its effect through the HPA.

The field as a whole faces major challenges, these include the need to ensure that all studies follow rigorous methodology during both study design and statistical analysis. In addition synthesis of a complex, and often conflicting, literature is challenging. While many animal models strongly implicate Il-1 β and TNF α in the generation of sickness or depressive behaviours, the human literature identifies Il-6 as the key biomarker. These disparate findings can be reconciled to some extent through the finding in some studies of links between TNF α and depressive disorders, or functional alterations associated with depression. In addition, the finding that Il-1ra is raised, may reflect the fact that although there are alterations in the Il-1 system, difficulties surrounding detection of Il-1 β in the circulation have hindered research into associations. Finally it is worth noting that a major challenge for the whole field of biomarkers in psychiatric disease is the relevance of the peripheral circulating compartment to what is going on in the CNS.

Aside from these challenges, there is increasing evidence of a role for chemokines in both human depressive disease and sickness behaviours. While this link will require further investigation to clarify it is an attractive area for research. This is due to the fact that modulation of major pro-inflammatory

cytokines is frequently associated with significant side effects, particularly an increased risks of infection that may make cytokine modulation unsuitable in a clinical setting. Chemokines, while important in co-ordinating immunity show high levels of redundancy and promiscuity within the immune system and therefore may be attractive targets if they have more specific roles within the CNS as Blank et al. suggest in their recent paper.

There is a clear need for further work to try to establish the role of chemokines in human depression and to identify if changes are robust across multiple studies. This work has bidirectional implications, identification of molecules that are altered in human disease become attractive candidates for study in animal models. Alongside this, if animal models of stress or sickness behaviour have identified candidate molecules and meta-analytical techniques can associate these with human depressive illness, there is a strong case for further investigation.

1.5 Justification and Thesis Aims

Overall it appears that innate immune pathways drive a variety of downstream changes that can, at least, be associated with alterations in mood and behaviour and potentially mechanistically linked. Activation of PRRs, and particularly TLRs, is associated with IFN and/or NF- κ B responses. These responses cause upregulation of a variety of molecules including, but not limited to, pro- and anti-inflammatory cytokines, such as IL-1 β , IL-6, TNF α and IL-10, and chemokines, such as CCL2 and CXCL10. In the case of both peripheral and central immune challenges with TLR agonists, cellular changes in the CNS are observed alongside molecular alterations. Resident glial cells of the CNS, particularly microglia and astrocytes, become reactive and produce inflammatory mediators of their own, and alongside resident cell activation circulating immune cells are recruited from the circulation and enter into the CNS parenchyma where they can sustain and effect inflammatory responses.

Immune responses of the CNS are increasingly associated with changes in CNS function. Alterations in neurotransmitter function, decreases in neurogenesis and HPA activation have all been identified within inflammatory models. These functional changes are linked with phenotypic changes characterised by mood

changes identified through behavioural studies. Mood changes include increases in anhedonia, decreases in social exploration and overall wellbeing, and altered memory and learning.

These functional and phenotypic changes share many characteristics with depressive symptomatology and pathology that has been observed in human populations. This has led to a variety of hypotheses surrounding the pathogenesis of depressive behaviour. One of these, the sickness behaviour hypothesis of depression, supposes that immune alteration in the human population drives a sickness behaviour phenotype driven by the pro-inflammatory cytokines $IL-1\beta$ and $TNF\alpha$, alongside potentially unidentified mediators. This sickness behaviour phenotype predisposes people to depressive illness and it is thought that restoring normal immune homeostasis within the CNS may help to alleviate depressive symptomatology.

Despite identification of these initial associations and the myriad of hypotheses arising from them, identifying and providing strong evidence for mechanistic links has been challenging. Well-designed multi-modal studies such as the study by Blank et al. that use more specialized techniques and specifically engineered mice that lack receptors only on cells of interest have begun to provide stronger mechanistic links between immune molecules and behavioural alteration. Finding animal models that mimic human biology and pathology as closely as possible is always a challenge, and use of a variety of methodologies and models is required for findings to be generalizable. As such identification, characterisation and validation of animal models that may be suitable for this purpose is a critical requirement in a field that has typically used the LPS endotoxin model of septicaemia as a 'work horse'. Work in our laboratory has identified the Aldara model of peripheral inflammation as a potentially advantageous model for the study of these innate immune phenomena.

Alongside animal work, human studies have begun to identify not only the major pro-inflammatory cytokines but also other immune molecules as being associated with depressive disorders. One class of molecules that is receiving increased attention, due to their pleiotropic functions that include cellular recruitment and possibly neuromodulation, are the chemotactic cytokines, or chemokines. Two recent meta-analyses have identified potential associations between CCL2

and depressive disease, however the role of other chemokines, such as CXCL10, remains unclear. Further work should aim to establish if this link exists for the other chemokines and to replicate evidence of pre-existing associations.

Based on the existing information presented above, the work in this thesis aimed to test three major hypotheses at the outset. The first hypothesis was:

“There is a significant association between circulating chemokine biomarkers, beyond CCL2, and human depression.”

To this end a systematic review and meta-analysis of the role of chemokines in human depressive disorder, examining and synthesising the evidence presented in human biomarker studies to date was undertaken.

The second hypothesis was:

“TLR7 driven changes in ISG expression in the Aldara model of peripheral inflammation are accompanied by changes in cytokine and chemokine expression and cellular alterations”

To test this the immune responses within the Aldara model of peripheral inflammation were further characterised, utilising a combination of gene and protein expression analysis and immunohistochemistry (IHC). It is acknowledged that this is a broad hypothesis and that much of the work done in this area was exploratory with the aim of characterising the Aldara model more completely.

The third and final hypothesis was:

“The Aldara model of peripheral inflammation is an appropriate tool for the study of peripheral-central inflammation”

To investigate whether this was true peripheral responses were examined alongside the central responses, and this work attempted to ascertain mechanisms through which Aldara may be inducing a response within the CNS.

Chapter 2

Materials and Methods

Chapter 2 Materials and Methods

2.1 Companies

Full contact details of all companies listed within this Thesis are available in Appendix 1.

2.2 Systematic Review and Meta-Analysis

This study was performed by Dr. Sam Leighton (SL) and Louis Nerurkar (LN) in collaboration. All work for data collection and analysis was contributed to equally by both individuals. Any work presented in this Thesis was written by LN alone.

2.2.1 Search Strategy

Searches were performed within the EMBASE, PsycINFO and Medline databases up to March 5th 2016. To improve the scope of the review non-english language papers and conference abstracts were included, alongside full journal articles. The search strategy was based on the PICO framework:

- Population - Humans
- Intervention/Exposure - Depression
- Comparison - No Depression
- Outcome - Blood or CSF Chemokines

Full details of final search strategies can be found in Appendix 2

2.2.2 Study Selection

Studies were selected for inclusion in the review based on the following criteria:

- Original research study measuring blood or CSF chemokine concentration in depressed and non-depressed subjects

- Subjects had a formal diagnosis of depression or a validated depressive scale was used
- Control subjects had sufficient information to allow for exclusion of depression

Studies were excluded based on the following characteristics:

- Subjects had comorbid or higher order psychiatric disorders (e.g. Bipolar disorder, schizophrenia)
- *In-vitro* studies
- Non-human studies
- Studies looking at stimulated responses (e.g. following *in vivo* or *ex vivo* LPS stimulation)
- Studies including pre-pubescent participants

Note that studies including participants with a physical comorbidity were not excluded, if control subjects had comparable comorbidity (e.g. Heart disease (+) depression (-) vs Heart disease (+) depression (+)). Using subgroup analysis, differences between studies with healthy or physically comorbid patients were still examinable.

Duplicate papers were excluded initially and titles were examined to exclude papers clearly not relevant to the current review. Subsequently, abstracts of all remaining studies were read. Those found to still meet inclusion criteria at this point were included for full text review and data extraction. If there were any ambiguities over inclusion or exclusion of a study, both reviewers discussed the study until a consensus was reached.

2.2.3 Data Extraction

Both reviewers (SL and LN) used a custom data extraction template (Available in Appendix 3) modified from the Cochrane Review criteria to extract relevant data

from studies. Where possible non-English studies were translated or data were extracted from English abstracts. For meta-analysis mean \pm standard deviation (SD) and N numbers were extracted from comparison groups. If the mean \pm SD, or raw data, were not available in the paper or supplemental materials, corresponding authors were contacted directly and allowed at least 28 days for a reply. If correspondence failed data were extracted from figures using Engauge data extraction software(326). Where only median \pm interquartile range was available data were converted using a previously published approximation method(327) to approximate mean \pm SD. If only raw data were available patients were dichotomised based on established cut-offs for depressive scales and calculated the mean \pm SD for the two groups. Finally for studies where SD was not available SD was inferred by using the pooled SD of all other studies for that chemokine.

2.2.4 Quality Assessment

To assess the quality of papers a combined approach was used to allow for the case-control nature of the studies assessed. To assess potential bias, the Cochrane collaboration guidelines(328) alongside modified Newcastle-Ottawa criteria(329) for observational studies were used. A selection of confounders previously shown to influence immune markers were also included. Finally two additional points were added to account for the need to extract data and whether the study was an abstract or complete article. This system generated a maximum possible score of 17 as below:

- Newcastle-Ottawa Criteria (1 if present or 0 if absent, total 3 points)
 - Representative controls
 - Clearly state diagnostic criteria
 - Tissue sampled, measurement technique used and units stated
- Cochrane (2 if low risk of bias, on1 if unclear, 0 if high risk, total 6 points)
 - Blinding of outcome assessment

- Incomplete outcome data
- Selective reporting of outcome data
- Confounders (1 if matched/adjusted, 0 if not mentioned or not matched/adjusted, total 6 points)
 - Body mass index (BMI)
 - Age
 - Sex
 - Smoking
 - Circadian [Time of blood draw]
 - Medications
- Other (total 2 points)
 - Article (1 point)/Abstract (0 points)
 - No data extraction required (1 point)/Data extraction or inference required (0 points)

All studies were included in the meta-analysis regardless of quality score however subgroup analysis was undertaken to assess only high quality studies $\geq 12/17$ where possible.

2.2.5 Statistical Analysis

All meta-analysis was performed in RevMan 5.3 Software(330) and effect sizes were replicated using R(331) with the metafor package(332). SMD was used rather than mean difference as the absolute values of results varied between different studies making direct comparison of mean differences inappropriate. An inverse variance random effects model was used to provide final estimates of

effect size and 95% confidence interval (CI). Inverse variance weights studies based on the variance observed, lower variance within a study results in greater weight for the study in the final model. Random effects should be utilised wherever heterogeneity may be high and it provides a more conservative estimate of effect size when compared to fixed effects models.

Additional statistics were generated to allow for assessment of statistical robustness and meta-analytic characteristics. I^2 values were calculated to provide an estimate of how much of the variance observed may be attributable to heterogeneity between studies, rather than sampling error. Publication bias was assessed using a combined approach of generating funnel plots and Egger's regression test in the metafor package. Egger's test provides a formal method for assessing funnel plot asymmetry. It is important to note that publication bias should not be considered absent if Egger's test is non-significant while there is strong evidence of asymmetry from the funnel plot. Finally if significant publication bias was suspected or detected using Egger's test, the trim and fill method of adjustment for publication bias was attempted in the R package.

2.3 General Materials

2.3.1 Plastics

Unless stated otherwise all sterile filter tips, 0.2ml polymerase chain reaction (PCR) tubes and 2ml tubes were purchased from Starlab. 1.5ml, 15ml and 50ml tubes were purchased from Greiner. Cryovials were purchased from Alphas laboratories.

2.3.2 Buffers and solutions

Ethylenediaminetetraacetic acid (EDTA) (0.5M) (100ml)

- 18.61g EDTA
- 80ml double distilled (dd) H₂O
- Add NaOH until fully dissolved

- pH to 8.0
- ddH₂O to 100ml

Li-Hep Phosphate buffered saline (PBS) (500ml)

- 500ml PBS
- 100KU Heparin-lithium salt from porcine intestinal mucosa (Sigma-Aldrich)

10x Tris-buffered saline (TBS) (1L)

- 78.8g Tris-HCl or 60.6g Tris-Base (0.5M)
- 87.6g NaCl (1.5M)
- 800ml ddH₂O
- ≈30ml HCl 37%
- pH to 7.5
- ddH₂O to 1L

1x TBS (1L)

- 100ml 10x TBS
- 900ml ddH₂O

1x TBX (1L)

- 100ml 10x TBS
- 900ml ddH₂O
- 250ul Triton-X 100

10x Sodium Citrate Buffer

- 29.4g Sodium Citrate Trihydrate (0.1M)
- ddH₂O to 800ml
- pH to 6.0
- ddH₂O to 1L

1x Sodium Citrate Antigen Retrieval Solution

- 100ml 10x Sodium Citrate Buffer
- 900ml ddH₂O
- pH to 6.0

Scott's Tap Water (STW)

- 3.5g Sodium Bicarbonate
- 20g Magnesium Sulphate Heptahydrate
- 1L Tap water

Eosin Stain

- 500ml Putt's Eosin Stain (CellPath)
- 500ml Tap Water

1% Acid Alcohol

- 990ml 70% Ethanol (EtOH)
- 10ml Concentrated HCl

50x TAE Buffer

- 252g Tris-Base (2M)
- 650ml ddH₂O
- Dissolve Tris-Base completely
- 57.1ml Acetic Acid (Slowly add down side of bottle)
- 100ml 0.5M EDTA pH8.0 (50mM)
- ddH₂O to 1L

1x TAE Buffer

- 100ml 50x TAE Buffer
- 4900ml ddH₂O

2% Agarose Gel

- 50ml TAE Buffer
- 1g Agarose
- Heated in microwave until fully dissolved
- 2.5ul Ethidium Bromide

2.4 Animals

C57BL/6 mice were obtained from Harlan Laboratories/Envigo. CCR1/2/3/5KO also known as inflammatory chemokine receptor KO (iCCRKO) and IFNARKO mice were maintained at the Beatson Laboratories University of Glasgow and transferred to the Central Research Facility prior to experimental protocols. Mice were kept for a minimum of a week within the Central Research Facility to

allow for acclimatisation prior to commencement of procedures. Mice were maintained in specific pathogen free conditions. Mice were treated between at the age of 8-9 weeks and were all female unless otherwise stated. All experiments received local ethical approval and were performed under the authority of UK Home Office Licence 70/8377.

2.5 Aldara Model of Inflammation

2.5.1 Aldara Model of Psoriasiform Inflammation Overview

Mice were treated with a quarter sachet (≈ 62.5 mg) of Aldara™ (Meda AB) cream containing 5% IMQ or an equivalent volume of control cream (Boots Aqueous Cream/10% Vaseline Lanette Cream) at each treatment point. Cream was applied to shaved dorsal skin near the base of the tail (Figure 2.1). For experiments longer than 24 hours in length mice were weighed daily to ensure that there was no more than 20% body weight loss as per Home Office licence conditions. Mice were euthanised with an increasing concentration of CO₂ after the completion of the experimental protocol.

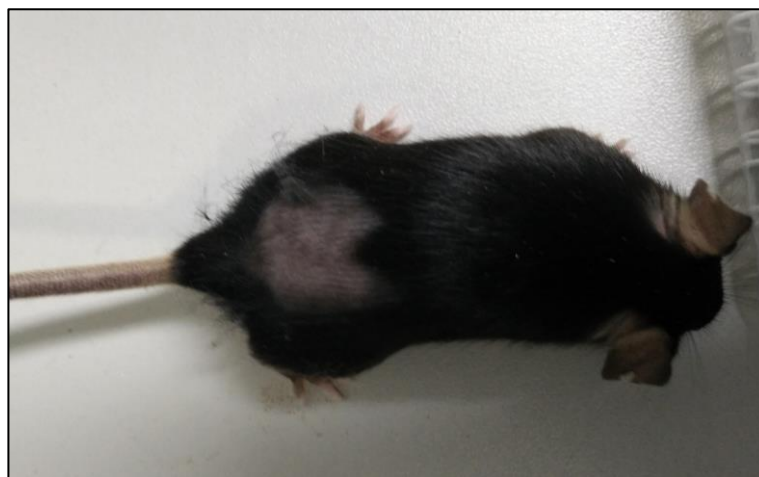


Figure 2.1 Image demonstrating treatment area on dorsal skin of mouse

2.5.2 Three Day Aldara Model

8.5 week old C57BL/6 female mice were treated daily with $\frac{1}{4}$ sachet Aldara (≈ 62.5 mg) or an equivalent volume of control cream as described. Mice were euthanised 24 hours after the third application of cream.

2.5.3 Time-course Aldara Models of Inflammation

8.5 week old C57BL/6J female mice were treated daily with ¼ sachet Aldara (≈62.5mg) or an equivalent volume of control cream as described. Mice were euthanised at 4 hours, 12 hours and 24 hours after the first treatment, or 24 hours after the 3rd and 5th treatment (4h, 12h, 24h/1d, 3d, 5d groups respectively)

2.5.4 Single Treatment Time-course Model of Inflammation

8.5 week old C57BL/6J female mice were treated once with ¼ sachet Aldara (≈62.5mg) or an equivalent volume of control cream as described. Mice were euthanised 24 hours, 72 hours and 120 hours after the first treatment. (1d, 3d, 5d groups respectively).

2.5.5 Knockout Models of Inflammation

IFNARKO (A129) or iCCRKO (C57BL/6N) mice were treated daily with ¼ sachet Aldara (≈62.5mg) or an equivalent volume of control cream as described. Mice were euthanised 24 hours after the 3rd treatment for IFNARKO or 4th treatment for iCCRKO mice. Details of these experiments are given in Table 2.1:

Experiment	Timepoint	Mice	Groups (total N)
iCCRKO 1 (Figure 5.2, Figure 5.3)	4d	8 wk C57BL/6N Female	N=4-6 (16) [WT, HET, KO]
iCCRKO 2 (Figure 5.4, Figure 5.5)	4d	10 wk C57BL/6N Female	N=5 or 6 (21) [Treated, Control] WT and KO
IFNARKO1 (Figure 5.9, Figure 5.12, Figure 5.13)	3d	8.5 wk A129 Female	N=4 (8) [Treated, Control]
IFNARKO2 (Figure 5.10, Figure 5.11)	3d	10 wk, 11.5 wk [Treated, Control] A129 Female	N=4 (16) [Treated, Control] WT and KO

Table 2.1: Details of animals used in KO experiments

Figures listed under each experiments title are to direct reader to the corresponding gene expression data

2.6 Tissue Collection following Animal Models

2.6.1 Peripheral blood leukocytes (PBL) collection for RNA

Blood was collected from mice immediately after euthanasia using a syringe flushed with 0.5M EDTA. The pleural cavity was opened, the right atrium was cut and blood collected. PBL were obtained from blood by separating the plasma and cellular compartments of the blood initially using centrifugation at 300g for 10 minutes. Plasma was removed from the top layer. PBL were obtained following red cell lysis treatment for 10 minutes with ammonium chloride (STEMCELL Technologies), and a series of washes in PBS. PBL were then re-suspended in buffer RLT (Qiagen) prior to storage. Both PBL and Plasma were stored at -80°C.

2.6.2 Tissue collection for RNA

After opening of the right atrium, mice were perfused with 20ml PBS through the left ventricle to clear tissues of remaining blood. Following perfusion tissues (skin, lungs, liver, spleen, colon, right hemisphere of brain) were collected, placed in cryovials (AlphaLaboratories) and 'snap frozen' in liquid nitrogen (3 day experiments and repeated treatment time-course experiment) or submerged in RNAlater (Thermo Fisher Scientific) at 4°C for 24-48 hours (all subsequent experiments). Tissues were then stored at -80°C until RNA extraction was performed.

2.6.3 Tissue collection for Protein Analysis

After opening of the right atrium, mice were perfused with 20ml PBS through the left ventricle to clear tissues of remaining blood. Following perfusion the left hemisphere of the brain was collected, placed in a cryovial and 'snap frozen' in liquid nitrogen. Tissue was stored at -80°C until protein extraction was performed.

2.6.4 Tissue collection for formalin-fixed paraffin embedded (FFPE) sections

Brain (left hemisphere/whole brain) was collected from mice after euthanasia, with or without perfusion and placed into 10% neutral buffered formalin for 24-48 hours before being transferred to 70% EtOH prior to tissue processing.

2.6.5 Tissue collection for Mass Spectrometry

After opening the right atrium whole blood was collected in syringes flushed with lithium-heparin PBS before being placed into a 1.5ml Eppendorf containing 40ul lithium-heparin PBS (8U lithium-heparin). Following blood collection mice were perfused with 20ml lithium-heparin PBS and brains were collected, placed in cryovials and 'snap frozen' in liquid nitrogen. Plasma was immediately collected from whole blood by centrifugation at 10,000g for 5 minutes. Supernatant was then spun again at 10,000g for 5 minutes and plasma collected. Both plasma and brains were stored at -80°C until shipping on dry ice.

2.7 Tissue Processing

2.7.1 RNA Extraction

Under RNase-free conditions, tissues were homogenized using the TissueLyser LT (Qiagen) in 1ml of Qiazol® (Qiagen). Following homogenisation, tissues were allowed to stand at room temperature (RT) for 5 minutes before 200ul of chloroform was added. Samples were then mixed and allowed to stand for a further 2 minutes. Qiazol/Chloroform homogenate was then spun at 12,000g for 15 minutes at 4°C and supernatant drawn off. Supernatant was further purified and genomic deoxyribonucleic acid (DNA) removed using an RNeasy Mini Kit (Qiagen) with optional DNase I (Qiagen) on-column treatment as per manufacturer's instructions. In brief, RNA was bound to silica membrane within RNeasy column and washed once with RW1 buffer. On-column DNase treatment was performed for 15 minutes, after which a series of washes were performed and the column dried. Once dried 50ul of RNase free water was added to the column and RNA was eluted. RNA quality for all time-course and knockout experiments was assessed using Agilent Bioanalyzer (Agilent Technologies), to

generate an RNA integrity number (RIN), at Glasgow Polyomics and details of this can be found in Appendix 4.

2.7.2 RNA to complementary DNA (cDNA) conversion

RNA was converted to cDNA using AffinityScript Multi-Temperature cDNA Synthesis Kit (Agilent) or High-Capacity RNA-to-cDNA Kit (Thermo Fisher Scientific) as per manufacturer's instructions. RNA quantity was measured using Nanodrop 1000 (Thermo Fisher Scientific). An equal quantity of RNA (maximum amount recommended by kit or maximum amount possible from lowest concentration sample) was used to generate cDNA as per manufacturer's instructions. For each batch of cDNA, a "-RT" control was generated where the reverse transcriptase was omitted from the PCR reaction to allow for assessment of genomic DNA contamination.

2.7.3 Protein Extraction

Protein was extracted using neuronal protein extraction reagent (N-PER) (Thermo Fisher Scientific) as per manufacturer's instructions. In brief, Pierce mini protease tablets (Thermo Fisher Scientific) were added to N-PER reagent, homogenisation tubes were placed on dry ice and tissue was added. Tubes were transferred to wet ice to prevent lysis buffer freezing. Lysis buffer was added and tissue was homogenised using Tissue Lyser LT (Qiagen). Homogenate was then centrifuged at 10,000g for 10 minutes at 4°C and supernatant was collected, 'snap frozen' on dry ice and stored at -80°C prior to use. Protein concentration was determined using Pierce BCA Protein Assay Kit (ThermoFisher Scientific) as per manufacturer's instructions. In brief, sample was added to a 96 well plate with a set of bovine serum albumin standards, BCA reagent was added prior to incubation at 37°C for 30 minutes, the plate was then placed in the fridge for 2 minutes to stop the reaction. Optical density was then measured using a Sunrise plate reader (Tecan) and protein quantity was determined from the standard curve.

2.7.4 Tissue processing and paraffin embedding for FFPE sections

After formalin fixation and storage in 70% EtOH, tissues were processed using KOS microwave HistoSTATION (Milestone SRL) using a 4mm tissue processing cycle and proprietary reagents. This system is Xylene free to help avoid excessive drying of tissues. For IFNARKO 2 (Figure 5.14, Figure 5.15, Figure 5.16) brains were processed using a Thermo Shandon Excelsior (Thermo Fisher Scientific) on an overnight processing cycle, this system was not Xylene-free. Tissues were then embedded in paraffin prior to storage at RT.

2.7.5 FFPE sectioning

FFPE Tissue were sectioned on a Shandon Finesse 325 Microtome (Thermo Fisher Scientific) at 5 μ m. Ribboned sections were floated on a water bath at \approx 40°C and then collected onto SuperfrostPlus Slides (VWR). Slides were then placed onto a heated slide drier for >1 hour prior to storage at RT.

2.8 Gene Expression Analysis

2.8.1 Primer Design

Primers were designed using primer3 software(333, 334) using the following conditions:

- Between 18 and 23 base-pair (bp) length (20bp optimal)
- Between 40 and 65% GC content (50% optimal)
- Annealing temperature (T_m) of primers between 59.5C and 61C (60C optimal)
- Max self-complementarity: 2
- Max 3' self-complementarity: 1
- Amplicon size 50-150bp

- No more than two G or C bases in last 5 at 3' end
- No stretches of G or C >4
- Use of rodent mispriming library

In addition, where possible, primers were designed to be exon-spanning using information available from NCBI RefSeq Sequences to help avoid amplification of genomic DNA.

Primers were checked for specificity using NCBI Primer Blast(335) for species *Mus Musculus* (taxid: 10090). Standard primers were designed using primer3 software as per the above specification with the following modifications:

- Included region was defined as the quantitative real time PCR (qRT-PCR) amplicon region +20bp at both the 3' and 5' end
- Amplicon size was extended to be 100-500bp

If no standard primers could be designed using the above specifications the Tm range was widened to allow for greater flexibility in primer design. Once primers were designed they were ordered from Integrated DNA Technologies.

Details of all designed primers can be seen in Table 2.2 and Table 2.3 for qRT-PCR and standard primers respectively.

Target	qRT-PCR Primer 1	qRT-PCR Primer 2
<i>Ccl2</i>	CTC ACC TGC TGC TAC TCA TTC A	CCA TTC CTT CTT GGG GTC A
<i>Ccl3</i>	CAG CCA GGT GTC ATT TTC CT	CAG GCA TTC AGT TCC AGG TC
<i>Ccl4</i>	TGA CCA AAA GAG GCA GAC AGA T	GCT GTG CCA CAT CTC TTG GT
<i>Ccl5</i>	CTG CTG CTT TGC CTA CCT CT	ACA CAC TTG GCG GTT CCT T
<i>Ccl9</i>	CTC ACA ACC ACG GAC CTA CA	CAC TGG GGA AGA CCA AAG AA
<i>Ccl11</i>	GCA CCC TGA AAG CCA TAG TCT	TGG GGT CAG CAC AGA TCT CT
<i>Ccl19</i>	GTG CCT GCT GTT GTG TTC AC	CAA GAC ACA GGG CTC CTT CTG
<i>Cxcl1</i>	CCG AAG TCA TAG CCA CAC TCA	AGG TGC CAT CAG AGC AGT CT
<i>Cxcl10</i>	GCT CAA GTG GCT GGG ATG	GAG GAC AAG GAG GGT GTG G

Target	qRT-PCR Primer 1	qRT-PCR Primer 2
<i>Cxcl13</i>	CAT ACC CAA CCC ACA TCC TT	GCC TGT TCT CAA ATA GCC TTT C
<i>Cxcl16</i>	TGC TGA CCC TTT GCC TCT AC	GGC TGG CTT GGA CTA AAT AAC A
<i>Cx3cl1</i>	CAA CTT CCG AGG CAC AGG AT	AGA TGT CAG CCG CCT CAA AA
<i>Ccr5</i>	TTT GTT CCT GCC TTC AGA CC	TTG GTG CTC TTT CCT CAT CTC
<i>Il-1B</i>	CGC TCA GGG TCA CAA GAA AC	GAG GCA AGG AGG AAA ACA CA
<i>TNFa</i>	CAC CAC CAT CAA GGA CTC AA	GAG GCA ACC TGA CCA CTC TC
<i>Il-6</i>	TTC CAT CCA GTT GCC TTC TT	ATT TCC ACG ATT TCC CAG AG
<i>Il-10</i>	CAG AGA AGC ATG GCC CAG AA	GCT CCA CTG CCT TGC TCT TA
<i>Tbp</i>	TGC TGT TGG TGA TTG TTG GT	AAC TGG CTT GTG TGG GAA AG

Table 2.2: Primers for qRT-PCR

Target	Standard Primer 1	Standard Primer 2
<i>Ccl2</i>	CAC CAG CAC CAG CCA ACT	GCA TCA CAG TCC GAG TCA CA
<i>Ccl3</i>	CCA CGC CAA TTC ATC GTT	TAT GCA GGT GGC AGG AAT GT
<i>Ccl4</i>	CTA ACC CCG AGC AAC ACC AT	CTG AAC GTG AGG AGC AAG GA
<i>Ccl5</i>	CCC TCA CCA TCA TCC TCA CT	TCA GAA TCA AGA GGC CCT CTA TCC
<i>Ccl9</i>	GCC CTC TCC TTC CTC ATT CT	CTT CAG ACC TTC CAG GCA TC
<i>Ccl11</i>	TGC TGC TCA CGG TCA CTT C	CTT AGG CTC TGG GTT AGT GTC AA
<i>Ccl19</i>	GCC TTC CGC TAC CTT CTT AAT GA	GCA CAG ACT TGG CTG GGT TA
<i>Cxcl1</i>	ACA CTC CAA CAC AGC ACC AT	AGC AGA ACT GAA CTA CCA TCG A
<i>Cxcl10</i>	CGA TGG ATG GAC AGC AGA GAG CCT	GAC AAG GAG GGT GTG GGG AGC A
<i>Cxcl13</i>	AAC GCT GCT TCT CCT CCT G	CCA TCT CGC AAA CCT CTT GT
<i>Cxcl16</i>	CGC CTA CAG CAA GAG TGG A	AAG AGT GTT CCC CAA GAG CA
<i>Cx3cl1</i>	GCC TGA ATC CGC CAC ATT G	CCT GAG GAG ATG GGG CTG TA
<i>Ccr5</i>	ACC CAT TGA GGA AAC AGC AA	CCT CTG AGG GGC ACA ACA AC
<i>Il-1B</i>	TGG GCT GGA CTG TTT CTA ATG C	CCA CAC GTT GAC AGC TAG GT
<i>TNFa</i>	TCT GTG AAG GGA ATG GGT GT	GGC TGG CTC TGT GAG GAA
<i>Il-6</i>	TCC AGA AAC CGC TAT GAA GT	CTC CAG AAG ACC AGA GGA AA
<i>Il-10</i>	TGC TAA CCG ACT CCT TAA TGC A	GGC CTT GTA GAC ACC TTG GT
<i>Tbp</i>	GAG TTG CTT GCT CTG TGC TG	ATA CTG GGA AGG CGG AAT GT

Table 2.3: Primers for generation of standard curves

2.8.2 Standard Curve Generation

Standard curves were generated using Expand Hi Fi master mix (Roche) or Phusion master mix (Thermo Fisher Scientific) as per manufacturer's instructions using a positive sample of cDNA. Optimal Tms were calculated using New England Biolabs (NEB) Tm Calculator (Available at: tmcalculator.neb.com). A small aliquot was analysed by gel electrophoresis. If amplification was non-specific the total PCR product was separated by gel electrophoresis and the specific band extracted using PureLink Gel Extraction Kit (Thermo Fisher Scientific), as per manufacturer's instructions.

The standard aliquot concentration was then quantified using triplicate nanodrop readings. To obtain an estimate of the number of DNA molecules present, molecular weight of the standard sequence was estimated using OligoCalc: Oligonucleotide Properties Calculator(336). The following formula was then used to obtain an estimate of the number of molecules present in the raw standard per μl :

$$\frac{\text{concentration (g/\mu l)}}{\text{molecular weight (g)}} \times 6.23 \times 10^{23} \text{ OR } \text{mol/\mu l} \times \text{avogadro's constant}$$

This was multiplied by 10^{-4} for input into the machine (first point on the standard curve)

The raw standard was diluted 100 fold to generate a 10^{-2} stock prior to storage at -20°C .

2.8.3 Primer Validation PCR

Primers for qRT-PCR were validated using SYBR Green PerfeCTa master mix, along with a positive sample:

- 5ul PerfeCTa 2x master mix
- 3.85ul RNase-free H₂O
- 0.15ul primer pair
- 1ul cDNA sample

PCR was performed for 40 cycles in a Veriti 96 well thermal cycler (Thermo Fisher Scientific) under the following conditions:

- 95°C - 3'
- 95°C - 3"  x 40
- 60°C - 30"

The PCR product was analysed by gel electrophoresis with a 100bp ladder to confirm that there was only one specific product of the expected amplicon size.

2.8.4 Gel Electrophoresis

Gel electrophoresis of PCR product was performed using 2% agarose gel with a 100bp ladder (New England Biolabs). Sample and ladder were loaded with BlueJuice Gel Loading Buffer (10x) (Thermo Fisher Scientific) and run at 80-100V until clear individual bands were visible.

2.8.5 Quantitative Real-time Polymerase Chain Reaction qRT-PCR

qRT-PCR was performed using 7900HT and QuantStudio7 (ThermoFisher Scientific), qRT-PCR machines. PerfeCTa SYBR Green FastMix with ROX reference dye (QuantaBio) was used:

- 5ul PerfeCTa 2x master mix
- 3.85ul RNase-free H₂O
- 0.15ul primer pair
- 1ul cDNA sample

Samples were run in triplicate on 384 Well PCR Plates (Starlab) and calibrated using a standard curve for either relative or absolute quantification. 6 point standard curves started at 10⁻⁴ dilution with a final point of 10⁻⁹. In the case of relative quantification, all standard curves were set at a range of 1,000,000 to 10. A dissociation step was included at the end of thermal cycling to generate a melt curve so that product specificity could be assessed. Thermal cycles for the machines are shown in Table 2.4

	7900HT	QuantStudio7
Amplification	95°C - 3'	95°C - 20"
	95°C - 3" 60°C - 30" } x 40	95°C - 1" 60°C - 20" } x 40
Dissociation	95°C - 15" 60°C - 15" 95°C - 15"	95°C - 15" 60°C - 1' 95°C - 15"

Table 2.4: Thermal cycles of qRT-PCR machines

2.8.6 Analysis

Raw cycle threshold (Ct) values and quantities were exported from the qRT-PCR software after checking that amplification had occurred and that standard curves, melt curves and negative controls were of sufficient quality. All subsequent analysis was performed in Excel 2013 (Microsoft) and statistical analysis was performed using GraphPad7 software (GraphPad Software). The analysis workflow was as follows:

- 1) Assess coefficient of variation of Ct triplicates
 - a) Any triplicates with a coefficient of variation >2.5% (SD = 0.5, @ Ct = 20) had an outlier excluded if it was >1.5 from median values
- 2) Generate means of quantities calculated from standard curve
- 3) If required subtract background levels from no template or no reverse transcriptase controls (whichever was highest)
- 4) Calculate gene expression value relative to TATA-binding protein (*Tbp*)
 - a) For absolute quantification this was the final value for gene expression presented as copies/ 10^3 *Tbp*
 - b) For relative quantification, arbitrary value relative to *Tbp* was compared to the average of all control arbitrary values to generate a fold change compared to the control sample

NB: For the first 3 day single time-point experiments in Chapter 2 (Figure 4.2, Figure 4.3, Figure 4.4) background subtraction was not performed.

2.9 LegendPlex Protein Assay

2.9.1 LegendPlex Protein Assay

Protein expression was measured using the Legendplex assay (BioLegend) as per the manufacturer's instructions. In brief, beads were incubated with protein

extract for 2 hours at 600rpm on a plate shaker. Beads were then conjugated with streptavidin-phycoerythrin (SA-PE) for 30 minutes and two washes were performed prior to sample reading using a BD LSR-II flow cytometer (BD Biosciences). Samples were differentiated on the basis of bead size and allophycocyanin fluorescence, while protein quantity was determined using SA-PE fluorescence calibrated to a standard curve.

2.10 Immunohistochemistry

2.10.1 Haematoxylin and eosin staining

FFPE sections were initially deparaffinised in Xylene and rehydrated in reducing concentrations of EtOH (100%, 90%, 70%). Sections were briefly washed in running tap water and then stained in Haematoxylin Z (CellPath) solution. Sections were washed again until the water ran clear. Haematoxylin stain was regressed in 1% acid alcohol and then blueed in STW. Counterstaining in Eosin Y was performed prior to dehydration in increasing concentrations of alcohol and Xylene. Finally sections were mounted with DPX (Leica Microsystems).

2.10.2 Chromogenic Immunohistochemistry

Chromogenic immunohistochemistry was performed on FFPE sections after sectioning. Sections were de-paraffinised in Xylene before undergoing rehydration in decreasing concentrations of EtOH. Antigen retrieval was performed in boiling sodium citrate antigen retrieval buffer for 6 minutes in a microwave at full power. Slides were subsequently washed in TBX and endogenous peroxidase activity was quenched using 3% H₂O₂ in methanol for 20 minutes or BLOXALL Endogenous Peroxidase and Alkaline Phosphatase Blocking Solution (Vector Laboratories) for 10 minutes. Prior to antibody incubation, sections were isolated on the slide using an ImmEdge Hydrophobic Barrier Pen (Vector Laboratories) and blocked in TBX + 10% serum for one hour @ RT. Serum was derived from the animal that the secondary antibody was raised in. Primary antibody or isotype was diluted in TBX + 2% serum at equal concentrations and then applied to sections overnight @4°C.

Following overnight incubation, sections were washed in TB, and secondary biotinylated anti-species antibody was applied to sections for 30 minutes @ RT. After washing in TB, ABC reagent (prepared >30 minutes in advance) with horseradish peroxidase (Vector Laboratories) was applied to sections for 30 minutes @ RT. After a final wash in TB, 3,3'-diaminobenzidine (DAB) was applied to sections and allowed to develop for an appropriate amount of time. Sections were then washed in running water, counterstained with Haematoxylin QS, then dehydrated and mounted using DPX.

All CD3 staining was performed by the Veterinary Diagnostic Services Core Facility at the University of Glasgow. (Vector Laboratories CD3 VP-RM01; Abcam CD3 Ab16669).

Details of antibodies used can be found in Table 2.5

Antibody	Dilution (Final Concentration)	Species	Catalogue No.
Primary Antibodies			
Iba1	1:2000 (0.25µg/ml)	Rabbit	019-19741 [AlphaLabs]
GFAP	1:2000 (1.3µg/ml)	Rabbit	Z0334 [DAKO]
Secondary Biotinylated Antibodies			
Anti-Rabbit	1:4000 (0.375ug/ml)	Horse	BA-1100 [Vector Laboratories]

Table 2.5: Primary and Secondary Antibodies used in IHC

2.10.3 Image Analysis and Quantification

Following immunohistochemistry slides were scanned at 20x resolution using Leica SCN400F (Leica Microsystems). Full scans of slides were then available to view in ImageScope software (Leica Microsystems). For each animal 2-3 sections were analysed for each stain. All image capture and analysis was performed on blinded slides.

For Iba1 a single field of view was taken from both the hippocampus and cortex, for GFAP three fields of view were taken from hippocampus. Using ImageJ software an automated analysis algorithm was used to quantify percentage area stained. Briefly, background was subtracted in an automated fashion, images were separated into haematoxylin and DAB channels. Threshold was then set to

a pre-determined value on the DAB separated image and the area above threshold quantified. Validity of analysis technique was confirmed by three independent individuals through the use of random image matching with a single dummy image. All individuals confirmed the six matched images were accurate representations and correctly identified the dummy slide in a blind fashion.

For CD3 staining cell counts were performed, for hippocampus all CD3+ cells within the hippocampus were counted. For the cortex three fields of view were counted.

2.11 Mass Spectrometry Analysis

2.11.1 Mass Spectrometry Analysis

Plasma and brain samples were sent to the Biomarker and Drug Analysis Core Facility at the University of Dundee (<http://medicine.dundee.ac.uk/biomarker-and-drug-analysis-core-facility>) for mass spectrometry analysis. Briefly, samples were extensively homogenized prior to solid phase extraction using in-house strong cation exchange SpinTip. Eluents were vacuum dried and then reconstituted in 25 μ L elution solution. Liquid chromatography coupled with tandem mass spectrometry was performed using a HILIC column (Intersil, GL Sciences) and a Thermo Quantum Ultra mass spectrometer (ThermoFisher Scientific). The lower limit of quantification was 1.57 ng/mL.

2.12 Statistical Analysis

2.12.1 Between group comparisons

All statistical analysis was performed in Prism 7 software. Non-parametric data were log transformed prior to parametric tests. Student's t-test, one-way analysis of variance (ANOVA) (with post-hoc tests) or two-way ANOVA (with post-hoc tests) were used to test for significant differences between groups. If multiple genes or time points were tested in the same experiment Bonferroni's multiple correction testing was applied to account for the increased probability of type I errors. For protein data, if samples were below the limit of detection they were set to the limit of detection for statistical analysis. A p-value of <0.05 was considered significant.

2.12.2 Linear regression analysis

For linear regression all non-normally distributed samples were log-transformed prior to analysis. Linear regression was performed in Prism 7 software. For protein and mRNA analysis all samples with an mRNA fold change <2 were excluded from analysis. A p-value of <0.05 was considered significant.

2.12.3 Power calculation

Power calculation for 5.3.2 was performed using normalised means obtained from both iCCRKO experiments and a pooled standard deviation from both groups. Power calculation was performed using <https://www.stat.ubc.ca/~rollin/stats/ssize/n2.html>

Chapter 3

A Systematic Review and Meta-Analysis of Chemokines in Human Depression

Chapter 3 A Systematic Review and Meta-Analysis of Chemokines in Human Depression

3.1 Introduction

The burden of depression on health and social care systems, as well as affected individuals is great (1), yet current treatment options are limited(3). An association between depressive disorders and inflammation has been established through both individual biomarker studies and large meta-analyses of this field (15-17, 300-303). This has helped to support a growing field of research into psychoneuroimmunology and aided in the identification of potential molecular pathways to be investigated. Despite this growing body of research, there has been a paucity of reviews on the chemokine molecule family, aside from CCL2/MCP-1 and CXCL8/IL-8. As discussed earlier, chemokines are highly pleiotropic and increasingly associated with CNS functions (30, 101, 337) making them attractive candidates for study.

This is likely due to two main reasons, firstly, chemokines are a newer field of study in psychoneuroimmunology particularly in a clinical context. Secondly, until standardisation of nomenclature most chemokines had multiple variant names making review of the literature challenging and many studies on chemokines can be difficult to identify(338).

To fill this gap in the literature, SL and LN carried out a comprehensive review of the human biomarker literature examining chemokine expression in depressed individuals compared to controls. It is worth noting that throughout the course of this process two meta-analyses were published that looked at chemokines (15, 300) however these only presented results for CCL2, CCL3 and CXCL8 and identified a relatively limited number of studies for each.

This review used a broad approach, including grey literature (e.g. conference abstracts) where appropriate. Through use of a highly structured search strategy based on the PICO framework; Population was human; Intervention was depression; Comparison was no depression; Outcome was change in chemokine levels, and utilising multiple variant names for chemokine molecules this

analysis hopes to have overcome some of the challenges that review of the chemokine literature present.

3.2 Results

3.2.1 Search Results and Study Inclusion

Systematic search of EMBASE, PsycINFO and MEDLINE databases up until 5th March 2016 identified a total of 8497 studies (Figure 3.1). Removal of duplicates resulted in 7440 unique studies. Exclusion based on title removed 4105 studies. Subsequently 3335 abstracts were reviewed, with 2981 studies excluded. 354 full texts were then reviewed with 72 meeting the criteria for inclusion in the meta-analysis (339-410).

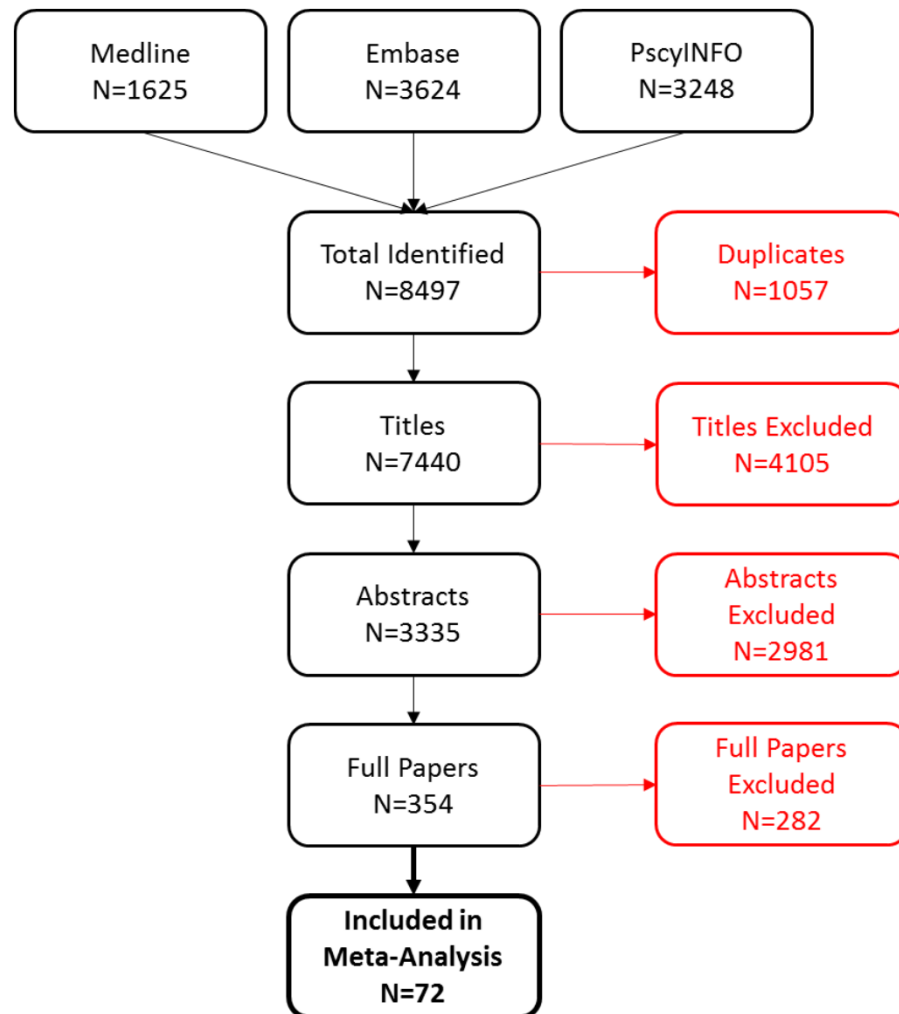


Figure 3.1: PRISMA Flow Chart demonstrating study selection process for meta-analysis

3.2.2 Study Quality

Assessment of study quality based on modified Cochrane collaboration and Newcastle-Ottawa criteria, combined with assessment for confounders, revealed large differences in quality between studies. Out of a total of 17 possible points a range of 3 to 17 was found within the identified studies (Table 3.1). Most studies were contained within a narrower interquartile range of 10 to 13.

Study ID	Study Design (Max. 3)	Outcomes (Max. 6)	Confounders (Max. 6)	Other (Max. 2)	Total Score
Bai 2014	2	5	3	2	12
Bai 2015	2	5	2	2	11
Bazzichi 2007	2	5	3	2	12
Blasko 2006	2	5	2	2	11
Byrne 2013	3	5	3	2	13
Cizza 2008	3	6	3	1	13
Corwin 2015	3	5	6	1	15
Dahl 2014	3	5	5	1	14
Daniele 2015	3	5	1	1	10
Dantoft 2014	2	5	1	2	10
Dekker 2014	2	5	3	1	11
Dong 2013	2	5	1	1	9
Einvik 2012	3	5	4	1	13
Eller 2008	2	5	5	2	14
Fontenelle 2012	3	4	1	2	10
García-Lozano 2008	3	5	1	0	9
Gehi 2010	3	5	2	2	12
Grassi-Oliveira 2012	2	5	3	2	12
Gur 2002	3	5	1	2	11
Halaris 2015	3	4	5	1	13
Hallberg 2010	3	5	3	2	13
Ho 2015	2	5	4	2	13
Hocaoglu 2012	3	4	3	2	12
Hüfner 2015	3	5	5	2	15
Janelidze 2013	3	5	1	1	10
Janelidze 2015	3	3	5	2	13
Jonsdottir 2009	3	3	3	2	11
Juengst 2015	2	5	4	2	13
Kahl 2009	2	5	6	2	15
Karege 2005	3	5	2	2	12
Kelly 2015	2	5	2	1	10

Study ID	Study Design (Max. 3)	Outcomes (Max. 6)	Confounders (Max. 6)	Other (Max. 2)	Total Score
Kern 2014	3	5	2	2	12
Kudoh 2001	3	1	1	2	7
Kuijpers 2002	3	5	3	2	13
Laake 2014	3	5	1	1	10
Laghrissi-Thode 1997	3	4	3	2	12
Lebedeva 2014	2	1	0	0	3
Lee 2009	3	4	4	2	13
Lehto 2010	3	4	4	2	13
Lindqvist 2009	3	5	4	2	14
Lindqvist 2011	3	5	3	2	13
Lu 2013	3	5	5	2	15
Mantur 2006	3	5	1	2	11
Marksteiner 2011	1	5	1	2	9
Mikova 2001	2	5	4	2	13
Miller 2002	3	3	4	2	12
Motivala 2005	3	5	6	2	16
Musselman 2002	3	6	2	2	13
Neupane 2015	3	5	0	1	9
O'brien 2007	3	5	2	2	12
Oglodek 2014	2	2	4	1	9
Piletz 2009	3	6	6	2	17
Pisetsky 2014	2	3	1	2	8
Plourde 2011	2	5	0	1	8
Podlipny 2010	3	4	3	1	11
Pomara 2012	2	5	0	1	8
Pomara 2013	2	5	0	1	8
Rajagopalan 2001	2	6	4	2	14
Rybka 2012	0	4	2	1	7
Schins 2004	3	5	4	2	14
Serebruany 2003	3	4	1	2	10
Shelton 2015	3	5	1	2	11
Simon 2008	2	5	3	2	12
Song 1998	2	5	3	2	12
Sutcigil 2007	2	2	3	2	9
Tajfard 2014	3	5	2	1	11
van Sloten 2014	3	5	2	1	11
Weng 2004	2	5	0	1	8
Whyte 2001	3	4	2	2	11
Wong 2008	3	1	4	2	10
Xiong 2015	3	6	1	1	11

Study ID	Study Design (Max. 3)	Outcomes (Max. 6)	Confounders (Max. 6)	Other (Max. 2)	Total Score
Zahn 2015	3	5	3	2	13
Zhen 2015	3	5	1	2	11

Table 3.1: Risk of bias scores from studies included in meta-analysis. Higher scores indicate lower risks of bias.

3.2.3 CCL2

For blood CCL2 21 studies with 4688 participants were identified. There was a significant increase in CCL2 concentrations in depressed compared to non-depressed subjects (SMD 0.21; 95% CI 0.02, 0.40; $p=0.03$) (Figure 3.2). There was significant heterogeneity identified ($I^2=81\%$; $p<0.00001$). The funnel plot displayed evidence of asymmetry (Figure 3.3) and Egger's test found significant evidence of this ($p=0.0071$). Despite this, trim and fill, did not impute any studies. Analysis of studies after manual removal of the funnel plot outlier Suticigil et al. 2007 did not retain significance (SMD 0.11; 95% CI -0.03, 0.25; $p=0.12$)

Sensitivity analysis in studies with only healthy participants ($n=17$) retained significance (SMD 0.26, 95% CI 0.01, 0.51; $p=0.04$) however this significance was lost again once Suticigil et al. were manually removed. Sensitivity analysis of plasma and serum samples, demonstrated significant differences in serum ($n=12$) (SMD 0.33; 95% CI 0.09, 0.58; $p=0.007$) but not plasma, following manual removal of Suticigil et al. this difference was borderline significant (SMD 0.17; 95% CI -0.00, 0.34; $p=0.05$). Final sensitivity analysis of only those studies with a low risk of bias ($n=12$) did not retain significance (SMD 0.18; 95% CI -0.05, 0.40; $p=0.12$) and this group did not contain the Suticigil et al. study.

2 studies with 81 participants were also identified for CSF CCL2, there was no significant difference between depressed and non-depressed subjects (SMD -0.20; 95% CI -0.66, 0.26; $p=0.40$), due to the low number of studies no further sensitivity analysis was performed.

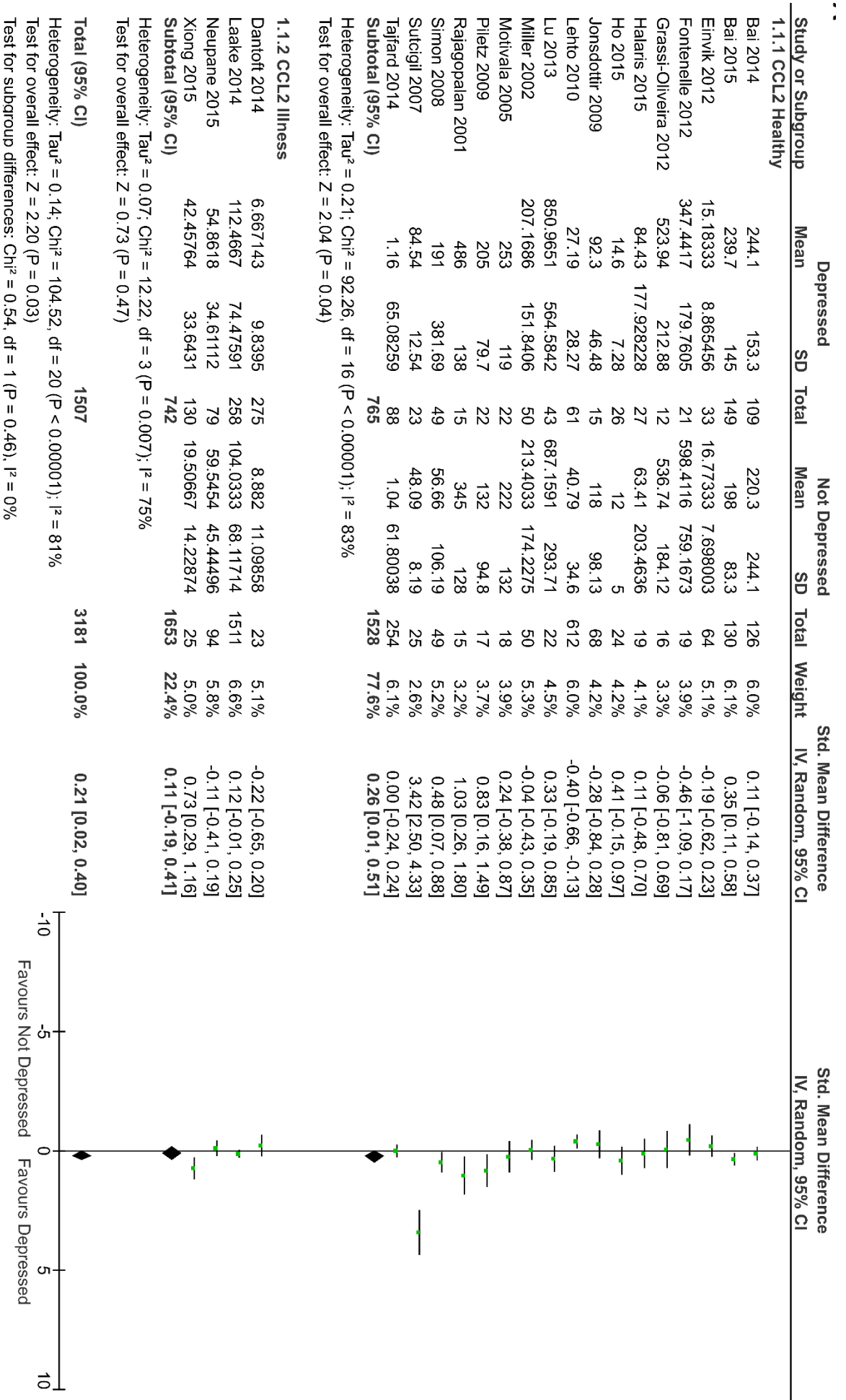


Figure 3.2: (Previous page) Meta-analysis of blood CCL2 in depressed and non-depressed subjects.

Forest plot of CCL2 meta-analysis generated in RevMan 5.3 software using random effects inverse variance model. SD = Standard Deviation, IV = Inverse Variance, CI = Confidence Interval.

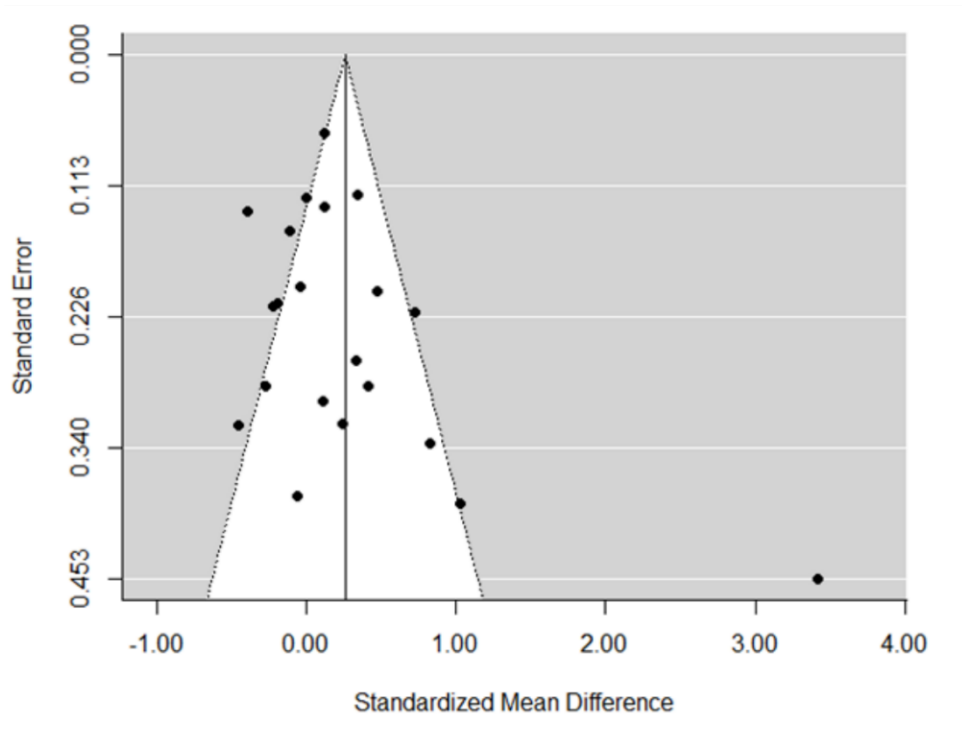


Figure 3.3: Funnel plot of blood CCL2 studies generated in R using metafor package.

3.2.4 CCL3

For blood CCL3 6 studies with 510 participants were identified. There was no significant difference in CCL3 concentrations in depressed compared to non-depressed subjects (SMD 0.33; 95% CI -0.06, 0.71; $p=0.10$) (Figure 3.4). There was significant heterogeneity identified ($I^2=76\%$; $p=0.0008$). There was no evidence of asymmetry in the funnel plot (Figure 3.5) and Egger's test was not significant.

Sensitivity analysis in studies with only healthy participants ($n=5$) found a significant increase in blood CCL3 concentrations in depressed individuals (SMD 0.48, 95% CI 0.20, 0.76; $p=0.0007$). Sensitivity analysis of plasma and serum samples demonstrated no significant differences. Final sensitivity analysis of only those studies with a low risk of bias ($n=4$) did demonstrate significant increases in blood CCL3 concentrations in depressed subjects (SMD 0.58, 95% CI -0.35, 0.82, $p<0.00001$).

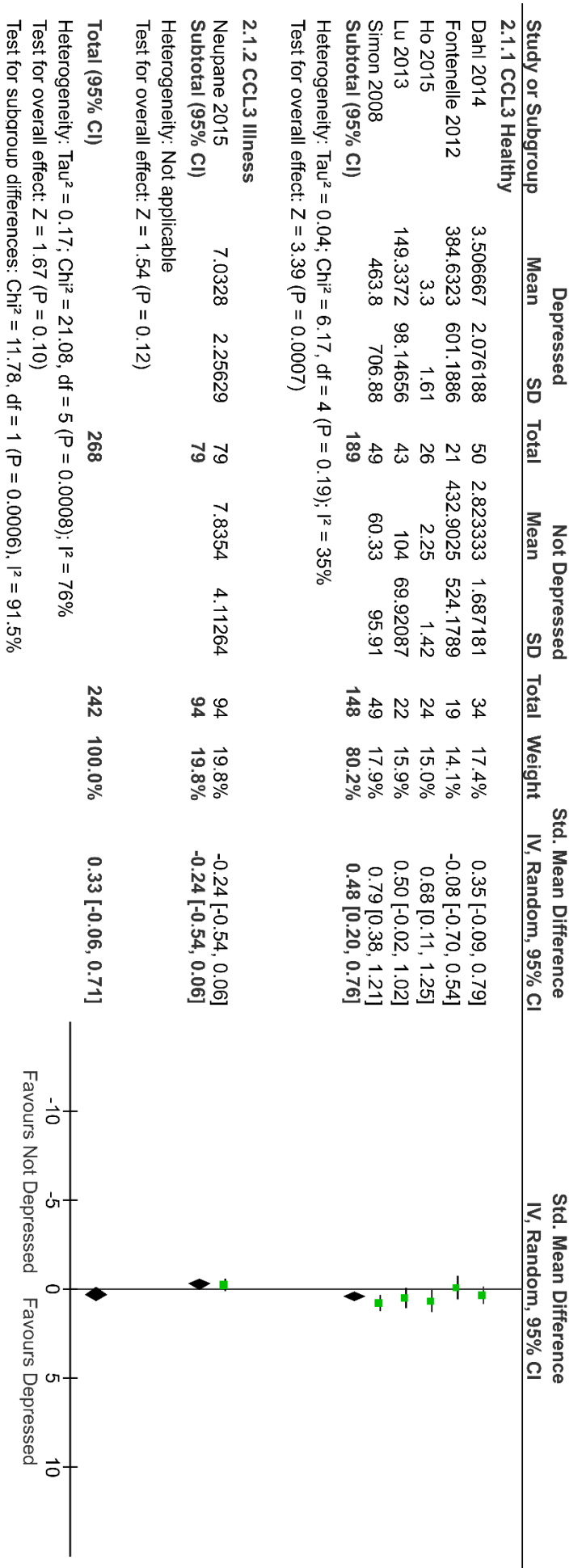


Figure 3.4: Meta-analysis of blood CCL3 in depressed and non-depressed subjects.
 Forest plot of blood CCL3 meta-analysis generated in RevMan 5.3 software using random effects inverse variance model. SD = Standard Deviation, IV = Inverse Variance, CI = Confidence Interval.

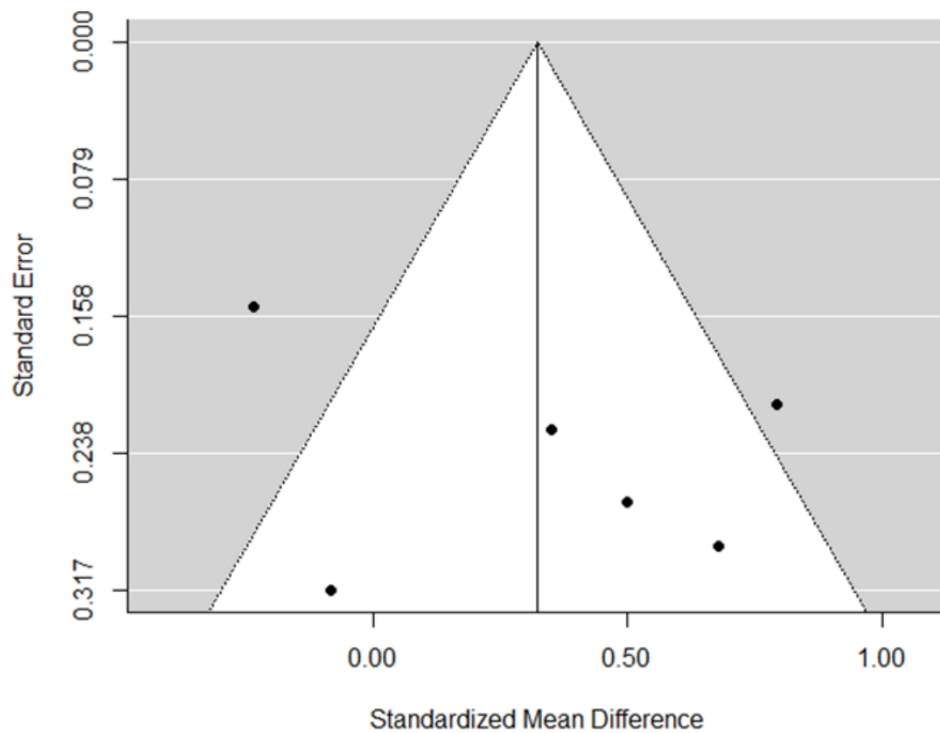


Figure 3.5: Funnel plot of blood CCL3 studies generated in R using metafor package.

3.2.5 CCL4

For blood CCL4 5 studies with 507 participants were identified. There was a significant decrease in CCL4 concentrations in depressed compared to non-depressed subjects (SMD -0.31; 95% CI -0.49, -0.13; $p=0.0007$) (Figure 3.6). There was no significant heterogeneity identified ($I^2=0\%$; $p=0.85$). There was no evidence of asymmetry in the funnel plot (Figure 3.7) and Egger's test was not significant.

Sensitivity analysis in studies with only healthy participants ($n=4$) retained significance (SMD -0.32, 95% CI -0.54, -0.10; $p=0.005$). In addition, these studies all had a low risk of bias. Sensitivity analysis of plasma and serum samples demonstrated significant differences in serum ($n=3$) (SMD -0.33; 95% CI -0.54, -0.12; $p=0.002$) but not plasma.

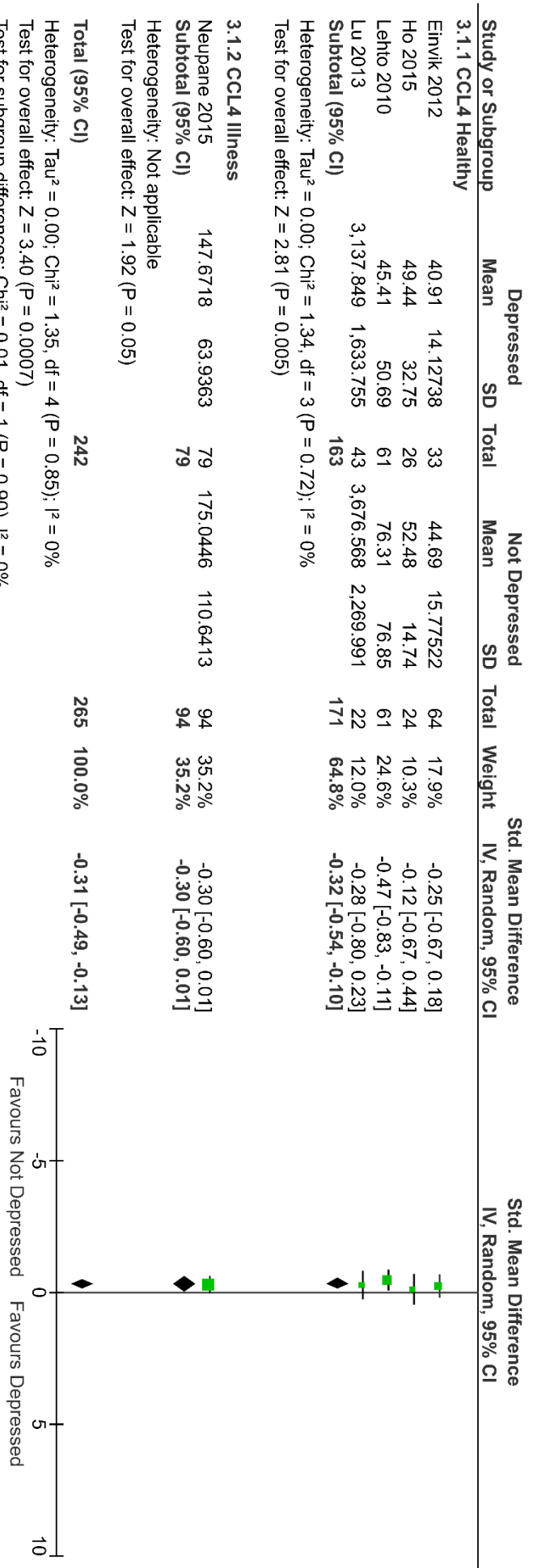


Figure 3.6: Meta-analysis of blood CCL4 in depressed and non-depressed subjects.
 Forest plot of blood CCL4 meta-analysis generated in RevMan 5.3 software using random effects inverse variance model. SD = Standard Deviation, IV = Inverse Variance, CI = Confidence Interval.

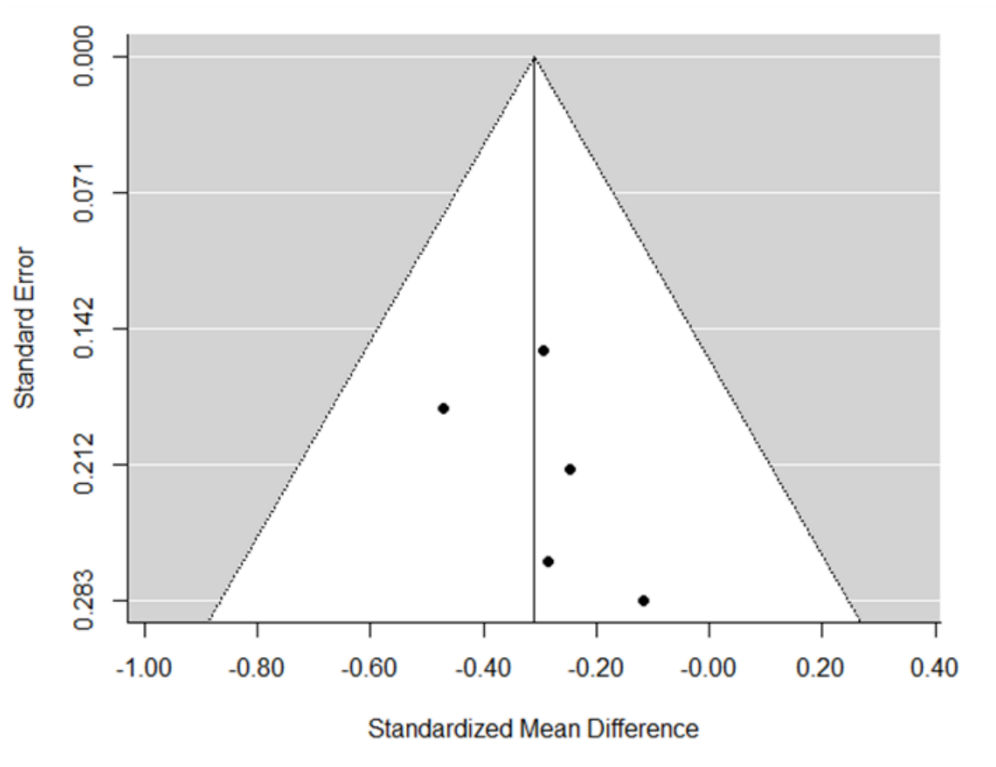


Figure 3.7: Funnel plot of blood CCL4 studies generated in R using metafor package.

3.2.6 CCL5

For blood CCL5 6 studies with 444 participants were identified. There was no significant difference in CCL5 concentrations in depressed compared to non-depressed subjects (SMD -0.10; 95% CI -0.59, 0.40; $p=0.70$). There was significant heterogeneity identified ($I^2=82\%$; $p<0.00001$). There was some evidence of asymmetry in the funnel plot, however, Egger's test was not significant.

Sensitivity analysis in studies with only healthy participants or ill participants, using plasma or serum or examining only those studies with a low risk of bias did not achieve significance.

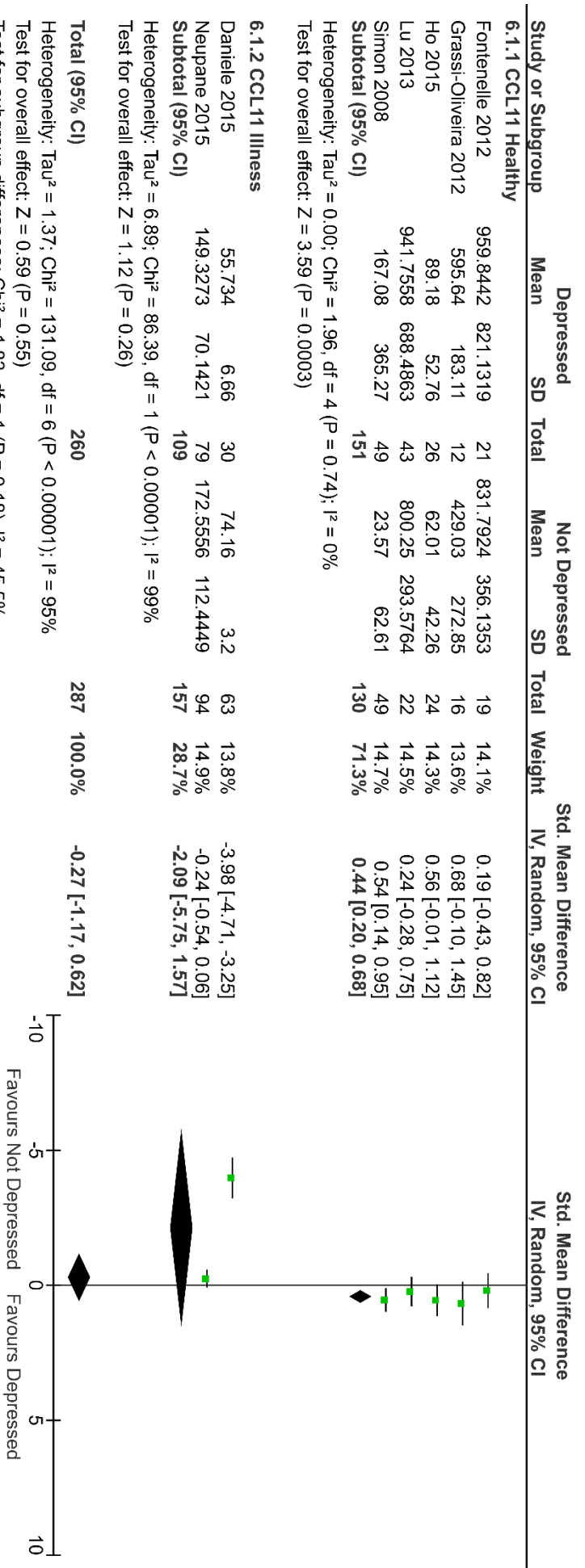


Figure 3.8: Meta-analysis of blood CCL11 in depressed and non-depressed subjects.
 Forest plot of blood CCL11 meta-analysis generated in RevMan 5.3 software using random effects inverse variance model. SD = Standard Deviation, IV = Inverse Variance, CI = Confidence Interval.

3.2.7 CCL11

For blood CCL11 7 studies with 547 participants were identified. There was no significant difference in CCL11 concentrations in depressed compared to non-depressed subjects (SMD -0.27; 95% CI -1.17, 0.62; $p=0.55$) (Figure 3.8). There was significant heterogeneity identified ($I^2=64\%$; $p=0.02$). There was some evidence of asymmetry in the funnel plot (Figure 3.9), however, Egger's test was not significant.

Sensitivity analysis in studies with only healthy participants ($n=5$) found a significant increase in blood CCL11 concentrations in depressed individuals (SMD 0.44, 95% CI 0.20, 0.68; $p=0.0003$). Sensitivity analysis of plasma and serum samples demonstrated no significant differences. Final sensitivity analysis of only those studies with a low risk of bias ($n=4$) did demonstrate significant increases in blood CCL11 concentrations in depressed subjects (SMD 0.48, 95% CI 0.22, 0.74, $p=0.0003$).

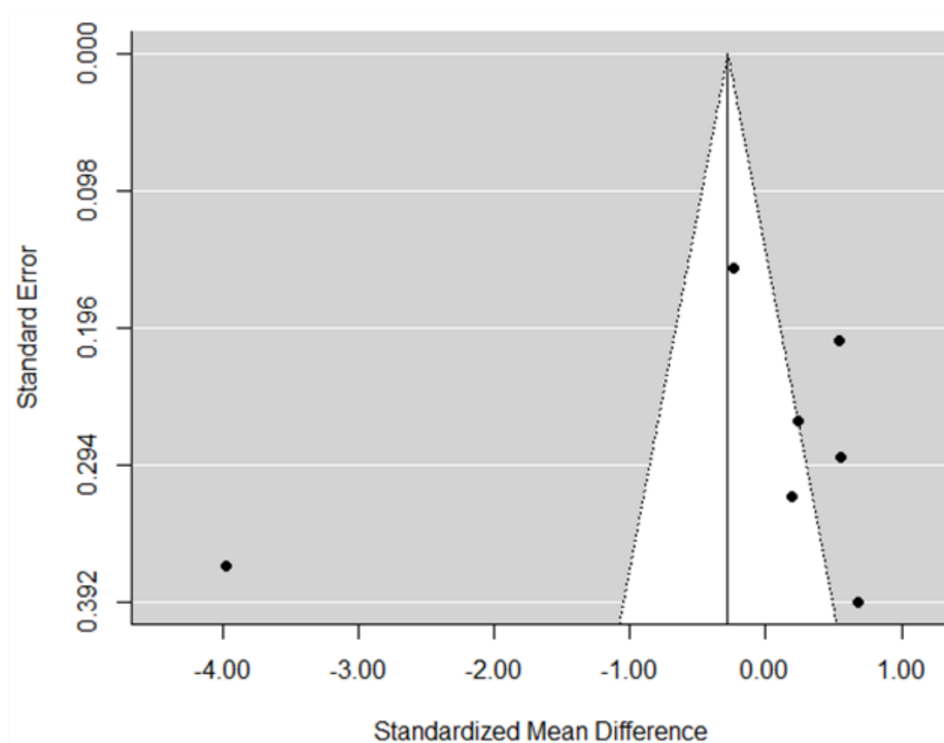


Figure 3.9: Funnel plot of blood CCL11 studies generated in R using metafor package.

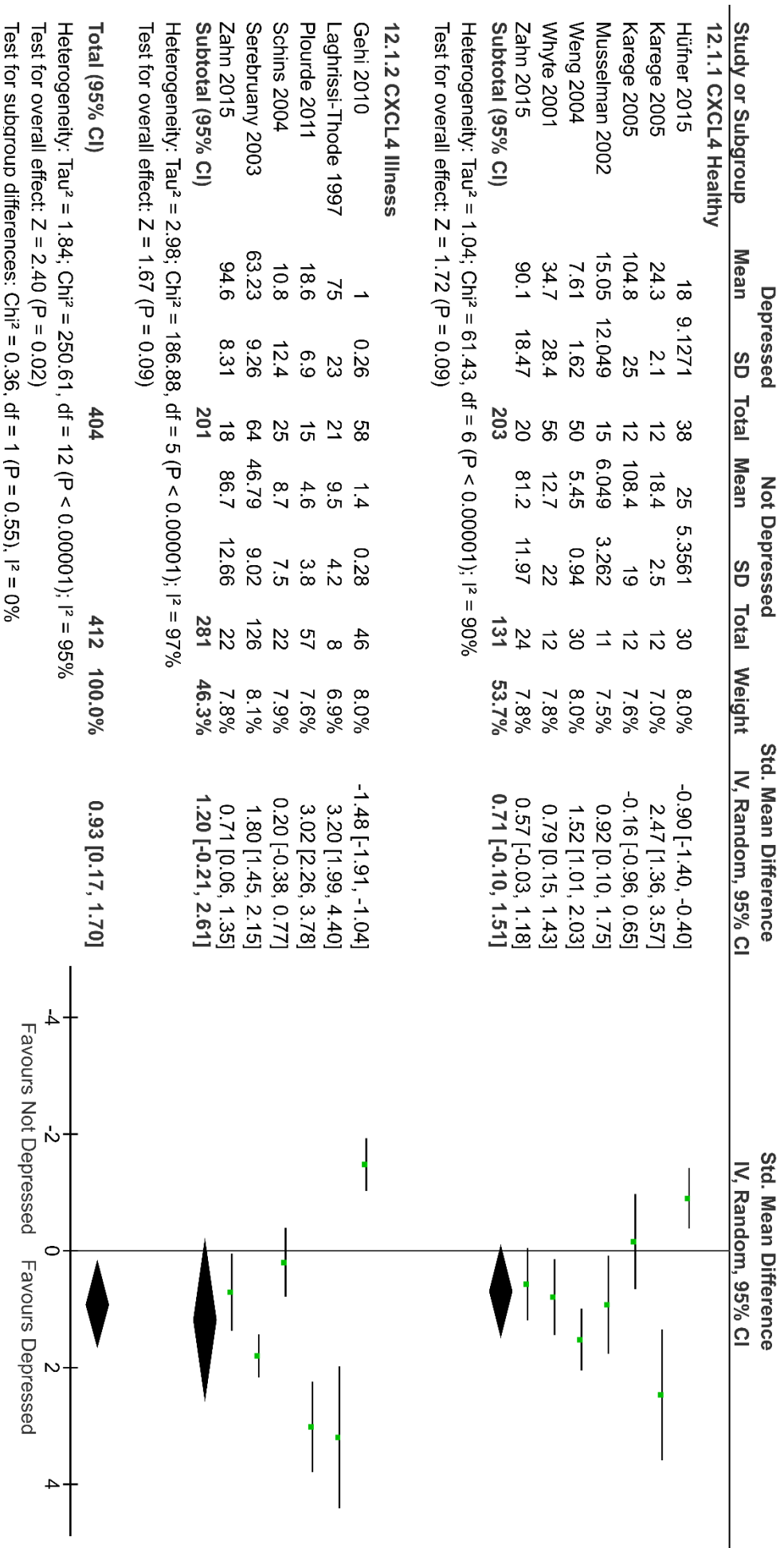


Figure 3.10: Meta-analysis of blood CXCL4 in depressed and non-depressed subjects.
 Forest plot of blood CXCL4 meta-analysis generated in RevMan 5.3 software using random effects inverse variance model. SD = Standard Deviation, IV = Inverse Variance, CI = Confidence Interval.

3.2.8 CXCL4

For blood CXCL4 11 studies with 816 participants were identified. There was a significant increase in CXCL4 concentrations in depressed compared to non-depressed subjects (SMD 0.93; 95% CI 0.17, 1.70; $p=0.02$) (Figure 3.10). There was significant heterogeneity identified ($I^2=96%$; $p<0.00001$). There was evidence of asymmetry in the funnel plot (Figure 3.11), however, Egger's test was not significant. Karege et al. 2005 had values for both serum and plasma, sensitivity analysis removing either of these retained significance.

Sensitivity analysis in studies with only healthy participants or ill participants, using plasma or serum or examining only those studies with a low risk of bias did not achieve significance.

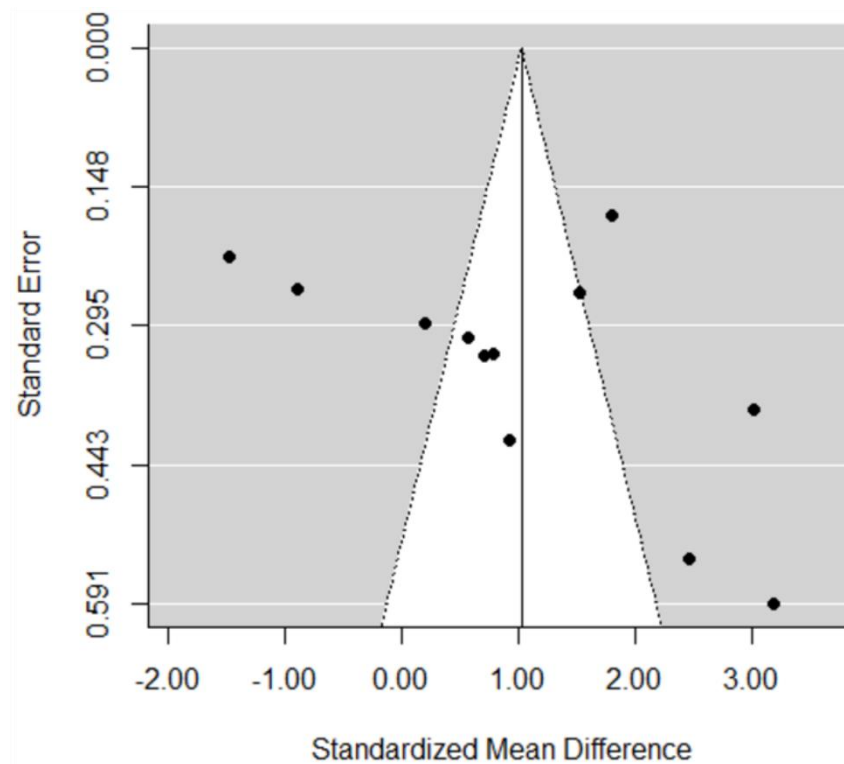


Figure 3.11: Funnel plot of blood CXCL4 studies generated in R using metafor package

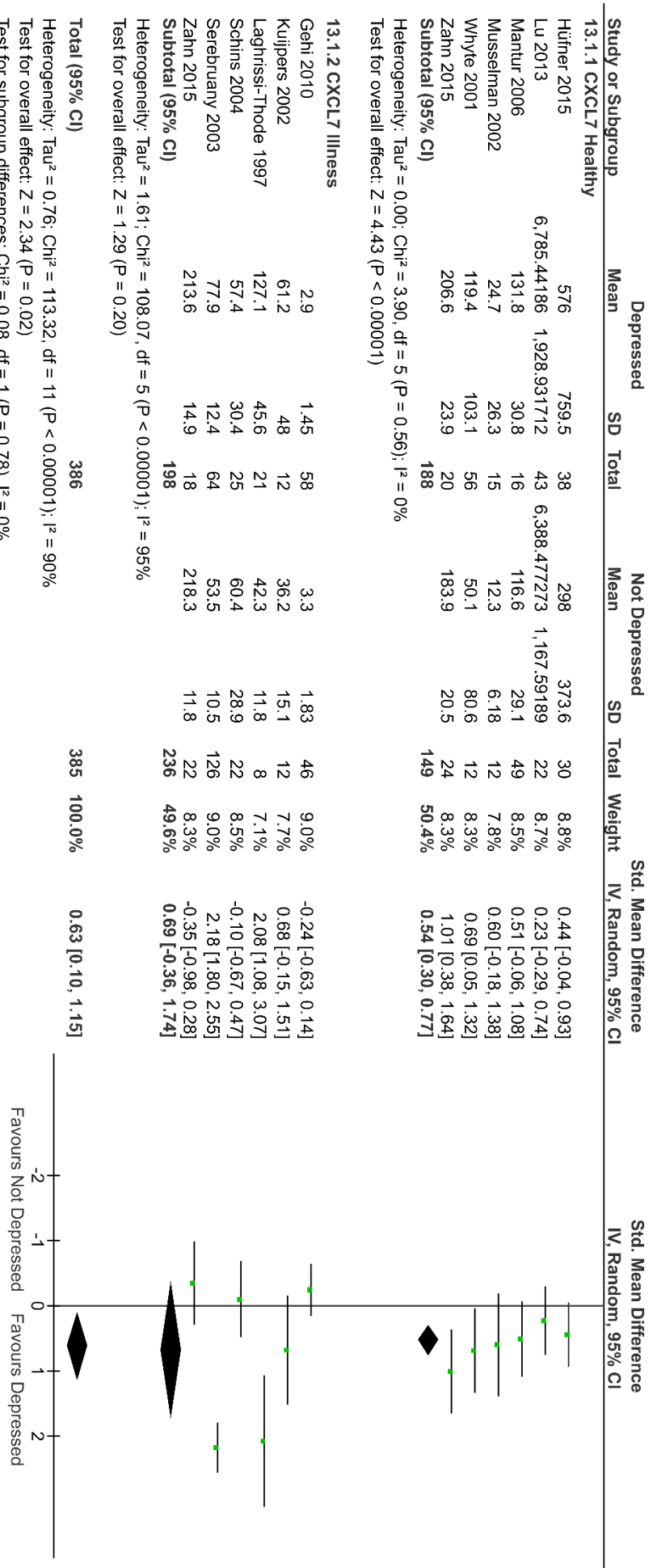


Figure 3.12: Meta-analysis of blood CXCL7 in depressed and non-depressed subjects. Forest plot of blood CXCL7 meta-analysis generated in RevMan 5.3 software using random effects inverse variance model. SD = Standard Deviation, IV = Inverse Variance, CI = Confidence Interval.

3.2.9 CXCL7

For blood CXCL7 11 studies with 711 participants were identified. There was a significant increase in CXCL7 concentrations in depressed compared to non-depressed subjects (SMD 0.63; 95% CI 0.10, 1.70; $p=0.02$) (Figure 3.12). There was significant heterogeneity identified ($I^2=90\%$; $p<0.00001$). There was some evidence of asymmetry in the funnel plot (Figure 3.13), however, Egger's test was not significant.

Sensitivity analysis in studies with only healthy participants ($n=6$) retained significance (SMD 0.54, 95% CI 0.30, 0.77; $p<0.00001$). Sensitivity analysis of plasma and serum samples demonstrated significant increases in plasma ($n=9$) (SMD 0.71; 95% CI 0.05, 1.37; $p=0.04$) but not serum. Final sensitivity analysis of only those studies with a low risk of bias ($n=8$) was borderline significant (SMD 0.40, 95% CI -0.00, 0.80, $p=0.05$).

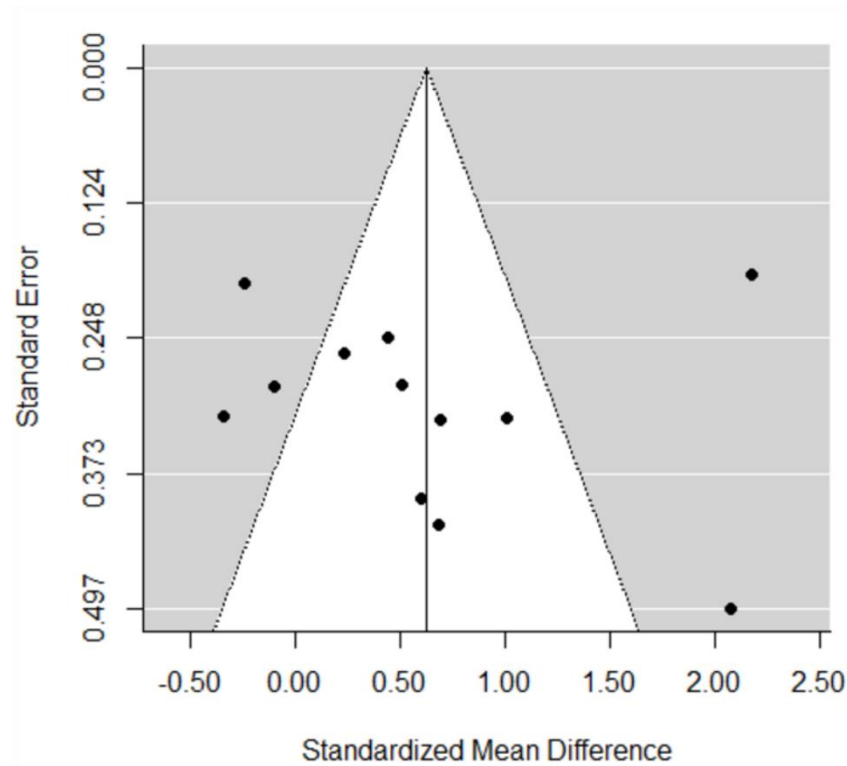
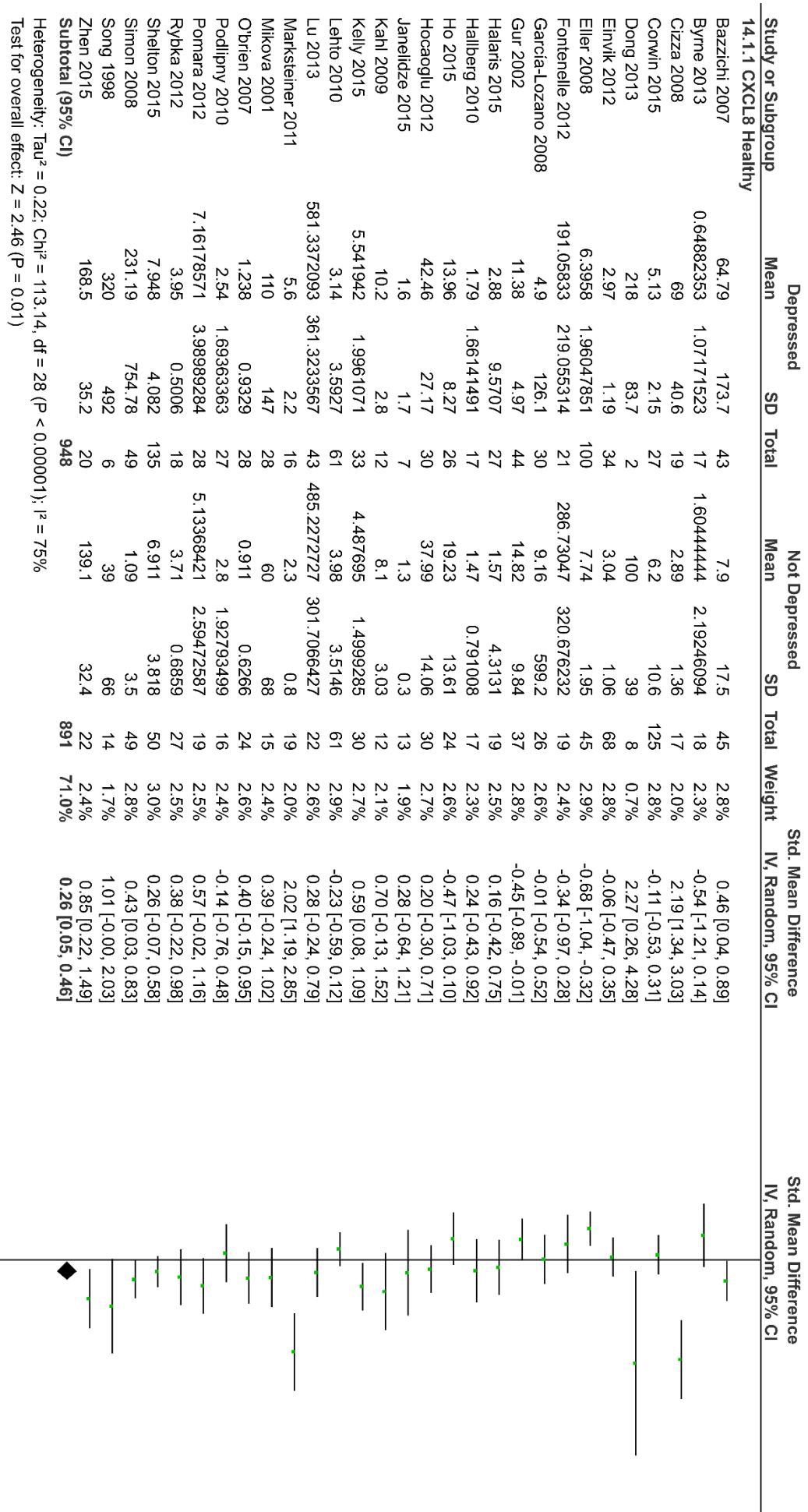


Figure 3.13: Funnel plot of blood CXCL7 studies generated in R using metafor package.



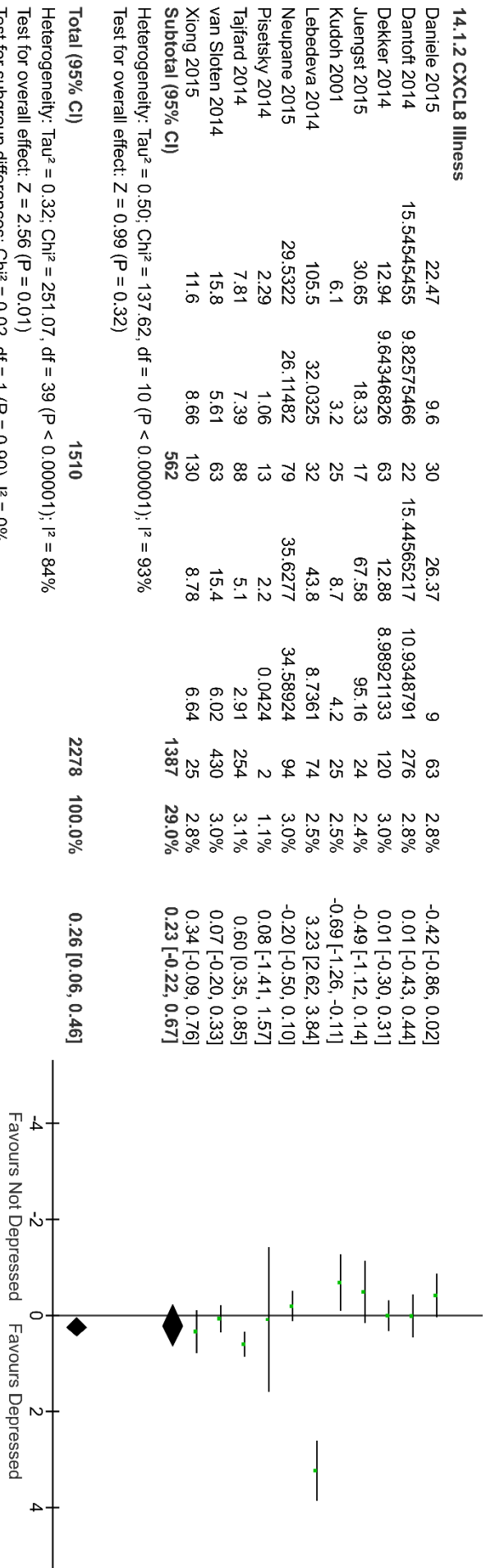


Figure 3.14: Meta-analysis of blood CXCL8 in depressed and non-depressed subjects.
 Forest plot of blood CXCL8 meta-analysis generated in RevMan 5.3 software using random effects inverse variance model SD = Standard Deviation, IV = Inverse Variance, CI = Confidence Interval.

3.2.10 CXCL8

For blood CXCL8 40 studies with 3788 participants were identified. There was a significant increase in CXCL8 concentrations in depressed compared to non-depressed subjects (SMD 0.26; 95% CI 0.06, 0.46; $p=0.01$) (Figure 3.14). There was significant heterogeneity identified ($I^2=84%$; $p<0.00001$). There was moderate evidence of asymmetry in the funnel plot (Figure 3.15), however, Egger's test was not significant.

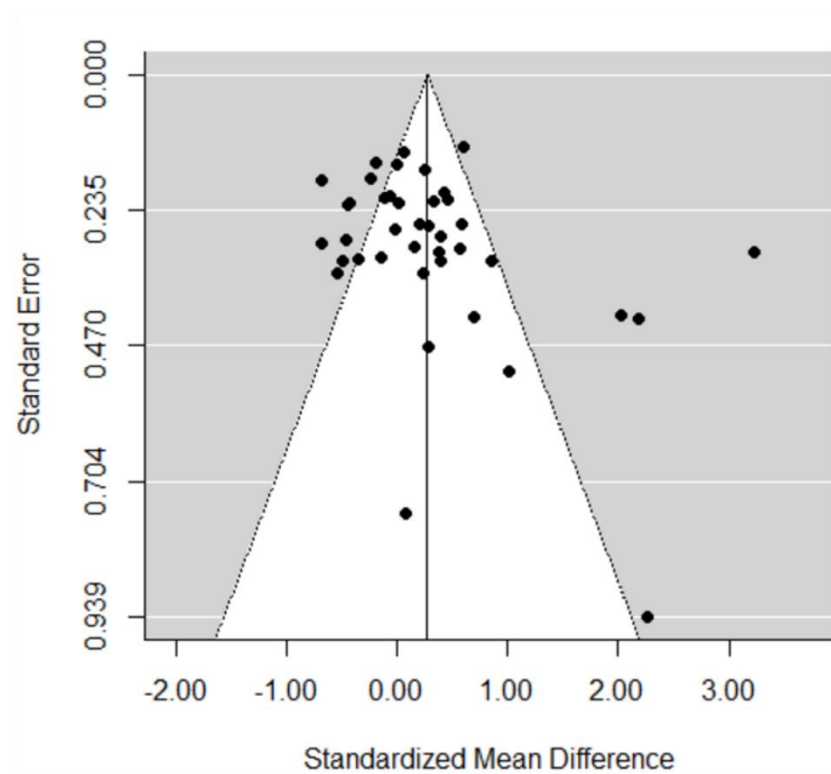


Figure 3.15: Funnel plot of blood CXCL8 studies generated in R using metafor package.

Sensitivity analysis in studies with only healthy participants ($n=29$) retained significance (SMD 0.26, 95% CI 0.05, 0.46; $p=0.01$). Sensitivity analysis of plasma and serum samples demonstrated significant increases in plasma ($n=17$) (SMD 0.57; 95% CI 0.17, 1.00; $p=0.006$) but not serum. Final sensitivity analysis of only those studies with a low risk of bias did not retain significance.

We also identified 6 studies with 361 participants for CSF CXCL8, there was no significant difference between depressed and non-depressed subjects (SMD 0.19; 95% CI -0.15, 0.54; $p=0.40$). Funnel plot did not show evidence of asymmetry

and Egger's test was not significant. Sensitivity analysis on healthy individuals or studies with a low risk of bias did not reveal significant differences.

3.2.11 CXCL10

For blood CXCL10 3 studies with 350 participants were identified. There was no significant difference in CXCL10 concentrations in depressed compared to non-depressed subjects (SMD 1.17; 95% CI -0.26, 2.61; $p=0.11$). No further analysis was performed due to the low number of studies.

We also identified 4 studies with 208 participants for CSF CXCL10, there was no significant difference between depressed and non-depressed subjects (SMD -0.06; 95% CI -0.35, 0.22; $p=0.66$). Due to the low number of studies no further analysis was performed.

3.2.12 CXCL12

For blood CXCL12 2 studies with 121 participants were identified. There was a significant increase in CXCL12 concentrations in depressed compared to non-depressed subjects (SMD 0.44; 95% CI 0.05, 0.82; $p=0.03$) (Figure 3.16). No further analysis was performed due to the low number of studies.

3.2.13 Other chemokines

A number of other chemokines (CCL7, CCL15, CCL18, CCL24, CCL27, CXCL1 and CXCL9) that had ≤ 3 studies and no significant results were also analysed. Details of effect sizes for these chemokines can be seen in Table 3.2.

Chemokine	Studies	Participants	Effect Estimate [95% CI]
CCL7	3	156	0.07 [-0.65, 0.79]
CCL15	2	100	0.09 [-0.31, 0.50]
CCL18	2	100	0.15 [-0.26, 0.56]
CCL24	2	105	-0.11 [-0.76, 0.53]
CCL27	2	121	-0.21 [-0.78, 0.37]
CXCL1	2	121	0.28 [-0.10, 0.66]
CXCL9	3	161	-0.05 [-0.60, 0.49]

Table 3.2: Non-significant results from chemokines with ≤ 3 studies included in meta-analysis.

Effect size generated in RevMan 5.3 software. CI = Confidence interval.

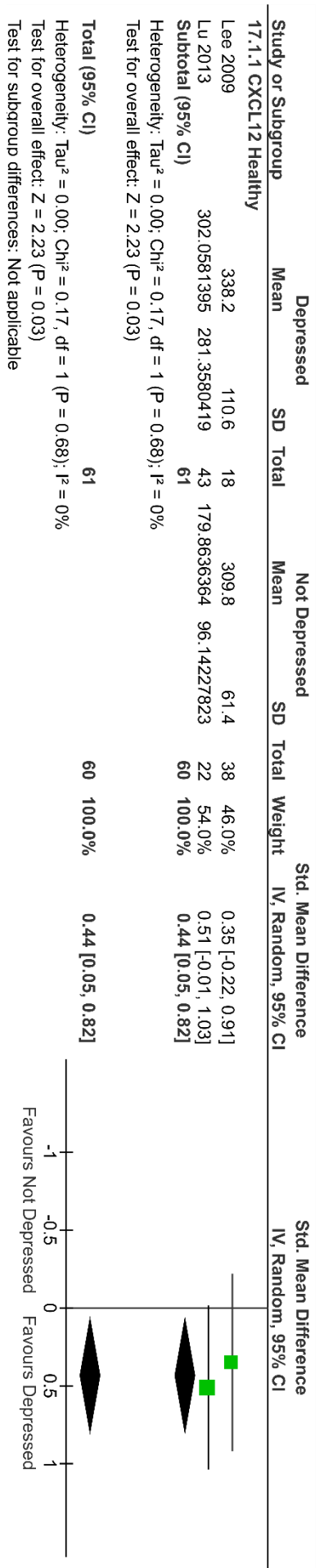


Figure 3.16: Meta-analysis of blood CXCL12 in depressed and non-depressed subjects.

Forest plot of blood CXCL12 meta-analysis generated in RevMan 5.3 software using random effects inverse variance model. SD = Standard Deviation, IV = Inverse Variance, CI = Confidence Interval.

3.3 Discussion

3.3.1 Summary of results and concordance with existing literature

Overall significant increases in CCL2, CXCL4, CXCL7, CXCL8 and CXCL12 were found. In addition, a significant decrease in CCL4 was identified when comparing depressed and non-depressed subjects (Table 3.3). Sensitivity analysis of studies with only healthy participants revealed further differences with both CCL3 and CCL11 being significantly increased in depressed compared to non-depressed subjects, and only CXCL4 losing significance. Interestingly, no significant differences were identified when examining only studies in which subjects had physical comorbidities. This suggests that in the context of illness likely to affect inflammation, immune markers are not a useful tool for discriminating depressive illness. This is likely due to the fact that biological noise in already raised markers will mask the smaller increases expected from depressive illness.

Chemokine	Overall	Health	Illness	Plasma	Serum	Low Bias
CCL2	Increase	Increase	NS	NS	Increase	NS
CCL3	NS	Increase	NS	<i>Increase</i>	NS	Increase
CCL4	Decrease	Decrease	NS	NS	Decrease	Decrease
CCL11	NS	Increase	NS	NS	NS	Increase
CXCL4	Increase	NS	NS	NS	NS	NS
CXCL7	Increase	Increase	NS	Increase	NS	<i>Increase</i>
CXCL8	Increase	Increase	NS	Increase	NS	NS

Table 3.3: Significant results and sensitivity analysis in chemokines with >5 studies identified and a significant difference.

Italics indicates borderline significance ($=0.05$). NS = Not significant. Significance indicated by $p < 0.05$ in a random effects model using inverse variance weighting.

Further to this, examining differences in only plasma or only serum did not reveal any particular pattern. Analysis of only studies considered to have a low risk of bias also did not reveal a particular pattern. A number of studies lost significance within this context suggesting a role for poorer study design in the earlier identification of differences. However for both CCL3 and CCL11 significance was gained. This is likely a reflection of the fact that there was considerable overlap between the studies in healthy participants and those with a low risk of bias and this may have supported identification of these changes.

The significant differences identified within this study strongly support the idea of peripheral alterations in circulating chemokines in depressive disorder. However, it should be noted that CCL2's significance was largely due to a single study by Sutcgil et al. with a very large effect size (SMD=3.42)

Both CXCL9 and CXCL10 are IFN stimulated genes and CXCL10 was recently identified as a key mediator of sickness behaviour in a study by Blank et al. (103) Despite this study, and the strong association of IFNs with depressive disorder(14), CXCL9 and CXCL10 were not significantly altered in depressed subjects. This may be a reflection of the lower number of studies available for these analytes. However only blood CXCL10 showed a trend and both blood CXCL9 and CSF CXCL10 did not appear to show any suggestion of significant effects.

When comparing our findings to those observed in other meta-analyses by Eyre et al.(300) and Köhler et al.(15) significant increases in CCL2 were found, similar to these studies. However, unlike Eyre and Köhler increases in CXCL8 were also identified in this study. It is worth noting that Köhler et al. did not retain significance for CCL2 after exclusion of a study by Shen et al.(411). The paper by Shen et al. had been identified in this study, however, it was excluded prior to the meta-analysis due to a very high risk of bias and an inability to contact the authors. In addition, when examining studies with only a low risk of bias both of these analytes were not found to be significantly different in our meta-analysis. This suggests that more poorly designed studies may contribute to the significant alterations identified. Finally although Köhler et al. did not identify alterations in CCL3, the study in this chapter indicated the presence of significant increases that were retained even when considering only those studies with a lower risk of bias. Another possible explanation for the differences in CCL2, CCL3 and CXCL8 findings between our study and the other meta-analyses is that a much greater number of studies were identified for inclusion, possibly due to the use of a more complete search strategy.

Interestingly, Pantazatos et al. identified reductions in CCL4 at a transcriptional level in a post-mortem study of depressive disorder. This suggests that peripheral alterations observed here may also manifest within the CNS(412).

3.3.2 Biological relevance

Although not widely studied in the context of behavioural and CNS alterations, work has shown that some of the chemokines above appear to be able to alter CNS physiology. CCL2 has been shown to be associated with, an influx of CCR2+ monocytes to the CNS following LPS challenge and liver injury(102, 413) and, activation of resident microglia(414). This association with microglial activation also links with emerging theories that depression and other CNS diseases may in part be microglial pathologies(308). Overexpression of CCL2 has also been associated with elevation of Il-1 β and Il-6 cytokines that have been implicated in animal sickness behaviours (295) and human depression respectively (15-17, 301, 302).

Direct application of CCL2 to serotonergic neurons has been associated with decreases in action potential frequency and spontaneous discharge due to hyperpolarization and reductions in membrane resistance(102). Alongside these CCL2-associated electrophysiological alterations, CCL3 has been shown to alter hippocampal neuron firing and long-term potentiation effects that were linked to behavioural alterations in learning and memory. These effects could be reversed through co-administration of maraviroc a CCR5 antagonist(415). The finding that maraviroc blocked the effects of CCL3, suggests that the effects of CCL2 and CCL3 may be mediated through different receptors as CCL2 does not signal through CCR5 as CCL3 does(29). Alterations of chemokines may not necessarily be detrimental and could represent protective responses in stressed neurons. KO of CCR5 in a mouse model of nerve injury accelerated motor neuron death suggesting that CCR5 may be protective in the context of neurotoxicity (416). There is limited evidence currently available for CCL4 and a recent systematic review did not identify studies that implicated it in psychiatric disorders(417). Despite this, CCL4 has been associated with T_{reg} cells (418) that have themselves been associated with depression (419).

Villeda et al. found CCL11 to be mechanistically associated with reductions of hippocampal neurogenesis and impaired learning and memory(420), both of which have been associated with depressive disorders. Interestingly, this study also identified CCL2 as a factor that correlated with reductions in neurogenesis similar to CCL11.

CXCL4 and CXCL7 are predominantly known for their role as platelet chemokines. Of the chemokines identified within this meta-analysis CCL2, CCL3, CXCL8 and CXCL12 are also thought to be platelet chemokines or associated with platelet activation (421, 422). Other platelet chemokines were either not part of this study due to insufficient studies (e.g. CCL17, CXCL5) or found to not be significantly altered within a very small number of studies (e.g. CXCL1 [n=2]). The only exception being CCL5 that had a similar number of studies, and participants, to other chemokines examined. This suggests there may be a potential association of platelet dysfunction with depressive disorder. This is supported by work showing that there is increased platelet activation in depressed patients (423, 424), and that this activation is decreased following 6 months of cognitive and/or pharmaceutical therapy (423).

CXCL4 alone has also been shown to be expressed by microglia in response to LPS *in vitro* and to induce their migration, in addition it was able to suppress the synthesis of nitric oxide (NO) in BV-2 cells but not primary microglia, and microglial phagocytosis was reduced in the presence of CXCL4(425) suggesting that it may have protective effects with regards to neurotoxicity similar to CCL3. These possible protective responses suggest that elevation of these chemokines may not be a driving factor in depression but rather a protective response to neuronal stress.

It is harder to identify mechanistic links between CXCL8 and depressive behaviours as mice and rats do not have CXCL8, however CXCL1 is closely related to CXCL8(29). CXCL1 administered peripherally but not centrally was found to drive sickness behaviour responses in adult Wistar rats(426) suggesting that peripheral alterations may play a role in depressive phenotypes. Although alterations in CXCL1 were not found, there were only two studies and these did trend towards an increase in peripheral CXCL1. A recent study by Aguilar-Valles et al. identified neutrophils as mediators of sickness behaviour in the LPS model of inflammation(427), as CXCL8 is a neutrophil chemoattractant this suggests a possible mechanism through which elevated CXCL8 could contribute to depressive behaviours.

CXCL12 has been shown to have effects on serotonergic, gamma-aminobutyric acid, glutamate and other CNS systems(428, 429). In addition, CXCR7 a receptor

for CXCL12 has been found to be rapidly upregulated on endothelial cells in response to TNF α treatment,(430) another molecule that has been linked with depression(318). Evidence has also suggested that CXCL12 can modulate neuroendocrine systems(337) and neurogenesis(30). Dysfunction of these CNS systems is implicated in depressive pathology (431, 432).

Overall these data provide equivocal, and at times conflicting, evidence for a mechanistic role of identified chemokines in depressive behaviours. There is evidence that many of these chemokines can contribute to cellular recruitment and activation during neuroinflammation and promote alterations in CNS function associated with depressive behaviour such as reduction in neurogenesis, changes in neuronal function and HPA axis alteration. These lines of evidence promote the idea that raised chemokine levels are mechanistically associated with psychological disturbances. On the other hand, there is also evidence that some of these chemokines may have neuroprotective roles, while not mutually exclusive to the data presented above this would suggest a more reactionary rather than mechanistic role for chemokines in the context of depressive pathology.

3.3.3 Limitations and Strengths of Study

Throughout the course of this study a number of limitations within the human literature were identified. First and foremost, nearly all of the analytes assessed were taken from blood. This is a peripheral compartment and may not necessarily reflect what is observed in the brain. Differences in CCL2 and CXCL8 that were observed in the blood of depressed subjects were not replicated in the CSF compartment. Although this may be partly due to the lower number of studies examined, it casts some doubt on the direct biological relevance of these findings.

Secondly, there is large variability in the number of confounders that people account for. Evidence suggests that age(433), gender(434), BMI(435), smoking(436), circadian rhythms(437) and medications (e.g Nonsteroidal anti-inflammatory drugs) can all influence immune status. When looking for the small differences anticipated in conditions like depressive disorder, accounting for these confounders is incredibly important. In addition, depressive disorder is

also associated with nearly all of these confounders; depressive prevalence varies by age (438); depressive prevalence is greater in women(438); depressive prevalence varies based on BMI (439, 440), partly due to anti-depressant treatments(441); depression is associated with higher rates of smoking and lower rates of smoking cessation(442, 443); depression is associated with disturbances of circadian rhythmicity (444); and anti-depressant medication is associated with immune alterations as discussed in the introduction (16, 307). These associations between depression and inflammatory confounders increase the likelihood of confounding when effective matching does not occur. Unmatched confounders can easily lead to bias, particularly when there is non-reporting of these clinical demographics making it impossible to assess whether they are likely to be influencing perceived outcomes.

Thirdly, small outlying studies can have large effects on meta-analysis results. In our study Sutcgil et al. provided an excellent example of this as removal of it from the analyses caused the significant difference in CCL2 to be lost, despite an overall n = 21. This is a challenging area to navigate as, if the study shows a high level of rigour and is conducted appropriately, it should be included in a meta-analysis. However this can be difficult to ascertain particularly for older studies where online supplemental material may be lacking and identification of immune confounders was less advanced, meaning that there may be more limited reporting of demographics.

Alongside these limitations, it is worth noting two major strengths of this study. Firstly the use of a comprehensive search strategy allowed for the inclusion of many more studies and chemokines than have previously been examined and allowed for more in depth sensitivity analysis. This identified alterations in chemokines that have not previously been reported in earlier meta-analyses. Secondly through the use of a more conservative random effects model it is possible to have increased confidence in the significant results identified, particularly from a statistical perspective.

3.3.4 Conclusion

Overall this study has demonstrated that there is significant evidence across multiple studies for peripheral alterations in circulating chemokine

concentrations. Despite this, there are methodological concerns when examining human biomarker studies. These include the relevance of peripheral biomarkers to CNS immunology and the role of unseen confounders in these studies, particularly emerging confounders such as circadian rhythm and the role of anti-depressive medication in altering immune profiles. In addition, mechanistic conclusions are nearly impossible to draw from cross-sectional studies such as those examined in this meta-analysis.

Moving forward it would be beneficial to encourage future studies to try to account for more of these confounders. When it is challenging or impossible to accurately match groups, efforts should be made to provide complete demographic reporting and attempt adjustment for potential confounding factors. In addition, with the increasing availability of affordable proteomic arrays, where possible these should be employed particularly in exploratory studies. This allows for an increased range of analytes and helps to prevent over interpretation of results with a narrow scope and to provide increased data availability for future analyses. Examining the differences between healthy and ill populations suggests that looking for alterations in peripheral immune biomarkers in depressed populations with comorbidities is unlikely to be very successful. As mentioned, this is probably due to the fact that when peripheral immune biomarkers are already raised, biological noise would mask the smaller effect size expected between a depressed and non-depressed population.

Finally while it is possible to link these findings to mechanistic animal models and emerging theories of depression, it is worth noting that due to the highly complex nature of depression and the numerous theories surrounding its pathophysiology it is possible to link a very large number of molecular targets to depressive disease. While this does not preclude these associations being true it does shed some doubt on the mechanistic relevance of every finding. Rigorous mechanistic studies in animal models of depressive behaviours and more methodologically sound human cross-sectional studies combined with prospective longitudinal studies may help to overcome these issues and provide evidence of which molecules appear to be most mechanistically relevant to human depression. Despite this doubt, the work here clearly supports further research into the chemokine family as potential mediators of depressive disease.

Chapter 4

Initial Characterisation of the Aldara Model

Chapter 4 Initial characterisation of the Aldara Model

4.1 Introduction

It has previously been established that peripheral inflammatory stimuli using TLR agonists can result in immune alterations within the CNS. TLR3, TLR4 and TLR7 agonists administered to a peripheral site either topically, i.p. or i.v. result in the central upregulation of ISGs, chemokines and cytokines (24, 25, 81, 245, 246, 248, 445).

Previous work within our laboratory has established that the Aldara model of psoriasiform inflammation utilising the TLR7 agonist imiquimod results in upregulation of ISGs and some chemokines (24, 25) from 24 hours post-treatment. This has been associated with an influx of T cells, reductions in neurogenesis and alterations in behavioural measures (24, 446). Recent work, has shown that this inflammatory response is associated with an influx of, not just T cells, but also other peripheral immune cells, into the CNS (24). Alongside this, work by other laboratories has demonstrated that both the liver and lungs may become inflamed in response to Aldara treatment, however, these organs were studied in isolation (447, 448). Earlier data from our laboratory have also suggested that the PBL and brain responses are temporally distinct (24, 446).

This chapter aims to address several questions surrounding the Aldara model that have been identified from these data:

1. What is the transcriptional response with regards to cytokines and a broader range of chemokines?
2. How rapidly does the brain response become evident?
3. How does the response within the brain compare to the response within the peripheral organs?
4. Are transcriptional alterations evident at a protein level?

5. Are transcriptional responses associated with changes in glial populations of the CNS (microglia and astrocytes) and/or changes in a recruited cellular population (T-cells)?”

To address these questions and to better understand the characteristics of the Aldara model, we aimed to perform a more widespread analysis of transcriptional responses that included a broader range of chemokines and some major cytokines, examining both the brain and the periphery. In addition to studying transcriptional responses, associated changes were assessed through assay of protein levels and immunohistochemical examination of cellular alterations. To assess the temporal nature of the response and the speed at which brain responses occur earlier time-points than have been previously examined were investigated. Together these data will form the foundation of an immunological characterisation of the Aldara model in both the periphery and CNS, and provide additional insight into functional changes within the brain itself.

Based on current conceptions surrounding brain immunology, which suppose that the brain is a site of modified immune function (198-200), it was hypothesised that the brain response to Aldara would be distinct compared to the peripheral organs. In addition, based on the signalling pathways associated with TLR7 activation, and the previous findings of ISG upregulation, it was hypothesised that various chemokines and cytokines that were previously unexamined would also be upregulated, and that this upregulation would be associated with increases in protein levels within the CNS. Considering the evidence from other models of TLR activation, and studies examining viral responses within the CNS, it was also hypothesised that this upregulation would be associated with alterations in microglial and astrocytic populations of the CNS.

To this end, this chapter will present initial systemic data examining the peak response point of 3 days identified in earlier studies, followed by a more extensive time-course characterisation. To assess the functional implication of altered immunity it will next be determined, if transcriptional changes become evident at a protein level and, whether there are altered cellular responses to this peripheral stimulus using immunohistochemical techniques.

4.2 Results

4.2.1 The effect of repeated cutaneous treatment with Aldara on mouse weight and skin thickness after 3 days

Initially, changes in weight, and the skin response, up to 3 days of treatment were investigated. This time-point was chosen as it was the previously identified peak ISG transcriptional response point. Examining changes in weight from baseline identified that after 1 day of treatment mice treated with Aldara cream had significant reductions in weight compared to control mice (Figure 4.1A). This reduction continued for the 3 days of treatment. As Aldara treatment is characterised by changes in skin that are supposed to mimic psoriasiform inflammation we also examined skin histological changes using H&E. Examination of skin sections showed clear evidence of epidermal thickening and there were significant increases in epidermal:dermal ratios in mice treated with Aldara indicative of epidermal hyperplasia (Figure 4.1B/C).

4.2.2 The effect of repeated cutaneous treatment with Aldara on systemic chemokine and cytokine transcription after 3 days

Following the confirmation of a clear phenotype in treated animals the skin, lungs, liver and spleen alongside the brain were investigated at the 3-day time-point. For all transcripts examined (*Ccl2*, *Ccl3*, *Ccl5*, *Ccl9*, *Ccl19*, *Cxcl10*, *Cxcl13*, *Cxcl16*, *Ccr5*, *Il1b*, *Tnfa*, *Il6*, *Il1b*) the brain demonstrated a significant upregulation when compared to control animals (Figure 4.2, Figure 4.3, Figure 4.4). In contrast, peripheral tissues did not show universal upregulation.

The skin did not demonstrate significant upregulation of any transcript after three days of Aldara treatment and this is in contrast to the histological changes that are clearly identifiable at this time-point. In the peripheral tissues, the lungs were the most significantly altered aside from the brain and there was significant upregulation of a number of chemokines and cytokines (*Ccl2*, *Ccl3*, *Ccl5*, *Ccl9*, *Cxcl10*, *Cxcl13*, *Il1b* and *Il10*) (Figure 4.2, Figure 4.3, Figure 4.4), although the magnitude of this upregulation was diminished when compared to that in the brain. Of all the transcripts examined *Il10* was found to be the most consistently upregulated with significant differences identified in all tissues aside from the skin at this time-point. Minimal significant changes were observed

in the liver and spleen with only *Tnfa* and *Il10* found to be significantly upregulated in the liver and only *Il6* and *Il10* being significantly upregulated in the spleen. Interestingly, *Ccl19* was the only transcript found to be significantly down-regulated in any tissue and this downregulation was only present in the spleen.

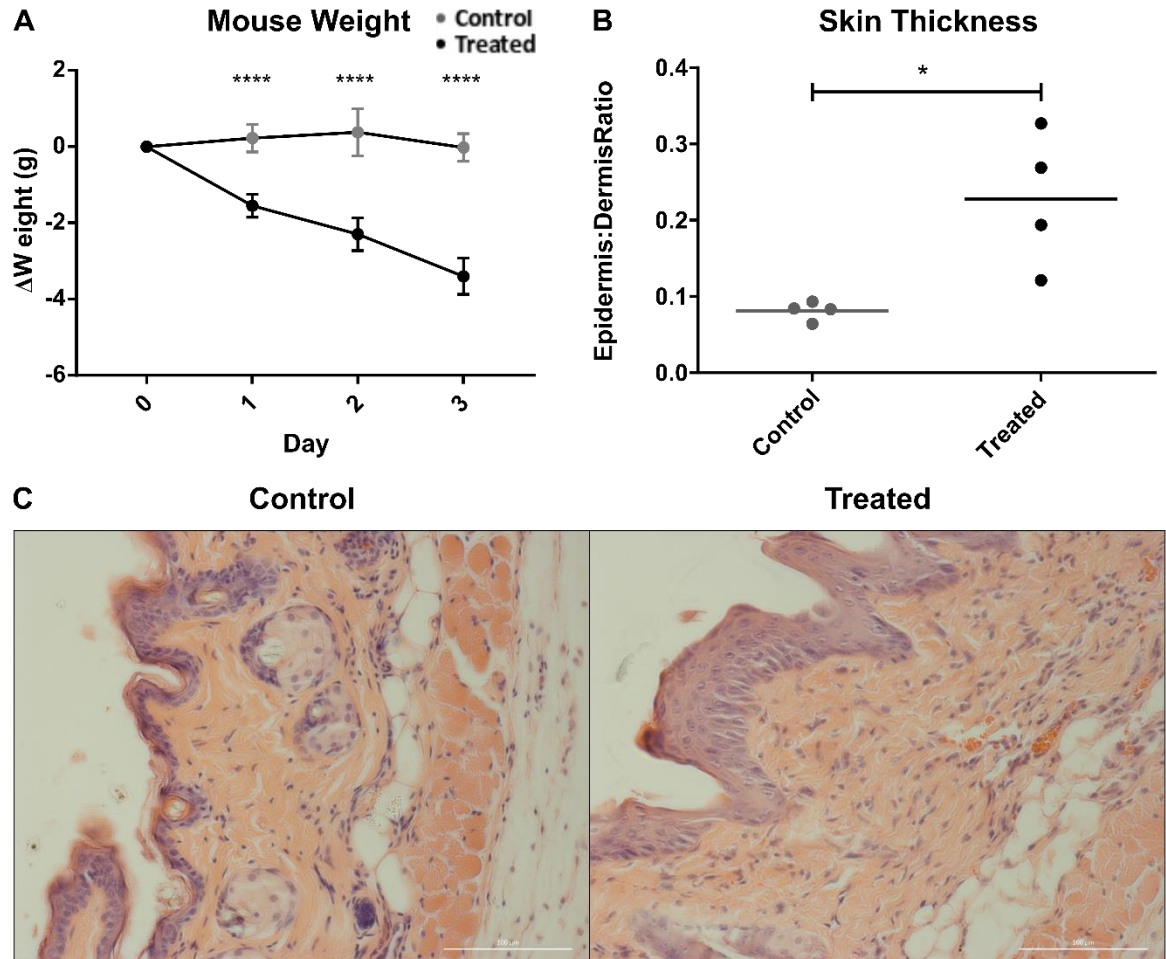


Figure 4.1: 3-day Aldara Model Weight Change and Skin Haematoxylin & Eosin.

Mice were treated daily with 62.5mg Aldara cream (5% imiquimod) or control cream on the dorsal skin for 3-days. (A) Mouse weight change from baseline over 3 days of treatment (n=4, 1 representative experiment of 2 shown) tested using One-way ANOVA and post-hoc Student's t-test with Bonferroni multiple testing correction. (B) Epidermis:dermis ratio as an average from 3 sections per mouse (n=4) Tested using unpaired Student's t-test. (C) Representative figures of skin H&E. *= $P < 0.05$; ****= $P < 0.0001$. Scale bars = 100 μ m. Bars represent mean \pm SD.

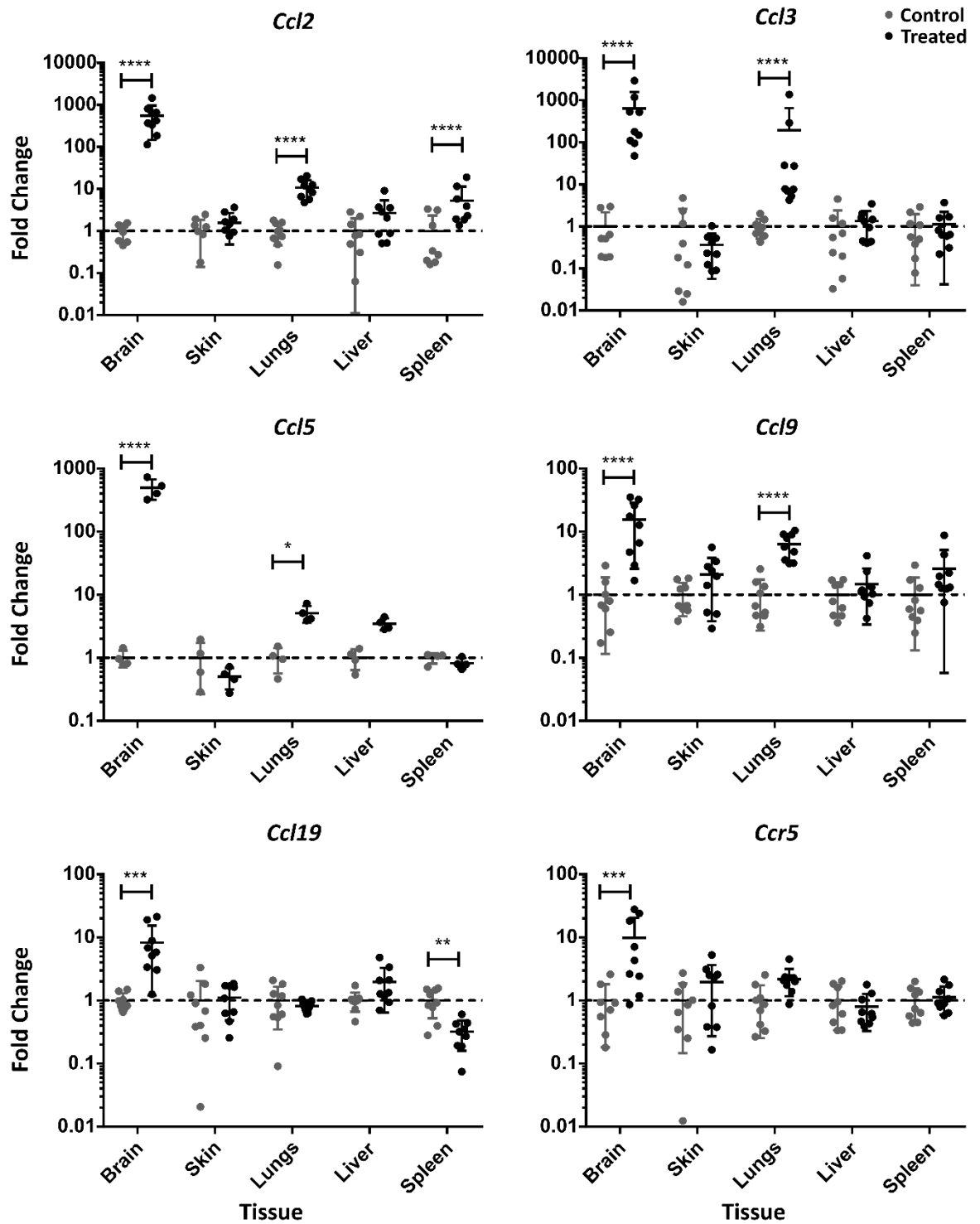


Figure 4.2: 3-day Aldara Model CC Chemokine Transcript.

Mice were treated daily with 62.5mg Aldara cream (5% imiquimod) or control cream on the dorsal skin for 3-days prior to perfusion and tissue collection. Arbitrary expression values from qRT-PCR were normalised to *tbp* housekeeping gene. Individual fold changes were calculated compared to average of controls for that tissue (n=9; 2 experiments shown, for Ccl15 n=4). Tested after log-transformation using Two-way ANOVA and post-hoc Student's t-test with Bonferonni multiple testing correction. *= $P < 0.05$; **= $P < 0.01$; ***= $P < 0.001$; ****= $P < 0.0001$. Bars represent mean \pm SD.

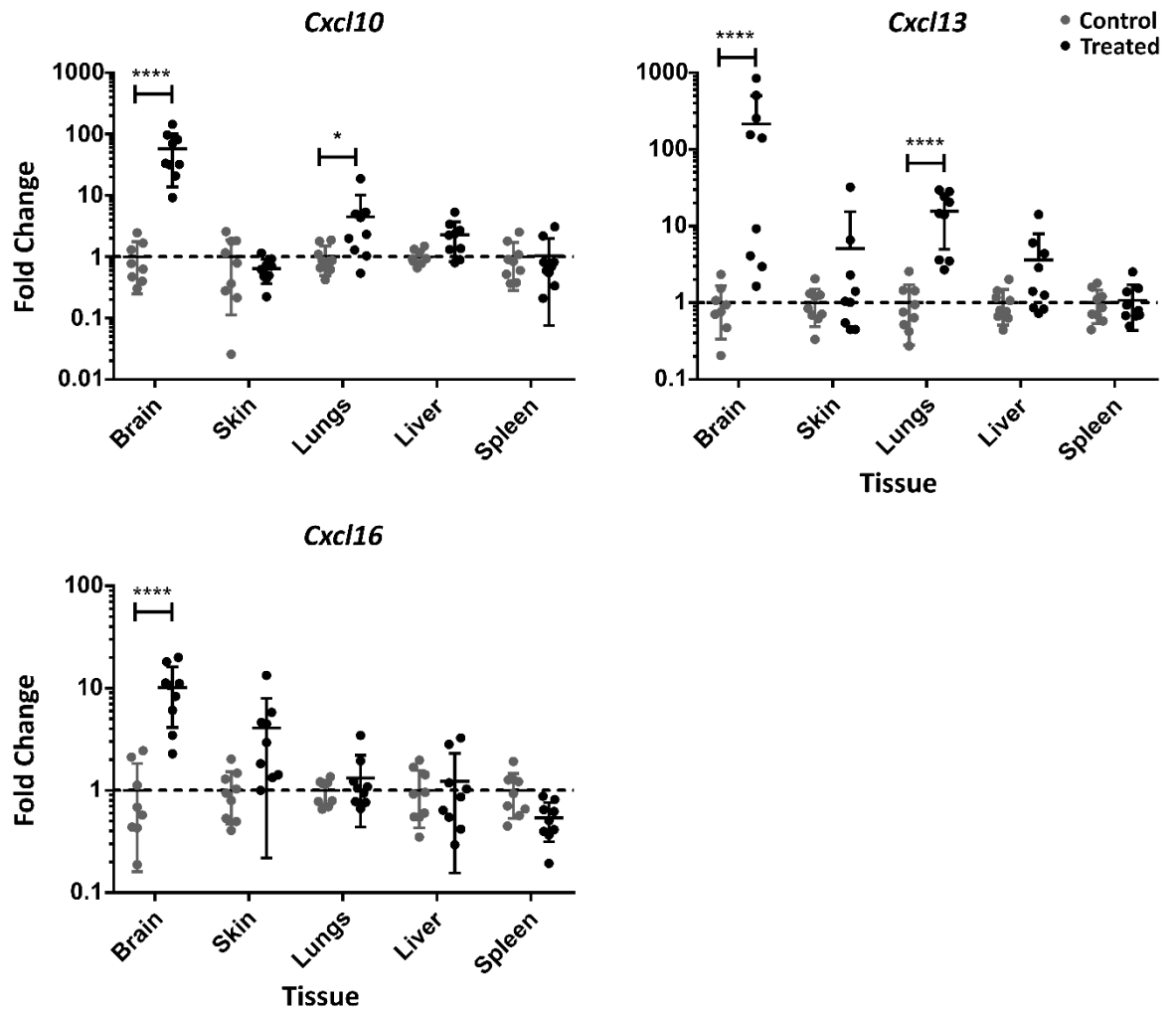


Figure 4.3: 3-day Aldara Model CXC Chemokine Transcript.

Mice were treated daily with 62.5mg Aldara cream (5% imiquimod) or control cream on the dorsal skin for 3-days prior to perfusion and tissue collection. Arbitrary expression values from qRT-PCR were normalised to *tbp* housekeeping gene. Individual fold changes were calculated compared to average of controls for that tissue (n=9; 2 experiments shown). Tested after log-transformation using Two-way ANOVA and post-hoc Student's t-test with Bonferonni multiple testing correction. * = P < 0.05; ** = P < 0.01; *** = P < 0.001; **** = P < 0.0001. Bars represent mean \pm SD.

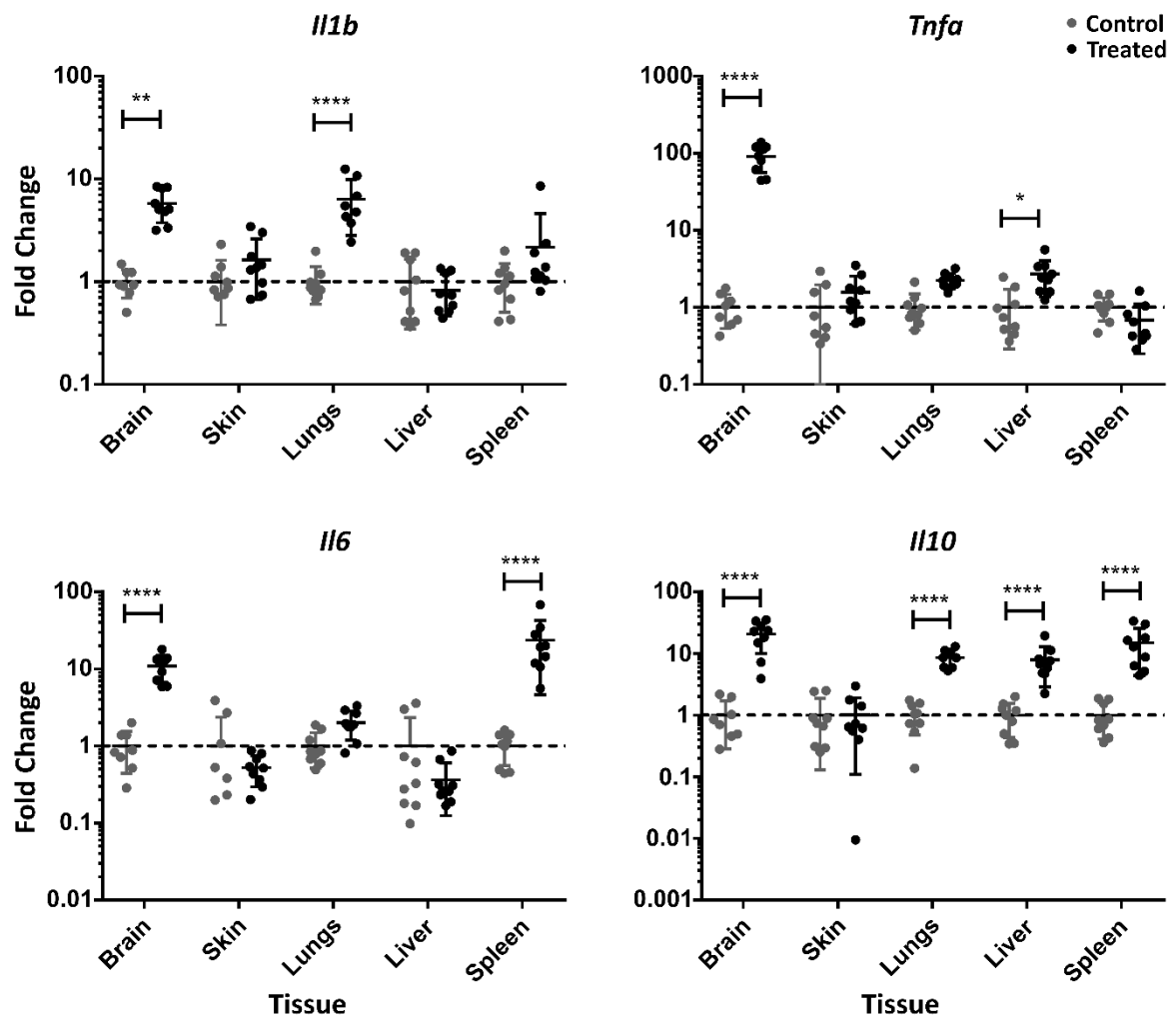


Figure 4.4: 3-day Aldara Model Cytokine Transcript.

Mice were treated daily with 62.5mg Aldara cream (5% imiquimod) or control cream on the dorsal skin for 3-days prior to perfusion and tissue collection. Arbitrary expression values from qRT-PCR were normalised to *tbp* housekeeping gene. Individual fold changes were calculated compared to average of controls for that tissue (n=9; 2 experiments shown). Tested after log-transformation using Two-way ANOVA and post-hoc Student's t-test with Bonferonni multiple testing correction. *= $P < 0.05$; **= $P < 0.01$; ***= $P < 0.001$; ****= $P < 0.0001$. Bars represent mean \pm SD.

4.2.3 The effect of repeated cutaneous treatment with Aldara on mouse weight and skin thickness over a 5-day timecourse

Following on from the identification of these changes after 3 days of treatment responses across a range of time-points were next examined to provide further information as to the time-course of the response. As had been done for the initial 3 day experiment, the skin and weight response of C57BL6/J mice to daily treatment of Aldara was examined. Similar to the 3-day experiment we found significant decreases in weight for treated animals when compared to controls (Figure 4.5A). After 2 days of treatment the mice appeared to begin to start

regaining weight. Despite this, significant differences in weight change persisted until 4 days after treatment.

Although within the first 24 hours there were no significant alterations in epidermal thickening, after three days of Aldara treatment there were significant increases in the epidermal:dermal ratio that persisted until 5 days of treatment (Figure 4.5B). There was no significant difference in epidermal:dermal ratio between 3 and 5 days of treatment. By 24 hours post-treatment there does appear to be some evidence of epidermal hyperplasia occurring (Figure 4.5C). However, this is not significant and is less obvious histologically than at 3 and 5 days post-treatment.

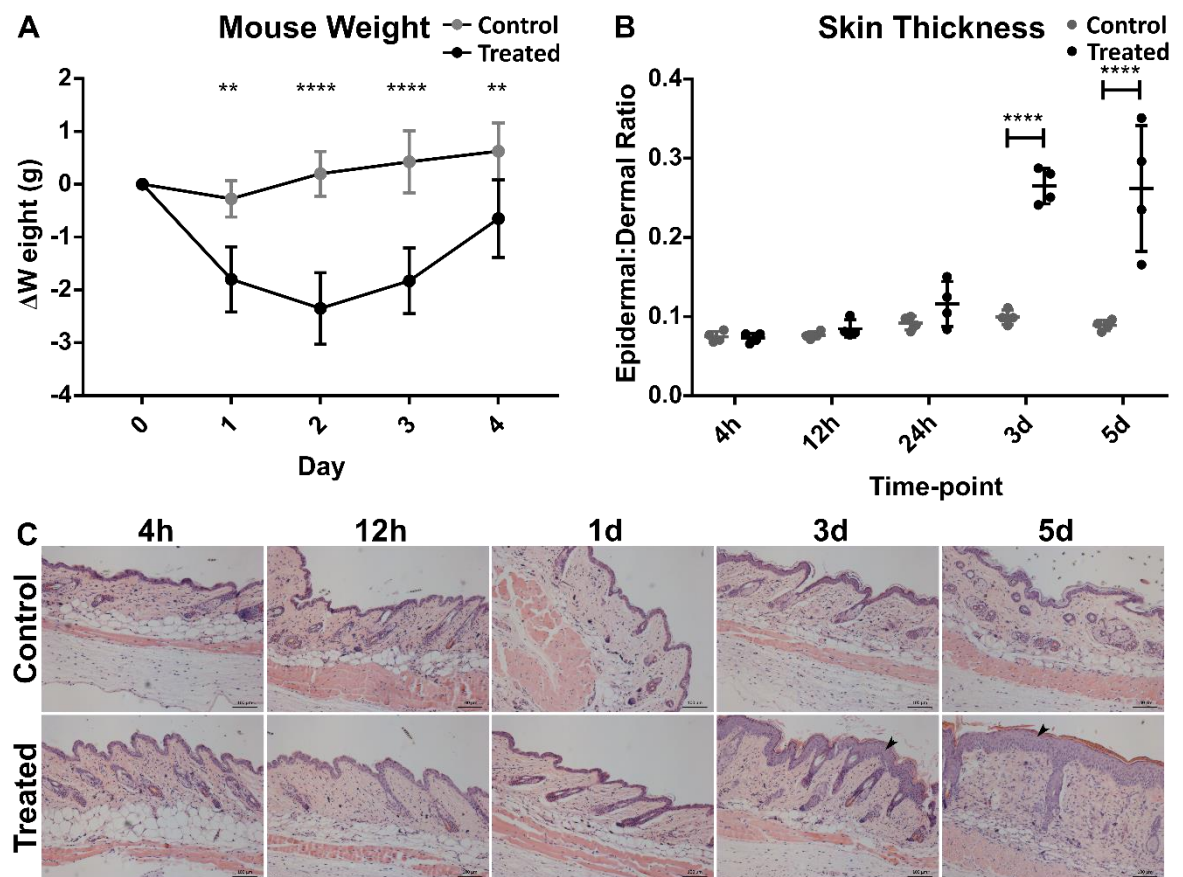


Figure 4.5: Time-course Aldara Model Weight Change and Skin Haematoxylin & Eosin. Mice were weighed and then treated daily with 62.5mg Aldara cream (5% imiquimod) or control cream on the dorsal skin. Tissue was collected at 4, 12 and 24 hours and 3 and 5 days. (A) Mouse weight change from baseline over 4 days of treatment (n=4, weight change for 5 day mice shown) Tested using Two-way ANOVA and post-hoc Student's t-test with Bonferroni multiple testing correction. (B) Epidermis:dermis ratio as an average from 3 sections per mouse (n=4) Tested using One-way ANOVA and post-hoc Student's t-test with Bonferroni multiple testing correction. (C) Representative figures of skin H&E. * $P < 0.05$; **** $P < 0.0001$. Scale bars = 100 μ m. Bars represent mean \pm SD.

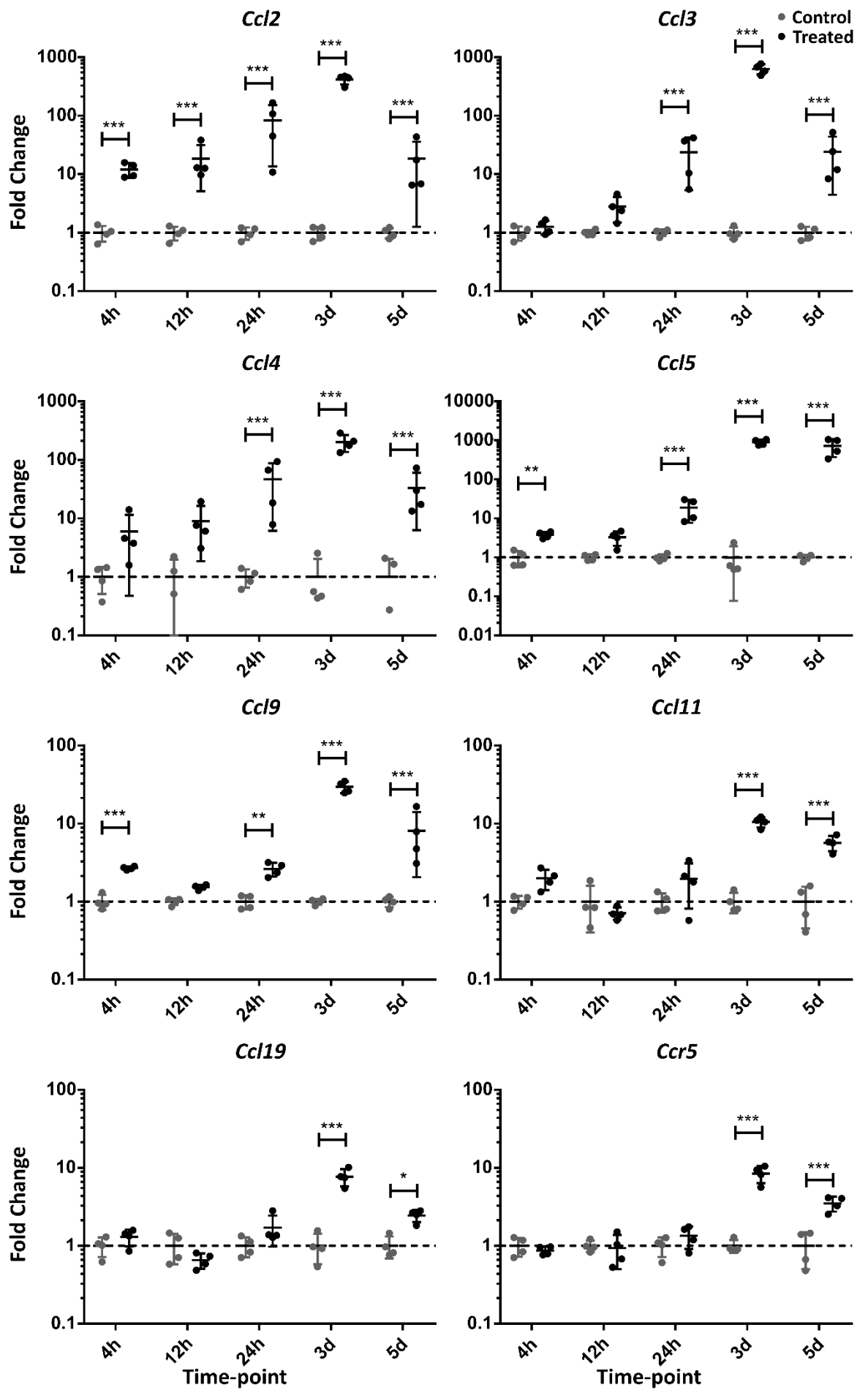
4.2.4 The effect of repeated cutaneous treatment with Aldara on chemokine and cytokine transcription in the brain over a 5-day timecourse

Following on from the finding of significant transcriptional upregulations within the brain after 3 days of treatment, it was asked how early these transcriptional responses manifested themselves within the brain and whether at a later time-point (5 days) they persisted. Previous work had demonstrated that ISGs and some chemokines are upregulated after 1-5 days of treatment but did not examine earlier time-points. In addition to the transcripts assayed in the initial 3 day time points we also investigated the expression of *Ccl4*, *Ccl11*, *Cxcl1* and *Cx3cl1* based on emerging evidence of their importance from both our own meta-analysis and other animal studies.

Time-course data revealed that all transcripts examined (*Ccl2*, *Ccl3*, *Ccl4*, *Ccl5*, *Ccl9*, *Ccl11*, *Ccl19*, *Ccr5*, *Cxcl1*, *Cxcl10*, *Cxcl13*, *Cxcl16*, *Il1b*, *Tnfa*, *Il6* and *Il10*) were significantly upregulated at 3 days post-treatment aside from *Cx3cl1* that was not significantly altered at any time point (Figure 4.6, Figure 4.7, Figure 4.8). The general pattern was that, by 1 day post-treatment, there was a significant upregulation of most transcripts, between 1 and 3 days post-treatment there was a continuing increase in the level of transcript compared to controls, and by 5 days post-treatment this had begun to subside although generally it still remained significant. Aside from these broad patterns it is worth identifying other notable results from this time-course. A small number of transcripts were rapidly upregulated by 4 hours post-treatment (*Ccl2*, *Ccl5*, *Ccl9* and *Cxcl10*), interestingly both *Ccl5* and *Ccl9* were not found to be significantly upregulated after 12 hours and upregulation of *Cxcl10* was ameliorated when compared to 4 hours (Figure 4.6, Figure 4.7). Aside from these rapidly upregulated transcripts, both *Cxcl1* and *Il1b* were only upregulated at 3 days post-treatment (Figure 4.7, Figure 4.8).

Figure 4.6: (Overleaf) Time-course Aldara Model Brain CC Chemokine Transcript.

Mice were treated daily with 62.5mg Aldara cream (5% imiquimod) or control cream on the dorsal skin. Brain tissue was collected at 4, 12 and 24 hours and 3 and 5 days. Arbitrary expression values from qRT-PCR were normalised to *tbp* housekeeping gene. Individual fold changes were calculated compared to average of controls for that time-point (n=4). Tested after log-transformation using One-way ANOVA and post-hoc Student's t-test with Bonferonni multiple testing correction. *= $P < 0.05$; **= $P < 0.01$; ***= $P < 0.001$; ****= $P < 0.0001$. Bars represent mean \pm SD.



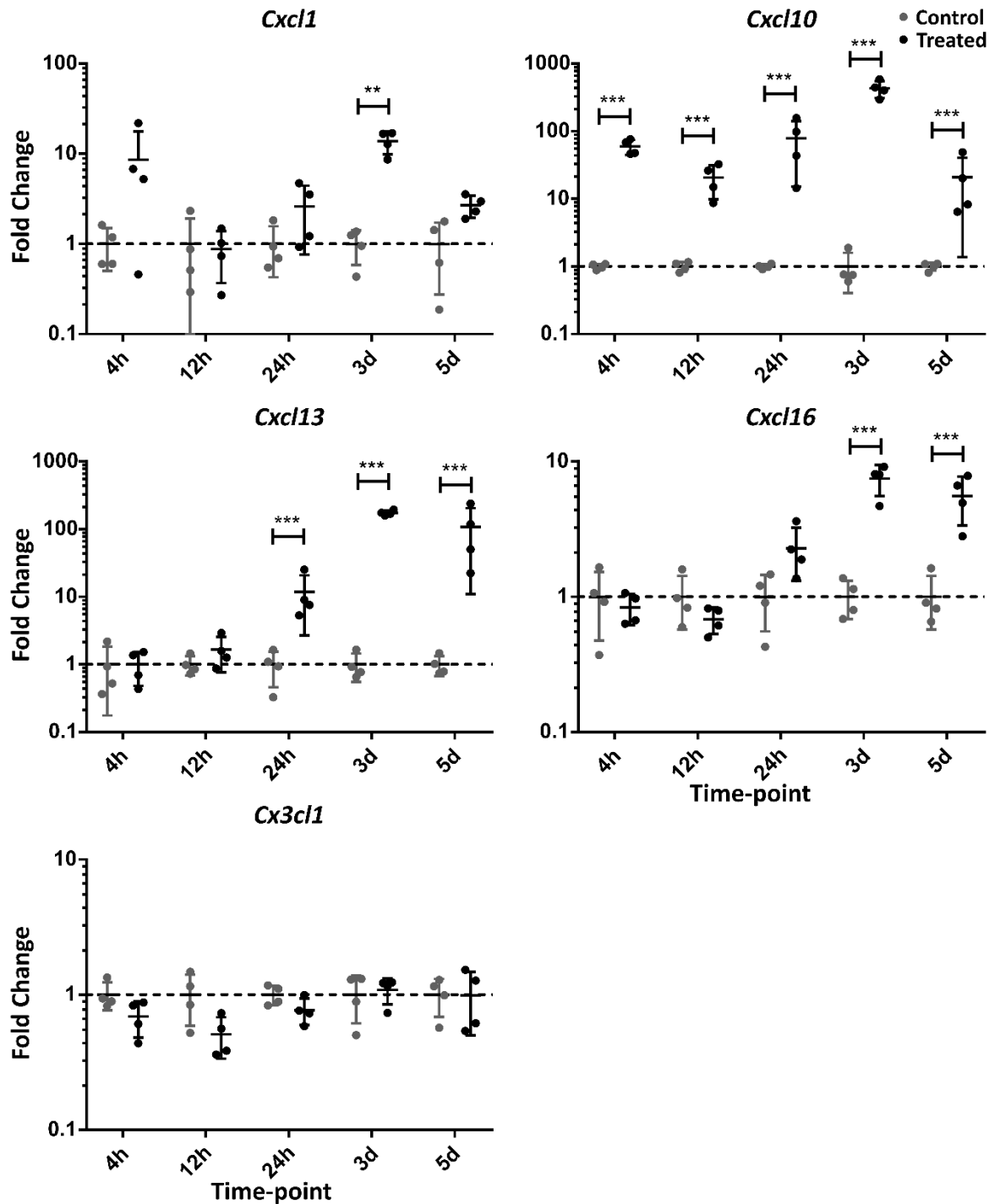


Figure 4.7: Time-course Aldara Model Brain CXC Chemokine Transcript.

Mice were treated daily with 62.5mg Aldara cream (5% imiquimod) or control cream on the dorsal skin. Brain tissue was collected at 4, 12 and 24 hours and 3 and 5 days. Arbitrary expression values from qRT-PCR were normalised to *tbp* housekeeping gene. Individual fold changes were calculated compared to average of controls for that time-point (n=4). Tested after log-transformation using One-way ANOVA and post-hoc Student's t-test with Bonferonni multiple testing correction. * = P < 0.05; ** = P < 0.01; *** = P < 0.001; **** = P < 0.0001. Bars represent mean ± SD.

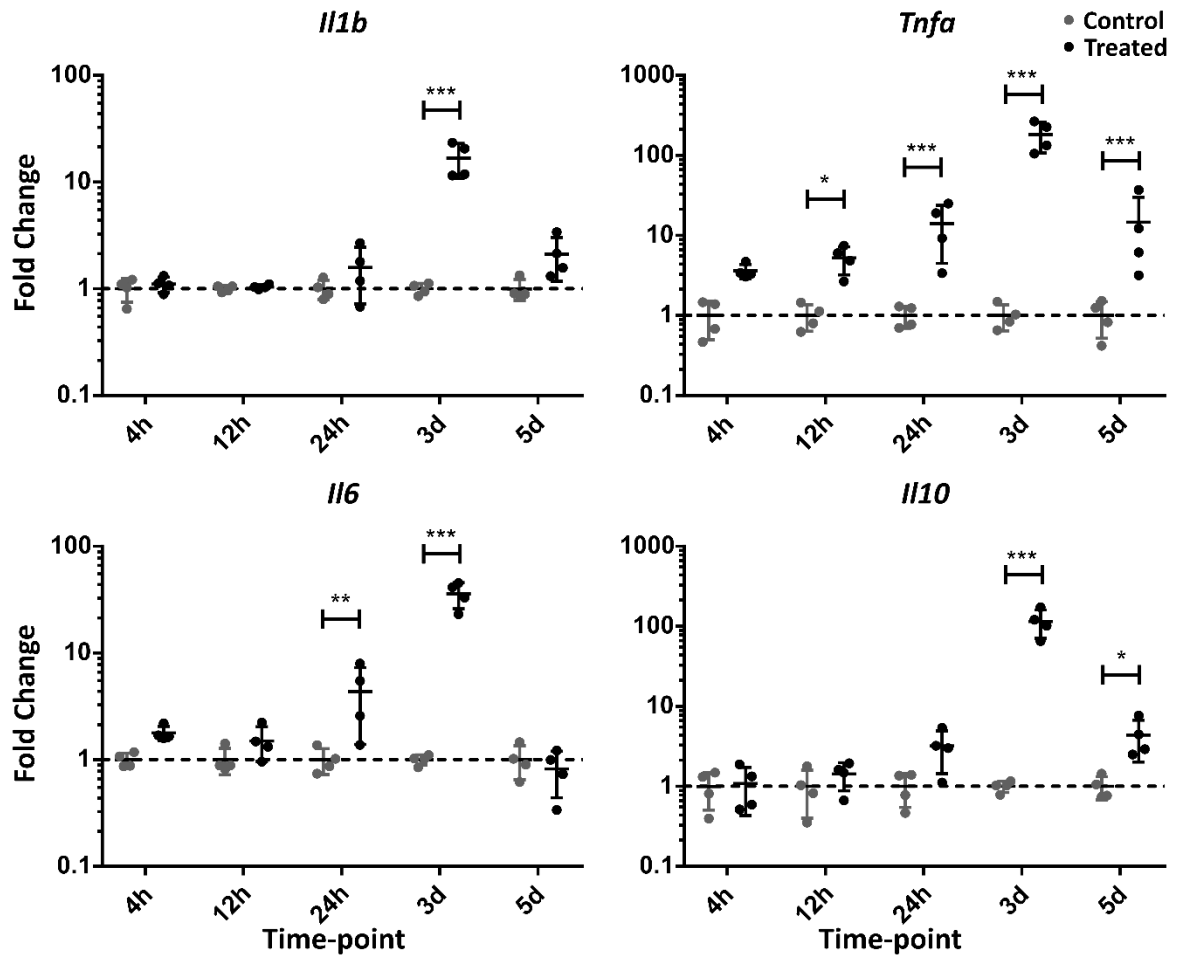


Figure 4.8: Time-course Aldara Model Brain Cytokine Transcript.

Mice were treated daily with 62.5mg Aldara cream (5% imiquimod) or control cream on the dorsal skin. Brain tissue was collected at 4, 12 and 24 hours and 3 and 5 days. Arbitrary expression values from qRT-PCR were normalised to *tbp* housekeeping gene. Individual fold changes were calculated compared to average of controls for that time-point (n=4). Tested after log-transformation using One-way ANOVA and post-hoc Student's t-test with Bonferonni multiple testing correction. * = P < 0.05; ** = P < 0.01; *** = P < 0.001; **** = P < 0.0001. Bars represent mean \pm SD.

4.2.5 The effect of repeated cutaneous treatment with Aldara on chemokine and cytokine transcription in the periphery over a 5-day timecourse

After the finding of large differences between the brain and the peripheral organs at 3 days post treatment the peripheral tissues were next examined in the time-course analysis to determine if transcriptional differences between the brain and peripheral organs were due to a lack of upregulation at any time point, or due to temporal differences between the brain and periphery. In addition, to assess the circulating transcriptional profile, PBL gene expression was also examined alongside the previously mentioned peripheral organs. Due to technical issues the spleen was excluded from this time course analysis.

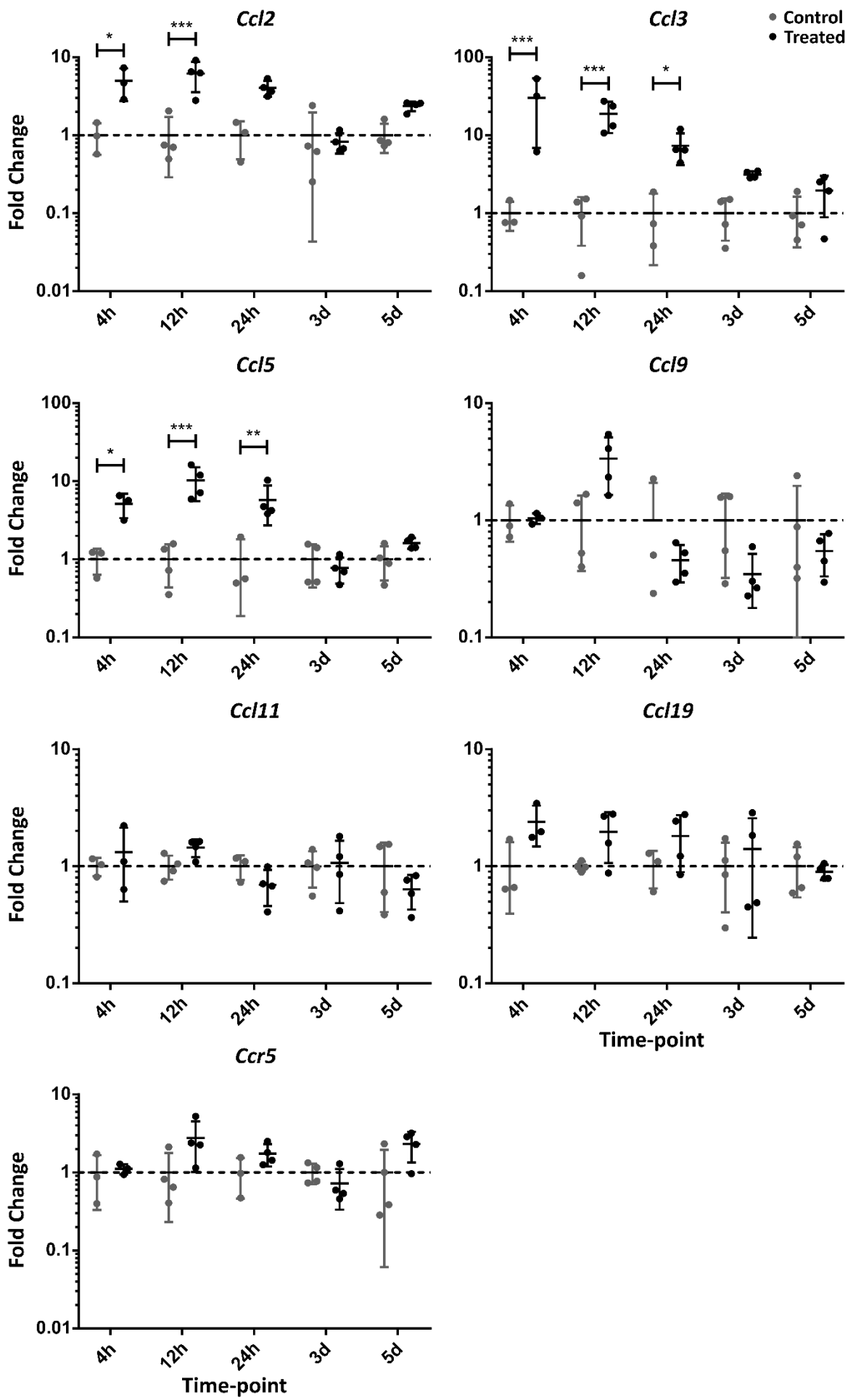


Figure 4.9: (Previous page) Time-course Aldara Model Skin CC Chemokine Transcript.

Mice were treated daily with 62.5mg Aldara cream (5% imiquimod) or control cream on the dorsal skin. Skin tissue was collected at 4, 12 and 24 hours and 3 and 5 days. Arbitrary expression values from qRT-PCR were normalised to *tbp* housekeeping gene. Individual fold changes were calculated compared to average of controls for that time-point (n=3-4). Tested after log-transformation using one-way ANOVA and post-hoc Student's t-test with Bonferonni multiple testing correction. *= $P < 0.05$; **= $P < 0.01$; ***= $P < 0.001$; ****= $P < 0.0001$. Bars represent mean \pm SD.

4.2.5.1 Skin and PBL chemokine and cytokine transcriptional responses

Examination of the skin showed that there was a limited transcriptional response to Aldara treatment, although *Ccl2*, *Ccl3*, *Ccl5* and *Cxcl10* were significantly upregulated after 4 hours persisting until 12 or 24 hours post-treatment (Figure 4.9, Figure 4.10). The remaining chemokines were not significantly upregulated at any time point. Examining the cytokine responses there was a transient upregulation of *Il10* at 12 hours post-treatment and *Il6* was significantly upregulated from 24 hours post-treatment until 3 days post-treatment returning to control levels by 5 days post-treatment (Figure 4.11). While striking that there was a lack of upregulation in some of the other transcripts RIN values (Appendix 4) indicated that the RNA was of adequate quality for qRT-PCR applications.

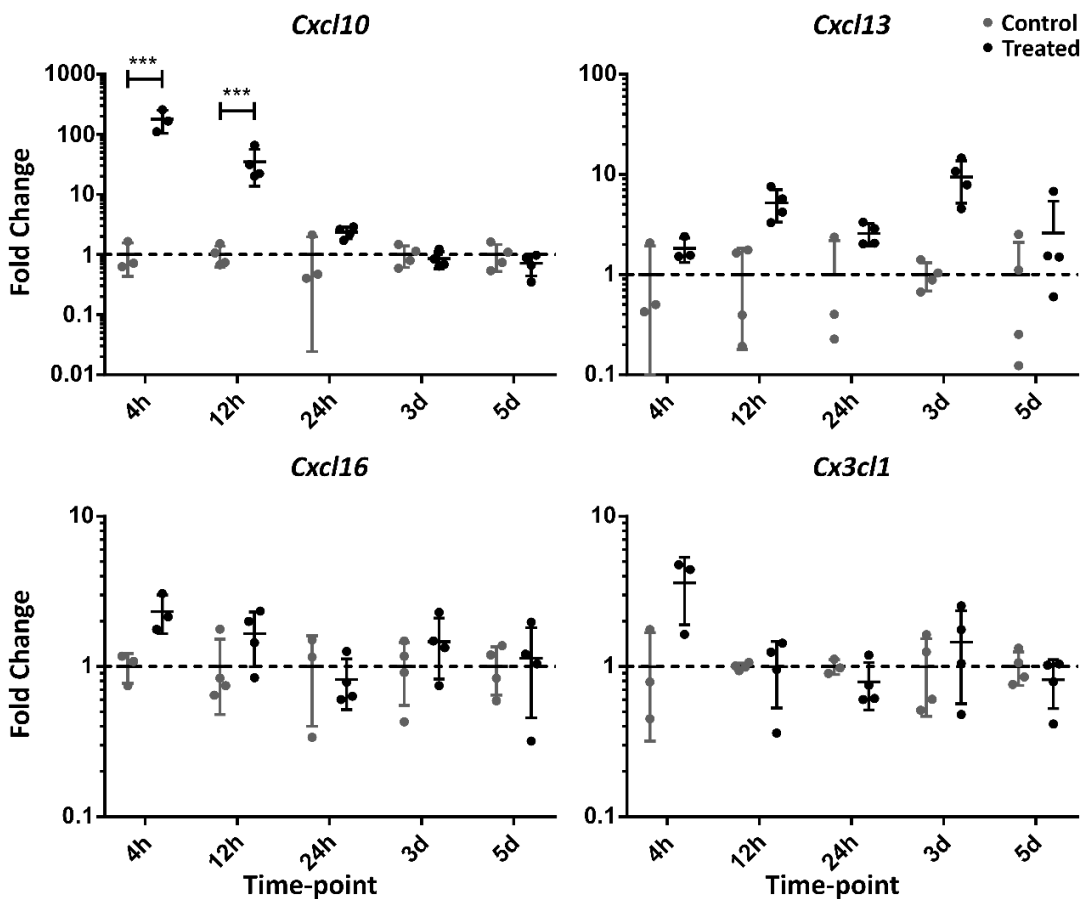
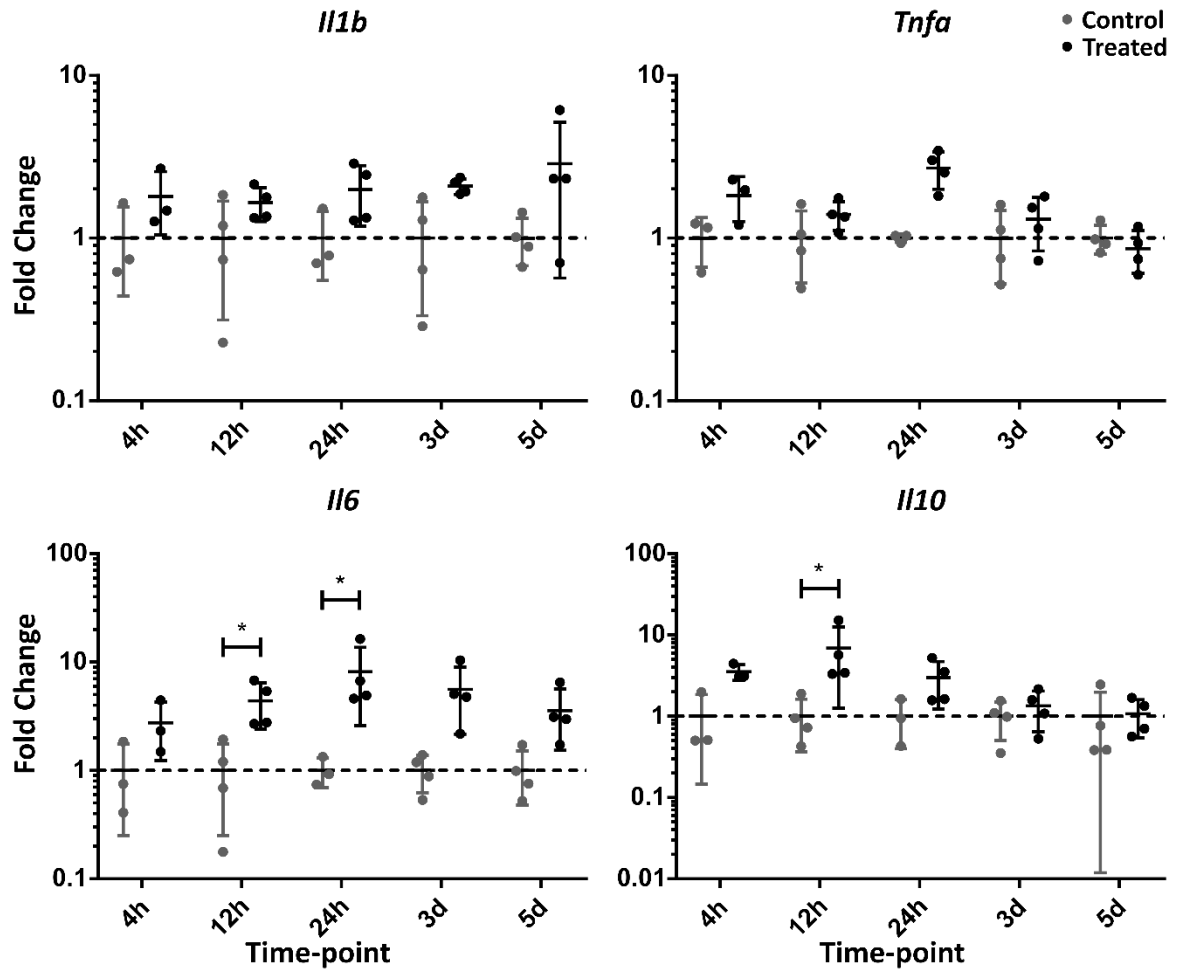


Figure 4.10: (Previous page) Time-course Aldara Model Skin CXC Chemokine Transcript.

Mice were treated daily with 62.5mg Aldara cream (5% imiquimod) or control cream on the dorsal skin. Skin tissue was collected at 4, 12 and 24 hours and 3 and 5 days. Arbitrary expression values from qRT-PCR were normalised to *tbp* housekeeping gene. Individual fold changes were calculated compared to average of controls for that time-point (n=3-4). Tested after log-transformation using one-way ANOVA and post-hoc Student's t-test with Bonferonni multiple testing correction. *= $P < 0.05$; **= $P < 0.01$; ***= $P < 0.001$; ****= $P < 0.0001$. Bars represent mean \pm SD.

**Figure 4.11: Time-course Aldara Model Skin Cytokine Transcript.**

Mice were treated daily with 62.5mg Aldara cream (5% imiquimod) or control cream on the dorsal skin. Skin tissue was collected at 4, 12 and 24 hours and 3 and 5 days. Arbitrary expression values from qRT-PCR were normalised to *tbp* housekeeping gene. Individual fold changes were calculated compared to average of controls for that time-point (n=3-4). Tested after log-transformation using one-way ANOVA and post-hoc Student's t-test with Bonferonni multiple testing correction. *= $P < 0.05$; **= $P < 0.01$; ***= $P < 0.001$; ****= $P < 0.0001$. Bars represent mean \pm SD.

Next, the circulatory response was investigated as represented by the transcriptional response of PBL. Here, there was a more diverse upregulation of transcript when compared to the skin. Similarly to the skin, *Ccl2*, *Ccl3*, *Ccl5* and *Cxcl10* were significantly upregulated when compared to controls, in addition there were significant alterations of *Ccl9*, *Cxcl13* and *Ccr5* (Figure 4.12, Figure 4.13). Alongside these changes in chemokine gene expression, there was also significant upregulation of all cytokine transcripts (*Il1b*, *Tnfa*, *Il6*, *Il10*) (Figure 4.14). Although the precise pattern of upregulation varied between transcripts generally speaking by 4 hours post-treatment significant changes were present and these persisted for up to 3 days of treatment. An exception to this was *Il1b* that was only significantly upregulated at 4 hours (Figure 4.14). In addition, *Cxcl13* and *Ccl9* did not become significantly altered until 12 hours and 24 hours post-treatment respectively (Figure 4.12, Figure 4.13).

Overall gene expression changes in both the skin and the PBL demonstrated a pattern of upregulation that was rapid and transient returning to control levels between the 24 hour and 3 day time-point for most transcripts. All measured transcripts returned to control levels after 5 days of treatment. In addition, for all transcripts that were significantly altered peak response points were within the first 24 hours aside from *Il10* in PBL that showed a similar magnitude of upregulation at both 24 hour and 3 day time-points.

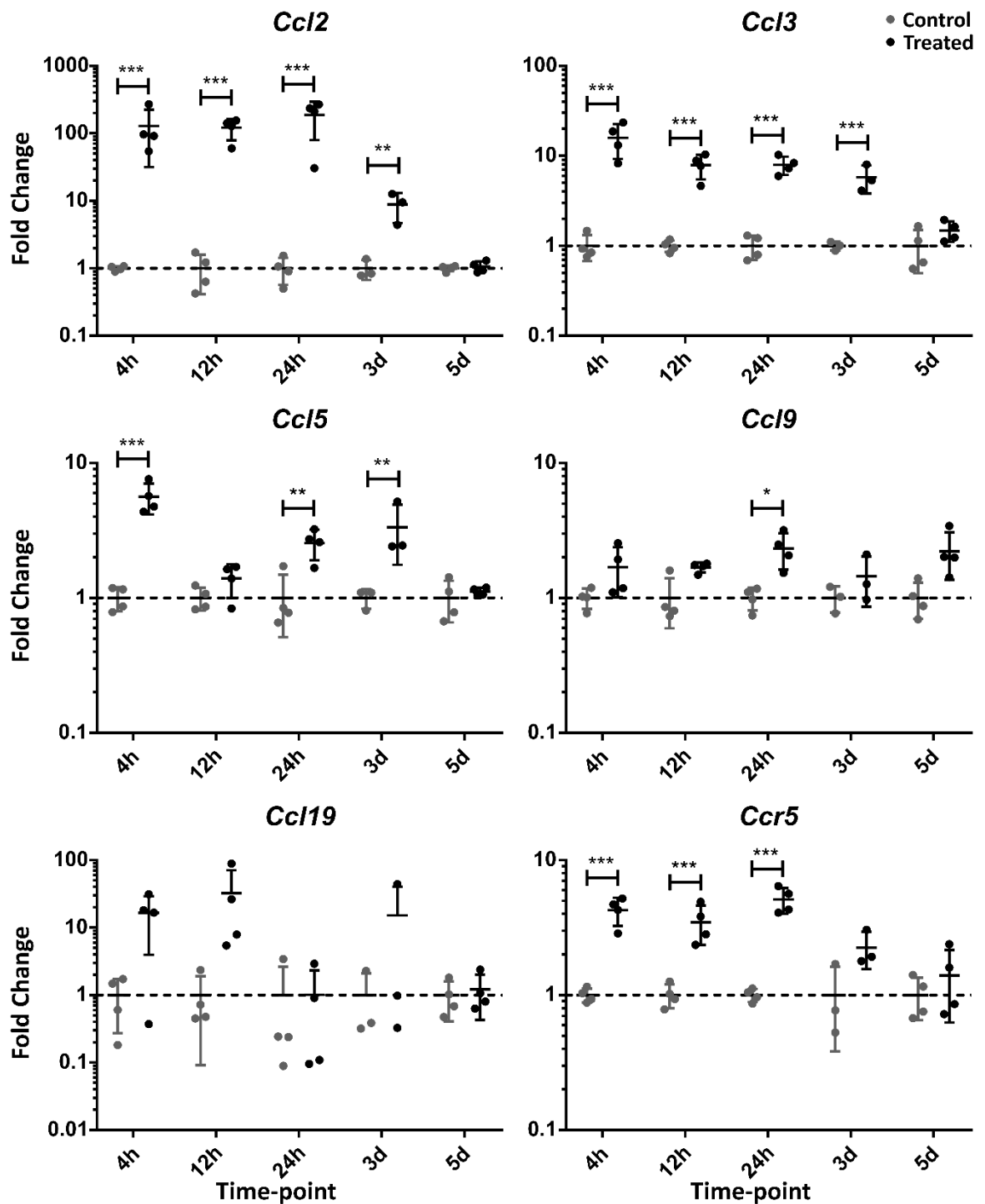


Figure 4.12: Time-course Aldara Model PBL CC Chemokine Transcript.

Mice were treated daily with 62.5mg Aldara cream (5% imiquimod) or control cream on the dorsal skin. PBL were collected at 4, 12 and 24 hours and 3 and 5 days. Arbitrary expression values from qRT-PCR were normalised to *tbp* housekeeping gene. Individual fold changes were calculated compared to average of controls for that time-point (n=3-4). Tested after log-transformation using one-way ANOVA and post-hoc Student's t-test with Bonferonni multiple testing correction.

*=P<0.05; **=P<0.01; ***=P<0.001; ****=P<0.0001. Bars represent mean \pm SD.

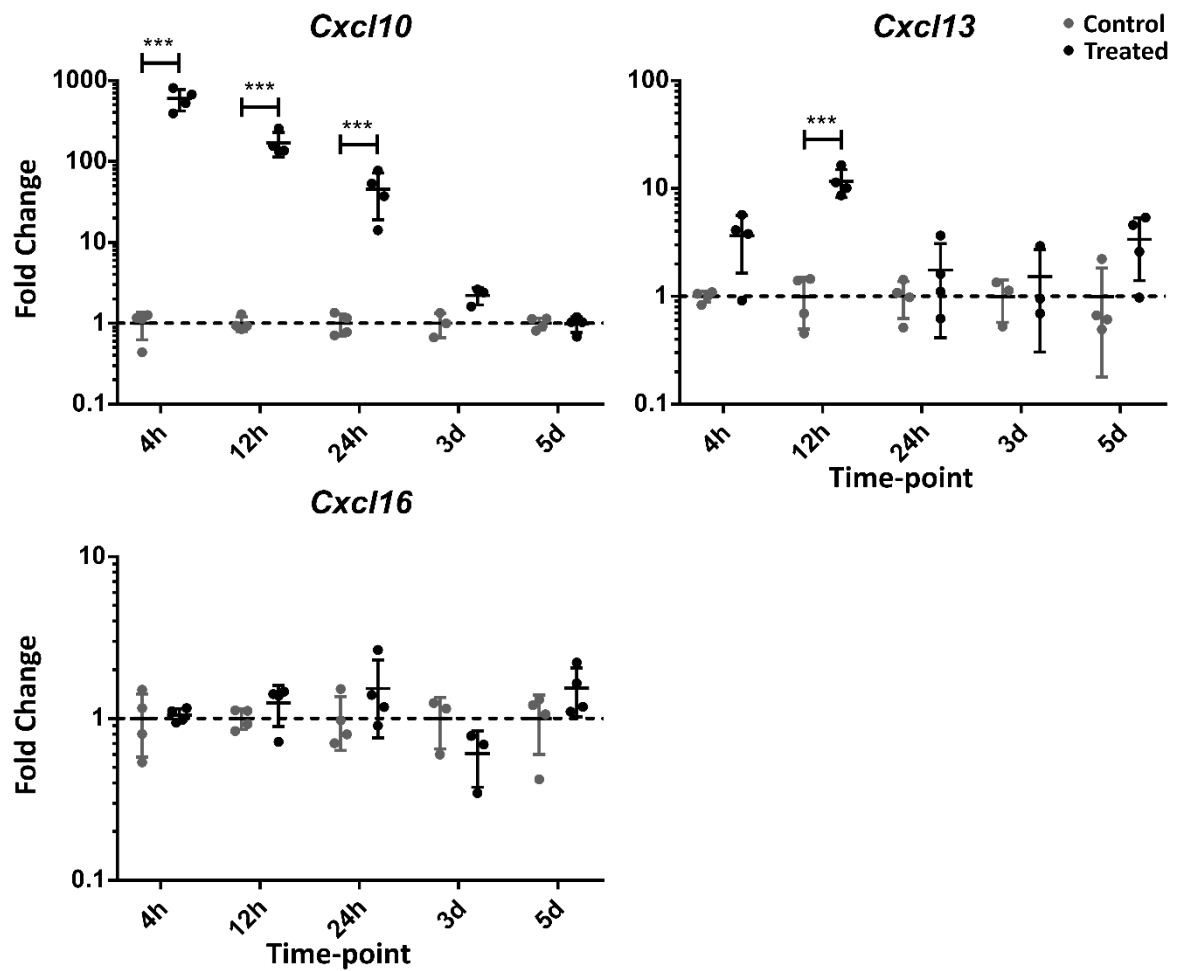


Figure 4.13: Time-course Aldara Model PBL CXC Chemokine Transcript.

Mice were treated daily with 62.5mg Aldara cream (5% imiquimod) or control cream on the dorsal skin. PBL were collected at 4, 12 and 24 hours and 3 and 5 days. Arbitrary expression values from qRT-PCR were normalised to *tbp* housekeeping gene. Individual fold changes were calculated compared to average of controls for that time-point (n=3-4). Tested after log-transformation using one-way ANOVA and post-hoc Student's t-test with Bonferonni multiple testing correction. *= $P < 0.05$; **= $P < 0.01$; ***= $P < 0.001$; ****= $P < 0.0001$. Bars represent mean \pm SD.

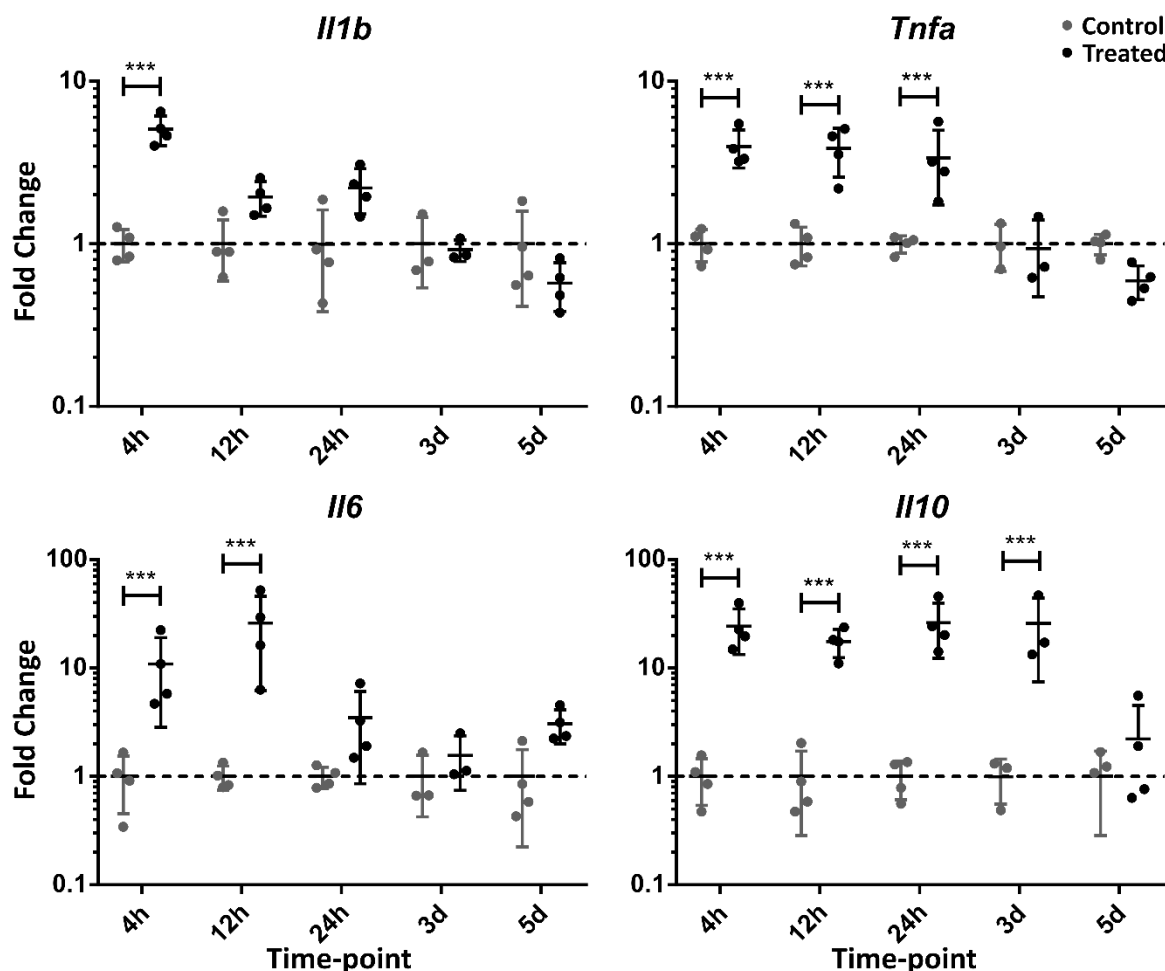


Figure 4.14: Time-course Aldara Model PBL Cytokine Transcript.

Mice were treated daily with 62.5mg Aldara cream (5% imiquimod) or control cream on the dorsal skin. PBL were collected at 4, 12 and 24 hours and 3 and 5 days. Arbitrary expression values from qRT-PCR were normalised to *tbp* housekeeping gene. Individual fold changes were calculated compared to average of controls for that time-point (n=3-4). Tested after log-transformation using one-way ANOVA and post-hoc Student's t-test with Bonferonni multiple testing correction. *= $P < 0.05$; **= $P < 0.01$; ***= $P < 0.001$; ****= $P < 0.0001$. Bars represent mean \pm SD.

4.2.5.2 Liver chemokine and cytokine transcriptional responses

Analysis of the liver showed a change in the pattern of upregulation when compared to the skin and PBL, with more prolonged alterations in a number of transcripts. Similar to the PBL there was a significant upregulation of *Ccl2*, *Ccl3*, *Ccl5*, *Cxcl10* and *Cxcl13* alongside the cytokines *Tnfa*, *Il6* and *Il10* (Figure 4.15, Figure 4.16, Figure 4.17). Like both the PBLs and skin, peak responses within the liver occurred within the first 24 hours including for *Il10*. In contrast, there were no significant alterations in *Ccl9*, *Ccr5* or *Il1b*. Unlike the PBLs and skin a small number of transcripts remained elevated after 5 days of treatment in the liver (*Ccl3*, *Ccl5*, *Cxcl13* and *Il10*), although the magnitude of upregulation was relatively small compared to peak response points.

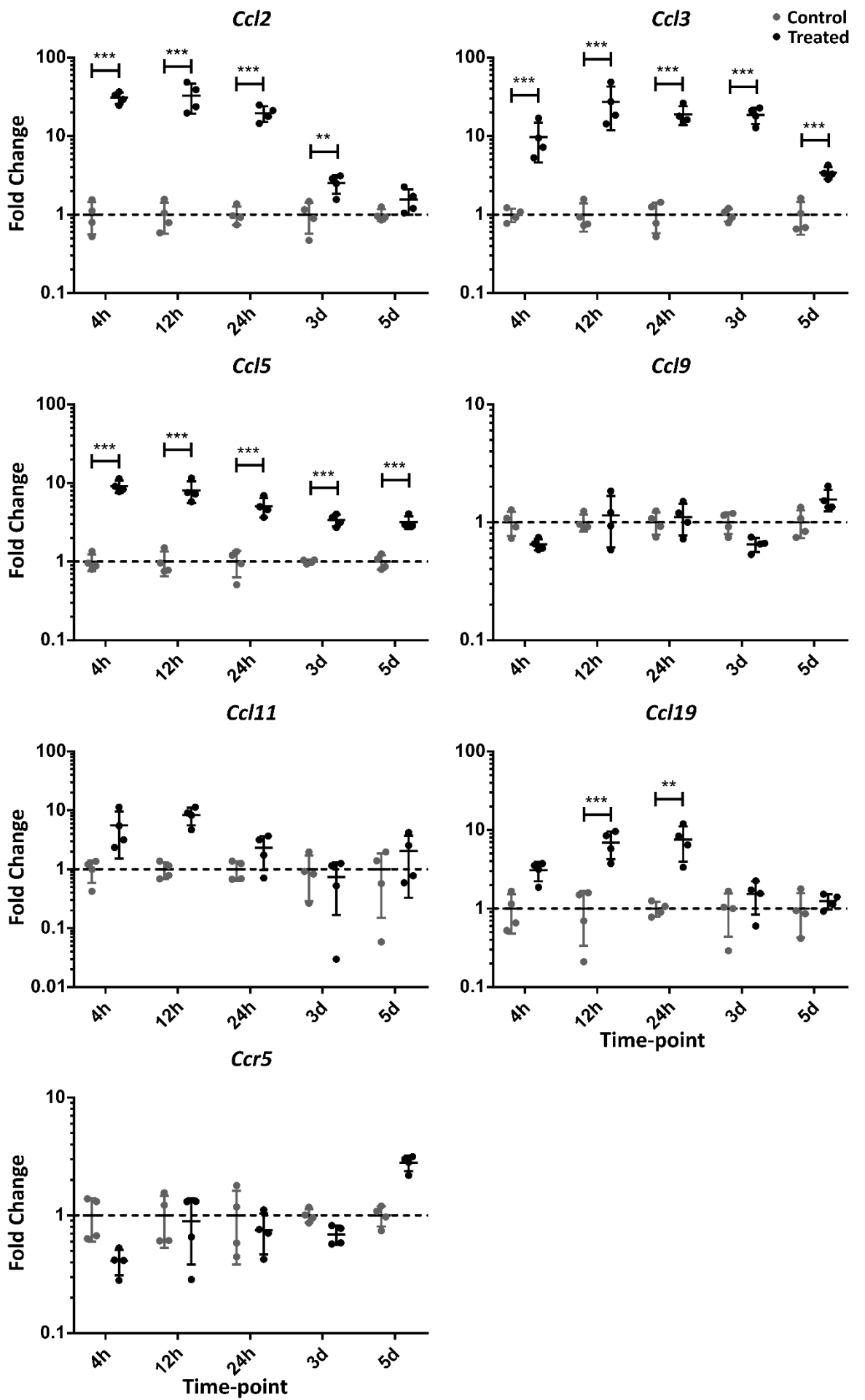
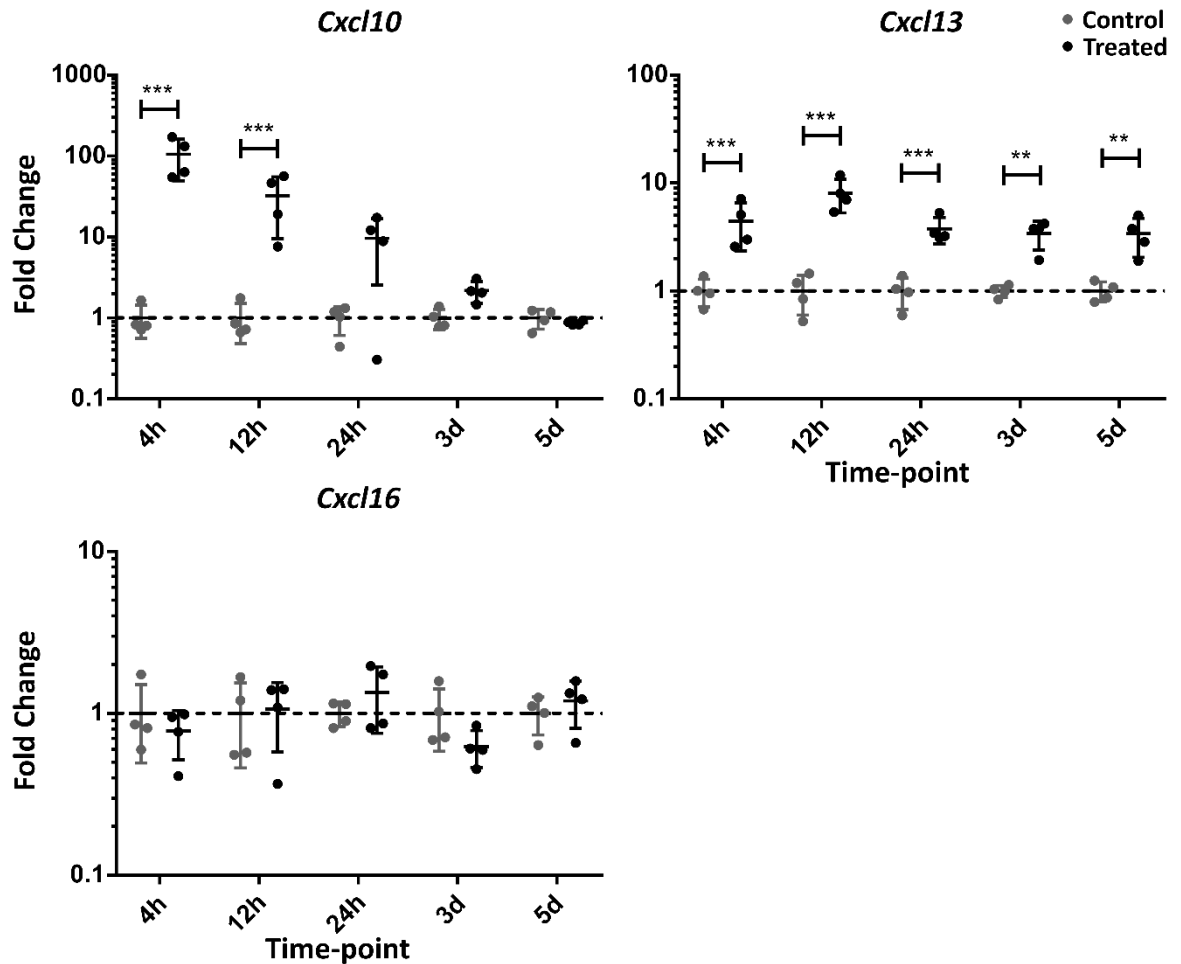


Figure 4.15: (Previous page) Time-course Aldara Model Liver CC Chemokine Transcript.

Mice were treated daily with 62.5mg Aldara cream (5% imiquimod) or control cream on the dorsal skin. Liver tissue was collected at 4, 12 and 24 hours and 3 and 5 days. Arbitrary expression values from qRT-PCR were normalised to *tbp* housekeeping gene. Individual fold changes were calculated compared to average of controls for that time-point (n=4). Tested after log-transformation using one-way ANOVA and post-hoc Student's t-test with Bonferonni multiple testing correction. *= $P < 0.05$; **= $P < 0.01$; ***= $P < 0.001$; ****= $P < 0.0001$. Bars represent mean \pm SD.

**Figure 4.16: Time-course Aldara Model Liver CXC Chemokine Transcript.**

Mice were treated daily with 62.5mg Aldara cream (5% imiquimod) or control cream on the dorsal skin. Liver tissue was collected at 4, 12 and 24 hours and 3 and 5 days. Arbitrary expression values from qRT-PCR were normalised to *tbp* housekeeping gene. Individual fold changes were calculated compared to average of controls for that time-point (n=4). Tested after log-transformation using Two-way ANOVA and post-hoc Student's t-test with Bonferonni multiple testing correction. *= $P < 0.05$; **= $P < 0.01$; ***= $P < 0.001$; ****= $P < 0.0001$. Bars represent mean \pm SD.

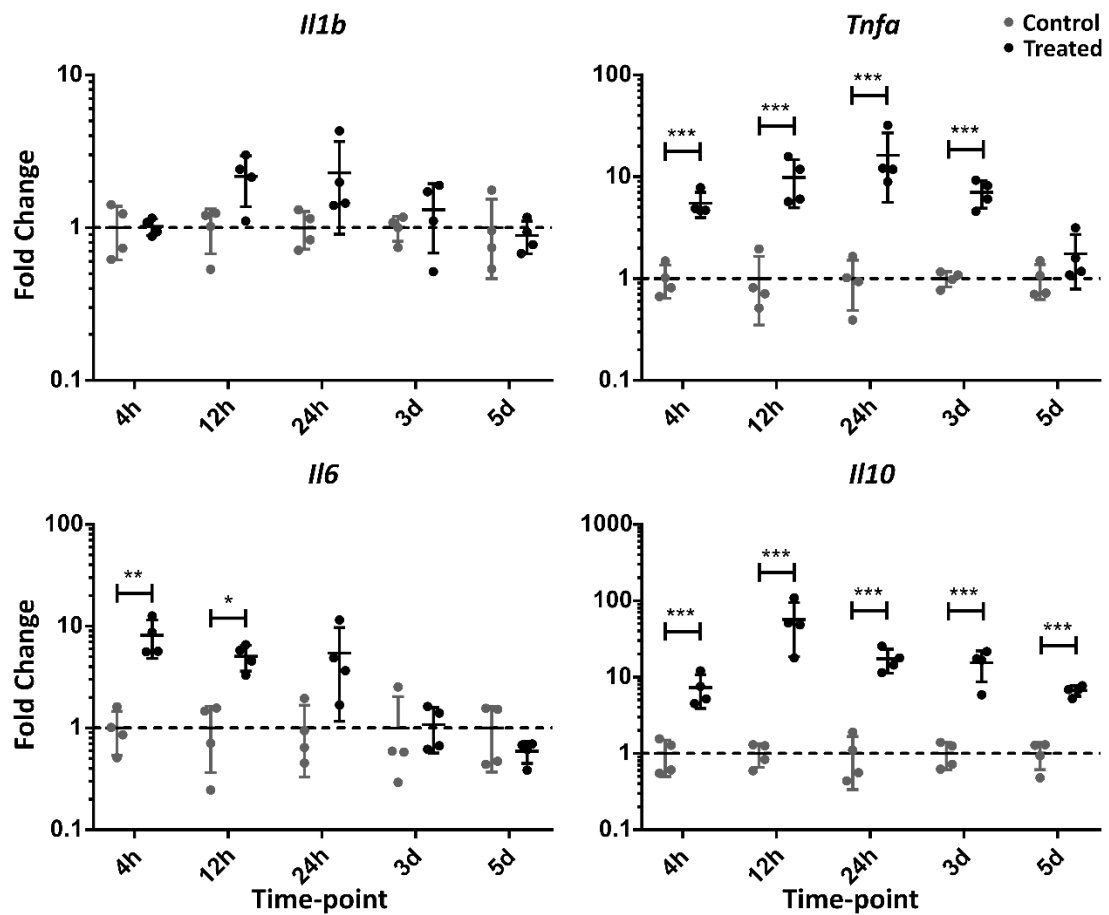


Figure 4.17: Time-course Aldara Model Liver Cytokine Transcript.

Mice were treated daily with 62.5mg Aldara cream (5% imiquimod) or control cream on the dorsal skin. Liver tissue was collected at 4, 12 and 24 hours and 3 and 5 days. Arbitrary expression values from qRT-PCR were normalised to *tbp* housekeeping gene. Individual fold changes were calculated compared to average of controls for that time-point (n=4). Tested after log-transformation using one-way ANOVA and post-hoc Student's t-test with Bonferonni multiple testing correction. *= $P < 0.05$; **= $P < 0.01$; ***= $P < 0.001$; ****= $P < 0.0001$. Bars represent mean \pm SD.

4.2.5.3 Lungs chemokine and cytokine transcriptional responses

Finally, the transcriptional response within the lungs was examined, this response was similar to other organs in that the chemokines *Ccl2*, *Ccl3*, *Ccl5*, *Ccl9*, *Cxcl10*, *Cxcl13* and *Ccr5* and the cytokines *Il1b*, *Tnfa*, *Il6* and *Il10* were upregulated (Figure 4.18, Figure 4.19, Figure 4.20). Unlike any of the other peripheral organs there were small but significant upregulations of *Cxcl16* and *Cx3cl1* after 4 hours, although these did not persist past this time point. The lungs, like the liver, demonstrated a more prolonged upregulation of a number of transcripts that persisted until 5 days of treatment. Alongside those found to be upregulated in the liver at 5 days (*Ccl3*, *Ccl5*, *Cxcl13* and *Il10*) additional transcripts were still significantly altered (*Ccl2*, *Ccl9*, *Cxcl10*, *Ccr5*, *Il1b* and *Il6*) in the day 5 lung.

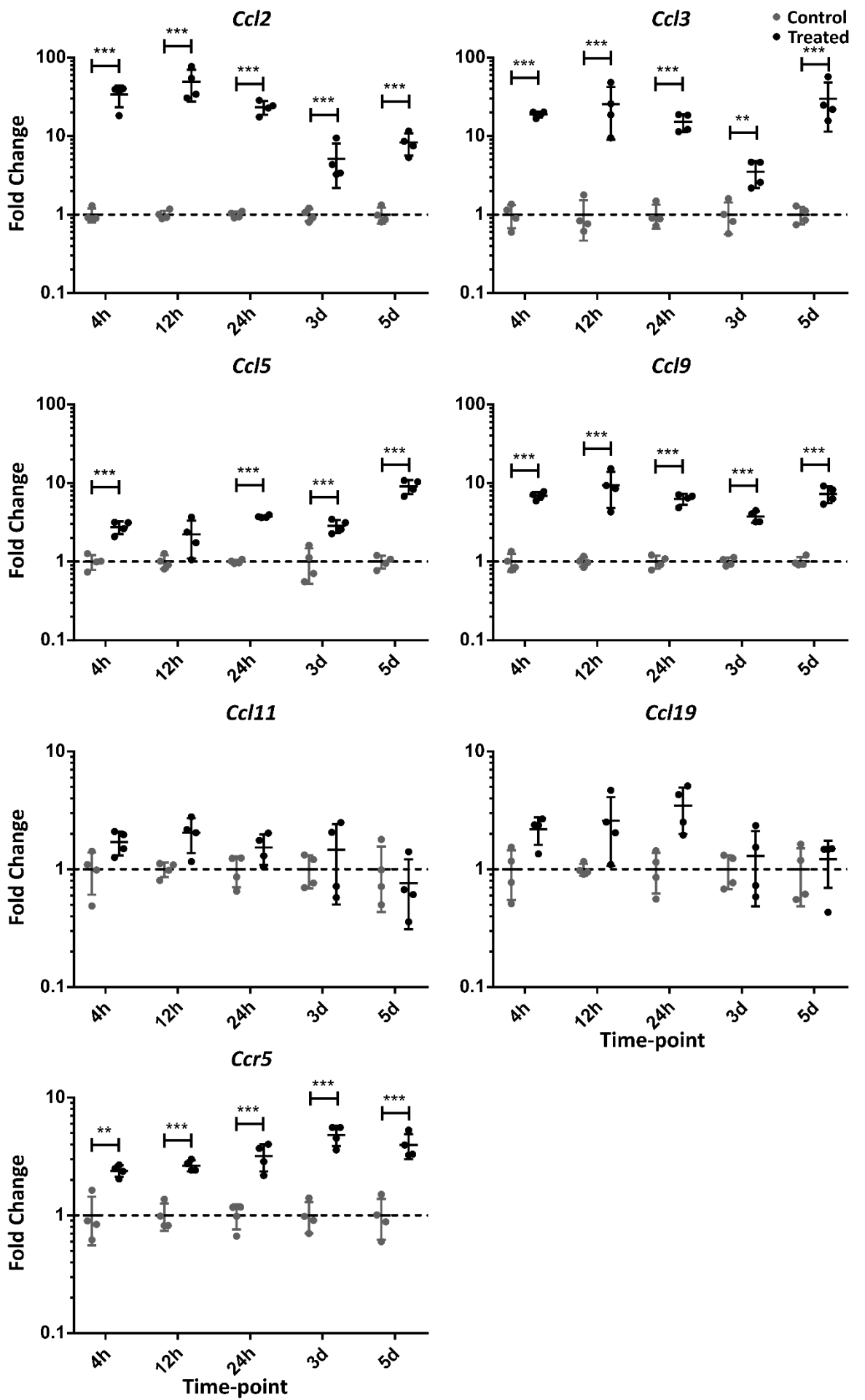
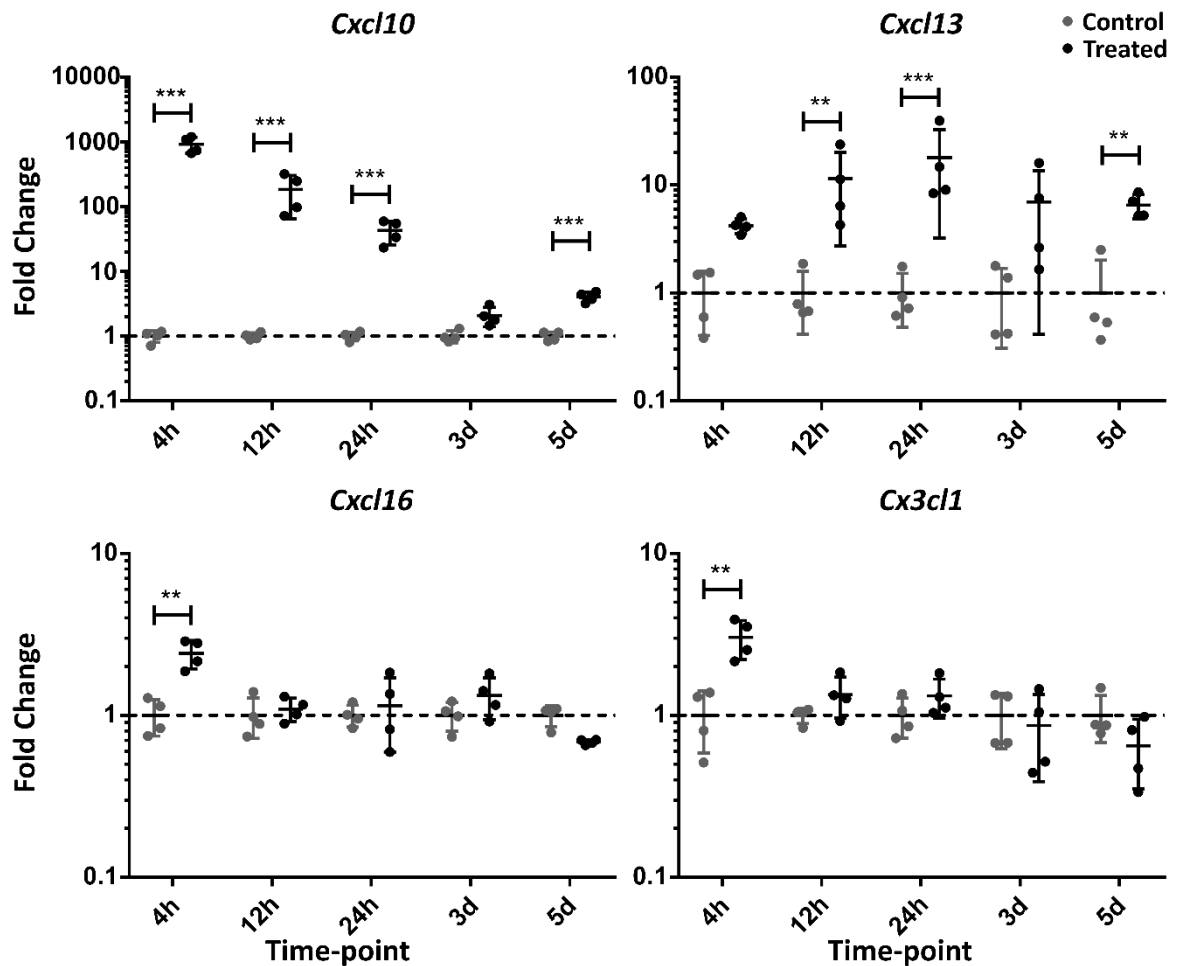


Figure 4.18: Time-course Aldara Model Lungs CC Chemokine Transcript.

Mice were treated daily with 62.5mg Aldara cream (5% imiquimod) or control cream on the dorsal skin. Lung tissue was collected at 4, 12 and 24 hours and 3 and 5 days. Arbitrary expression values from qRT-PCR were normalised to *tbp* housekeeping gene. Individual fold changes were calculated compared to average of controls for that time-point (n=4). Tested after log-transformation using one-way ANOVA and post-hoc Student's t-test with Bonferonni multiple testing correction. *= $P < 0.05$; **= $P < 0.01$; ***= $P < 0.001$; ****= $P < 0.0001$. Bars represent mean \pm SD.

**Figure 4.19: Time-course Aldara Model Lungs CXC Chemokine Transcript.**

Mice were treated daily with 62.5mg Aldara cream (5% imiquimod) or control cream on the dorsal skin. Lung tissue was collected at 4, 12 and 24 hours and 3 and 5 days. Arbitrary expression values from qRT-PCR were normalised to *tbp* housekeeping gene. Individual fold changes were calculated compared to average of controls for that time-point (n=4). Tested after log-transformation using one-way ANOVA and post-hoc Student's t-test with Bonferonni multiple testing correction. *= $P < 0.05$; **= $P < 0.01$; ***= $P < 0.001$; ****= $P < 0.0001$. Bars represent mean \pm SD.

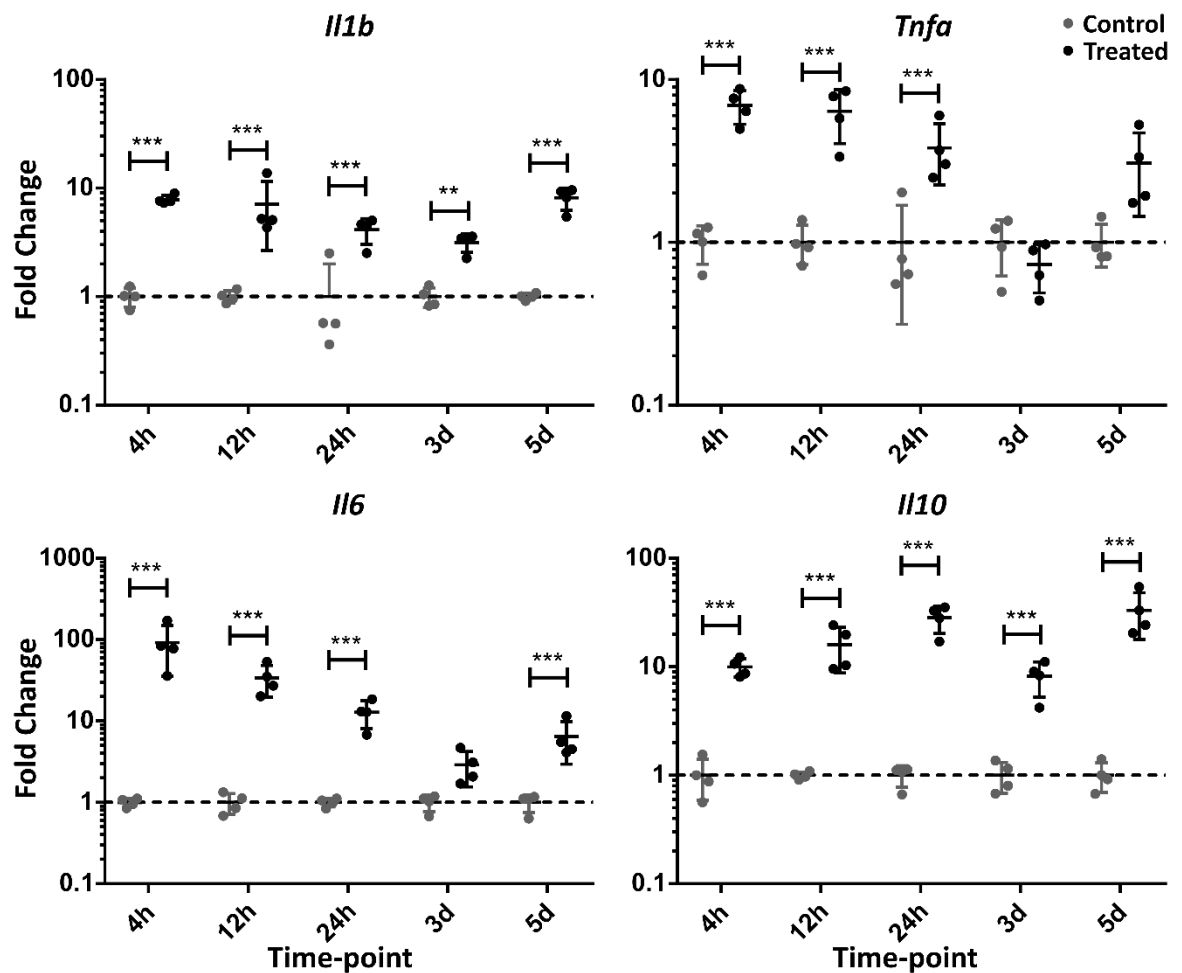


Figure 4.20: Time-course Aldara Model Lungs Cytokine Transcript.

Mice were treated daily with 62.5mg Aldara cream (5% imiquimod) or control cream on the dorsal skin. Lung tissue was collected at 4, 12 and 24 hours and 3 and 5 days. Arbitrary expression values from qRT-PCR were normalised to *tbp* housekeeping gene. Individual fold changes were calculated compared to average of controls for that time-point (n=4). Tested after log-transformation using one-way ANOVA and post-hoc Student's t-test with Bonferonni multiple testing correction. *= $P < 0.05$; **= $P < 0.01$; ***= $P < 0.001$; ****= $P < 0.0001$. Bars represent mean \pm SD.

4.2.6 Comparison of the response between 1- and 3-days in the brain and periphery

Considering the fact that nearly all peripheral transcripts peaked within the first 24 hours and the brain response appeared to consistently peak at 3 days post-treatment, temporal differences between the brain and periphery were next compared. To this end, the relative change in magnitude of response between 1 day and 3 days post-treatment was examined. This clearly revealed that for all transcripts examined within the brain there was a continuing upregulation of the response whereas when looking at peripheral responses to Aldara treatment there was a return towards control levels in nearly all transcripts examined (Figure 4.21). The only major exception to this was *Ccl19* in the PBL, but this is

likely attributable to the outlier present for this transcript at this time-point and removal of this sample abolished this effect.

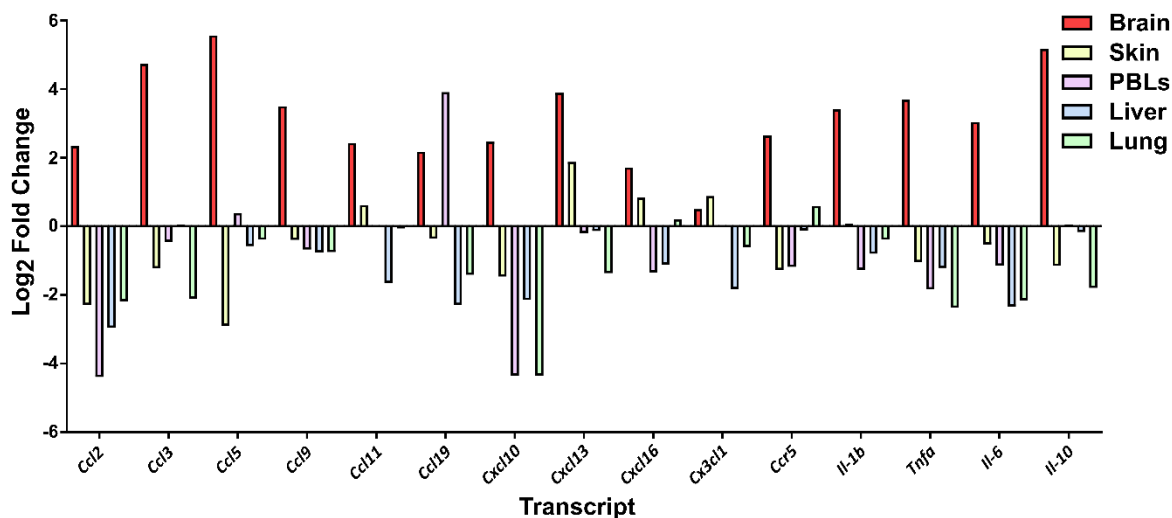


Figure 4.21: Time-course Aldara Model 1 day to 3 day relative gene expression change. Mice were treated daily with 62.5mg Aldara cream (5% imiquimod) or control cream on the dorsal skin. Tissue was collected at 24 hours and 3 days. Fold change values for 3 days were compared to 24 hours and relative fold changes calculated.

4.2.7 The effect of repeated cutaneous treatment on chemokine and cytokine protein levels in the brain over a 5-day time-course

After identifying a significant upregulation of chemokine and cytokine gene expression within the brain following Aldara treatment, it was important to determine if this transcriptional response was translated to changes in protein levels and over what time period. Using a multiplex array approach that had as much overlap with our previously examined genes as possible we assessed protein levels in the brains of mice treated with Aldara.

Protein assay showed that for all qRT-PCR targets that were included in the array there was significant upregulation at the protein level (CCL2, CCL3, CCL4, CCL5, CCL11, CXCL1, CXCL10, CXCL13, Il-1 β , TNF- α , Il-6 and Il-10) (Figure 4.22, Figure 4.23, Figure 4.24). Alongside these upregulations another ISG CXCL9 was found to be significantly upregulated and both IFN β and IFN γ were raised. The peak response point for all proteins was after 3 days of treatment which matches up with transcriptional data. Alongside this, many proteins were found to be significantly altered within 4 hours suggesting a rapid brain response to the peripheral immune stimulus. It is interesting to note that many of the

chemokines and cytokines examined appear to be constitutively expressed within the CNS as demonstrated by levels consistently above the limit of detection. Overall patterns of upregulation were similar to those observed at a transcriptional level, although for CXCL1 there appeared to be much more significant alterations in protein levels than in transcriptional responses (Figure 4.7, Figure 4.24).

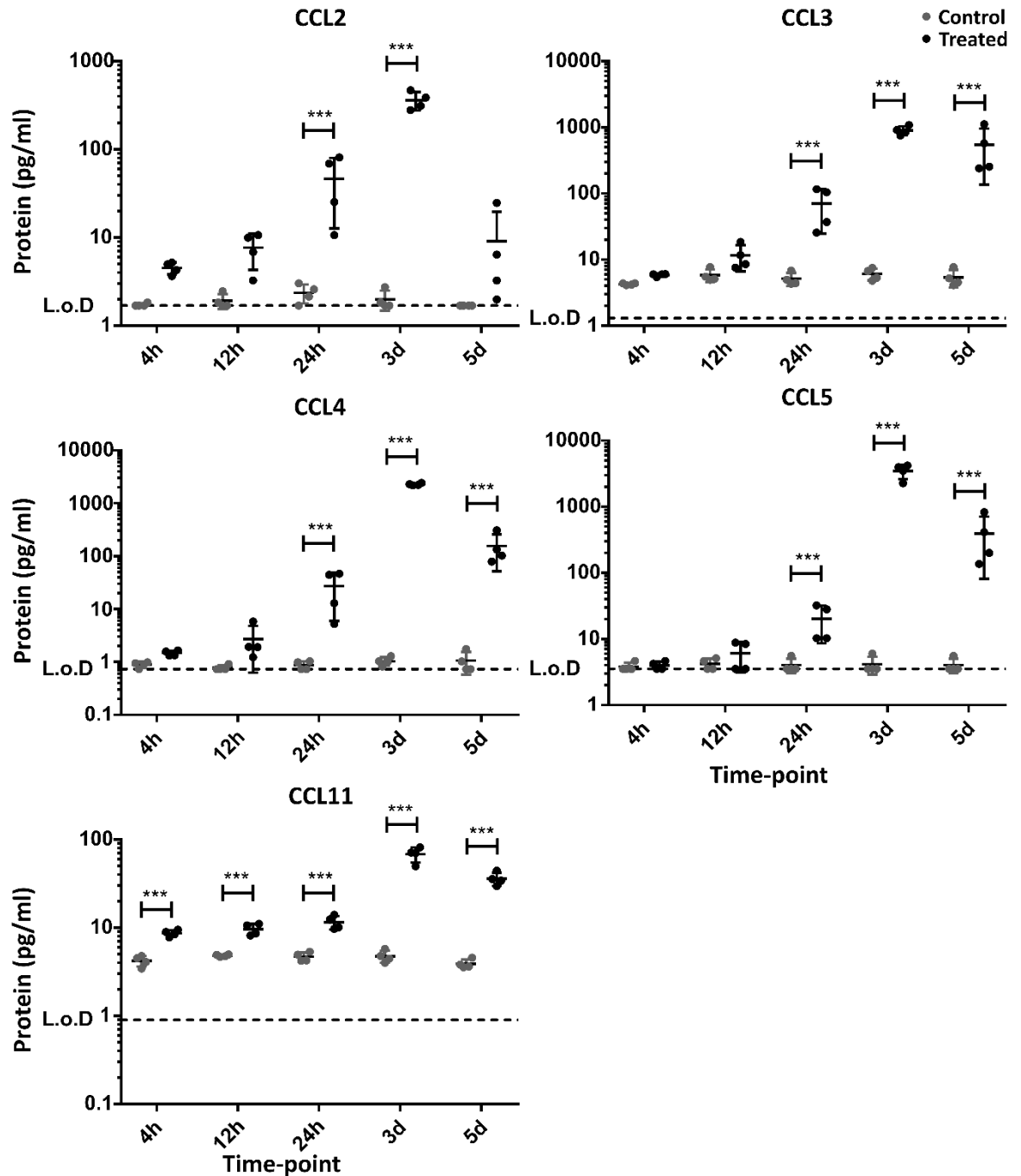


Figure 4.22: Time-course Aldara Model Brain CC Chemokine Protein Expression.

Mice were treated daily with 62.5mg Aldara cream (5% imiquimod) or control cream on the dorsal skin. Brain tissue was collected at 4, 12 and 24 hours and 3 and 5 days. Biologend LegendPlex assay was performed to generate absolute expression values. Tested using One-way ANOVA and post-hoc Student's t-test with Bonferroni multiple testing correction. * = $P < 0.05$; ** = $P < 0.01$; *** = $P < 0.001$; **** = $P < 0.0001$. Bars represent mean \pm SD.

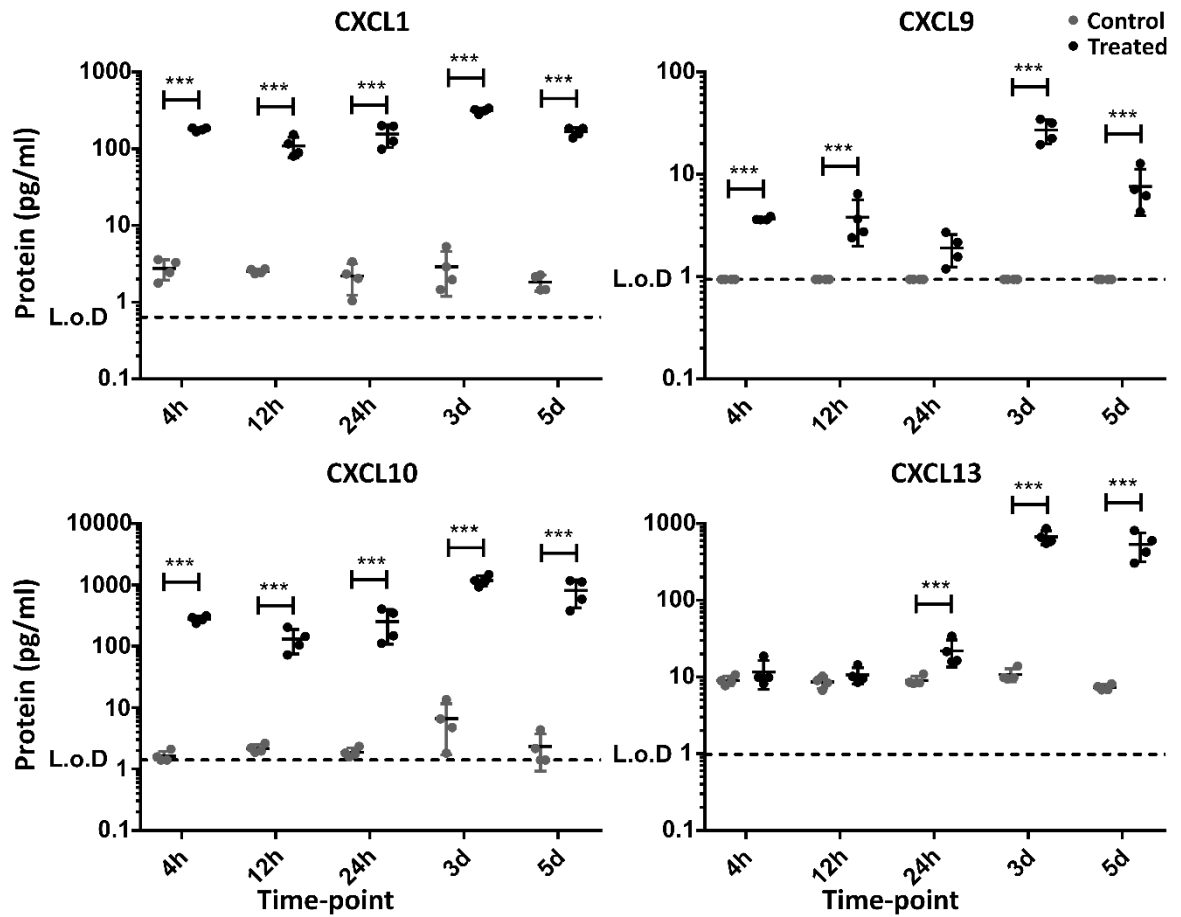


Figure 4.23: Time-course Aldara Model Brain CXC Chemokine Protein Expression.

Mice were treated daily with 62.5mg Aldara cream (5% imiquimod) or control cream on the dorsal skin. Brain tissue was collected at 4, 12 and 24 hours and 3 and 5 days. Biologend LegendPlex assay was performed to generate absolute expression values. Tested using One-way ANOVA and post-hoc Student's t-test with Bonferroni multiple testing correction. *= $P < 0.05$; **= $P < 0.01$; ***= $P < 0.001$; ****= $P < 0.0001$. Bars represent mean \pm SD.

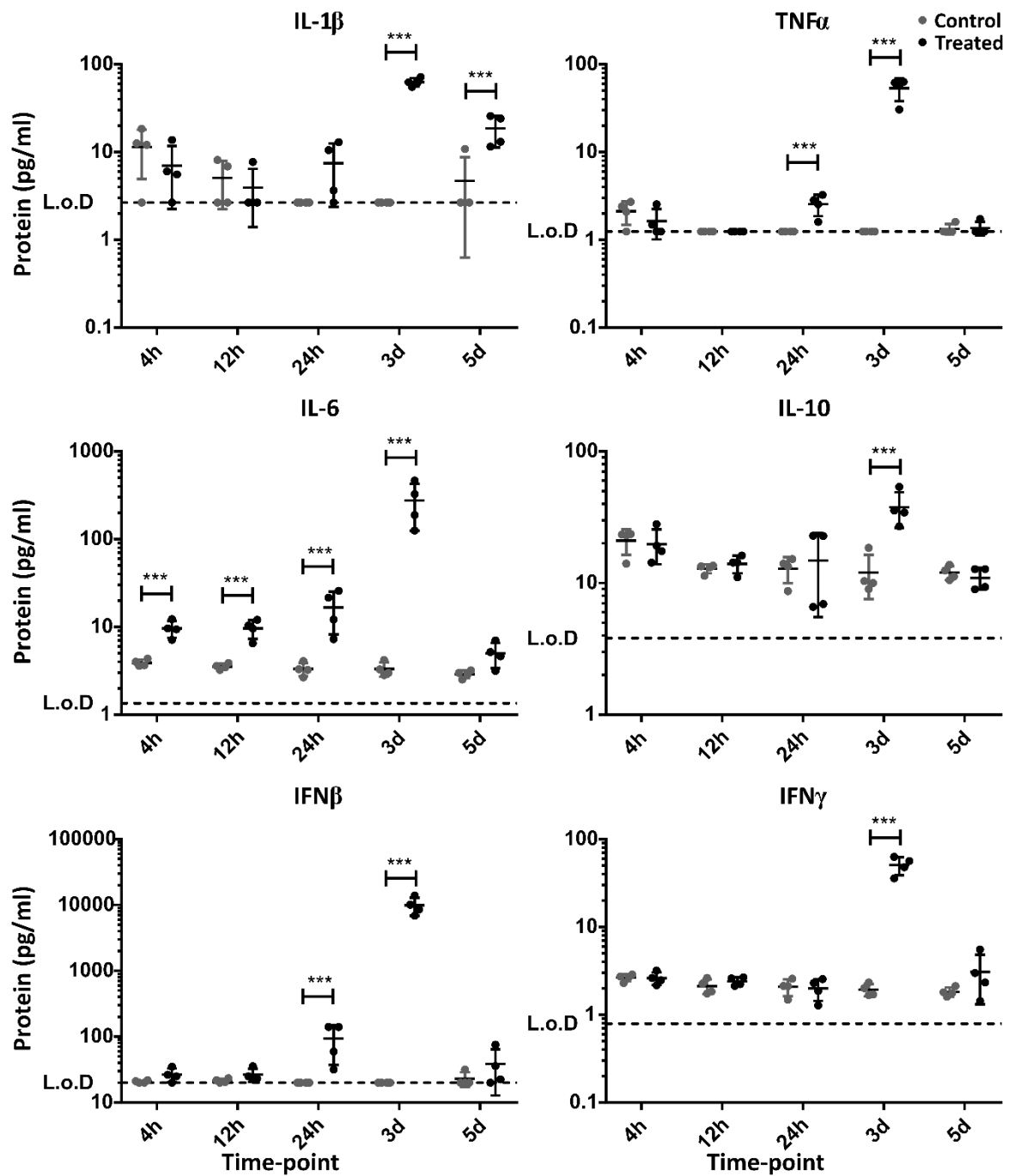


Figure 4.24: Time-course Aldara Model Brain Cytokine Protein Expression.

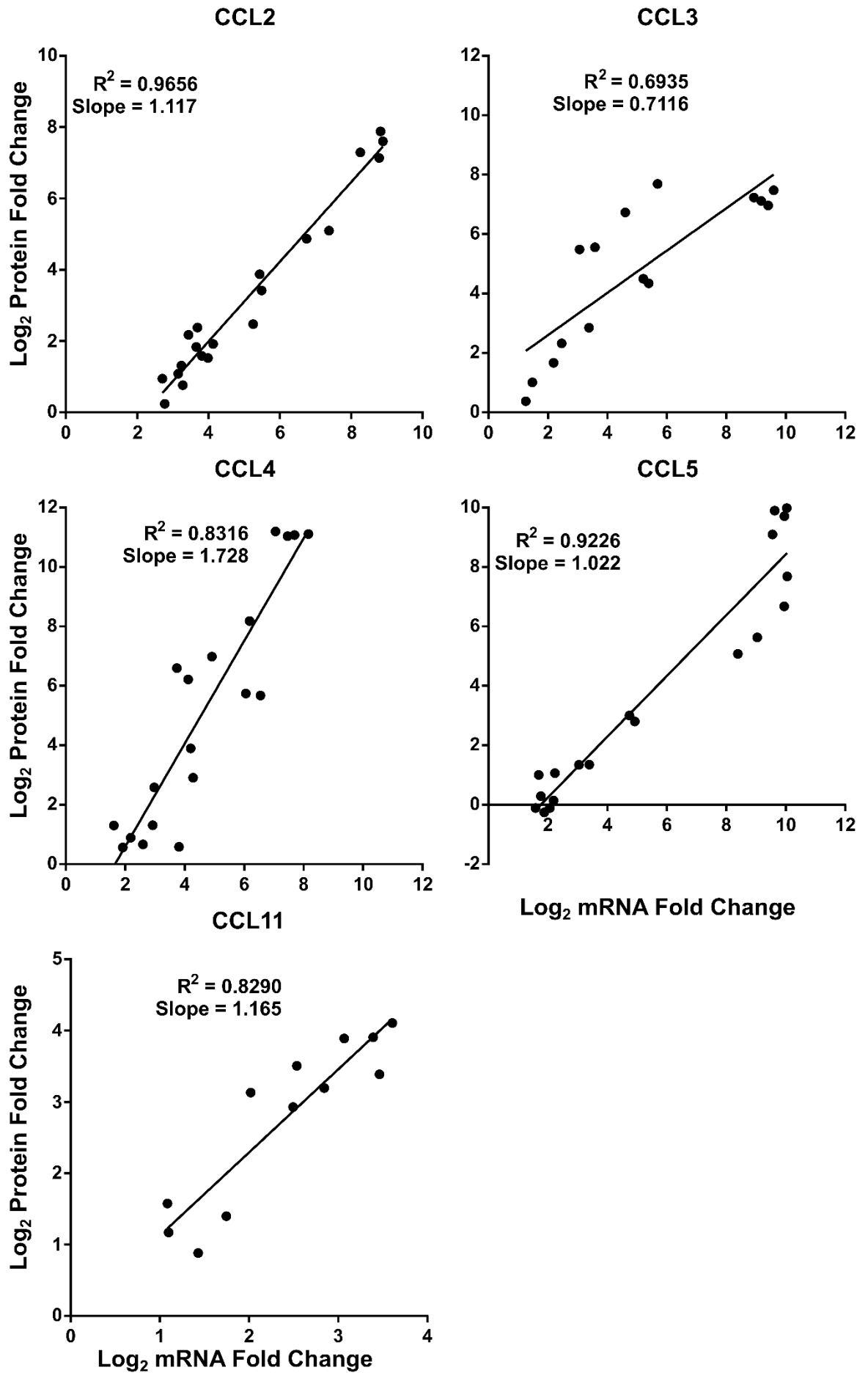
Mice were treated daily with 62.5mg Aldara cream (5% imiquimod) or control cream on the dorsal skin. Brain tissue was collected at 4, 12 and 24 hours and 3 and 5 days. Biologend LegendPlex assay was performed to generate absolute expression values. Tested using One-way ANOVA and post-hoc Student's t-test with Bonferroni multiple testing correction. *= $P < 0.05$; **= $P < 0.01$; ***= $P < 0.001$; ****= $P < 0.0001$. Bars represent mean \pm SD.

As the protein and gene expression assays had been performed on brains from the same animals it was possible to further investigate the relationship between fold changes in mRNA and fold changes in protein. Linear regression analysis on samples found to be above a 2 fold increase at an mRNA level revealed that

there were significant positive correlations between most analytes (CCL2, CCL3, CCL4, CCL5, CCL11, CXCL13, Il-1 β , TNF α , Il-6 and Il-10) (Figure 4.25, Figure 4.26, Figure 4.27). For *Cxcl10*/CXCL10 there was no significant correlation despite the large upregulation observed both transcriptionally and at a protein level. It is worth noting that for CCL5, TNF α and Il-10 there were samples where increased mRNA levels were actually associated with reduced protein (\log_2 fold change < 0), as such, caution should be taken when interpreting this association, particularly at lower levels of transcriptional upregulation. Despite this, transcriptional responses appeared to account for much of the variation in protein readings as demonstrated by the high R^2 values obtained.

Figure 4.25: (Overleaf) Linear regression of Brain CC chemokine mRNA and protein expression values in Aldara treated mice.

Mice were treated daily with 62.5mg Aldara cream (5% imiquimod) or control cream on the dorsal skin. Samples with a raw mRNA fold change compared to control >2 were used for analysis. Log-transformed mRNA fold change compared to control and log-transformed protein fold change compared to control were assessed for relationship using linear regression analysis. $P < 0.05$ for all analyses.



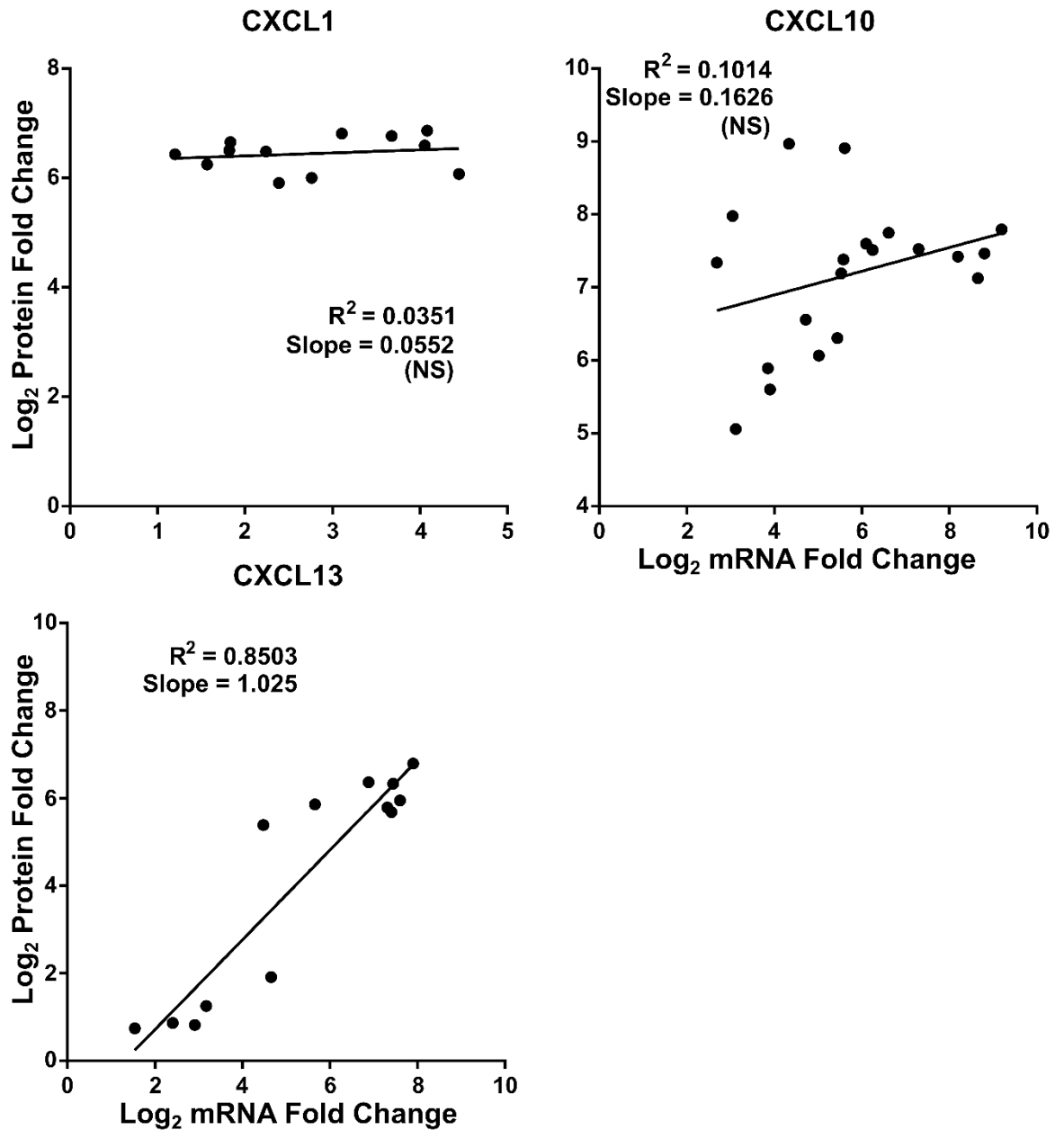


Figure 4.26: Linear regression of Brain CXC chemokine mRNA and protein expression values in Aldara treated mice.

Mice were treated daily with 62.5mg Aldara cream (5% imiquimod) or control cream on the dorsal skin. Samples with a raw mRNA fold change compared to control >2 were used for analysis. Log-transformed mRNA fold change compared to control and log-transformed protein fold change compared to control were assessed for relationship using linear regression analysis. $P < 0.05$ unless stated. NS=not significant.

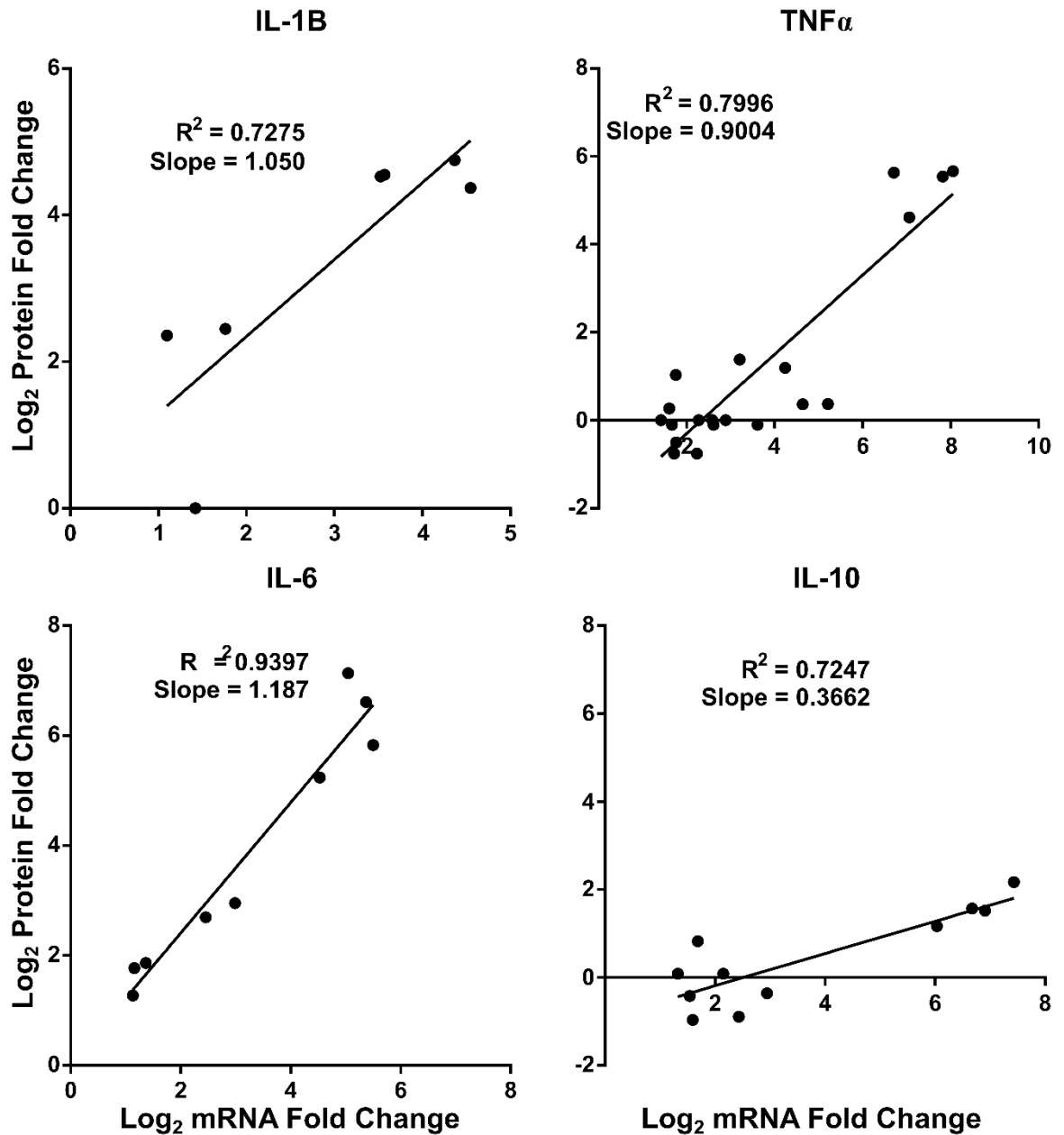


Figure 4.27: Linear regression of Brain cytokine mRNA and protein expression values in Aldara treated mice.

Mice were treated daily with 62.5mg Aldara cream (5% imiquimod) or control cream on the dorsal skin. Samples with a raw mRNA fold change compared to control >2 were used for analysis. Log-transformed mRNA fold change compared to control and log-transformed protein fold change compared to control were assessed for relationship using linear regression analysis. P<0.05 for all analyses.

4.2.8 The effect of repeated cutaneous treatment with Aldara on cellular populations within the brain parenchyma

Following on from the finding of chemokine and cytokine upregulation within the CNS it was investigated whether this was associated with cellular alteration or recruitment. At both 1 and 3 days post-treatment Iba1, GFAP and CD3 reactivity

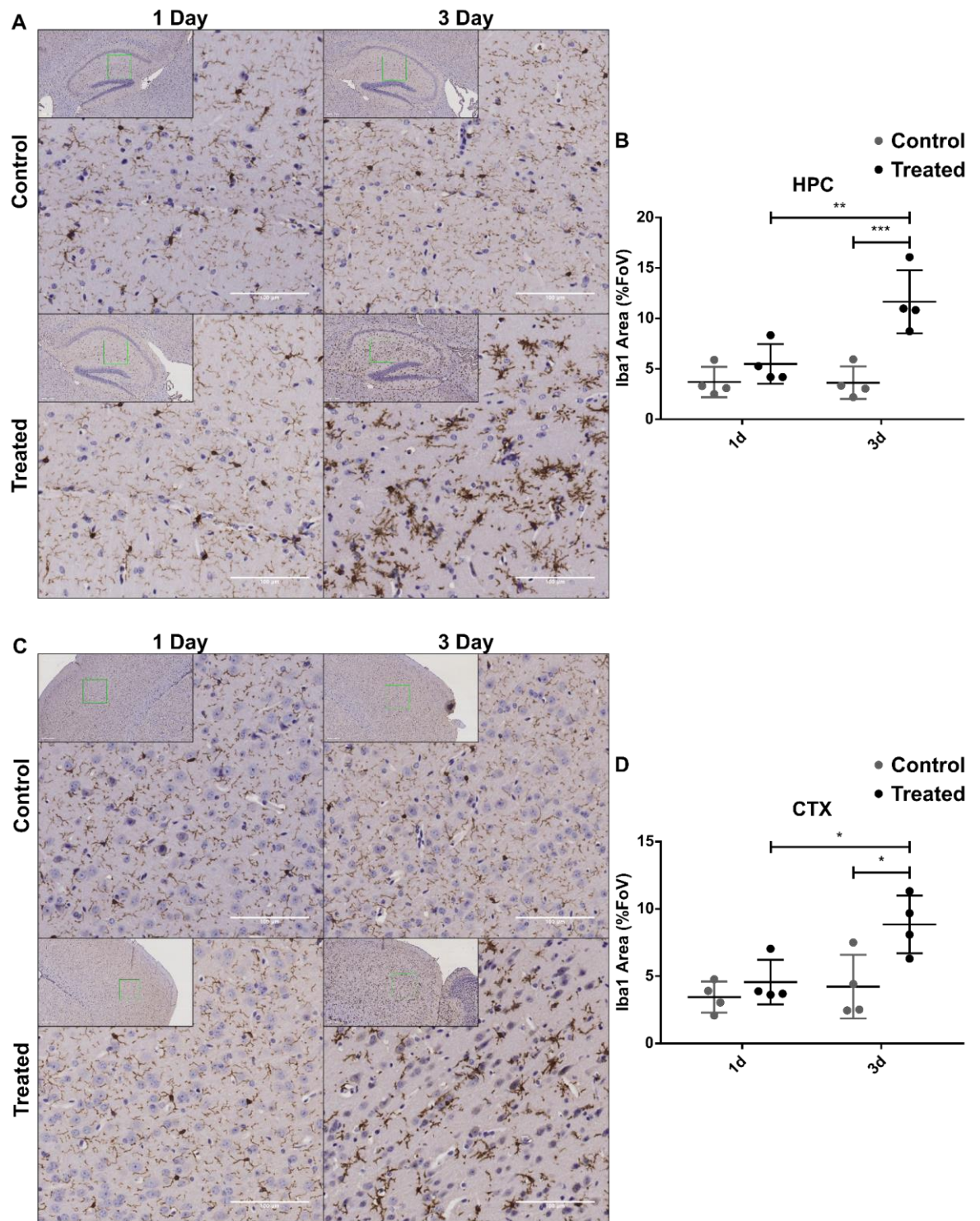
were investigated within the brain. Iba1 is a marker of microglia/macrophages, GFAP is a marker of astrocytes and CD3 is a T-cell marker.

4.2.8.1 Iba1+ staining of the hippocampus and cortex

Iba1 staining revealed that after 1 day of treatment there were no significant alterations in the quantity of Iba1 staining observed in either the hippocampus or the cortex. However, after three days of treatment, in both the hippocampus and cortex, gross morphological changes were observed (Figure 4.28). These were apparent, primarily as, a thickening and shortening of dendritic processes protruding from the cell body, changes associated with microglia taking on a more amoeboid appearance. In addition, automated quantification of 3 day Iba1 staining identified significant differences compared to both 1 day treated and 3 day control mice.

Figure 4.28: (Overleaf) Iba1 staining of brain in Aldara Model.

Mice were treated daily with 62.5mg Aldara cream (5% imiquimod) or control cream on the dorsal skin. Brains were collected after 24 hours and 3 days. Formalin-fixed paraffin embedded sections were stained using Iba1 antibody and haematoxylin QS counterstain. (A, C) Representative images of 20x hippocampal (A) and cortical (C) fields of view used for automated analysis. Inset image shows 10x view of area with 20x area highlighted in green. (B, D) Automated analysis of Iba1 area was performed using ImageJ software to quantify hippocampal (B) and cortical (D) Iba1 staining (n=4, 2-3 sections per mouse). Tested using One-way ANOVA and post-hoc Student's t-test with Bonferroni multiple testing correction. * $P < 0.05$; ** $P < 0.01$; *** $P < 0.001$. Scale bars = 100 μ m (main images), 200 μ m (inset images). Bars represent mean \pm SD. Abbreviations: HPC – Hippocampus; CTX - Cortex



4.2.8.2 GFAP staining of the hippocampus

Astrocytes are another important glial cell within the CNS. Due to their sparse distribution and the high background staining observed in the cortex GFAP reactivity was not assessed in this region. Despite this, in the hippocampus, a small but significant increase in GFAP staining was observed using the same methodology as for Iba1 (Figure 4.29). Gross morphological differences were less evident in this context than for Iba1.

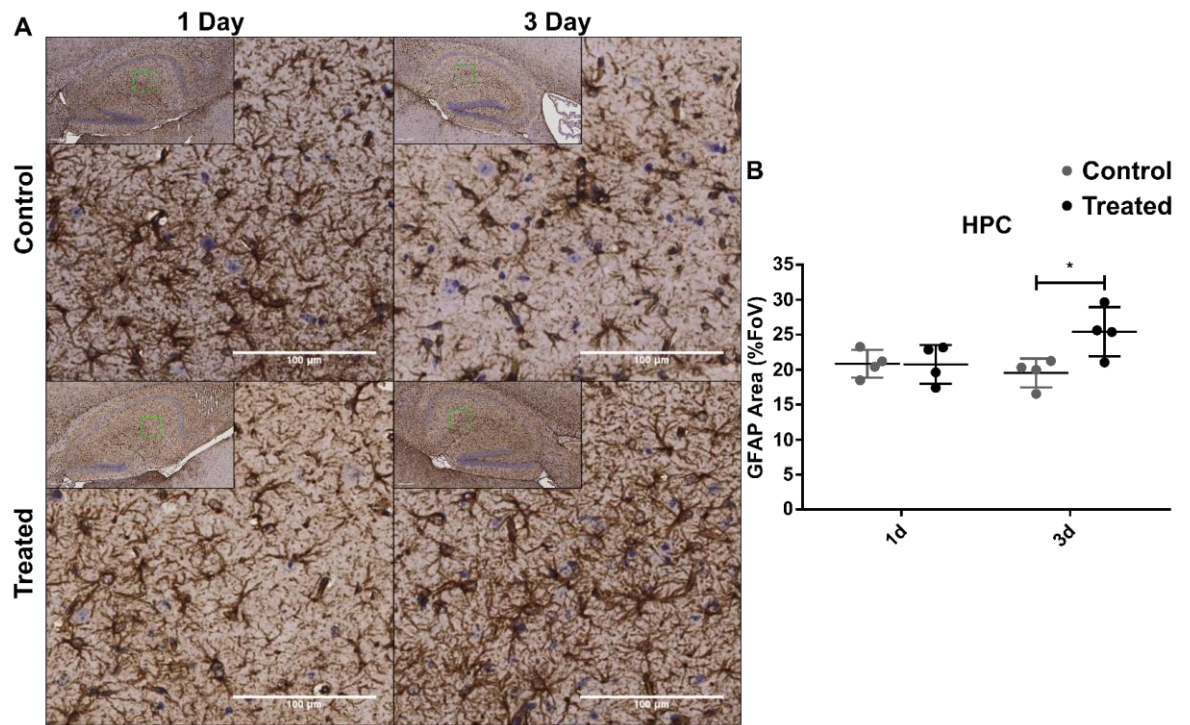


Figure 4.29: GFAP staining of brain in Aldara Model.

Mice were treated daily with 62.5mg Aldara cream (5% imiquimod) or control cream on the dorsal skin. Brains were collected after 24 hours and 3 days. Formalin-fixed paraffin embedded sections were stained using GFAP antibody and haematoxylin QS counterstain. (A) Representative images of 20x hippocampal fields of view used for automated analysis. Inset image shows 10x view of area with 20x area highlighted in green. (B) Automated analysis of GFAP area was performed using ImageJ software to quantify hippocampal GFAP staining (n=4, 2-3 sections per mouse). Tested using One-way ANOVA and post-hoc Student's t-test with Bonferroni multiple testing correction. *= $P < 0.05$. Scale bars =100µm (main images), 200µm (inset images). Bars represent mean \pm SD. Abbreviations: HPC – Hippocampus; CTX - Cortex

4.2.8.3 CD3+ cell counts of the hippocampus and cortex

Finally, evidence of exogenous cell recruitment into the CNS was examined. Using CD3 staining, combined with whole hippocampal cell counts and multiple fields of view from the cortex, significant evidence of T cell infiltration was found in response to peripheral Aldara treatment (Figure 4.30). In all control mice, and 1 day treated mice, there was little evidence of T cell infiltration with minimal or no CD3+ cells observed. Following three days of treatment there was consistent evidence of an increased number of CD3+ cells in both the hippocampus and cortex. These were located both perivascularly and within the parenchyma itself.

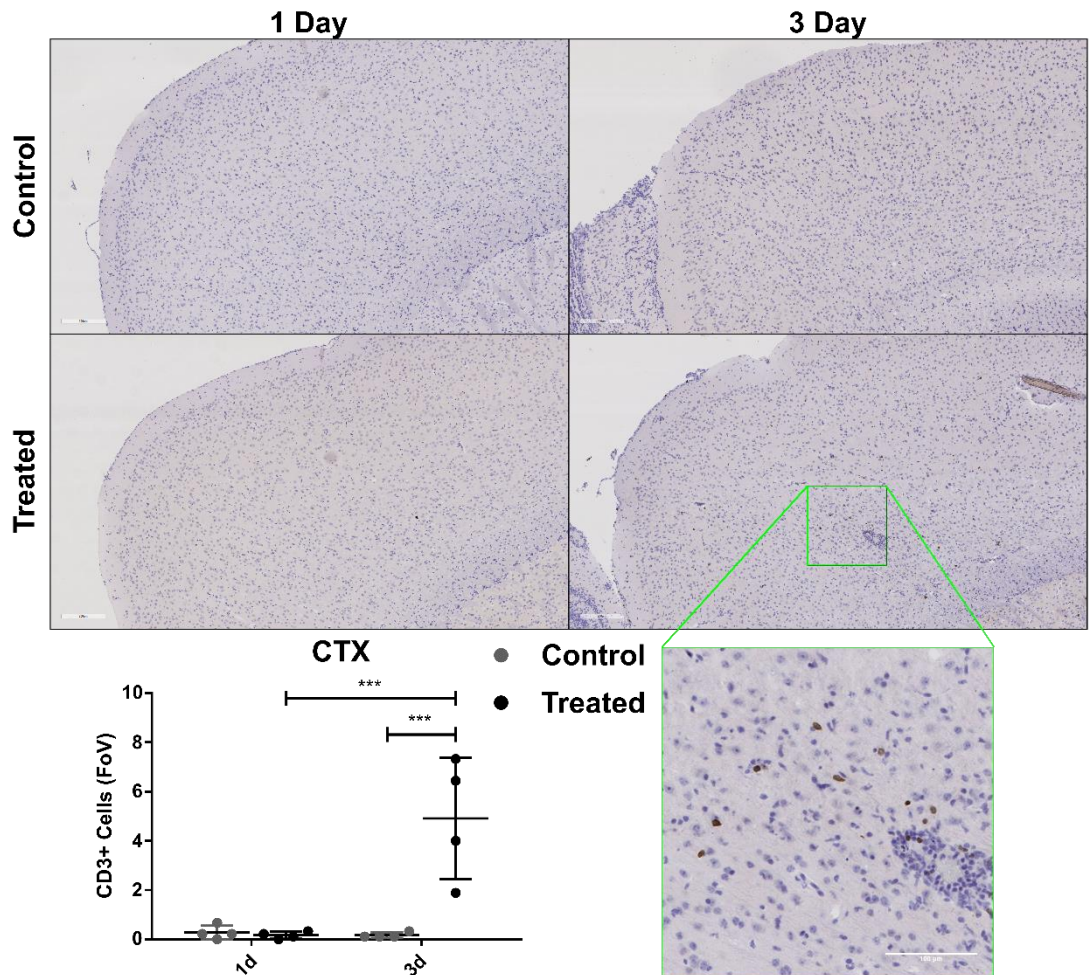
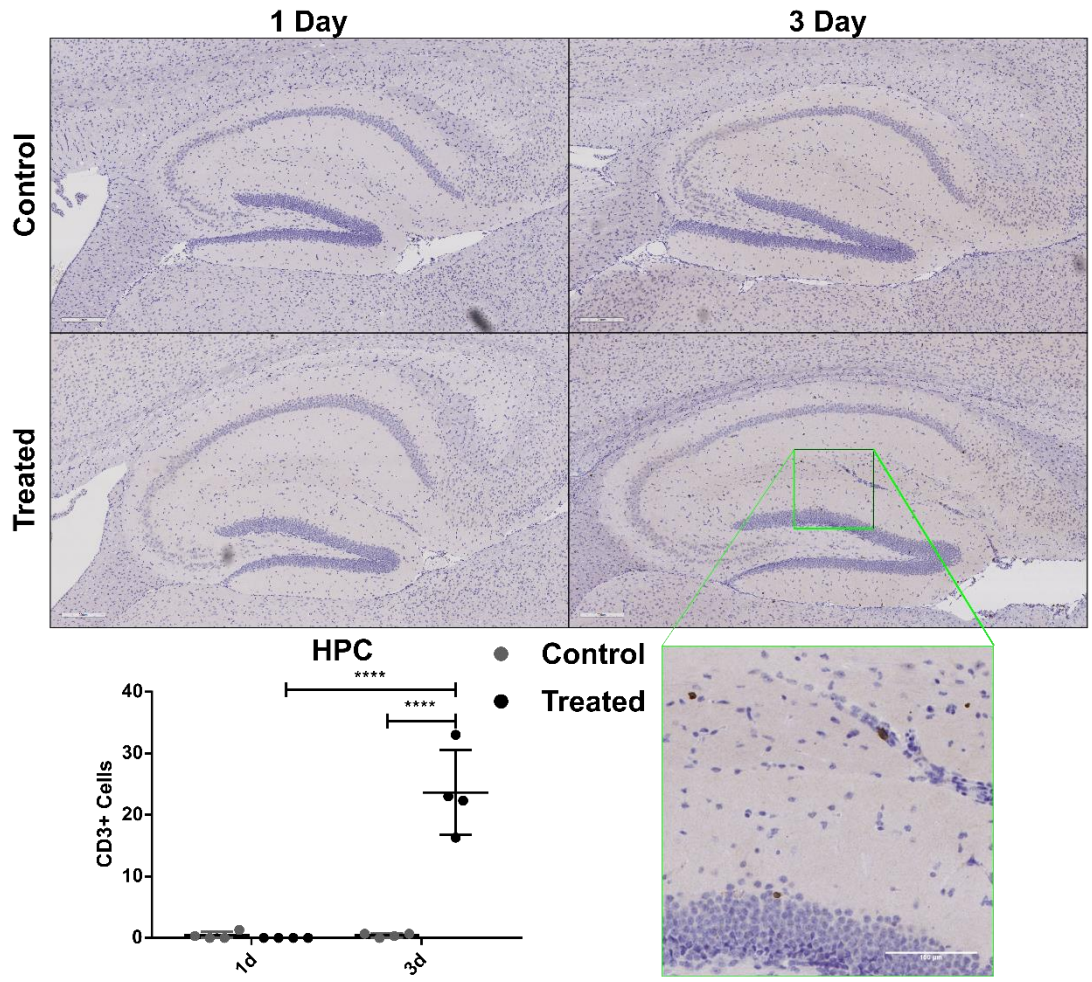


Figure 4.30: (Previous page) CD3 staining of brain in Aldara Model.

Mice were treated daily with 62.5mg Aldara cream (5% imiquimod) or control cream on the dorsal skin. Brains were collected after 24 hours and 3 days. Formalin-fixed paraffin embedded sections were stained using CD3 antibody and haematoxylin QS counterstain by Veterinary Diagnostic Services Laboratory at the University of Glasgow. (A, C) Representative images of 10x hippocampal (A) and cortical (C) fields of view. Expanded image is a 20x example of positive CD3 staining in 3 day treated sample. (B) Manual counting of all CD3+ cells in hippocampus (D) Manual counting of CD3+ cells in cortex, 3 fields of view were used per section (n=4, 2-3 sections per mouse). Tested using One-way ANOVA and post-hoc Student's t-test with Bonferroni multiple testing correction. *= $P < 0.05$; **= $P < 0.01$; ***= $P < 0.001$. Scale bars =100 μ m (main images), 200 μ m (inset images). Bars represent mean \pm SD. Abbreviations: HPC – Hippocampus; CTX - Cortex

4.3 Discussion

4.3.1 Summary of results

This chapter aimed to further characterise molecular responses to cutaneous Aldara treatment and their sequelae. To this end significant upregulation of a variety of chemokine and cytokine transcripts in the brain, skin, PBL and a number of peripheral organs was identified. Transcriptional data from the time-course are summarised in Figure 4.31. In addition to upregulation of measured transcripts temporal differences between the brain and the periphery were found. Further to this it was confirmed that transcriptional changes identified within the brain were translated into protein. Finally, these molecular alterations were found to be associated with significant changes in astrocytic, microglial and T cell populations.

	Brain					Skin					PBLS					Liver					Lungs				
	4h	12h	24h	3d	5d	4h	12h	24h	3d	5d	4h	12h	24h	3d	5d	4h	12h	24h	3d	5d	4h	12h	24h	3d	5d
Ccl2	3.59	4.20	6.37	8.71	4.21	2.31	2.63	2.02	-0.28	1.25	7.00	6.93	7.54	3.15	0.09	4.95	5.03	4.29	1.33	0.64	5.08	5.62	4.54	2.36	3.05
Ccl3	0.33	1.48	4.57	9.30	4.59	4.92	4.23	2.88	1.65	0.97	3.99	2.98	2.99	2.54	0.57	3.28	4.77	4.24	4.22	1.78	4.25	4.67	3.93	1.81	4.90
Ccl4	2.58	3.18	5.54	7.65	5.06	-	-	-	-	-	-	-	-	-	-	-	-	-	-	-	-	-	-	-	-
Ccl5	1.92	1.72	4.24	9.81	9.51	2.36	3.37	2.53	-0.37	0.69	2.49	0.48	1.35	1.74	0.16	3.19	3.01	2.34	1.76	1.67	1.46	1.15	1.91	1.51	3.18
Ccl9	1.43	0.61	1.39	4.89	3.01	0.06	1.75	-1.13	-1.53	-0.87	0.76	0.76	1.21	0.53	1.15	-0.62	0.19	0.15	-0.62	0.65	2.78	3.23	2.66	1.90	2.86
Ccl11	0.99	-0.49	0.97	3.40	2.50	0.40	0.53	-0.52	0.10	-0.65	-	-	-	-	-	2.48	3.06	1.22	-0.43	1.02	0.77	1.03	0.62	0.55	-0.39
Ccl19	0.38	-0.61	0.77	2.94	1.29	1.26	0.99	0.86	0.50	-0.16	4.05	5.01	0.01	3.93	0.29	1.62	2.79	2.92	0.62	0.32	1.13	1.37	1.79	0.38	0.29
Cxcl1	3.10	-0.19	1.38	3.78	1.42	-	-	-	-	-	-	-	-	-	-	-	-	-	-	-	-	-	-	-	-
Cxcl10	5.90	4.37	6.29	8.76	4.39	7.48	5.13	1.23	-0.23	-0.47	9.23	7.41	5.51	1.15	-0.02	6.72	5.02	3.28	1.12	-0.20	9.85	7.52	5.42	1.06	2.02
Cxcl13	0.01	0.73	3.56	7.45	6.75	0.87	2.38	1.36	3.24	1.38	1.86	3.54	0.81	0.61	1.76	2.15	3.01	1.91	1.77	1.76	2.07	3.52	4.16	2.80	2.70
Cxcl16	-0.26	-0.55	1.19	2.90	2.47	1.22	0.73	-0.28	0.55	0.19	0.07	0.32	0.62	-0.72	0.62	-0.36	0.09	0.43	-0.68	0.26	1.28	0.13	0.20	0.41	-0.55
Cx3cl1	-0.54	-0.97	-0.38	0.12	-0.02	1.85	0.00	-0.34	0.54	-0.29	-	-	-	-	-	-1.49	-1.79	1.75	-0.08	0.64	1.60	0.43	0.40	-0.21	-0.62
Ccr5	-0.20	-0.09	0.43	3.08	1.80	0.15	1.46	0.81	-0.47	1.22	2.09	1.80	2.35	1.17	0.48	-1.28	-0.17	-0.41	-0.54	1.48	1.26	1.41	1.68	2.27	1.98
Il11b	0.14	0.06	0.66	4.08	1.07	0.85	0.73	0.99	1.06	1.52	2.34	0.96	1.14	-0.12	-0.80	0.02	1.11	1.19	0.39	-0.17	2.97	2.83	2.05	1.66	3.02
Tnfa	1.85	2.39	3.82	7.51	3.87	0.87	0.48	1.43	0.38	-0.21	1.99	1.95	1.75	-0.09	-0.75	2.47	3.30	4.02	2.81	0.81	2.80	2.67	1.93	-0.45	1.62
Il6	0.83	0.59	2.12	5.16	-0.29	1.46	2.14	3.03	2.49	1.84	3.45	4.71	1.79	0.64	1.62	3.03	2.34	2.44	0.11	-0.75	6.53	5.09	3.69	1.53	2.69
Il10	0.11	0.51	1.67	6.85	2.13	1.83	2.79	1.58	0.43	0.10	4.60	4.14	4.71	4.69	1.15	2.87	5.83	4.11	3.94	2.74	3.31	4.00	4.83	3.03	5.05

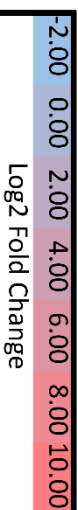


Figure 4.31: Heatmap of chemokine and cytokine gene expression after a repeated daily cutaneous treatments of Aldara cream.

Animals were treated once at day 0 with 62.5mg of Aldara cream (5% imiquimod) or control cream. At 4, hours, 12 hours, 24 hours, 3 days and 5 days after initial treatment tissues were collected and analysed by qRT-PCR. Log₂ fold changes compared to control levels of gene expression were calculated. Grey squares indicate samples where expression levels could not be determined. Student's T-test with Bonferroni multiple testing correction was used to determine significance. Results in bold demonstrate significant results P<0.05

4.3.2 Transcriptional responses to cutaneous Aldara treatment

The work presented here builds on earlier research performed in our laboratory that identified transcriptional alterations in many ISGs in the brain in response to cutaneous Aldara treatment. It was initially wished to extend this work to examine a broader range of chemokines, alongside previously unexamined cytokines. In addition, to expand our understanding of the Aldara model, transcriptional responses in several peripheral organs at multiple time-points were examined.

To this end significant upregulation of a broad array of CC and CXC chemokines in both the brain and periphery at a variety of time-points was identified. Alongside this, there was significant upregulation of the pro-inflammatory cytokines that were examined. Within the brain there was a significant upregulation of all measured transcripts aside from *Cx3cl1*. These chemokines (*Ccl2*, *Ccl3*, *Ccl4*, *Ccl5*, *Ccl9*, *Ccl11*, *Ccl19*, *Cxcl10*, *Cxcl13* and *Cxcl16*) are associated with the attraction of a broad range of cell types including monocytes(124, 125), neutrophils(449, 450) dendritic cells (451, 452), T cells (122, 123, 418, 453), eosinophils (454), B cells (455) and natural killer cells(456). Considering recent findings from our laboratory that many of these immune cell types are recruited to the CNS following cutaneous Aldara treatment (24), it is likely that the upregulation of these molecules is an important component of cellular recruitment. In addition a number of these chemokines have been implicated in sickness behaviours and/or neuronal modulation (102, 103, 457), suggesting one possible mechanism through which previously observed alterations in behaviour (24) may become manifest.

As discussed in the introduction, the cytokines $\text{IL-1}\beta$, $\text{TNF}\alpha$ and IL-6 have diverse actions within the immune system (33, 458, 459). Within the CNS the role of these cytokines appears variable with data showing that they can interact with resident CNS cells and have both protective and detrimental effects dependent on context (460-464). In addition, they may also be important regulators of chemokine mediated cellular recruitment (465, 466). Alongside their immune roles $\text{IL-1}\beta$ and $\text{TNF}\alpha$ have been closely linked to sickness behaviours (5, 9) and alterations of CNS function in animal models, including changes in the expression of the 5-HTT (467) in neurons. Finally, IL-10 is one of the key regulators of

immune responses and has potent anti-inflammatory properties (71, 468). Its widespread upregulation throughout all tissues highlights the importance of active immune resolution in the context of acute inflammatory responses. These data provide significant evidence that following cutaneous Aldara treatment there are molecular alterations within the brain that can not only induce inflammatory changes but also influence cellular populations and CNS function.

Considering that previous work has demonstrated that some of the chemokines examined here, and many ISGs, are upregulated in the brain after either 24 hours or 3 days, earlier time-points were investigated to understand how rapidly changes in the brain became apparent. This showed that a limited range of chemokines (*Ccl2*, *Ccl5*, *Ccl9* and *Cxcl10*) were significantly upregulated within the first 4 hours, suggesting that the beginnings of an inflammatory response are present even at this early time-point. In general the other transcripts were found to be upregulated at either 24 hours after treatment, or after 3 days of repeated treatment, and were largely sustained until 5 days.

Earlier work in our laboratory had demonstrated that the brain and PBL responses differ temporally, and work in other laboratories, has identified changes in the lung(447) and liver(448) in response to Aldara. The data presented here demonstrate that changes in transcriptional state between 1 and 3 days differ between the peripheral tissues and the brain. Between these two time-points the brain is continuing to upregulate its chemokine and cytokine transcriptional response, whereas the peripheral tissues are down-regulating and resolving their molecular inflammatory responses. This suggests that the peripheral response is rapid and transient in nature, particularly in the skin and PBLs, to some extent in the liver and to a lesser extent in the lungs. Whereas, in contrast to this, the brain response could be broadly considered to be slower but more sustained.

4.3.3 Protein responses in the CNS

While RNA samples are particularly useful for studies with a wider range of targets due to the minimal levels of starting material required, it is important, where possible, to assess if transcriptional changes are translated into protein responses. Protein array showed that for all transcripts included in the array

that were upregulated in the brains of Aldara treated mice, there were significant responses at a protein level. The high levels of association between mRNA and protein levels clearly suggests that translation for the studied molecules is closely related to transcriptional changes. This close association is also highlighted by the fact that, like the transcriptional responses, the peak response point for all of the measured proteins appeared to be after 3 days of treatment, with the majority of molecules studied appearing to down-regulate between 3 and 5 days. As part of the protein array both type I and type II IFNs (IFN β /IFN γ) were also identified upregulated in the brain at these time-points. This supports earlier work identifying the IFN signalling pathway as an important component of Aldara responses (25).

4.3.4 Cellular changes in the CNS

Molecular changes provide insight into immune responses and allow us to speculate on outcomes based on previous research. Despite this, where possible it is best to directly assess if there are downstream consequences of molecular alterations. Therefore, whether observed molecular changes were associated with alterations in Iba1+, GFAP+ and CD3+ cellular populations was examined.

Immunohistochemistry showed that after 3 days of Aldara treatment there were morphological changes associated with the Iba1+ microglial population with cells taking on a more amoeboid appearance. The functional implications of morphological changes in microglia are thought to be variable and depend on the context in which these changes occur, although they are consistently associated with enhanced phagocytosis (167, 469). Despite this it is reasonable to assume that morphological alterations are a reactive response to a stimulus, in this case cutaneous Aldara treatment. Astrocytes have been found to be a source of a number of chemokines and cytokines, particularly CXCL10 (182, 220) and, in this model, we did identify small but significant alterations of GFAP staining within the hippocampus. Upregulation of GFAP is characteristic of astrogliosis a response that is associated with many CNS inflammatory reactions(470). Thus, these changes may reflect a reactive response to cutaneous Aldara within the astrocyte population, similar to those observed within the microglial Iba1+ population.

Significant changes in astrocytes and microglia as measured by cellular staining do not become manifest until 3 days post-treatment. Despite this, the upregulation of both mRNA and protein observed within the CNS, at earlier time-points, suggests that these cells can produce molecular responses prior to the appearance of gross morphological changes.

Alongside reactive changes in brain resident cells, increases in CD3⁺ cells were identified in both the cortex and hippocampus after 3 days of cutaneous Aldara treatment, indicating significant increases in the T cell population. While these cells may contribute to the inflammatory response, their arrival also appears to coincide with the beginnings of immune regulation as evidenced by the rise in Il-10 and subsequent down-regulation of immune transcripts. This may in part be due to the fact that recruitment of regulatory T cells is a critical event in resolution of brain inflammatory responses (471, 472). Whilst further work would be needed to characterise this cellular population, it is possible that a subset of recruited CD3⁺ cells are regulatory.

4.3.5 Other findings of note

Alongside the questions we had aimed to answer in this chapter as part of a further characterisation of the Aldara model, the data presented above highlighted some interesting findings that are worth consideration.

Firstly, in this study we reported changes in skin histology at both 3 and 5 days yet we did not identify significant molecular alterations at either of these time-points. Similarly, splenic enlargement has been reported after repeated treatments of Aldara (446, 473) however we did not identify significant molecular alterations in this tissue after three days of treatment. These findings suggest that phenotypic responses do not necessarily correspond to ongoing inflammation but rather represent downstream sequelae of inflammatory responses that may have already resolved at a molecular level.

Secondly if we examine the magnitude of fold changes between tissues, the extent of upregulation within the brain appears to be greater than that observed in the peripheral tissues. While this is interesting, and at first glance may indicate that the brain may be responding more severely than the peripheral

organs, it is important to consider whether this increased magnitude is due to control levels in the brain being lower or whether it is a result of a more severe response within the brain itself (see Chapter 6).

4.3.6 Summary

Overall these data provide significant evidence that Aldara treatment and IMQ-mediated TLR7 agonism induces a rapid response at the local site of treatment in the skin, in the circulating PBLs and in peripheral organs. Within the CNS there is a rapidly induced immune response that increases in both magnitude and molecular diversity over time and with repeated treatments. Importantly the temporal nature of the response appears to differ between organs but this is particularly apparent between the brain and the periphery. The chemokine and cytokine transcriptional response observed within the brain has the potential to attract a multitude of cell types and to dramatically alter CNS function. Indeed, there appear to be alterations in the resident cellular populations of the CNS when examining microglia and astrocytes and there is a recruitment of CD3⁺ cells into the CNS. This suggests that the Aldara model is a compelling model for exploring neuroinflammation in the context of a systemic response to peripheral TLR stimulus.

Chapter 5

Exploring Mechanisms of Aldara-induced Brain Inflammation

Chapter 5 Exploring mechanisms of Aldara-induced brain inflammation

5.1 Introduction

In the previous chapter it was demonstrated that repeated applications of Aldara cream induce both peripheral and central inflammatory responses. CNS responses are of particular interest to our research, therefore, further investigation of potential mechanisms through which the CNS response may be induced was undertaken.

Previous work, and the work presented so far in this thesis, has identified the upregulation of interferon simulated genes (24, 25) and a wide range of chemokines in the brain. This led us to ask two questions about the response to cutaneous Aldara treatment:

What is the influence on chemokine and cytokine transcriptional responses, and associated microglial, astrocytic and T cell alterations of;

1. Inflammatory C-C chemokine receptor knockout (iCCRKO)?
2. Type 1 IFN knockout (IFNARKO)?

To investigate the role that these pathways play in brain inflammation the response to Aldara treatment was investigated in two knockout models. The first of these models involved inflammatory C-C chemokine receptor knockout mice (iCCRKO). These mice do not express CCR1/CCR2/CCR3 and CCR5. As discussed previously, chemokines exhibit high levels of promiscuity and redundancy (29), therefore these multi-receptor knockout mice can be used to overcome the challenges of studying a highly promiscuous and redundant molecular family. As many of the chemokines that can signal through these receptors (*Ccl2*, *Ccl3*, *Ccl4*, *Ccl5*, *Ccl9* and *Ccl11*) have been found to be altered in the brains of mice treated cutaneously with Aldara, exploring the influence of iCCRKO should provide insight into their role during CNS inflammation. The overlapping nature of signalling in the chemokines listed above is highlighted in Figure 5.1.

Chemokines are primarily associated with cellular recruitment and CCR5 is associated with T-cell recruitment(123). Therefore, it was hypothesised that iCCRKO would reduce the number of T cells that enter the brain. In addition, it was expected that decreases in cellular infiltration would lead to a reduced inflammatory burden, measured at both the transcriptional level and cellular level, through alterations in the microglial and astrocytic populations.

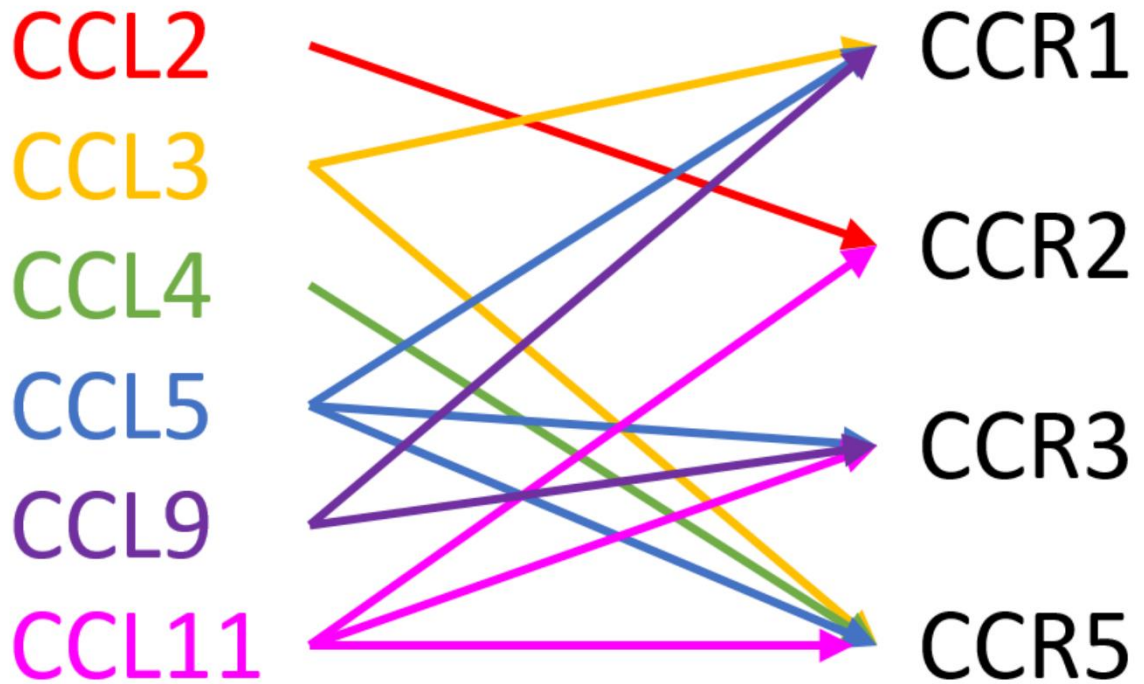


Figure 5.1: CCL-CCR Overlapping Interactions

Diagram illustrating the promiscuity of chemokine ligand and receptor interactions of those CC chemokines that were identified as raised in the initial time-course model and that signal through iCCRs. Based on (29)

The second of the models investigated the role of type I IFN signalling using IFNARKO mice. As discussed previously, IFN responses appear to be a shared pathway between TLR induced brain responses (25). IFNARKO mice are unable to initiate type I IFN signalling and therefore downstream responses should be ameliorated. However, IFNARKO should not prevent NF- κ B responses. As such, it would be expected that ISG expression (e.g. *Cxcl10*) and the expression of other IFN associated genes such as *Ccl2* would be reduced. Despite this, as the NF- κ B pathway remains intact pro-inflammatory cytokine responses would still be expected (49, 474), although these may be diminished due to the reduction of overall inflammatory stimulation. It was hypothesised that, reductions in type I IFN stimulated inflammation would reduce cellular infiltration, particularly due to reductions in *Cxcl10*.

Within this chapter and the following chapter a more focused analysis of the transcriptional response was undertaken. To this end *Ccl2*, *Ccl3*, *Ccl5*, *Cxcl10* and *Ccr5* were chosen as chemokines of interest, alongside the cytokines *Il1b*, *Tnfa*, *Il6* and *Il10*. The chemokines were chosen due to their association with our cells of interest, *Ccl2* and *Ccl3* are associated with microglia (231, 475, 476), *Ccl5* and *Cxcl10* are associated with T cells (122, 123), and *Ccr5* is associated with both microglia (477, 478) and T cells (123, 479). In addition, astrocytes have been associated with the production of some of these chemokines, particularly *Cxcl10* (232-234). The cytokines investigated have all been found to be altered in inflammatory TLR models and, particularly for *Il1b* and *Tnfa*, are consistently thought to be important mediators of CNS inflammatory reactions (226, 264) and subsequent behavioural changes (4, 9, 293). Finally, it is worth noting that for iCCRKO experiments, the animals were shared with others in the laboratory and therefore only the brain response could be investigated.

5.2 Results

5.2.1 The effect of iCCRKO on brain chemokine and cytokine transcriptional responses to repeated cutaneous Aldara treatment

Initial investigation of brain responses in iCCR^{+/+} (WT), iCCR^{+/-} (HET), and iCCR^{-/-} (KO) mice, after 4 days of daily cutaneous Aldara treatment, revealed no significant differences in chemokine and cytokine transcription between the genotypes, aside from in *Ccr5* (Figure 5.2, Figure 5.3). Reassuringly, significant reductions in *Ccr5* were identified in iCCRKO mice and while WT and HET mice did not differ significantly in expression, mean expression in HET mice was roughly halved (1395 vs 617.8 copies/10³ *Tbp*), indicative of haploinsufficiency. Although significant differences were not found in the other transcripts examined there did appear to be evidence of possible subtle differences. This was particularly true for *Il1b* where removal of the outlier present in the KO group did result in a significant difference between WT and KO mice.

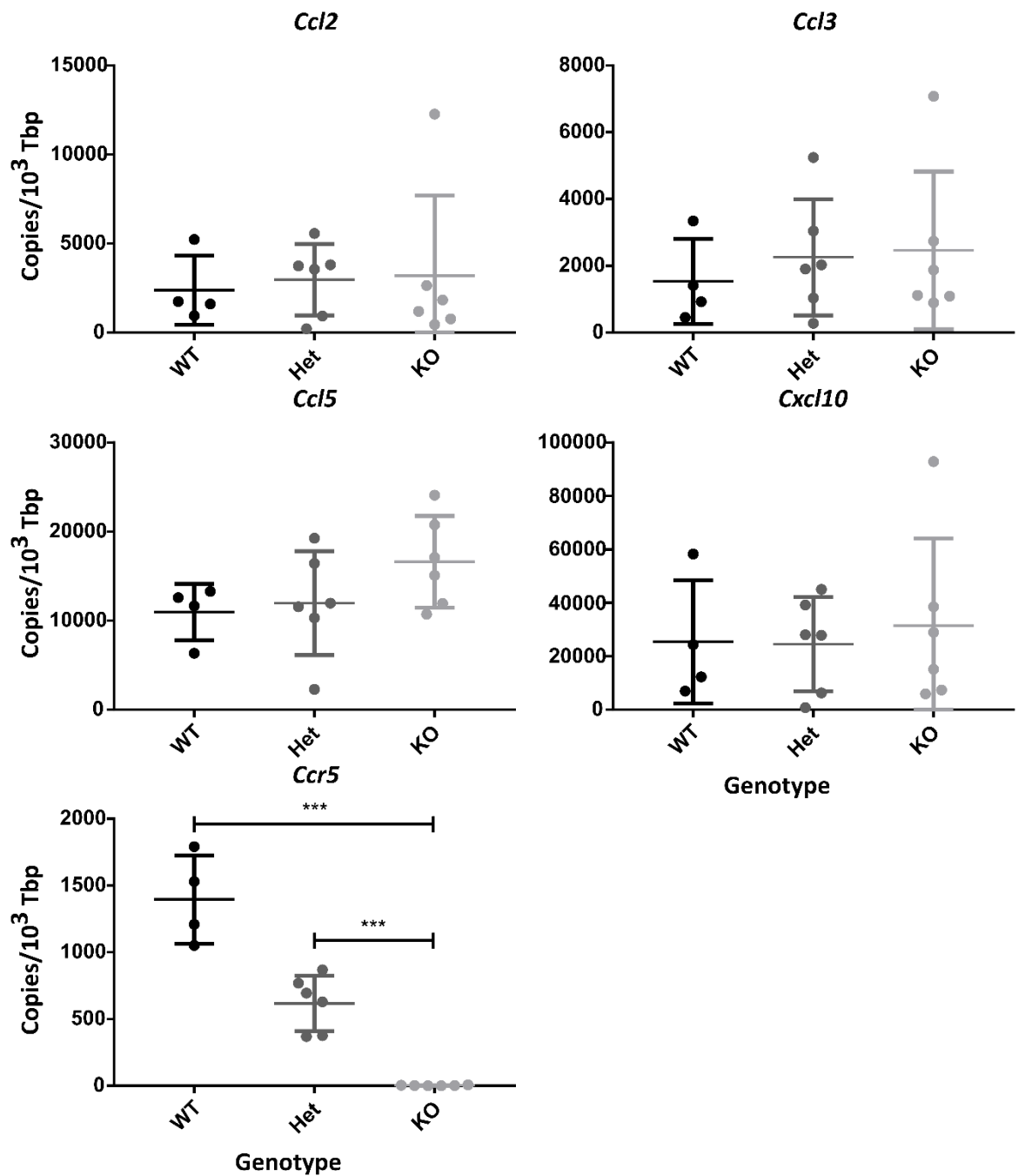


Figure 5.2: 4-day iCCRKO Aldara Model 1 Brain Chemokine Transcript.

iCCR^{+/+} (WT), iCCR^{+/-} (HET) and iCCR^{-/-} (KO) mice were treated daily with 62.5mg Aldara cream (5% imiquimod) on the dorsal skin. Brain tissue was collected 24 hours after the 4th application. Absolute quantification was performed by qRT-PCR and values were normalised to housekeeping gene Tbp. N=4-6 per group. One-way ANOVA followed by Student's T-test with Bonferroni multiple testing correction was used to determine statistical significance. ***= $P < 0.001$. Bars represent mean \pm SD.

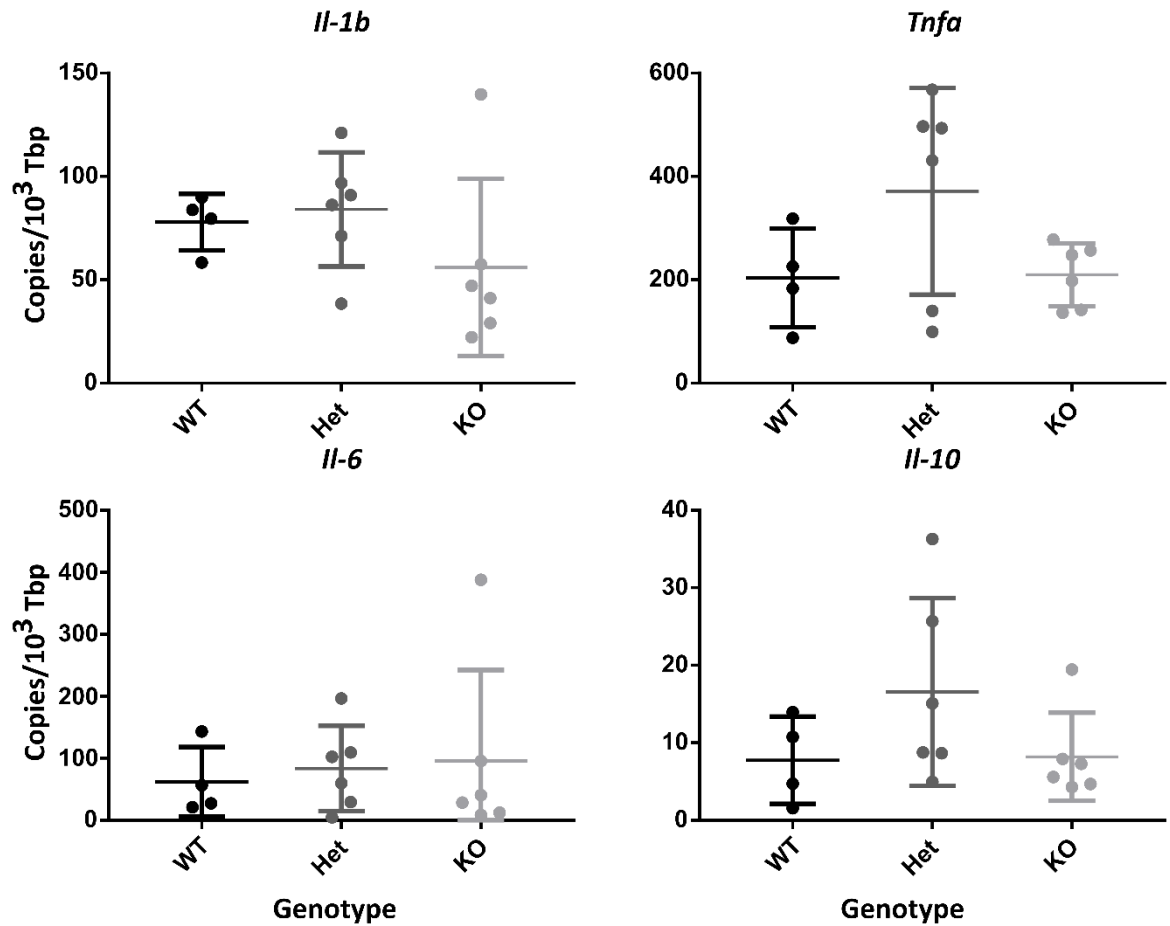


Figure 5.3: 4-day iCCRKO Aldara Model 1 Brain Cytokine Transcript

iCCR^{+/+} (WT), iCCR^{+/-} (HET) and iCCR^{-/-} (KO) mice were treated daily with 62.5mg Aldara cream (5% imiquimod) on the dorsal skin. Brain tissue was collected 24 hours after the 4th application. Absolute quantification was performed by qRT-PCR and values were normalised to housekeeping gene Tbp. N=4-6 per group. One-way ANOVA followed by Student's T-test with Bonferroni multiple testing correction was used to determine statistical significance. A P value <0.05 was considered significant. Bars represent mean \pm SD.

To further explore possible differences between WT and KO mice a repeat experiment was performed with both treated and control groups for each genotype. This experiment reproduced the findings of the earlier experiment with no significant differences identified between WT and KO mice apart from *Ccr5*. For all other transcripts examined (*Ccl2*, *Ccl3*, *Ccl5*, *Cxcl10*, *Il1b*, *Tnfa*, *Il6* and *Il10*) there were significant differences between treated and control mice in the iCCRKO group (Figure 5.4, Figure 5.5). *Il6* and *Il10* did not differ significantly between treated and control WT groups, however there was still a mean increase in the treated group consistent with previous findings.

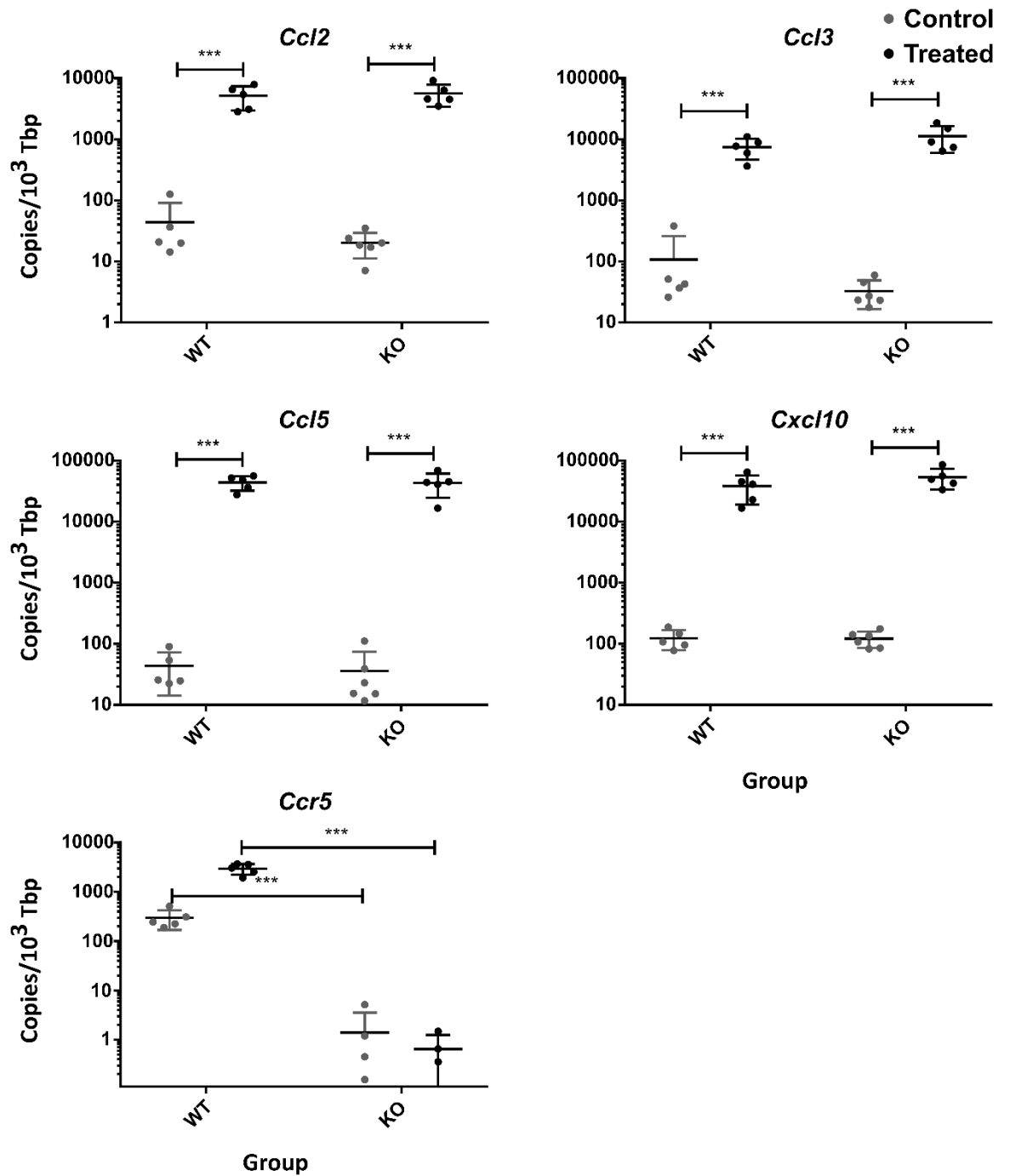


Figure 5.4: 4-day iCCRKO Aldara Model 2 Brain Chemokine Transcript

iCCR^{+/+} (WT) and iCCR^{-/-} (KO) mice were treated daily with 62.5mg Aldara cream (5% imiquimod) or control cream on the dorsal skin. Brain tissue was collected 24 hours after the 4th application. Absolute quantification was performed by qRT-PCR and values were normalised to housekeeping gene Tbp. N=5-6 per group. One-way ANOVA followed by Student's T-test with Bonferroni multiple testing correction was used to determine statistical significance. ***=P<0.001. Bars represent mean \pm SD.

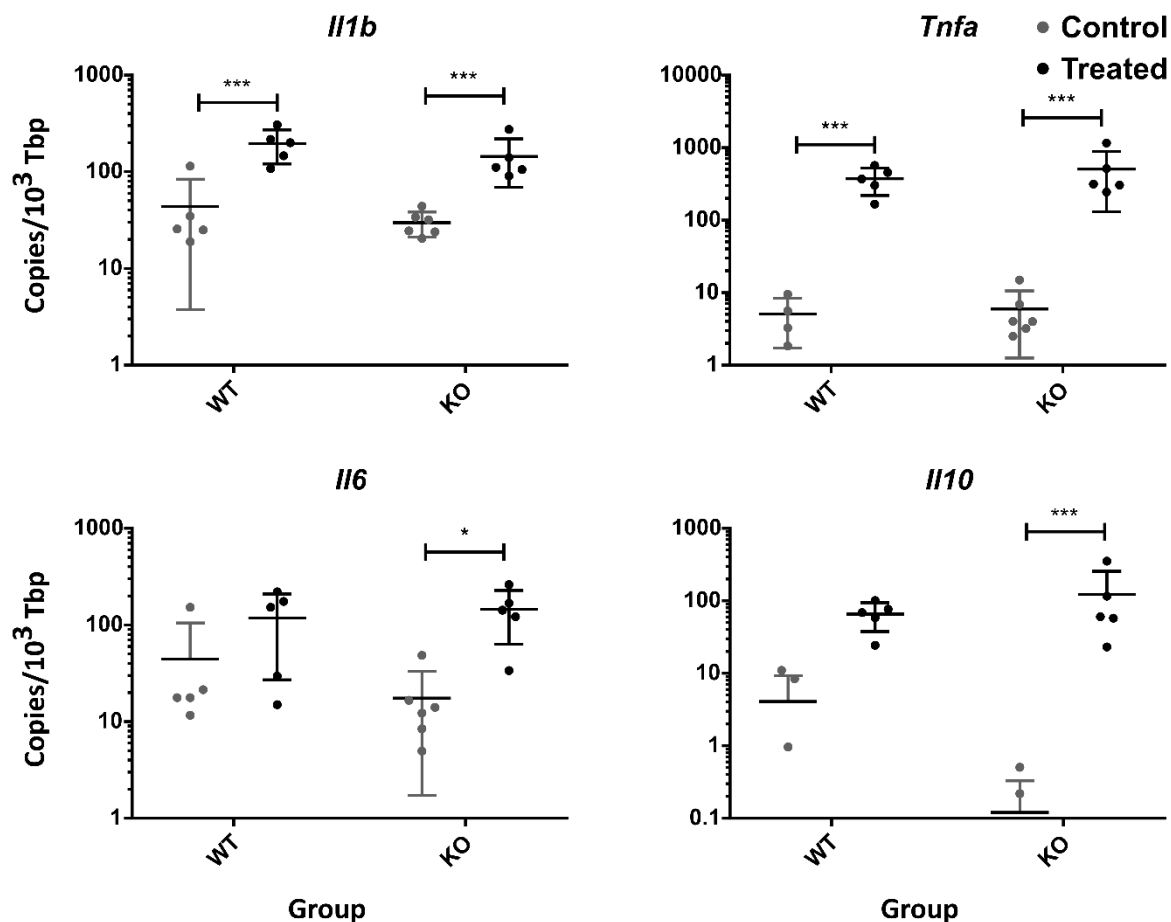


Figure 5.5: 4-day iCCRKO Aldara Model 2 Brain Cytokine Transcript

iCCR^{+/+} (WT) and iCCR^{-/-} (KO) mice were treated daily with 62.5mg Aldara cream (5% imiquimod) or control cream on the dorsal skin. Brain tissue was collected 24 hours after the 4th application. Absolute quantification was performed by qRT-PCR and values were normalised to housekeeping gene Tbp. N=5-6 per group. One-way ANOVA followed by Student's T-test with Bonferroni multiple testing correction was used to determine statistical significance. ***=P<0.001. Bars represent mean ± SD.

5.2.2 The effect of iCCRKO on brain cellular responses to repeated cutaneous Aldara treatment

5.2.2.1 Iba1⁺ staining of the hippocampus and cortex

To understand the influence of iCCRKO on cellular populations, immunohistochemical staining of the Iba1⁺, GFAP⁺ and CD3⁺ cellular populations was performed. Iba1⁺ staining of iCCRWT and KO mice reproduced earlier findings of increases in Iba1⁺ staining in Aldara treated animals that are accompanied by changes in gross morphology (Figure 5.6A, C, D, F). There was no evidence of significant alterations in Iba1⁺ staining in iCCRKO mice compared to WT mice (Figure 5.6B, C, E, F) and morphologically both treated groups appeared similar (Figure 5.6A, D).

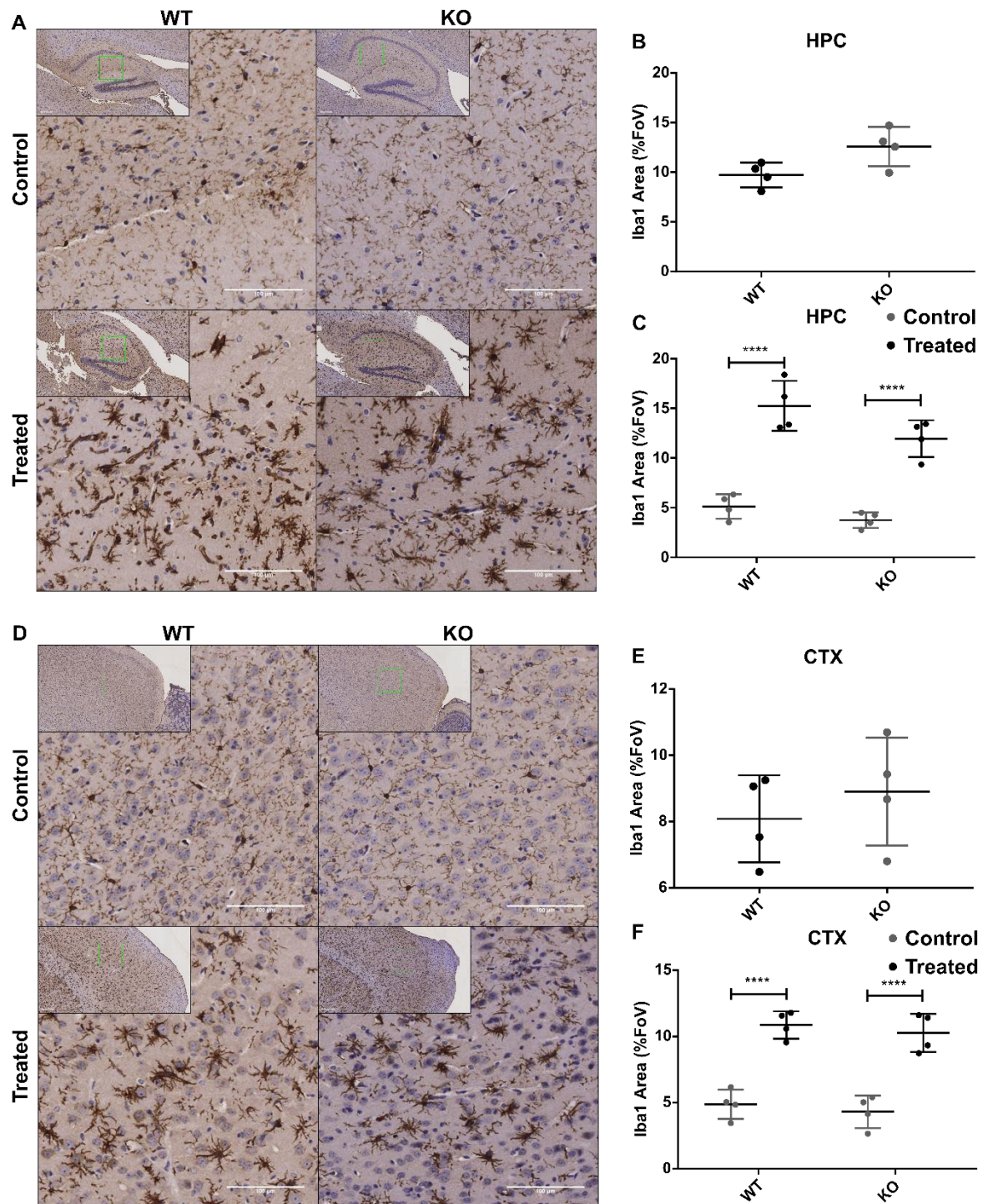


Figure 5.6: Iba1 staining of brain in iCCRKO Aldara Models

iCCR^{+/+} (WT) and iCCR^{-/-} (KO) mice were treated daily with 62.5mg Aldara cream (5% imiquimod) or control cream (A,C,D,F only) on the dorsal skin. Brain tissue was collected 24 hours after the 4th application. Formalin-fixed paraffin embedded sections were stained using Iba1 antibody and haematoxylin QS counterstain. (A, D) Representative images of 20x hippocampal (A) and cortical (D) fields of view used for automated analysis. Inset image shows 10x view of area with 20x area highlighted in green. Automated analysis of Iba1 area was performed using ImageJ software to quantify hippocampal (B, C) and cortical (E,F) Iba1 staining. Two separate experiments are shown; iCCRKO1 (B, E) iCCRKO2 (A, D, C, F) (n=4, 2-3 sections per mouse.) Tested using unpaired T-test (B, E) or one-way ANOVA and post-hoc Student's t-test with Bonferroni multiple testing correction (C, F). * $P < 0.05$; **** $P < 0.0001$. Scale bars = 100 μ m (main images), 200 μ m (inset images). Bars represent mean \pm SD. Abbreviations: HPC – Hippocampus; CTX – Cortex; FoV – Field of view.

5.2.2.2 GFAP staining of the hippocampus

As noted previously, due to its sparse distribution and high background staining GFAP was not examined in the cortex (Figure 5.7). Examination of hippocampal staining between WT and iCCRKO mice did not reveal any significant differences between the groups (Figure 5.7B, C). Unlike in the original 1d/3d GFAP staining, no significant differences in GFAP area were observed between treated and control groups in either WT or iCCRKO mice.

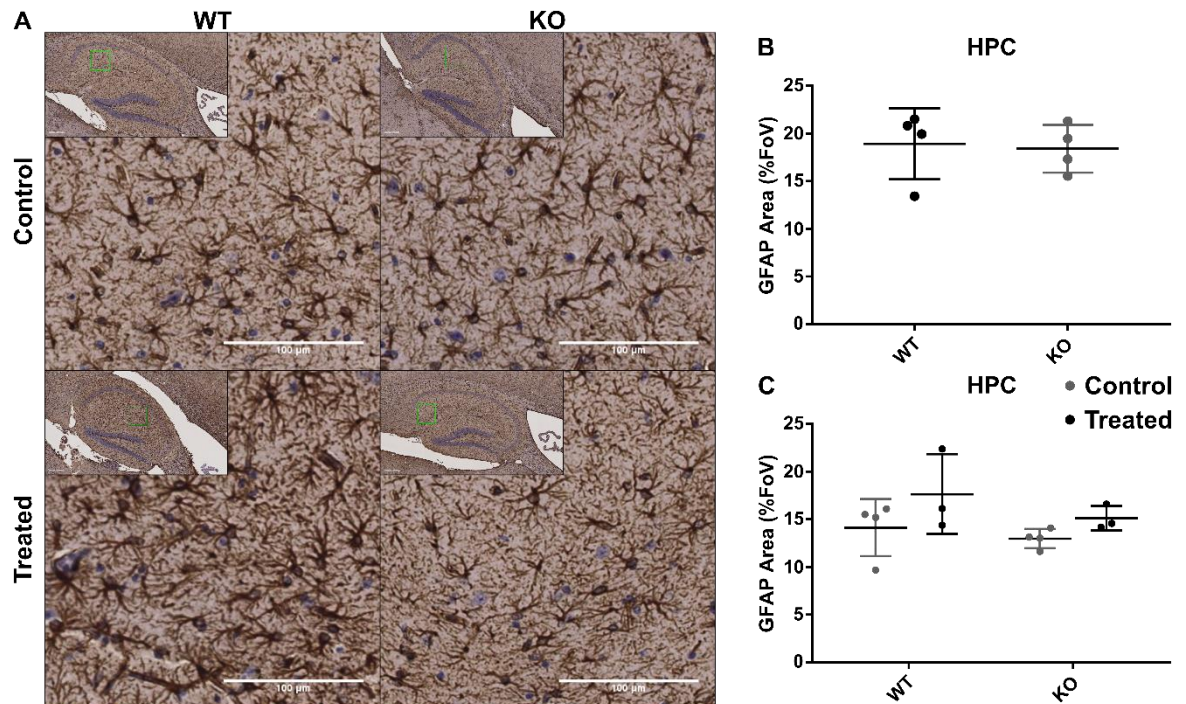


Figure 5.7: GFAP staining of brain in iCCRKO Aldara Models

iCCR^{+/+} (WT) and iCCR^{-/-} (KO) mice were treated daily with 62.5mg Aldara cream (5% imiquimod) or control cream (A,C only) on the dorsal skin. Brain tissue was collected 24 hours after the 4th application. Formalin-fixed paraffin embedded sections were stained using GFAP antibody and haematoxylin QS counterstain. (A) Representative images of 20x hippocampal fields of view used for automated analysis. Inset image shows 10x view of area with 20x area highlighted in green. Automated analysis of GFAP area was performed using ImageJ on three fields of view software to quantify hippocampal (B,C) GFAP staining. Two separate experiments are shown; iCCRKO1 (B) iCCRKO2 (C) (n=4, 2-3 sections per mouse.) Tested using unpaired T-test (B) or one-way ANOVA and post-hoc Student's t-test with Bonferroni multiple testing correction (C). **P*<0.05; Scale bars =100 μ m (main images), 200 μ m (inset images). Bars represent mean \pm SD. Abbreviations: HPC – Hippocampus; CTX – Cortex; FoV – Field of view.

5.2.2.3 CD3+ cell counts in the hippocampus and cortex

CD3+ cell numbers were examined in the hippocampus and cortex of iCCRKO and WT mice (Figure 5.8). Significant reductions in CD3+ cells were observed in the hippocampus but not in the cortex when comparing only treated WT and KO mice in the first experiment (Figure 5.8B, E). In the second experiment, although there were significant reductions in cortical CD3+ cell numbers, there was no significant difference within the HPC (Figure 5.8C, F). Reproducing earlier findings there were significant increases in CD3+ cells when comparing treated and control WT mice. Although not significant there was a mean increase in the number of CD3+ cells observed within the hippocampus and cortex of iCCRKO treated mice when compared to iCCRKO controls, and within the hippocampus this trended towards significance ($p=0.062$ after multiple testing correction) (Figure 5.8C, F).

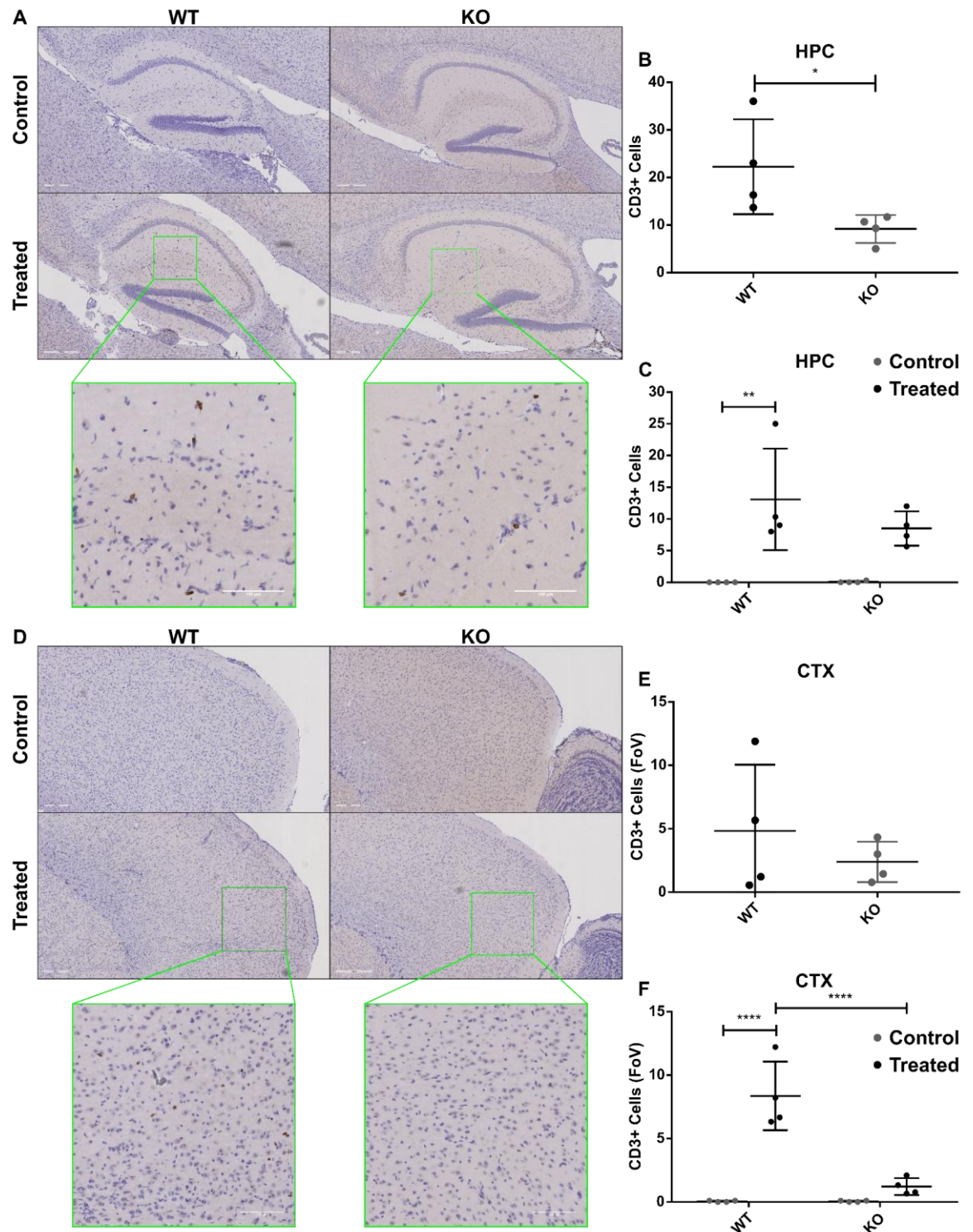


Figure 5.8: CD3 staining of brain in iCCRKO Aldara Models

iCCR^{+/+} (WT) and iCCR^{-/-} (KO) mice were treated daily with 62.5mg Aldara cream (5% imiquimod) or control cream (A,C,D,F only) on the dorsal skin. Brain tissue was collected 24 hours after the 4th application. Formalin-fixed paraffin embedded sections were stained using CD3 antibody and haematoxylin QS counterstain by Veterinary Diagnostic Services Laboratory at the University of Glasgow. (A, D) Representative images of 10x hippocampal (A) and cortical (D) fields of view. Expanded images are 20x examples of CD3 staining in treated samples. (B,C) Manual counting was performed on all CD3+ cells within the hippocampus. (E,F) Manual counting of CD3+ cells in the cortex, 3 fields of view were used per section. Two separate experiments are shown; iCCRKO1 (B, E) iCCRKO2 (A, D,C,F) (n=4, 3 sections per mouse.) Tested using unpaired T-test (B, E) or one-way ANOVA and post-hoc Student's t-test with Bonferroni multiple testing correction (C, F). **=P<0.01; ****=P<0.0001. Scale bars =100µm (main images), 200µm (inset images). Bars represent mean ± SD. Abbreviations: HPC – Hippocampus; CTX – Cortex; FoV – Field of view.

5.2.3 The effect of IFNARKO on chemokine and cytokine transcriptional responses to repeated cutaneous Aldara treatment

Following investigation of the iCCRKO response to cutaneous Aldara treatment, the effect of IFNARKO was explored in the brain, local site of immune stimulation, the skin, and, through examination of the PBL, the circulation.

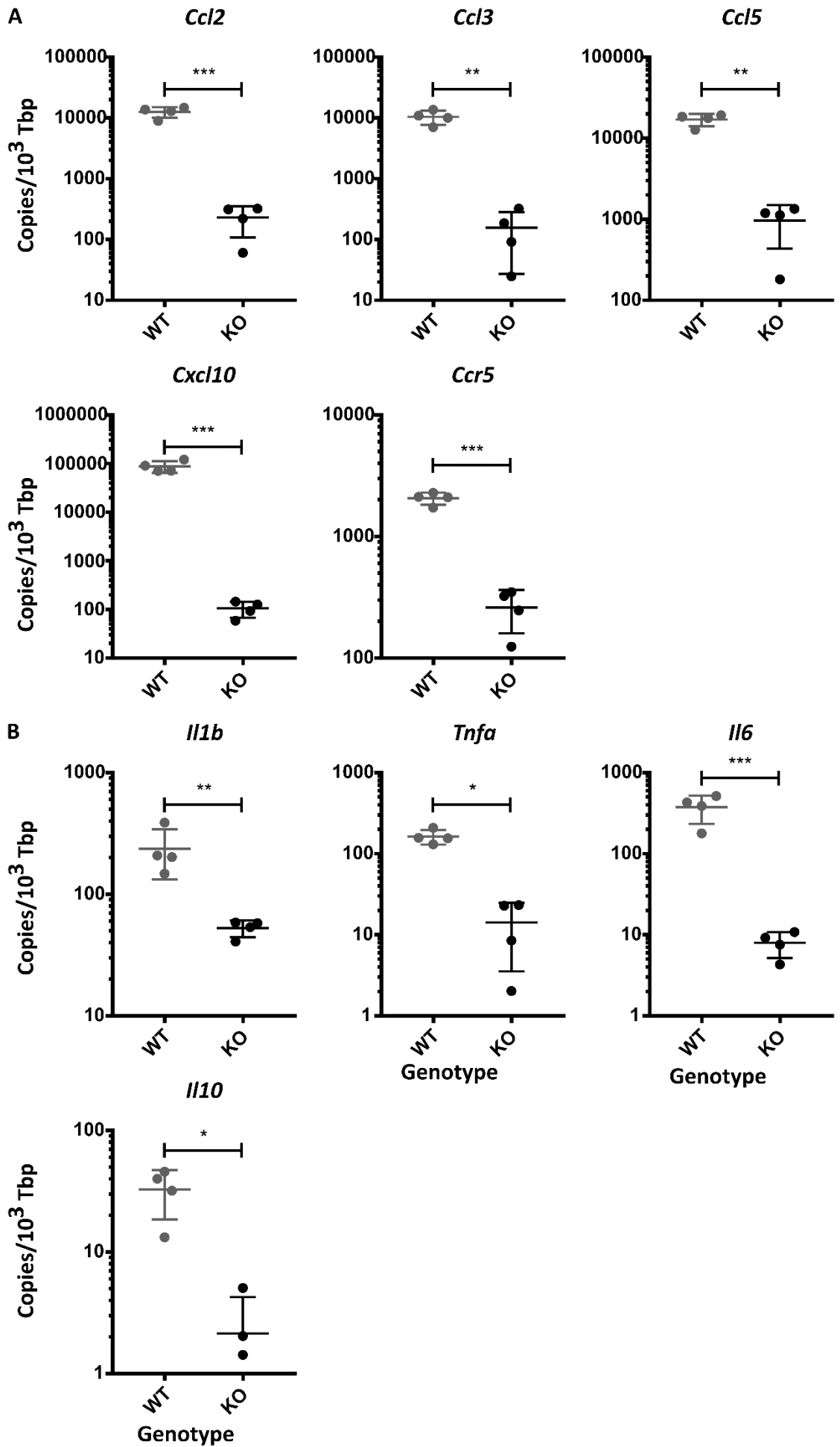
5.2.3.1 Brain chemokine and cytokine transcriptional responses

Initial investigation of the brain, after 3 days of daily cutaneous Aldara treatment, revealed significant reductions in all measured chemokine and cytokine transcripts (*Ccl2*, *Ccl3*, *Ccl5*, *Cxcl10*, *Ccr5*, *Il1b*, *Tnfa*, *Il6* and *Il10*) in IFNARKO mice (Figure 5.9). It is interesting to note that an archetypal ISG *Cxcl10* showed a much greater magnitude of reduction ($\approx 1000x$) when compared to genes that are more associated with NF- κ B responses (e.g. *Il1b* and *Tnfa*), which showed differences of ($\approx 10x$).

To further explore these differences a repeat experiment was performed using both treated and control groups for each genotype. This experiment reproduced the findings of the first experiment with significant reductions in the expression of all measured chemokine and cytokine transcripts (*Ccl2*, *Ccl3*, *Ccl5*, *Cxcl10*, *Ccr5*, *Il1b*, *Tnfa*, *Il6* and *Il10*) in IFNARKO mice when compared to WT mice (Figure 5.10, Figure 5.11). As expected, in WT treated mice there were significant increases in measured transcripts as compared to controls. Interestingly in the IFNARKO treated mice there were significant increases in the majority of measured transcripts (*Ccl2*, *Ccl3*, *Ccl5*, *Ccr5*, *Il1b*, *Tnfa*, *Il10*) when compared to IFNARKO controls. However, both *Cxcl10* and *Il6* did not differ significantly, suggesting that following cutaneous Aldara treatment IFNAR is required for their induction in the brain at this timepoint.

Figure 5.9: (Overleaf) 3-day IFNARKO Aldara Model 1 Brain Chemokine and Cytokine Transcript

IFNAR^{+/+} (WT) and IFNAR^{-/-} (KO) mice were treated daily with 62.5mg Aldara cream (5% imiquimod) on the dorsal skin. Brain tissue was collected 24 hours after the 3rd application. Absolute quantification was performed by qRT-PCR and values were normalised to housekeeping gene *Tbp*. N=4 per group. Unpaired Student's T-test with Bonferroni multiple testing correction was used to determine statistical significance. * = P < 0.05; ** = P < 0.01; *** = P < 0.001. Bars represent mean \pm SD.



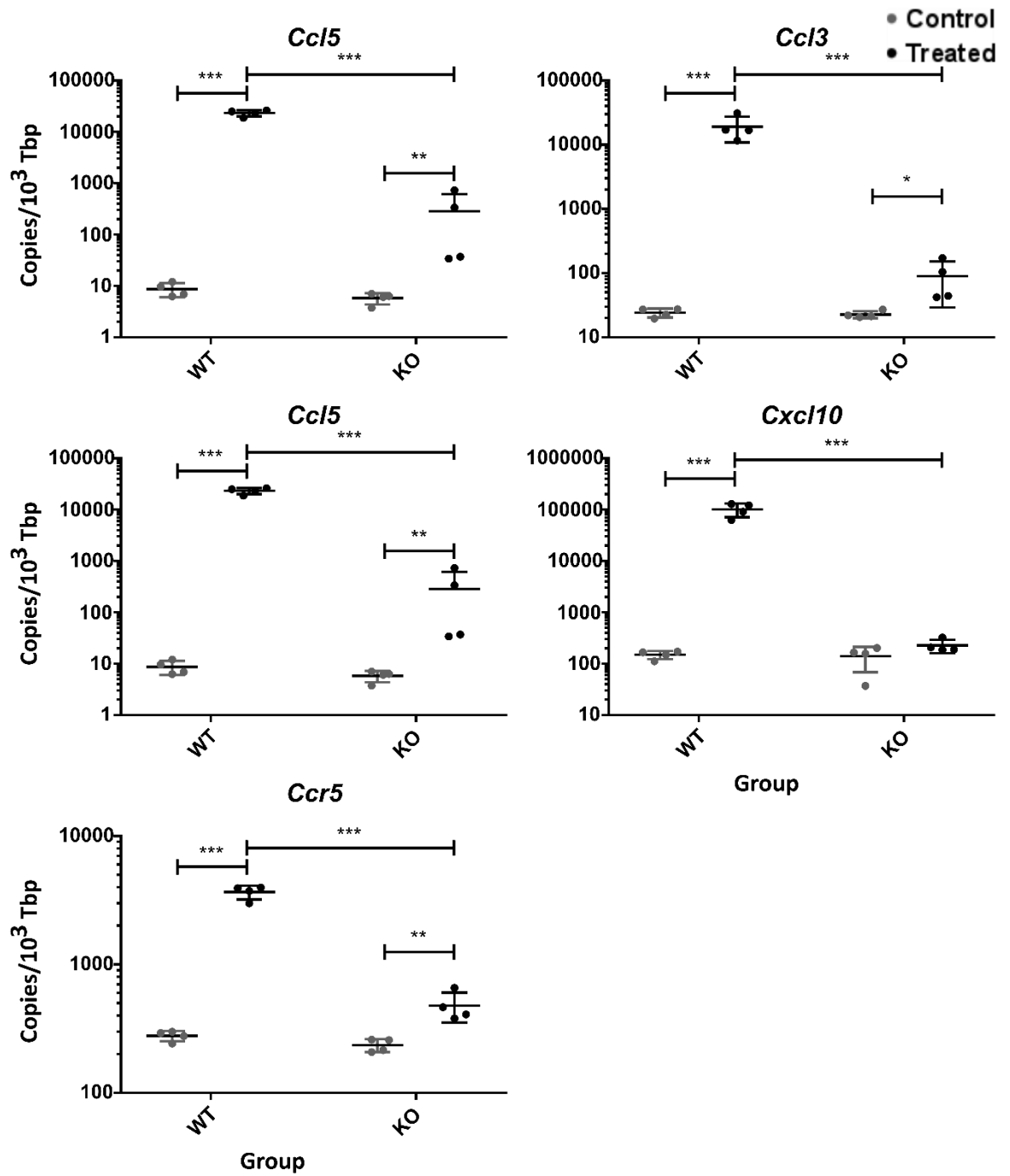


Figure 5.10: 3-day IFNARKO Aldara Model 2 Brain Chemokine Transcript

IFNAR^{+/+} (WT) and IFNAR^{-/-} (KO) mice were treated daily with 62.5mg Aldara cream (5% imiquimod) or control cream on the dorsal skin. Brain tissue was collected 24 hours after the 3rd application. Absolute quantification was performed by qRT-PCR and values were normalised to housekeeping gene Tbp. N=4 per group. One-way ANOVA followed by Student's T-test with Bonferroni multiple testing correction was used to determine statistical significance. * = P < 0.05; ** = P < 0.01; *** = P < 0.001. Bars represent mean ± SD.

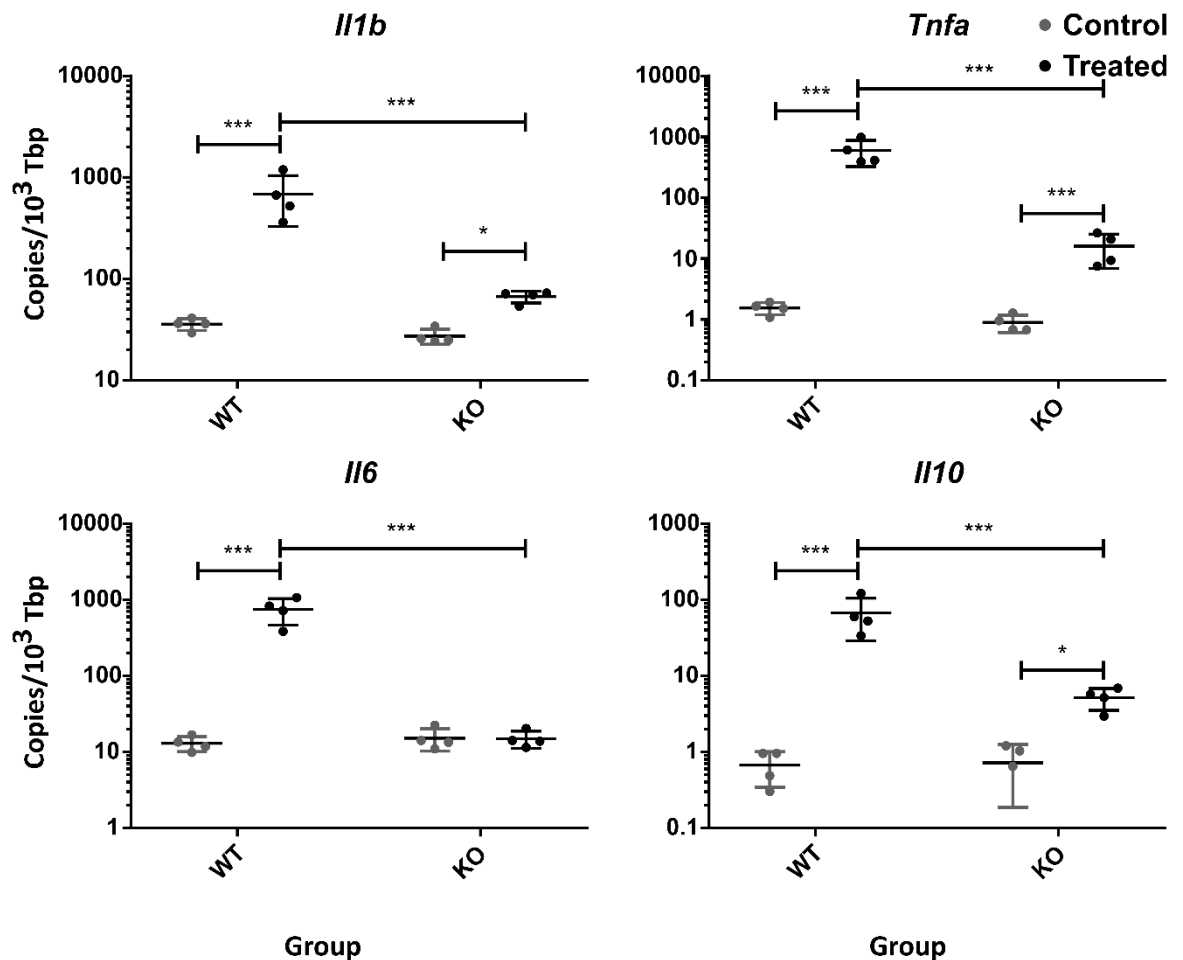


Figure 5.11: 3-day IFNARKO Aldara Model 2 Brain Cytokine Transcript

IFNAR^{+/+} (WT) and IFNAR^{-/-} (KO) mice were treated daily with 62.5mg Aldara cream (5% imiquimod) or control cream on the dorsal skin. Brain tissue was collected 24 hours after the 3rd application. Absolute quantification was performed by qRT-PCR and values were normalised to housekeeping gene *Tbp*. N=4 per group. One-way ANOVA followed by Student's T-test with Bonferroni multiple testing correction was used to determine statistical significance. *P<0.05; ***P<0.001. Bars represent mean ± SD.

5.2.3.2 Skin and PBL chemokine and cytokine transcriptional responses

Subsequent examination of peripheral transcriptional responses in the skin (Figure 5.12) and PBL (Figure 5.13) identified that in PBL alone, *Ccl5* and *Cxcl10* expression were significantly reduced in IFNARKO mice. In the skin, no measured chemokine or cytokine transcripts were significantly altered, as was the case for the remaining PBL transcripts. Finally, it is worth noting that there was no clear trend in the skin to suggest either an upregulation or downregulation of inflammatory mediators in this tissue for IFNARKO mice, indicating that there was likely no effect of IFNARKO on skin chemokine and cytokine transcriptional responses after three days of cutaneous Aldara treatment.

Figure 5.12: (Previous page) 3-day IFNARKO Aldara Model 1 Skin Chemokine and Cytokine Transcript

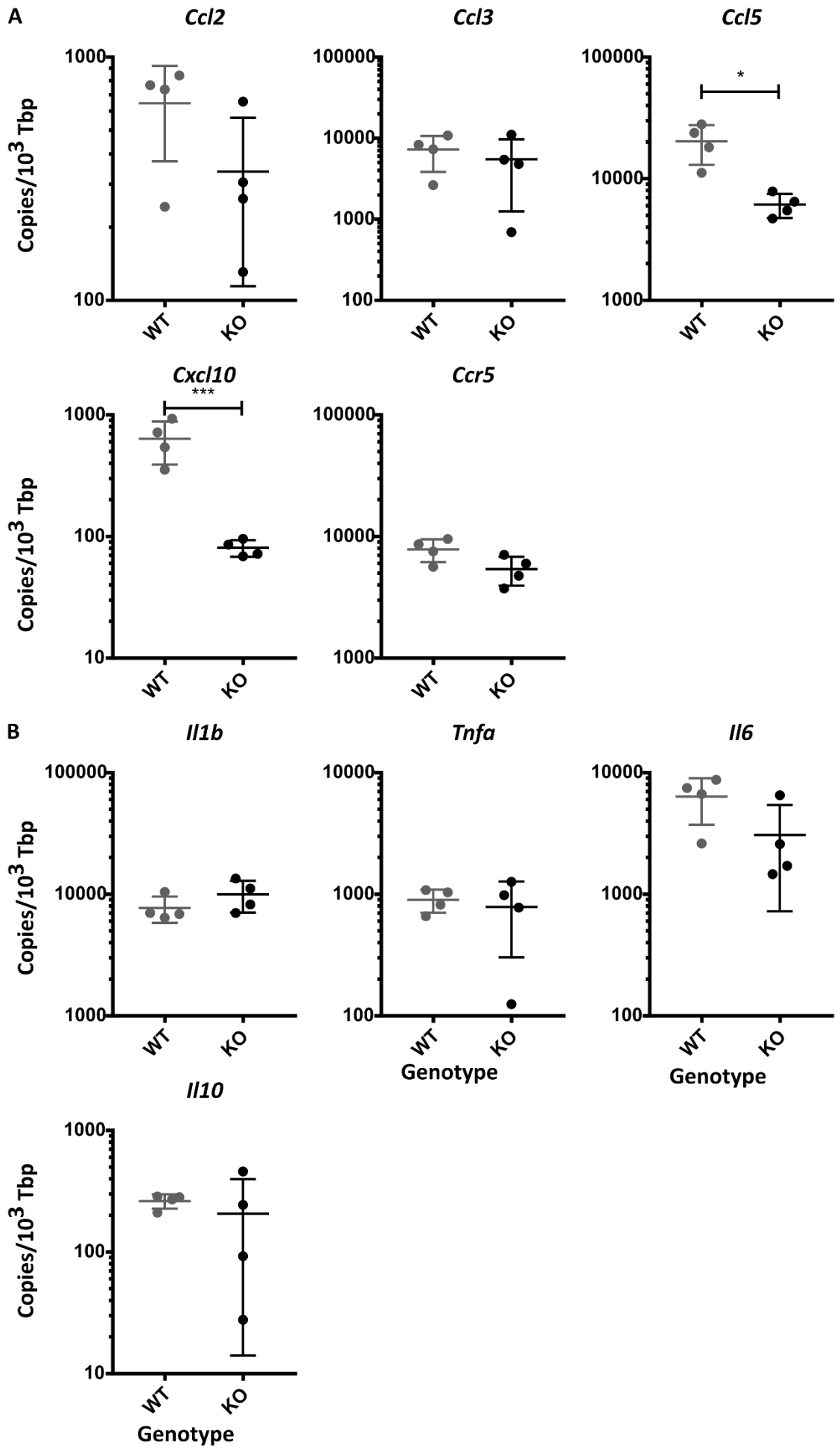
IFNAR^{+/+} (WT) and IFNAR^{-/-} (KO) mice were treated daily with 62.5mg Aldara cream (5% imiquimod) on the dorsal skin. Skin was collected 24 hours after the 3rd application. Absolute quantification was performed by qRT-PCR and values were normalised to housekeeping gene Tbp. N=4 per group. Unpaired Student's T-test with Bonferroni multiple testing correction was used to determine statistical significance. A P value < 0.05 was considered significant. Bars represent mean \pm SD.

5.2.4 The effect of IFNARKO on cellular responses to repeated Aldara treatment**5.2.4.1 Iba1+ staining of the hippocampus and cortex**

Initial Iba1+ staining of the hippocampus and cortex in treated IFNAR^{WT} and KO experiments demonstrated a significant reduction in hippocampal but not cortical, Iba1+ staining in KO mice (Figure 5.14B, E). In the repeat experiment this finding was not reproduced, and while there was no significant difference between treated WT and KO Iba1+ staining in the hippocampus, there was a trend towards a difference in the cortex (P=0.069 after multiple testing correction) (Figure 5.14C, F). Despite this lack of significance, morphological examination of Iba1 staining revealed that the clear changes in microglial appearance observed in treated WT mice do not appear to be as prominent in IFNARKO treated mice (Figure 5.14A, D).

Figure 5.13: (Overleaf) 3-day IFNARKO Aldara Model 1 PBL Chemokine and Cytokine Transcript

IFNAR^{+/+} (WT) and IFNAR^{-/-} (KO) mice were treated daily with 62.5mg Aldara cream (5% imiquimod) on the dorsal skin. PBL were collected 24 hours after the 3rd application. Absolute quantification was performed by qRT-PCR and values were normalised to housekeeping gene Tbp. N=4 per group. Unpaired Student's T-test with Bonferroni multiple testing correction was used to determine statistical significance. *=P<0.05; ***=P<0.001. Bars represent mean \pm SD.



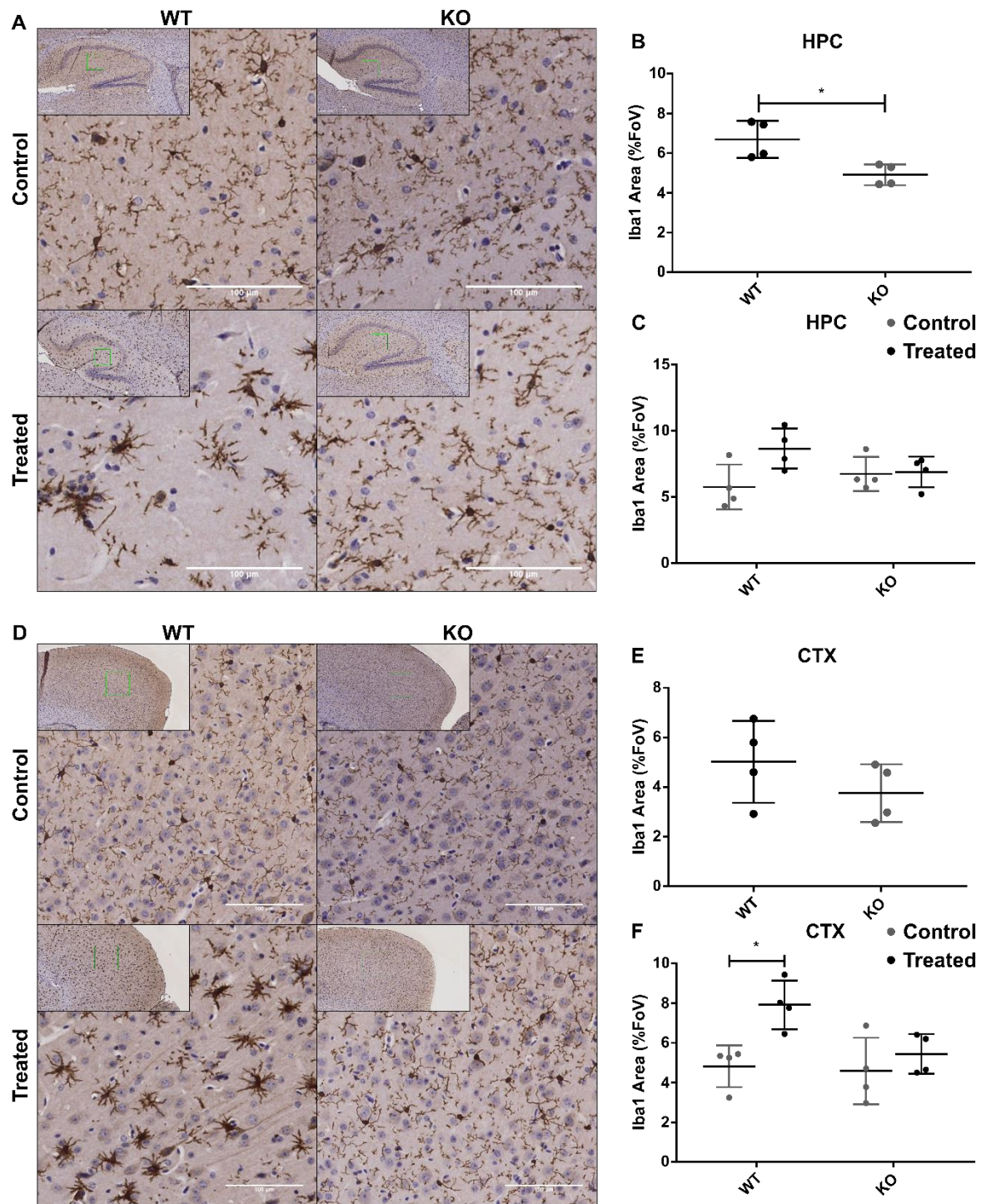


Figure 5.14: Iba1 staining of brain in IFNARKO Aldara Models

IFNAR^{+/+} (WT) and IFNAR^{-/-} (KO) mice were treated daily with 62.5mg Aldara cream (5% imiquimod) or control cream (A,C,D,F only) on the dorsal skin. Brain tissue was collected 24 hours after the 3rd application. Formalin-fixed paraffin embedded sections were stained using Iba1 antibody and haematoxylin QS counterstain. (A, D) Representative images of 20x hippocampal (A) and cortical (D) fields of view used for automated analysis. Inset image shows 10x view of area with 20x area highlighted in green. Automated analysis of Iba1 area was performed using ImageJ software to quantify hippocampal (B, C) and cortical (E,F) Iba1 staining. Two separate experiments are shown; IFNARKO1 (B, E) IFNARKO2 (A, D, C, F) (n=4, 2-3 sections per mouse.) Tested using unpaired T-test (B, E) or one-way ANOVA and post-hoc Student's t-test with Bonferroni multiple testing correction (C, F). * $P < 0.05$. Scale bars = 100 μ m (main images), 200 μ m (inset images). Bars represent mean \pm SD. Abbreviations: HPC – Hippocampus; CTX – Cortex; FoV – Field of view.

5.2.4.2 GFAP staining of the hippocampus

Examination of hippocampal GFAP revealed a small but significant increase in GFAP staining in treated IFNARKO mice compared to WT (Figure 5.15B), however in the second experiment this was not reproduced and the mean GFAP area in treated WT mice was increased non-significantly compared to treated IFNARKO mice (Figure 5.15C). Alongside this there did not appear to be gross morphological differences between the groups (Figure 5.15A).

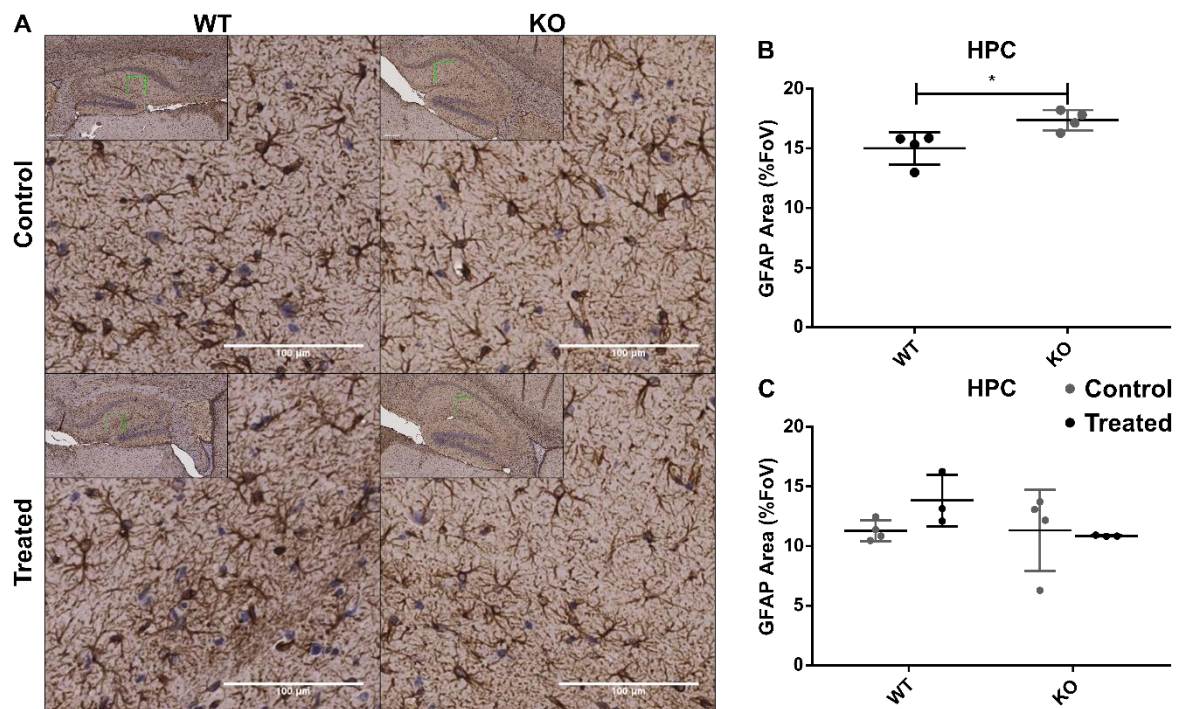


Figure 5.15: GFAP staining of brain in IFNARKO Aldara Models

IFNAR^{+/+} (WT) and IFNAR^{-/-} (KO) mice were treated daily with 62.5mg Aldara cream (5% imiquimod) or control cream (A,C only) on the dorsal skin. Brain tissue was collected 24 hours after the 3rd application. Formalin-fixed paraffin embedded sections were stained using GFAP antibody and haematoxylin QS counterstain. (A) Representative images of 20x hippocampal fields of view used for automated analysis. Inset image shows 10x view of area with 20x area highlighted in green. Automated analysis of GFAP area was performed using ImageJ on three fields of view software to quantify hippocampal (B, C) GFAP staining. Two separate experiments are shown; IFNARKO1 (B) IFNARKO2 (C) (n=4, 2-3 sections per mouse.) Tested using unpaired T-test (B) or one-way ANOVA and post-hoc Student's t-test with Bonferroni multiple testing correction (C). * $P < 0.05$; Scale bars = 100 μ m (main images), 200 μ m (inset images). Bars represent mean \pm SD. Abbreviations: HPC – Hippocampus; CTX – Cortex; FoV – Field of view.

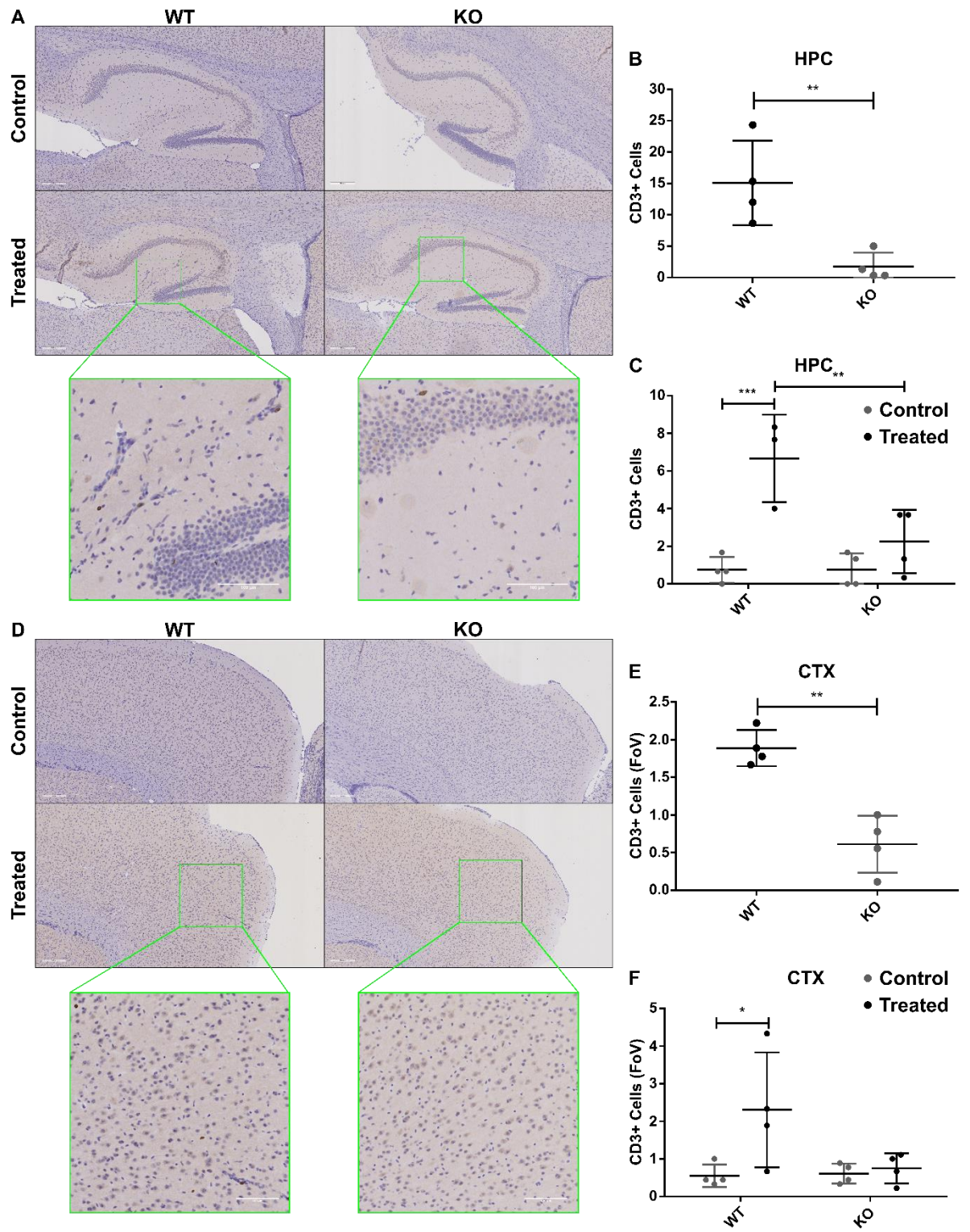
5.2.4.3 CD3+ cell counts in the hippocampus and cortex

CD3+ cells were investigated in both the hippocampus and cortex of IFNAR^{WT} and KO mice (Figure 5.16). In both experiments there were significant reductions in CD3+ cells in the hippocampus of treated IFNARKO mice when compared to WT (Figure 5.16B, C). Alongside this in the first experiment there was a

significant reduction in cortical CD3⁺ cells and in the second experiment there was a trend towards significance ($p=0.076$ after multiple testing correction) (Figure 5.16E, F). In both the hippocampus and the cortex earlier findings of increased CD3⁺ cells in treated animals were reproduced in WT mice. In contrast, there was no significant difference in CD3⁺ cell numbers between treated and control IFNARKO mice. Together these data strongly suggest that there are reductions in CD3⁺ cell numbers in treated IFNARKO mice when compared to WT animals.

Figure 5.16: (Overleaf) CD3 staining of brain in IFNARKO Aldara Models

IFNAR^{+/+} (WT) and IFNAR^{-/-} (KO) mice were treated daily with 62.5mg Aldara cream (5% imiquimod) or control cream (A,C,D,F only) on the dorsal skin. Brain tissue was collected 24 hours after the 3rd application. Formalin-fixed paraffin embedded sections were stained using CD3 antibody and haematoxylin QS counterstain by Veterinary Diagnostic Services Laboratory at the University of Glasgow. (A, D) Representative images of 10x hippocampal (A) and cortical (D) fields of view. Expanded images are 20x examples of CD3 staining in treated samples. (B, C) Manual counting was performed on all CD3⁺ cells within the hippocampus. (E, F) Manual counting of CD3⁺ cells in the cortex, 3 fields of view were used per section. Two separate experiments are shown; IFNARKO1 (B, E) IFNARKO2 (A, D, C, F) ($n=4$, 3 sections per mouse.) Tested using unpaired T-test (B, E) or one-way ANOVA and post-hoc Student's t-test with Bonferroni multiple testing correction (C, F). *= $P<0.05$; **= $P<0.01$; ****= $P<0.0001$. Scale bars =100 μ m (main images), 200 μ m (inset images). Bars represent mean \pm SD. Abbreviations: HPC – Hippocampus; CTX – Cortex; FoV – Field of view.



5.3 Discussion

5.3.1 Summary of results

The work presented in this chapter has investigated the role of inflammatory chemokine (CCR1, CCR2, CCR3 and CCR5) and IFNAR signalling in the induction of inflammation following cutaneous Aldara treatment. The data suggest that iCCRKO may influence CD3⁺ cellular response to cutaneous Aldara treatment, but does not have significant effects on transcriptional responses. In contrast, IFNARKO has significant effects on brain chemokine and cytokine transcriptional responses to cutaneous Aldara treatment that appear to be accompanied by changes in the response of Iba1⁺ and CD3⁺ cellular populations. Despite this IFNARKO does not appear to cause many significant differences in either the skin or PBL transcriptional response to 3 days of cutaneous Aldara treatment. Neither iCCRKO nor IFNARKO appeared to significantly influence the GFAP⁺ cellular population within the CNS in a consistent manner.

5.3.2 Role of iCCRs in response to cutaneous Aldara treatment

The data presented here suggest that, in contrast to our hypothesis, the iCCRs (CCR1, CCR2, CCR3 and CCR5) have no apparent effect on brain chemokine and cytokine transcriptional responses to cutaneous Aldara treatment. Despite this, there is evidence that there are reductions in the cellular CD3⁺ population. These data may be explained by a number of factors. Firstly iCCRs are most likely to influence cellular migration and recruitment(27), and, as such the responses of endogenous cellular populations such as microglia and astrocytes that are already present in the brain may not be significantly altered. This is particularly true when considering response to the type I IFNs and the cytokines examined here (*Il1b*, *Tnfa* and *Il6*). If the inflammatory signal from the periphery can be transmitted to the brain in the absence of cellular recruitment, for example, through circulating inflammatory mediators gaining access to the CNS parenchyma (254, 255, 257, 258), it would be unlikely that dramatic differences in the chemokine and cytokine response would be observed as the endogenous cells of the CNS would be able to respond to these signals and initiate an inflammatory response, independent of cellular recruitment. This would also

provide an explanation for the lack of consistent significant differences observed between iCCRKO and WT mice in the GFAP+ cellular populations.

Another possible explanation is that although significant differences were not observed in this experiment, this was due to insufficient power rather than a lack of any difference. Based on the data generated here and using *Il1b*, which was reduced non-significantly in both iCCRKO experiments, power calculations indicated that for 80% power at an alpha of 0.05, 32 animals per group would be required. As these animals were in short supply this would have been difficult to achieve, however it does highlight a limitation of this work and a consideration for future experiments.

A final possible explanation is that at this time-point transcriptional changes may not be present. Previous data from fluorescence-activated cell sorting (FACS) examination of recruited cellular populations in the brains of Aldara treated WT mice reveals that after 1 day there are limited changes with peak responses occurring at 3 or 5 days depending on the population(24). If recruitment begins to occur between 1 and 3 days, and there are deficits in this process in iCCRKO mice it is entirely possible that alterations in transcription may not become manifest until after the 4 day time-point examined here.

A reduction in CD3+ cellular recruitment was expected in the context of iCCRKO, because, as mentioned earlier, CCR5 is an important receptor for T-cell recruitment (123, 479). Although not conclusive there does appear to be evidence of reductions in CD3+ cell numbers in the brains of iCCRKO mice. The reason for this equivocal outcome may be that, in the absence of CCR5, CXCR3 will still be present in iCCRKO mice. The CXCR3-CXCL10 axis is also thought to be important for T-cell homing (122), particularly to the CNS (480, 481) and, as such, it might be expected that this redundancy would at least in part make up for deficits in CCR5. Increases in power or more quantitative methods such as FACS, may help to clarify the effect of iCCRKO on CD3+ cellular populations.

5.3.3 Role of IFNAR in response to cutaneous Aldara treatment

In line with our hypotheses IFNARKO resulted in significant reductions in brain transcriptional responses that were accompanied by changes in the Iba1+ and

CD3⁺ populations. The reductions in transcriptional response can be explained through the fact that IFNAR^{−/−} mice should lack type I IFN responses. As type I IFN signalling is a potent inducer of inflammatory responses (85), it is not surprising that in its absence chemokine and cytokine transcriptional responses are attenuated.

Two other, more interesting, findings from the transcriptional data are: (i) the extent to which all measured transcripts were downregulated (>10x) and; (ii) the fact that some (*Cxcl10* and *Il6*) but not all transcripts were unchanged in IFNAR^{−/−} mice in response to cutaneous Aldara treatment. Considering the first point, when examining genes that are more classically associated with NF- κ B such as *Il1b* and *Tnfa* (49, 474) one might expect that, although there may be reductions in their expression due to reduction in overall inflammation in IFNAR^{−/−}, their responses would be largely intact. The data presented here seem to suggest that this is not the case. While in the absence of IFNAR, many transcripts that are associated with NF- κ B signalling are still significantly upregulated following Aldara treatment these data suggest that IFNAR signalling is critical to augmenting this response. The second point demonstrates that, while there is crossover between IFNAR and NF- κ B signalling as discussed above, certain transcripts are strongly associated with specific signalling pathways. *Cxcl10* is an archetypal ISG and therefore the fact that its response is completely abrogated in IFNAR^{−/−} mice is not entirely surprising, although considering it was originally described as being induced by IFN γ a type II IFN, it is a little unexpected. However, without assessing the impact of IFNAR^{−/−} on IFN γ in this model, it is difficult to know how unexpected this result is as conflicting data shows that IFN γ can be both decreased (482) and increased (483) in IFNAR^{−/−} mice. *Il6* is not an archetypal ISG, however, the data presented here suggest that, at least within the brain, in response to cutaneous Aldara, its induction is dependent on intact type I IFN signalling. This conflicts with data from the same viral infection study (483) that demonstrated increase in IFN- γ , showing an increase in *Il-6* in IFNAR^{−/−} mice, although this may be accounted for by: (i) the fact that this model used a virus rather than a TLR ligand that may be able to activate other TLR signalling pathways; (ii) IFNAR^{−/−} increases viral load and lethality, and additional damage associated with this may potentiate further inflammatory responses.

Having observed reductions in transcription it is unsurprising that the cellular responses observed in treated mice are attenuated. As discussed, significant reductions in *Ccl5* and *Cxcl10* would be expected to result in a reduced number of CD3⁺ cells within the CNS parenchyma. Alongside these significant reductions in inflammatory transcripts, it is not surprising that morphological alterations, associated with reactive changes, in Iba1⁺ cells would be reduced. Considering that these changes in microglia are most strongly associated with phagocytosis, (167, 469) these data suggest that IFNAR signalling is important for inducing morphological alterations associated with a phagocytic phenotype in microglial cells. However, whether this is due to the fact that IFNAR signalling is required for the induction of phagocytic activity, whether IFNAR is required for morphological changes following phagocytosis or whether IFNARKO limits damage that stimulates a phagocytic phenotype is not clear from this set of experiments.

One challenge of the data presented above is that only two significant differences were identified in the chemokine and cytokine transcriptional responses of the skin and PBL. However, this would be expected, considering the fact that most transcripts in the time-course model appear to return to control levels by the 3 day time-point examined here. As such it is difficult to assess whether the reduction in inflammatory responses observed here is due to a reduction in the peripheral response that results in a reduction of CNS inflammation or is due to a brain specific role of IFNAR. A more complete time-course in IFNARKO mice would help investigate this.

5.3.4 Other findings of note

Two other findings of note are worth briefly mentioning here. Firstly the data presented here supports earlier findings of increases in chemokine and cytokine transcription after repeated daily cutaneous Aldara treatment compared to control cream. In addition although not always significant, in experiments that compared WT control and treated animals there were consistent increases in Iba1⁺ and GFAP⁺ area, and CD3⁺ cellular numbers. The consistent nature of these findings across not just multiple experiments but also multiple genotypes (C57BL6/J in the time-course, C57BL6/N in the iCCRKO and A129 in the IFNARKO) provides substantial evidence that observed effects are real.

Secondly it is interesting that there did not appear to be changes in GFAP between the genotypes. This is likely due to the fact that compared to the changes in Iba1 and CD3; the changes in GFAP appear to be relatively small. This may reflect that quantification of DAB GFAP area is not sensitive enough. As such, immunofluorescence that may be more easily quantifiable or alternate assays of astrocytic function, such as examination of the astrocyte population after cell sorting, may be more appropriate.

5.3.5 Summary

Overall these data have provided insight into the role of iCCRKO and IFNARKO in brain responses to cutaneous Aldara treatment. iCCRKO has minimal impact on transcriptional and CNS resident cellular responses to cutaneous Aldara, but, does appear to significantly impact the recruitment of CD3⁺ T cells. In contrast, IFNARKO has significant impacts on CNS transcriptional responses, even those more classically associated with NF- κ B. Alongside changes in the transcriptional response, IFNARKO also alters microglial responses as measured using Iba1 and reduces recruitment of CD3⁺ T cells into the brain. However, both of these studies raise questions that remain to be answered, particularly around the role of peripheral vs central mechanisms mediating these differences. In addition, much of the data presented here supported earlier findings from the Aldara model, allowing us to have greater confidence in findings of transcriptional and cellular alterations within the brain in response to cutaneous Aldara treatment.

Chapter 6

**The effect of a single Aldara treatment over time
and mass spectrometry of Imiquimod**

Chapter 6 The effect of a single Aldara treatment over time and mass spectrometry of Imiquimod

6.1 Introduction

Earlier in this thesis a number of features of the response to Aldara were identified to be investigated further. Firstly, it appeared that the magnitude of fold changes in the brain was greater than in the peripheral tissues. Secondly, examination of the brain transcriptional response to Aldara identified that for all examined chemokines and cytokines, the peak was after 3 days of repeated treatments, and, that this was not the case for the peripheral tissues that generally peaked within the first 24 hours. Based on these two findings the following questions were asked:

1. Is the absolute expression of examined chemokines and cytokines lower in the brain than in the periphery under control conditions thus accounting for the apparently greater fold change?
2. In the case of only a single treatment of Aldara does the brain still manifest a peak chemokine and cytokine transcriptional response after 3 days?

To this end the Aldara model was repeated looking at 1 day, 3 day and 5 day time-points after a single treatment of Aldara at day 0. The use of absolute measures of gene expression allowed for tentative comparisons of control expression between tissues. Based on data from other TLR models of inflammation suggesting that single peripheral insults resolve relatively quickly (239, 245, 246, 484), it was hypothesized that a single treatment would result in an earlier peak response point at 1 day post IMQ application.

In addition to the above findings, it was shown that there were profound systemic responses to Aldara treatment. Alongside this, human pharmacokinetic data shows that IMQ the TLR7 agonist present in Aldara can be absorbed into the circulation (485), and based on IMQ's low molecular weight and lipophilic

nature(486), it may subsequently be able to cross the blood-brain barrier. Therefore, it was asked:

3. Are the systemic and central responses to Aldara a consequence of imiquimod entry into the plasma and/or brain parenchyma?

To investigate the possible role of systemic IMQ further the biomarker and drug analysis core facility at Dundee University conducted mass spectrometry on the plasma and brains from mice treated with Aldara cream at a variety of time points.

Similar to the mechanistic investigations presented in the previous chapter the absolute expression of a select group of chemokines and cytokines identified as altered in the initial time-course investigations was investigated. In addition to the tissues studied in the time-course, the spleen was also examined as had been initially intended for the time-course experiment in Chapter 4. Alongside this, based on the paper by Grine et al. suggesting that Aldara's effects may be mediated by oral intake and colon activation (288), it was deemed worthwhile to include colon tissue to examine if there were inflammatory changes that could be indicative of IMQ ingestion.

6.2 Results

6.2.1 Comparison of control levels of gene expression between tissues

Due to the fact that a large quantity of absolute transcriptional data from control mice that had only been exposed to shaving was available, tissue specific expression levels were examined in these mice. The most striking finding from this analysis was that, for all chemokine and cytokine transcripts examined, absolute expression in the brain normalised to *Tbp* was either significantly lower or not significantly different from other tissues (Figure 6.1, Figure 6.2). For *Ccl2*, *Ccl5*, *Il1b* and *Tnfa* expression in the brain was significantly lower than all other tissues in control mice. For all transcripts except *Il6* the skin, spleen and colon had significantly higher gene expression than the brain.

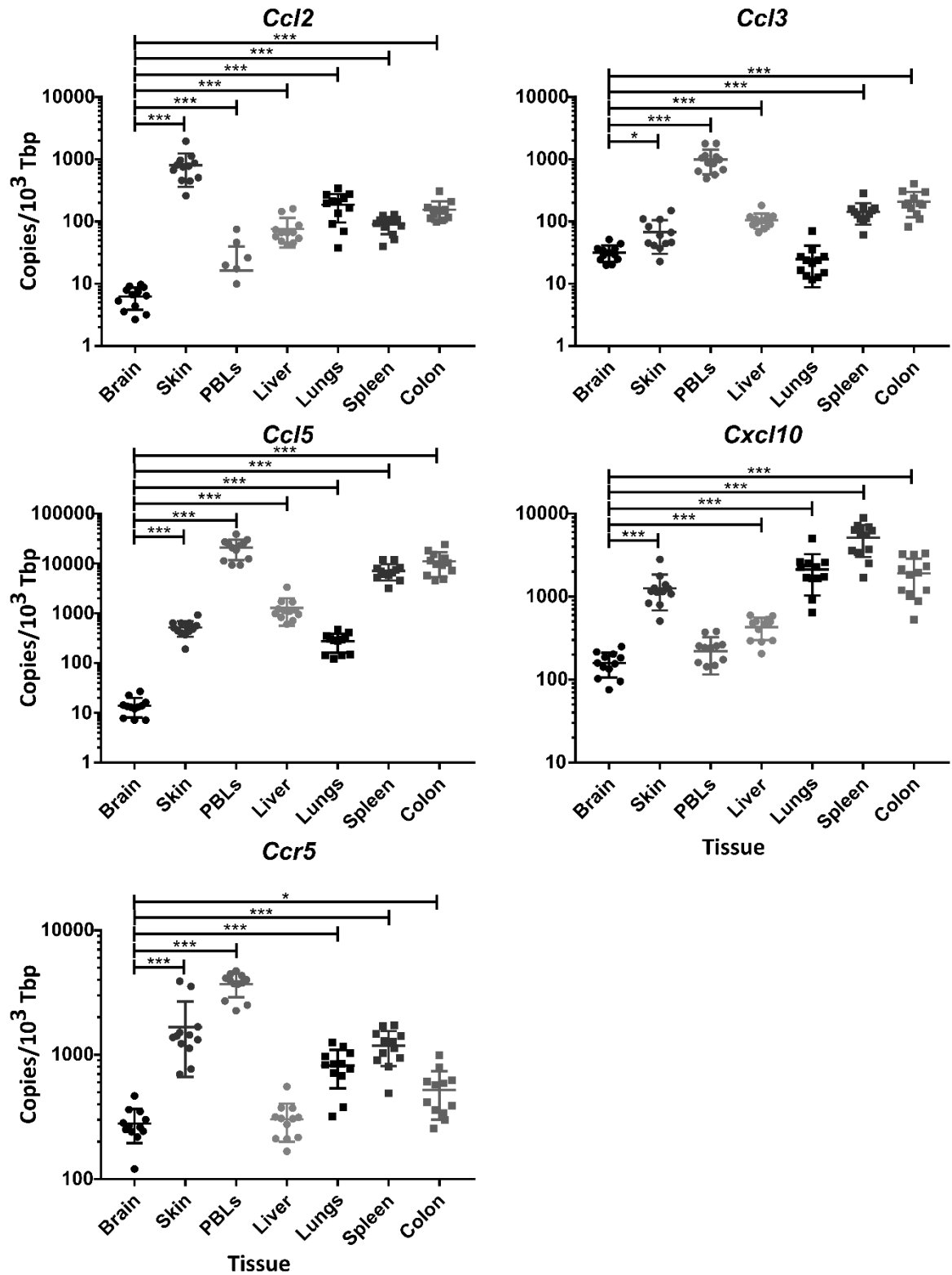


Figure 6.1: Chemokine transcription in control tissue

Tissue was isolated 1, 3 or 5 days after mice were treated with control cream on the dorsal skin. Absolute quantification was performed by qRT-PCR and values normalised to housekeeping gene *Tbp*. $n=12$. One-way ANOVA followed by Student's T-test with Bonferroni multiple testing correction was used to determine statistical significance. $*$ = $P<0.05$; $***$ = $P<0.001$. Bars represent mean \pm SD.

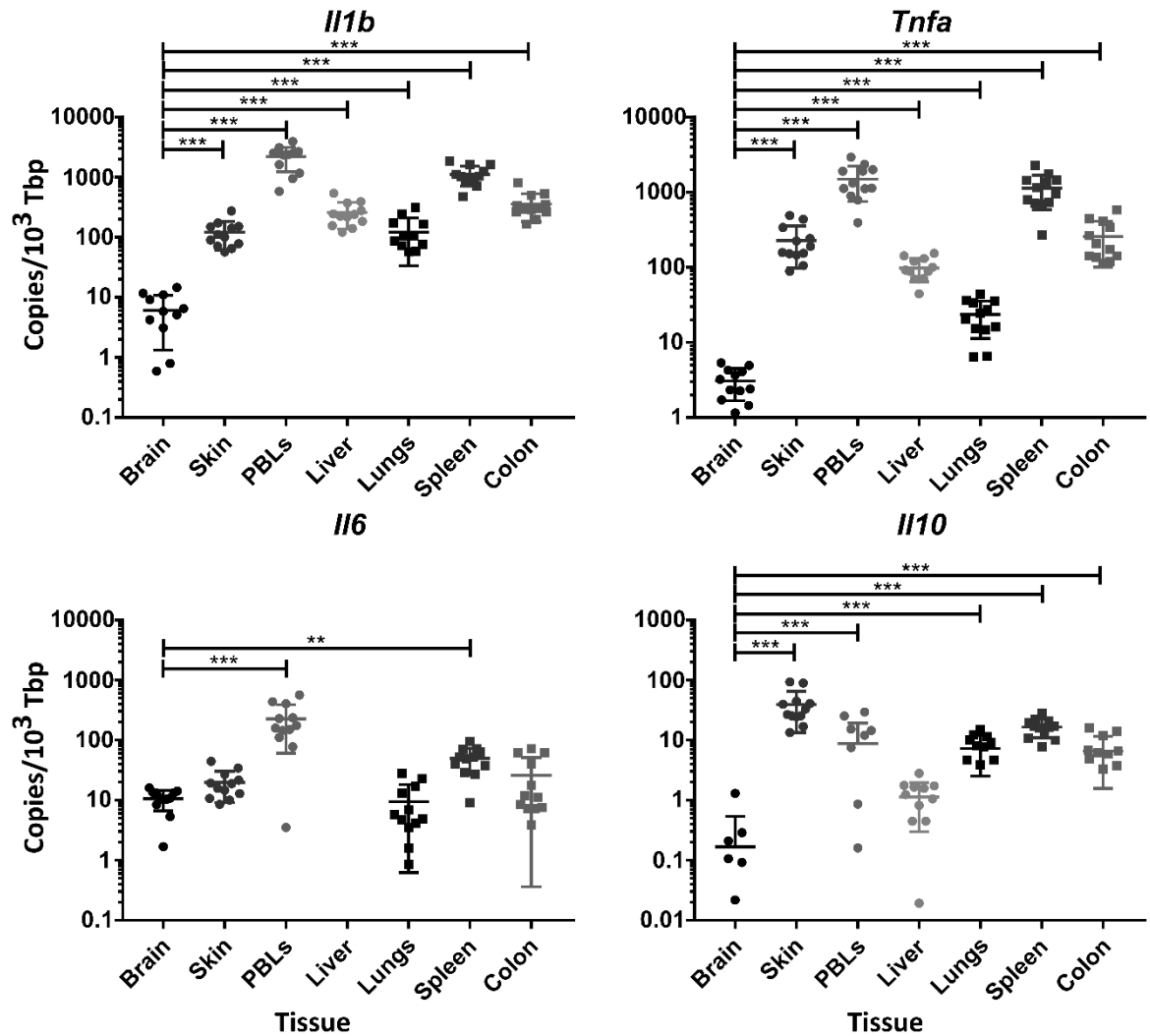


Figure 6.2: Cytokine transcription in control tissue.

Tissue was isolated 1, 3 or 5 days after mice were treated with control cream on the dorsal skin. Absolute quantification was performed by qRT-PCR and values normalised to housekeeping gene *Tbp*. $n=12$. One-way ANOVA followed by Student's T-test with Bonferroni multiple testing correction was used to determine statistical significance. **= $P<0.01$; ***= $P<0.001$. Bars represent mean \pm SD.

6.2.2 The effect of a single cutaneous treatment with Aldara on chemokine and cytokine transcription in the brain

Following examination of control levels of gene expression, the brain response to a single treatment of Aldara was investigated. As was expected, all transcripts (*Ccl2*, *Ccl3*, *Ccl5*, *Cxcl10*, *Tnfa* and *Il6*) found to be raised after 24 hours in the repeated treatments time-course were also found to be significantly upregulated compared to controls 24 hours after a single treatment in this model (Figure 6.3, Figure 6.4). Those transcripts not altered 1 day after a single treatment (*Ccr5*, *Il1b* and *Il10*) did not become significantly different from controls at either 3 or

5 days. Examining the later time-points *Ccl2*, *Ccl5*, *Cxcl10* and *Tnfa* all remained significantly upregulated at 3 days, however only *Ccl5* remained upregulated after 5 days (Figure 6.3). *Ccl5* was the only transcript that did not peak after 1 day, but instead peaked 3 days after Aldara treatment.

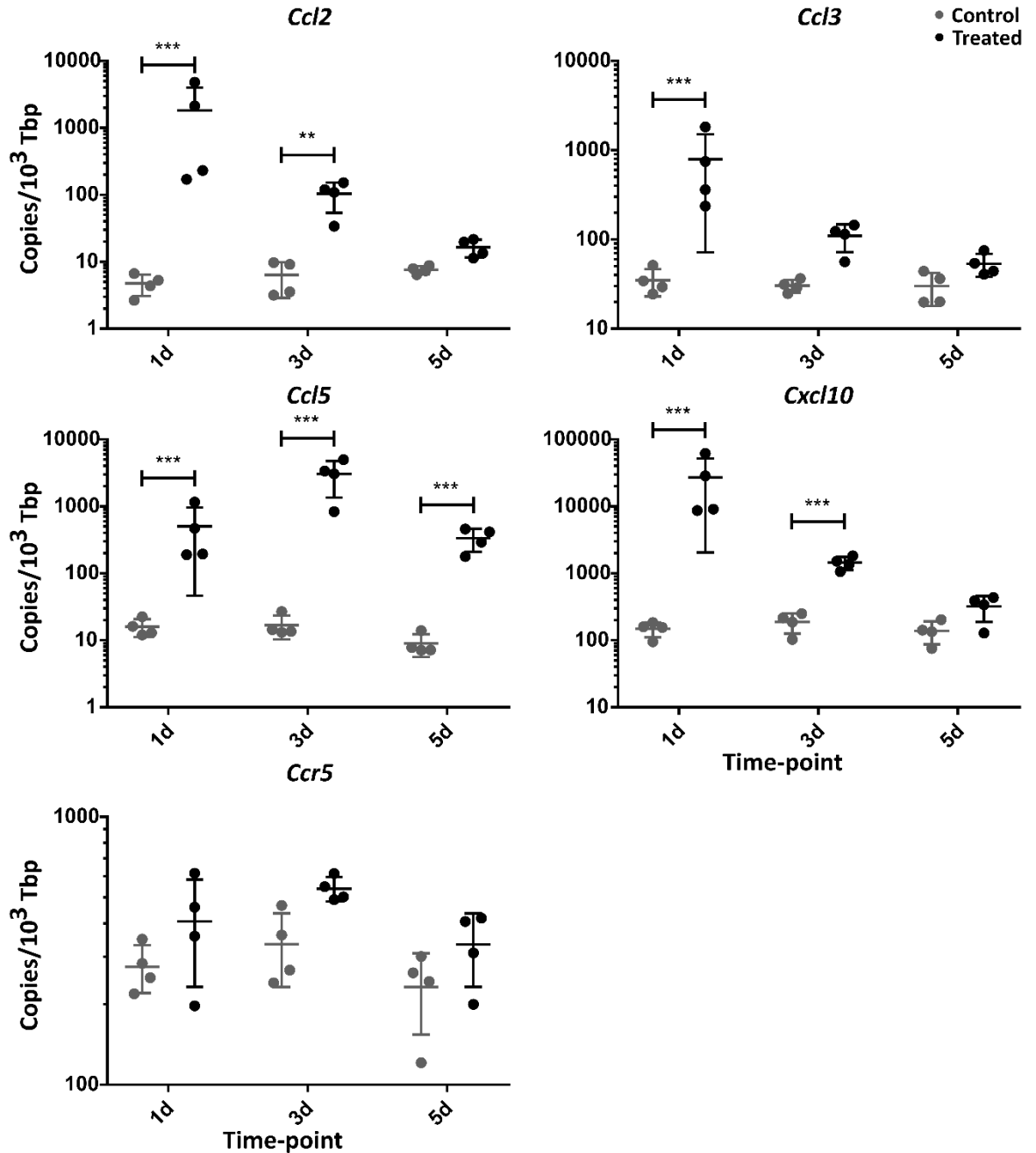


Figure 6.3: Brain chemokine transcript levels after a single Aldara treatment.

Brain tissue was isolated 1, 3 or 5 days after mice were treated with 62.5mg Aldara cream (5% imiquimod) or control cream on the dorsal skin. Absolute quantification was performed by qRT-PCR and values normalised to housekeeping gene *Tbp*. $n=4$ per group. One-way ANOVA followed by Student's T-test with Bonferroni multiple testing correction was used to determine statistical significance. **= $P < 0.01$; ***= $P < 0.001$. Bars represent mean \pm SD.

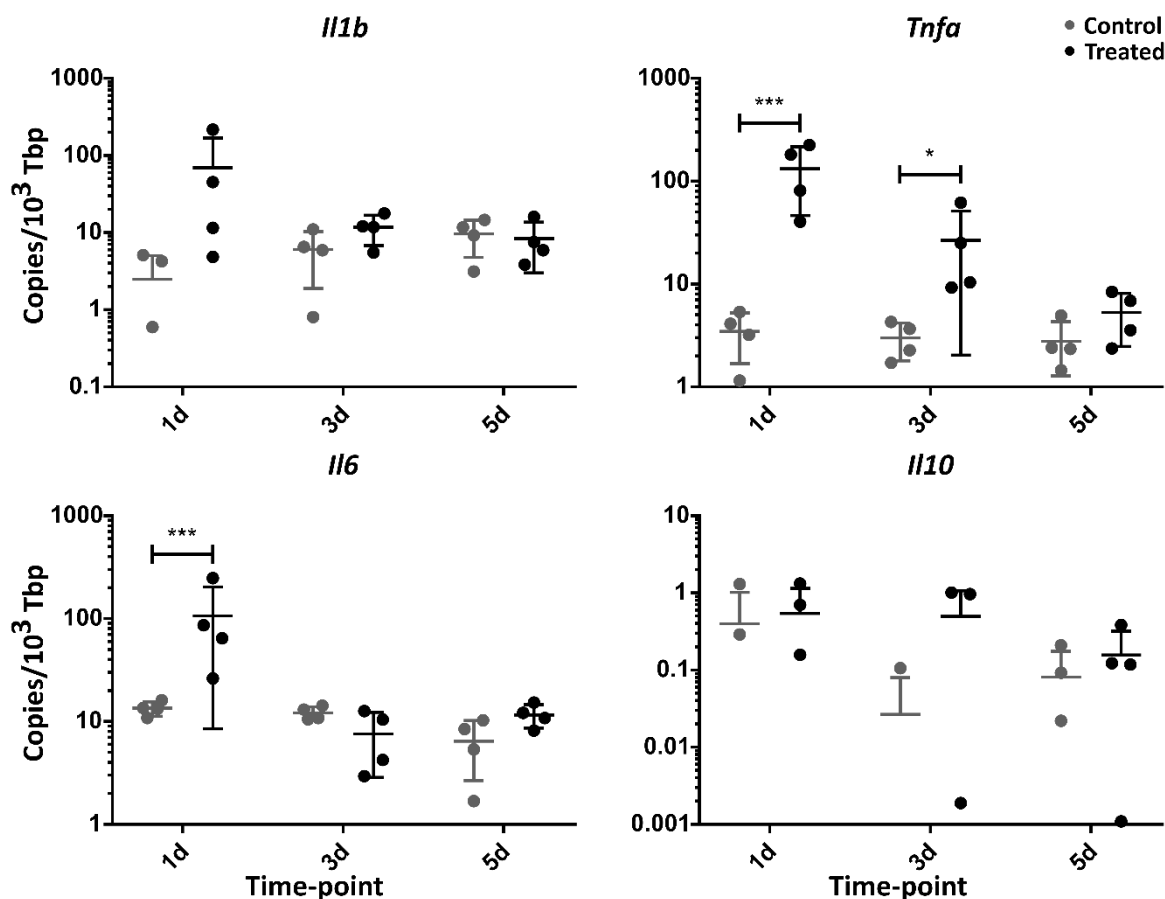


Figure 6.4: Brain cytokine transcript levels after a single Aldara treatment.

Brain tissue was isolated 1, 3 or 5 days after mice were treated with 62.5mg Aldara cream (5% imiquimod) or control cream on the dorsal skin. Absolute quantification was performed by qRT-PCR and values normalised to housekeeping gene *Tbp*. $n=4$ per group. One-way ANOVA followed by Student's T-test with Bonferroni multiple testing correction was used to determine statistical significance. $*=P<0.05$; $***=P<0.001$. Bars represent mean \pm SD.

6.2.3 The effect of a single cutaneous treatment with Aldara on chemokine and cytokine transcription in the periphery

6.2.3.1 Skin chemokine and cytokine transcriptional responses

Alongside investigation of the brain response, how the peripheral tissues responded to a single treatment was examined. Starting with the skin there was minimal upregulation of transcript at 1 day, with *Ccl2*, *Ccl3*, *Il1b*, *Il6* and *Il10* being the only measured transcripts that were significantly upregulated (Figure 6.5, Figure 6.6). Interestingly, in contrast to the repeated treatment model, *Ccl3* was also upregulated after 3 days of treatment, although no other transcripts were significantly altered from controls at this point.

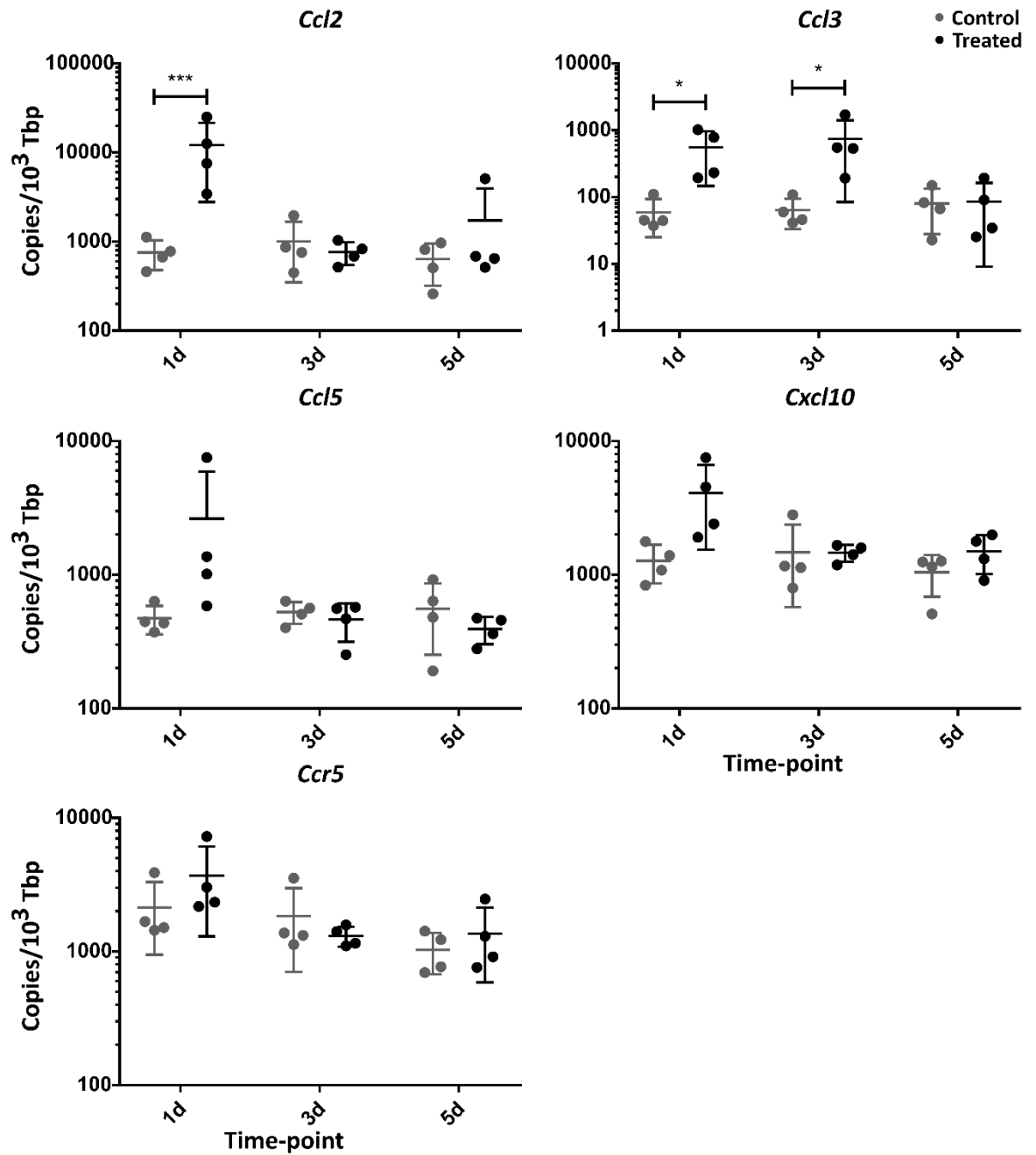


Figure 6.5: Skin chemokine transcript levels after a single Aldara treatment.

Skin tissue was isolated 1, 3 or 5 days after mice were treated with 62.5mg Aldara cream (5% imiquimod) or control cream on the dorsal skin. Absolute quantification was performed by qRT-PCR and values normalised to housekeeping gene *Tbp*. $n=4$ per group. One-way ANOVA followed by Student's T-test with Bonferroni multiple testing correction was used to determine statistical significance. $*=P<0.05$; $***=P<0.001$. Bars represent mean \pm SD.

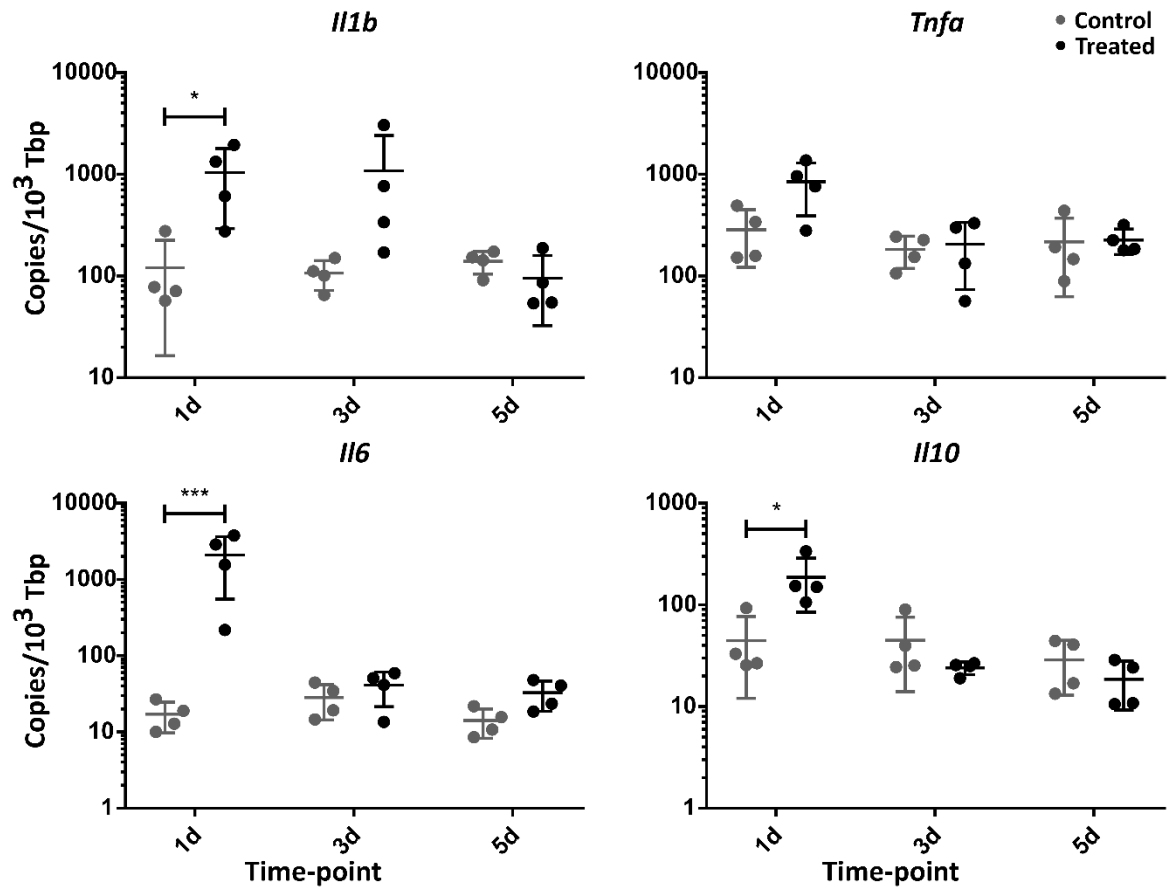


Figure 6.6: Skin cytokine transcript levels after a single Aldara treatment.

Skin tissue was isolated 1, 3 or 5 days after mice were treated with 62.5mg Aldara cream (5% imiquimod) or control cream on the dorsal skin. Absolute quantification was performed by qRT-PCR and values normalised to housekeeping gene *Tbp*. $n=4$ per group. One-way ANOVA followed by Student's T-test with Bonferroni multiple testing correction was used to determine statistical significance. $^* = P < 0.05$; $^{***} = P < 0.001$. Bars represent mean \pm SD.

6.2.3.2 PBLs chemokine and cytokine transcriptional responses

Next, cytokine and chemokine expression was examined in PBL. There was minimal upregulation of measured transcripts with only *Ccl3*, *Cxcl10* and *Ccr5* being significantly upregulated (Figure 6.7). No other chemokines or cytokines were significantly upregulated at any point, and it is interesting to note that in controls, and at later time-points, *Il10* expression was not higher than negative control levels in a number of samples suggesting minimal to no expression (Figure 6.8). No transcripts were found to be significantly altered at either 3 or 5 days after treatment.

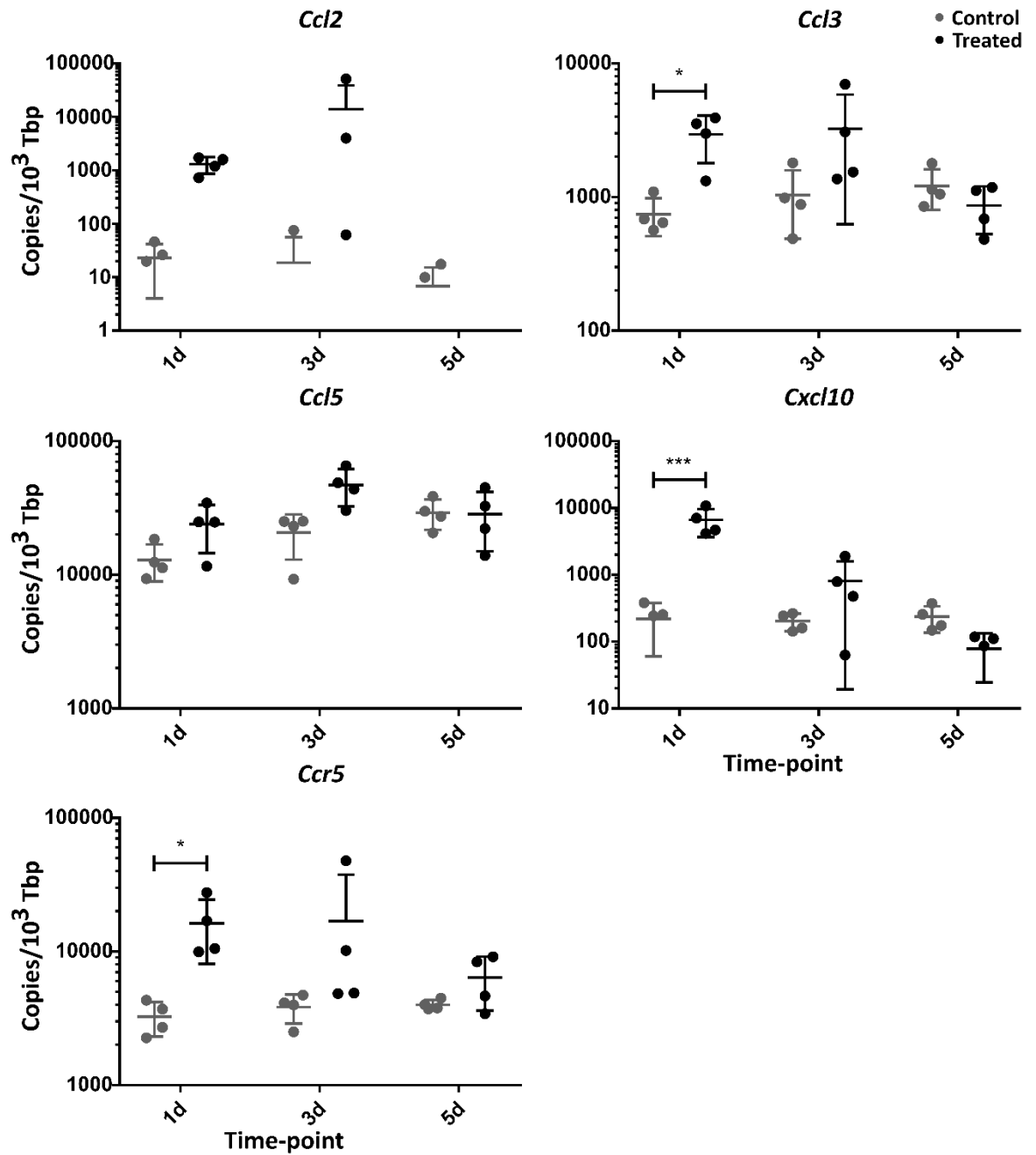


Figure 6.7: PBL chemokine transcript levels after a single Aldara treatment.

PBL were isolated 1, 3 or 5 days after mice were treated with 62.5mg Aldara cream (5% imiquimod) or control cream on the dorsal skin. Absolute quantification was performed by qRT-PCR and values normalised to housekeeping gene *Tbp*. $n=4$ per group. One-way ANOVA followed by Student's T-test with Bonferroni multiple testing correction was used to determine statistical significance. * = $P < 0.05$; *** = $P < 0.001$. Bars represent mean \pm SD.

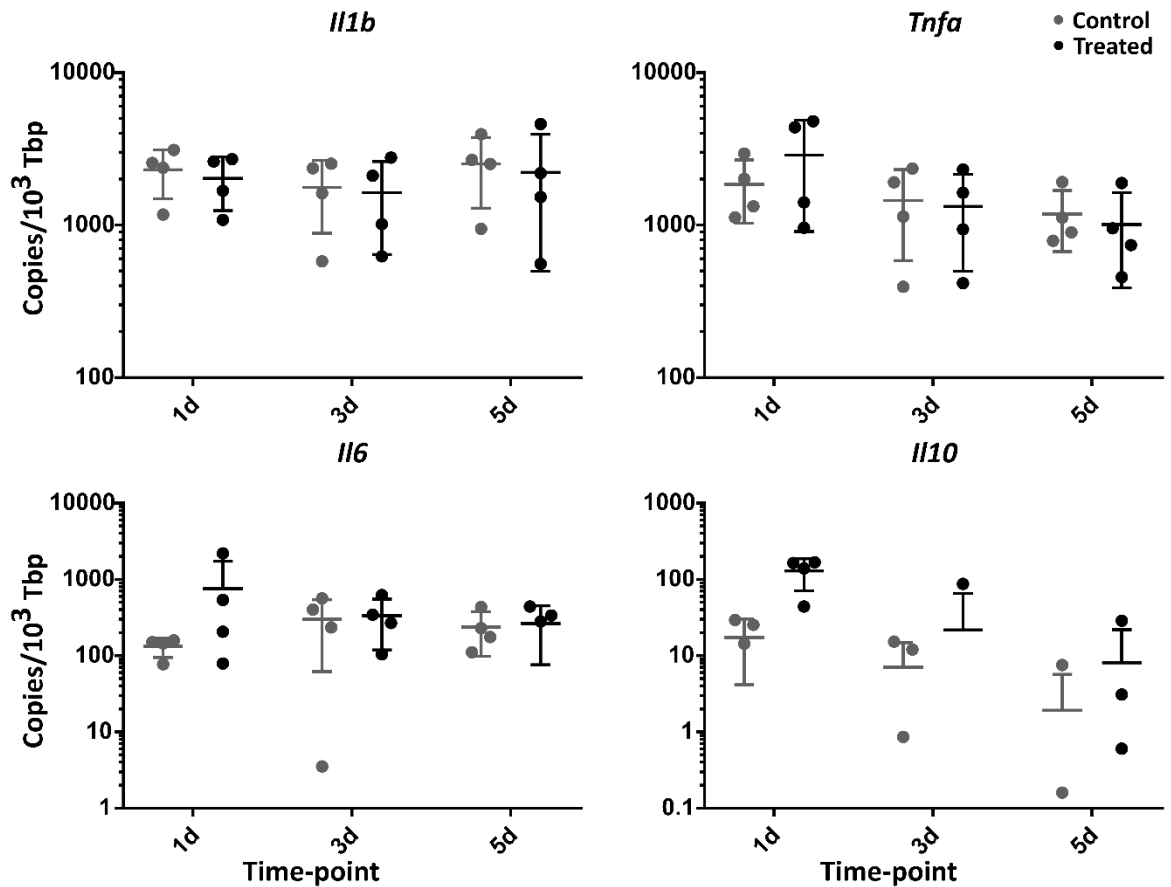


Figure 6.8: PBL cytokine transcript levels after a single Aldara treatment.

PBL were isolated 1, 3 or 5 days after mice were treated with 62.5mg Aldara cream (5% imiquimod) or control cream on the dorsal skin. Absolute quantification was performed by qRT-PCR and values normalised to housekeeping gene *Tbp*. $n=4$ per group. One-way ANOVA followed by Student's T-test with Bonferroni multiple testing correction was used to determine statistical significance. Bars represent mean \pm SD.

6.2.3.3 Liver chemokine and cytokine transcriptional responses

Analysis of the liver also revealed significant upregulation of a limited range of transcripts (*Ccl2*, *Ccl3*, *Cxcl10* and *Il10*) after 1 day of treatment (Figure 6.9, Figure 6.10). There were no significant alterations at any other time point. Although significance was lost after multiple testing correction it is worth noting that *Ccl5* also showed a trend towards upregulation ($p=0.088$). Liver *Il6* was excluded from analysis due to high non-specific background resulting in positive expression in only 3 of 24 samples.

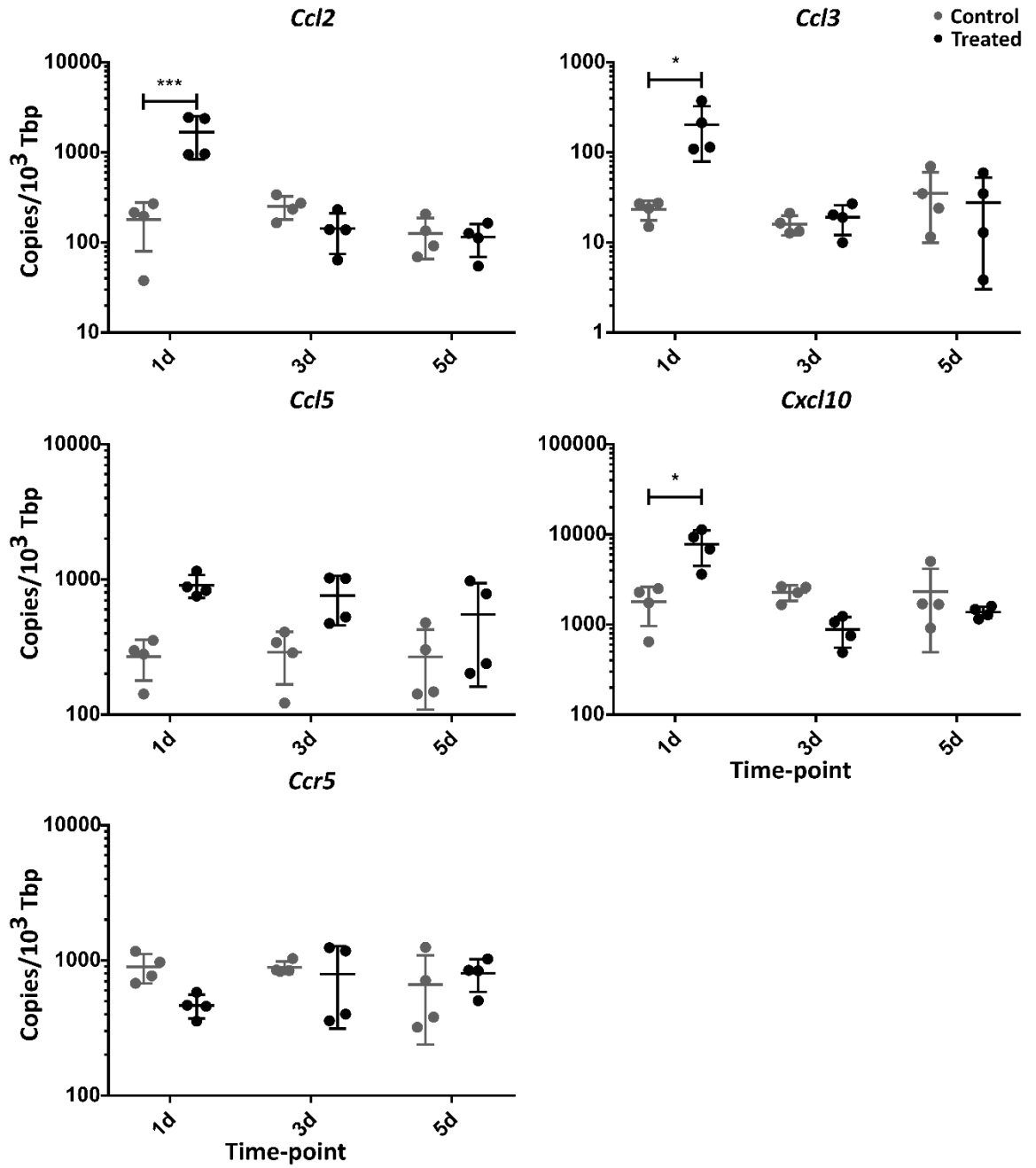


Figure 6.9: Liver chemokine transcript levels after a single Aldara treatment.

Liver tissue was isolated 1, 3 or 5 days after mice were treated with 62.5mg Aldara cream (5% imiquimod) or control cream on the dorsal skin. Absolute quantification was performed by qRT-PCR and values normalised to housekeeping gene *Tbp*. $n=4$ per group. One-way ANOVA followed by Student's T-test with Bonferroni multiple testing correction was used to determine statistical significance. $*=P<0.05$; $***=P<0.001$. Bars represent mean \pm SD.

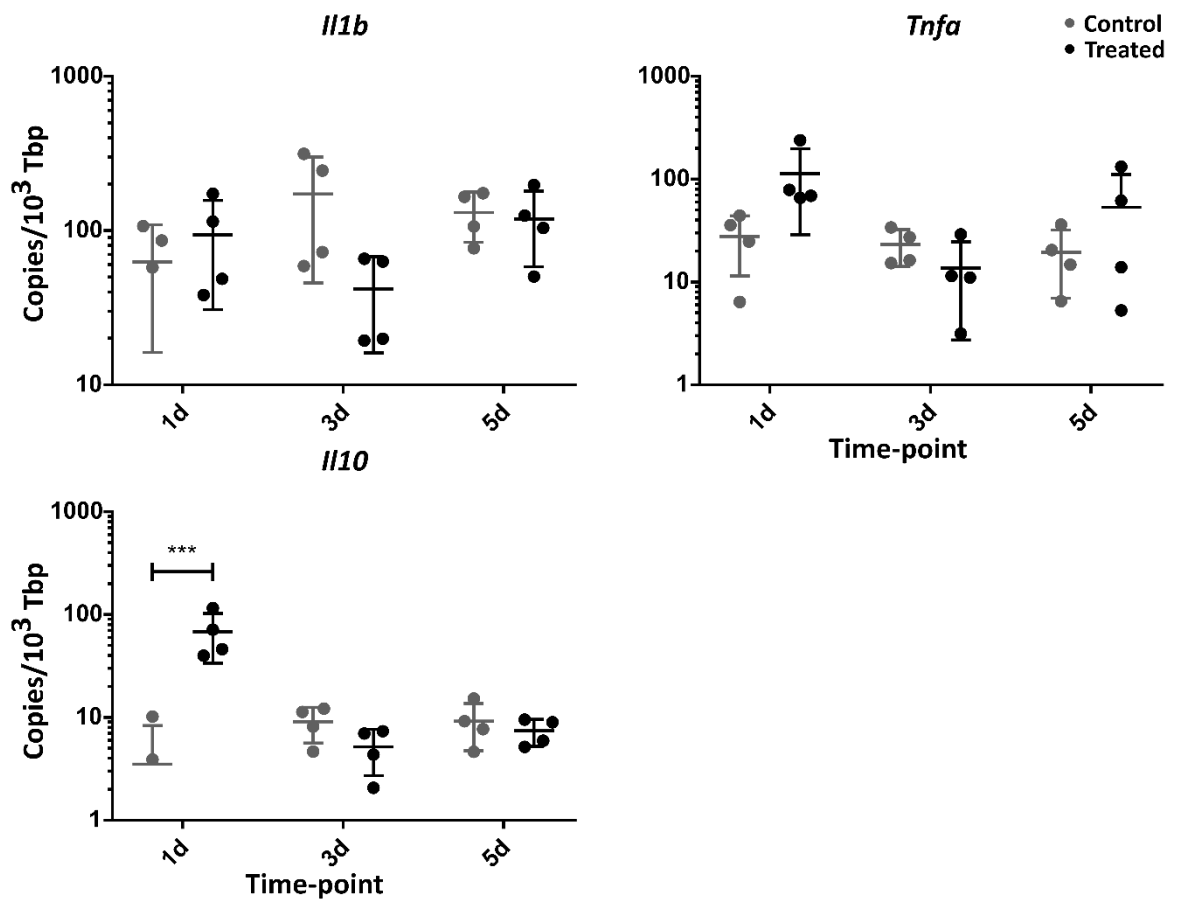


Figure 6.10: Liver cytokine transcript levels after a single Aldara treatment.

Liver tissue was isolated 1, 3 or 5 days after mice were treated with 62.5mg Aldara cream (5% imiquimod) or control cream on the dorsal skin. Absolute quantification was performed by qRT-PCR and values normalised to housekeeping gene *Tbp*. $n=4$ per group. One-way ANOVA followed by Student's T-test with Bonferroni multiple testing correction was used to determine statistical significance. ***= $P<0.001$. Bars represent mean \pm SD.

6.2.3.4 Lung chemokine and cytokine transcriptional responses

Investigation of the lung response revealed changes distinct from the other peripheral tissues. Expression of a wide range of transcripts was found to be significantly altered after 1 day (*Ccl2*, *Ccl3*, *Cxcl10*, *Ccr5*, *Il1b*, *Il6* and *Il10*), with only *Ccl5* and *Tnfa* showing no significant difference compared to controls (Figure 6.11, Figure 6.12). 3 days after Aldara treatment *Ccl5* became significantly upregulated and, alongside this, *Ccl2*, *Ccl3* and *Ccr5* remained significantly raised at this time-point. For all of the transcripts examined there were no significant differences at 5 days after treatment.

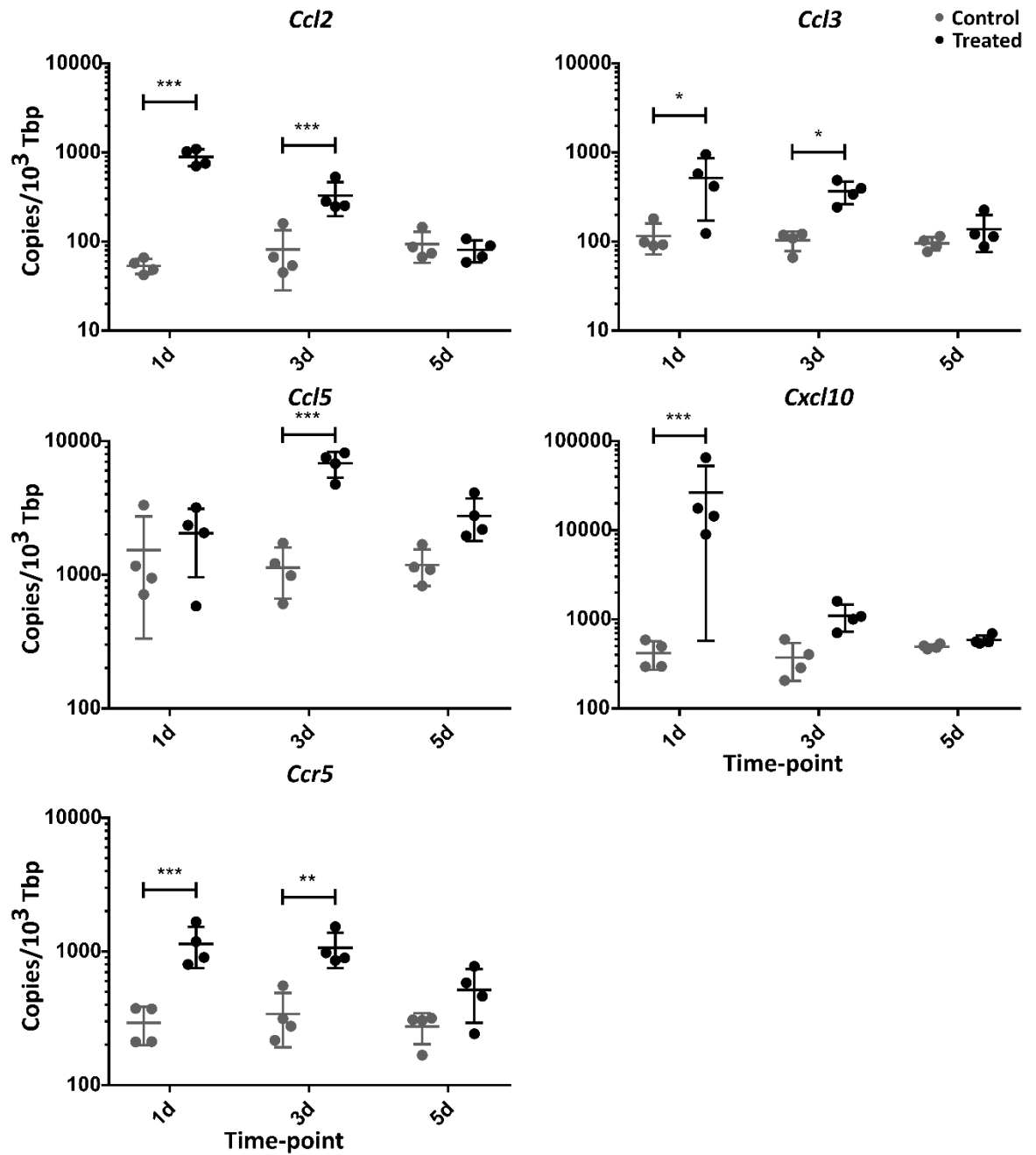


Figure 6.11: Lung chemokine transcript levels after a single Aldara treatment.

Lung tissue was isolated 1, 3 or 5 days after mice were treated with 62.5mg Aldara cream (5% imiquimod) or control cream on the dorsal skin. Absolute quantification was performed by qRT-PCR and values normalised to housekeeping gene *Tbp*. $n=4$ per group. One-way ANOVA followed by Student's T-test with Bonferroni multiple testing correction was used to determine statistical significance. *= $P<0.05$; **= $P<0.01$; ***= $P<0.001$. Bars represent mean \pm SD.

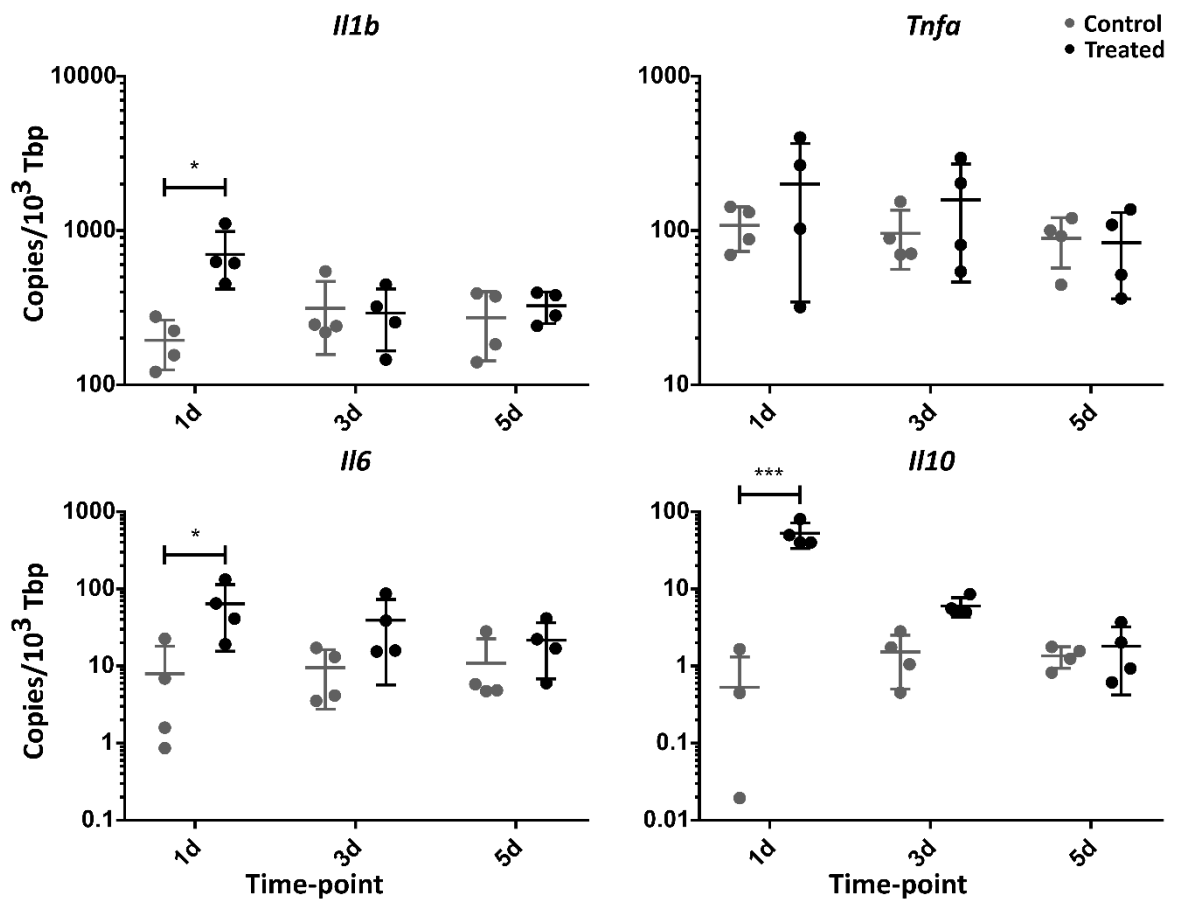


Figure 6.12: Lung cytokine transcript levels after a single Aldara treatment.

Lung tissue was isolated 1, 3 or 5 days after mice were treated with 62.5mg Aldara cream (5% imiquimod) or control cream on the dorsal skin. Absolute quantification was performed by qRT-PCR and values normalised to housekeeping gene *Tbp*. $n=4$ per group. One-way ANOVA followed by Student's T-test with Bonferroni multiple testing correction was used to determine statistical significance. $*=P<0.05$; $***=P<0.001$. Bars represent mean \pm SD.

6.2.3.5 Spleen chemokine and cytokine transcriptional responses

Investigation of the spleen demonstrated a significant upregulation of *Ccl2* and *Ccl3* after 1 day of treatment, similar to most of the other tissues examined (Figure 6.13). Expression of the cytokines *Il6* and *Il10* were also found to be significantly raised compared to control at this time-point (Figure 6.14). The only downregulation observed in this experiment occurred in the spleen, 3 days after Aldara treatment *Il1b* was found to be significantly downregulated. No other measured transcripts were significantly different from control at this time point. For all of the splenic transcripts examined there were no significant differences at 5 days after treatment.

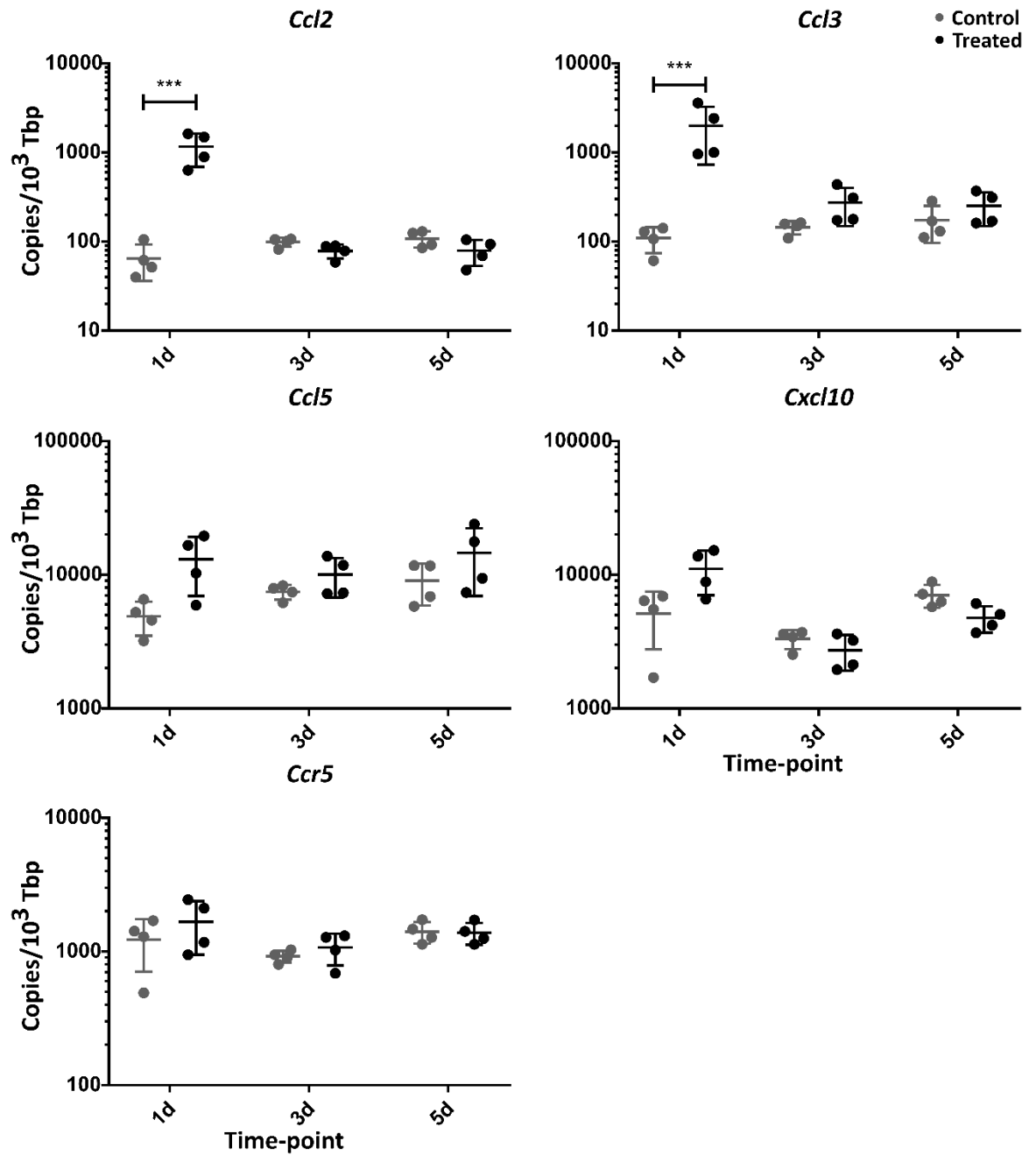


Figure 6.13: Spleen chemokine transcript levels after a single Aldara treatment.

Spleen tissue was isolated 1, 3 or 5 days after mice were treated with 62.5mg Aldara cream (5% imiquimod) or control cream on the dorsal skin. Absolute quantification was performed by qRT-PCR and values normalised to housekeeping gene *Tbp*. $n=4$ per group. One-way ANOVA followed by Student's T-test with Bonferroni multiple testing correction was used to determine statistical significance. ***= $P<0.001$. Bars represent mean \pm SD.

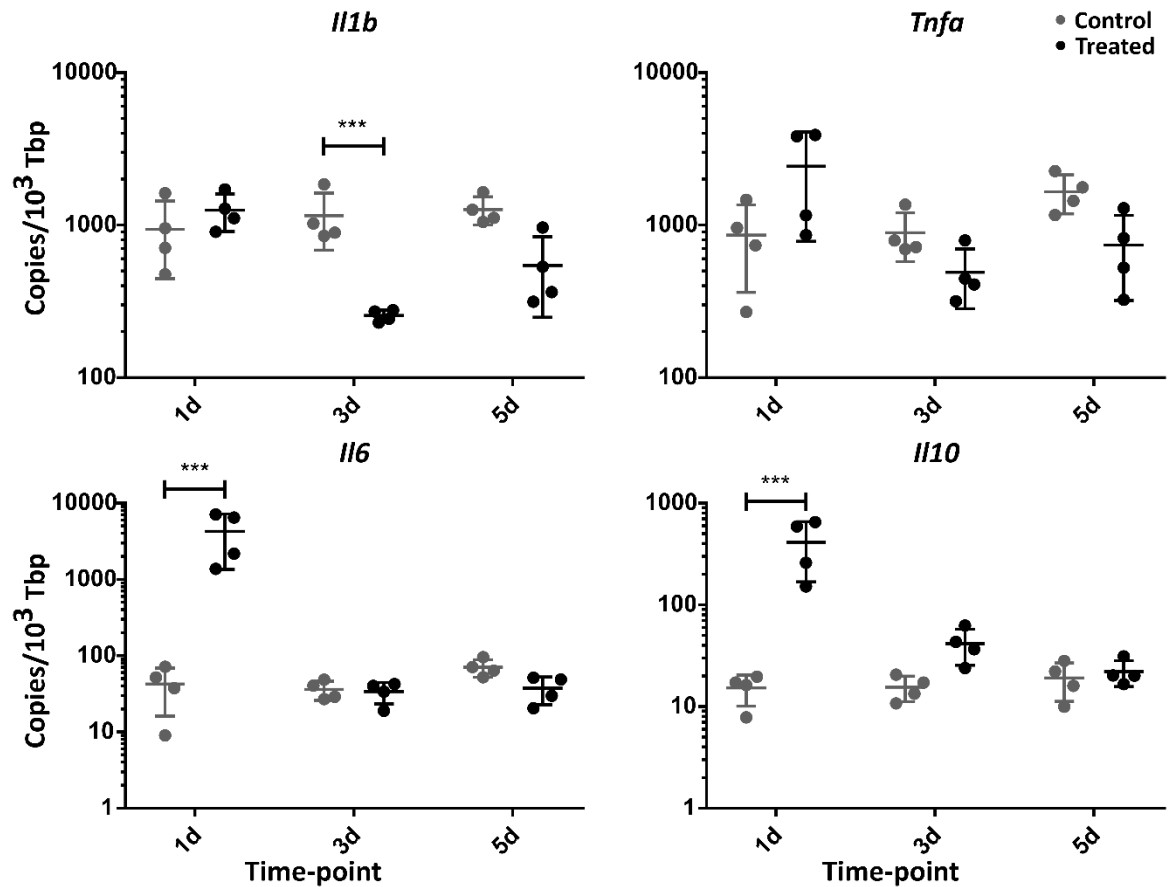


Figure 6.14: Spleen cytokine transcript levels after a single Aldara treatment.

Spleen tissue was isolated 1, 3 or 5 days after mice were treated with 62.5mg Aldara cream (5% imiquimod) or control cream on the dorsal skin. Absolute quantification was performed by qRT-PCR and values normalised to housekeeping gene *Tbp*. $n=4$ per group. One-way ANOVA followed by Student's T-test with Bonferroni multiple testing correction was used to determine statistical significance. ***= $P<0.001$. Bars represent mean \pm SD.

6.2.3.6 Colon chemokine and cytokine transcriptional responses

Finally the colon response to Aldara treatment was investigated. The colon response appeared very similar to the spleen response with *Ccl2*, *Ccl3*, *Il6* and *Il10* all being significantly upregulated after 1 day (Figure 6.15, Figure 6.16). No measured transcripts were significantly altered 3 or 5 days after treatment.

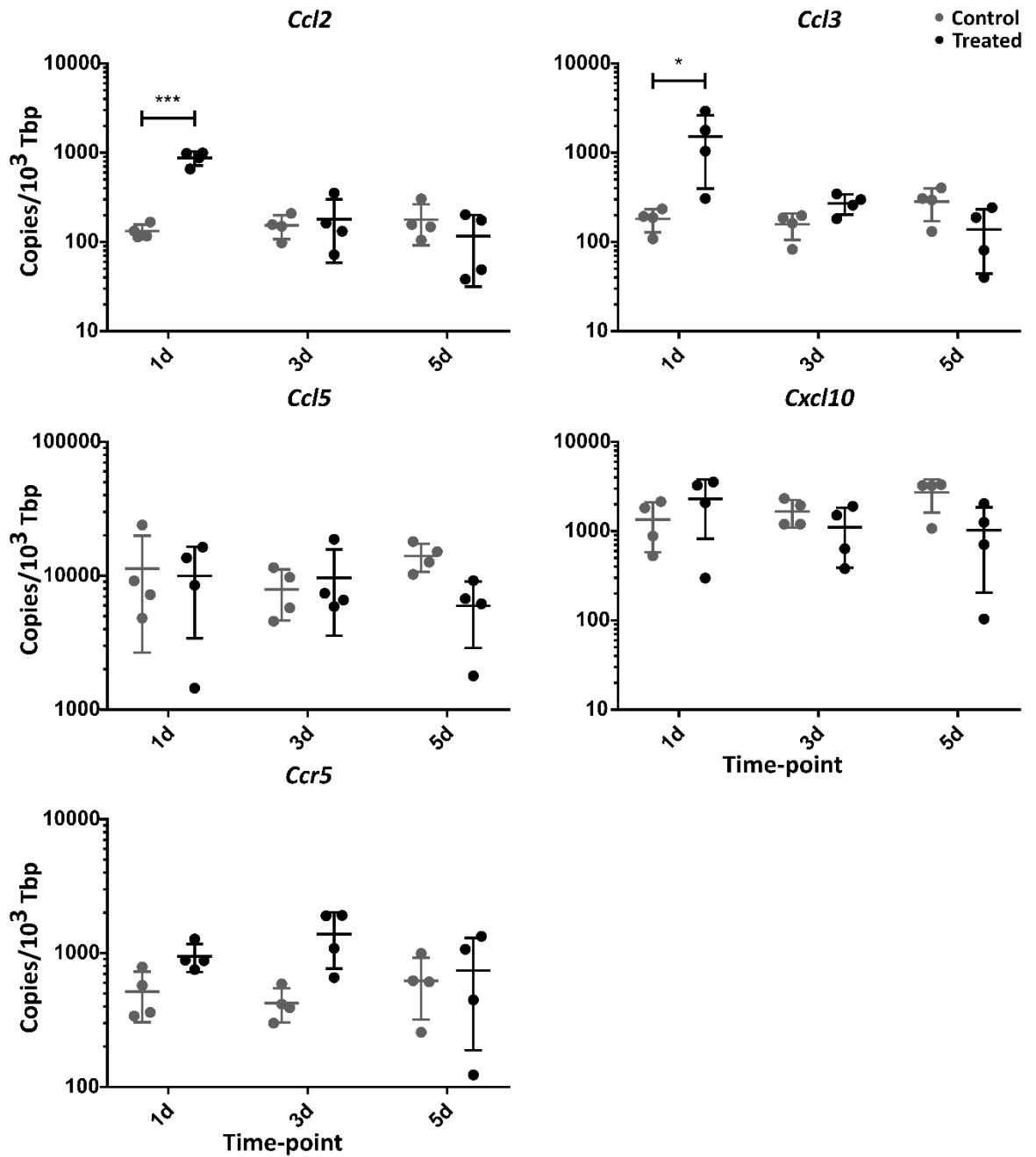


Figure 6.15: Colon chemokine transcript levels after a single Aldara treatment.

Colon tissue was isolated 1, 3 or 5 days after mice were treated with 62.5mg Aldara cream (5% imiquimod) or control cream on the dorsal skin. Absolute quantification was performed by qRT-PCR and values normalised to housekeeping gene *Tbp*. $n=4$ per group. One-way ANOVA followed by Student's T-test with Bonferroni multiple testing correction was used to determine statistical significance. * = $P < 0.05$; *** = $P < 0.001$. Bars represent mean \pm SD.

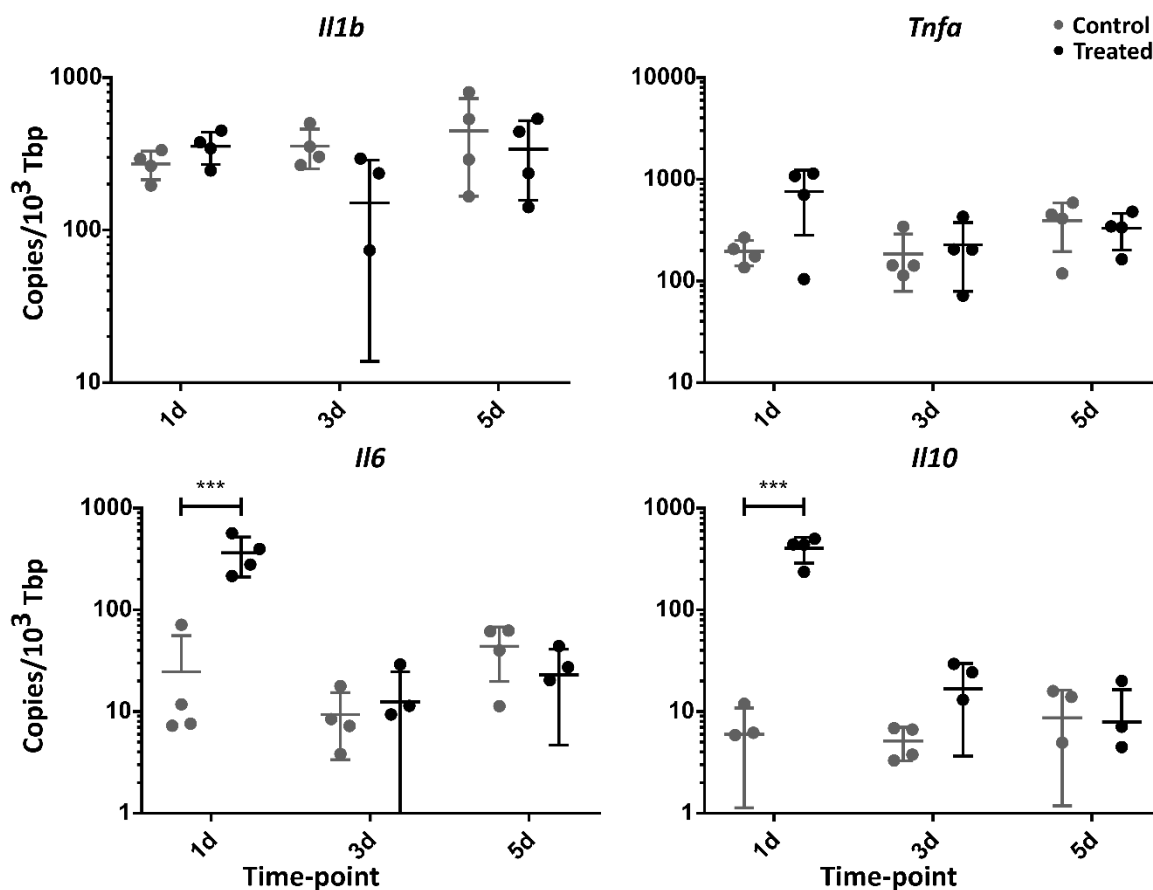


Figure 6.16: Colon cytokine transcript levels after a single Aldara treatment.

Colon tissue was isolated 1, 3 or 5 days after mice were treated with 62.5mg Aldara cream (5% imiquimod) or control cream on the dorsal skin. Absolute quantification was performed by qRT-PCR and values normalised to housekeeping gene *Tbp*. n=4 per group. One-way ANOVA followed by Student's T-test with Bonferroni multiple testing correction was used to determine statistical significance. ***=P<0.001. Bars represent mean ± SD.

6.2.4 Mass spectrometry of plasma and brain imiquimod in the Aldara model

To investigate the ability of IMQ, the TLR7 agonist present in Aldara, to enter the circulation and brain, mass spectrometry was performed at the University of Dundee. Initial investigation of IMQ levels after 3 days of Aldara treatment, the peak response point identified in earlier work, revealed that there was evidence that IMQ was not only present in the circulation but also within the brain (Figure 6.17A). IMQ reaches molar concentrations of 0.33 μ M (95% CI; 0.15-0.52) in the plasma with a total load of 0.76 nmol (95%CI; 0.31 - 1.21 nmol) in the brain after 3 days of treatment. After demonstrating that IMQ was present at this later time-point, how early it gained access to both the circulation and brain was assessed. To examine this IMQ levels 4 hours, 12 hours and 24 hours after a single cutaneous Aldara treatment were investigated. Examination of the plasma

found significant IMQ concentrations at 24 hours but not the earlier time-points, however it is important to note that at both 4 and 12 hours IMQ concentrations were above limits of quantification for all treated samples and absent in all controls (Figure 6.17B). This strongly supports the idea that by 4 hours after treatment IMQ has entered the circulation. In the brain significant IMQ concentrations were detected at both 12 and 24 hours after treatment. In addition, although not significant at 4 hours, similar to the plasma, all treated samples had levels of IMQ above the limit of quantification with no IMQ present in the controls.

Finally to assess if plasma and brain levels of IMQ were associated, linear regression analysis was performed. Linear regression revealed a strong association between plasma and brain levels ($R^2 = 0.8836$, Figure 6.17C), in addition the residual plot did not show any clear pattern, indicating that this linear analysis was likely appropriate (Figure 6.17D).

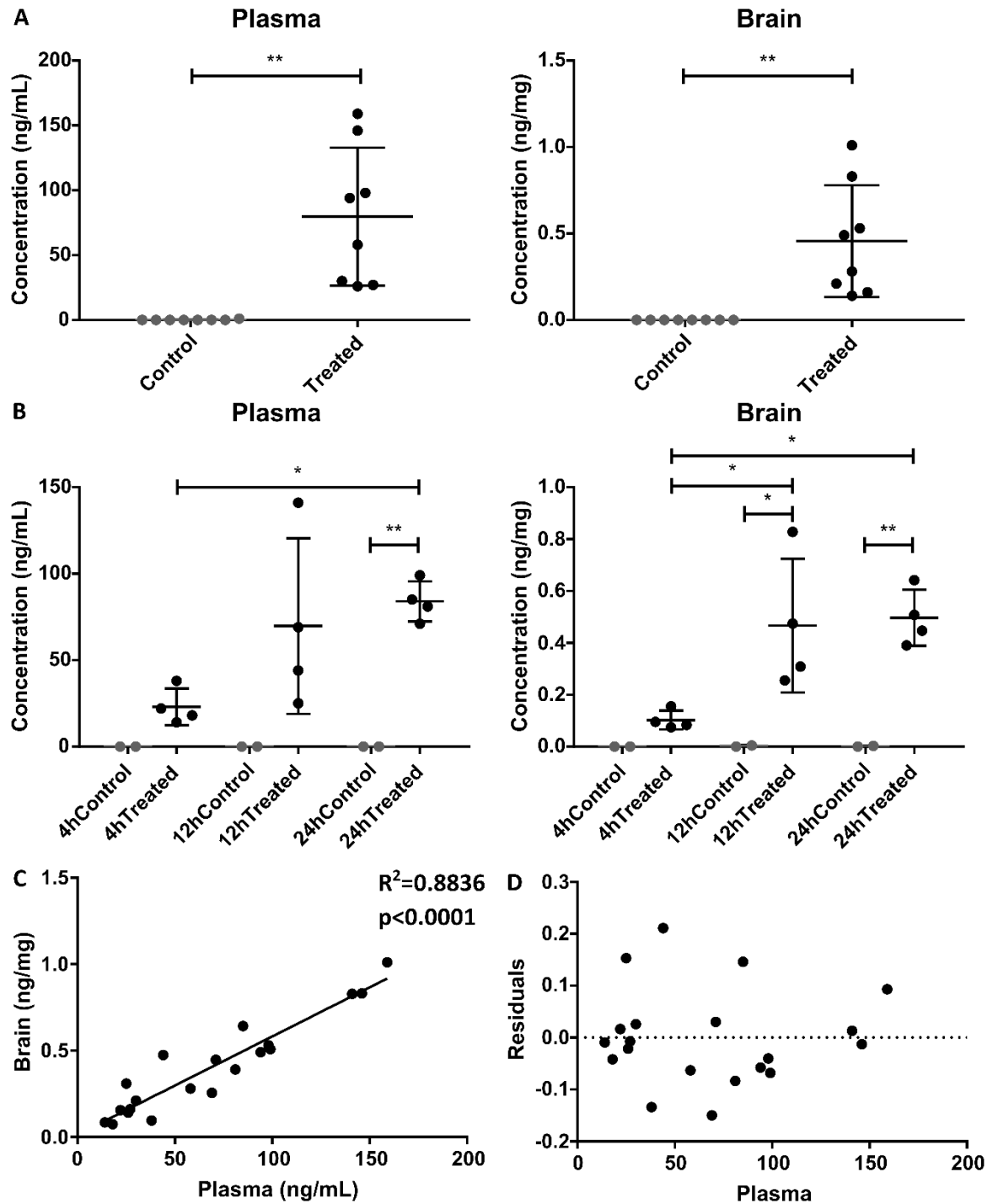


Figure 6.17: Mass spectrometry of imiquimod in Aldara treated mice.

Mice were treated with 62.5mg Aldara cream (5% imiquimod) or control cream. Brains and plasma were isolated from mice and frozen prior to mass spectrometry analysis at the University of Dundee. (A) Imiquimod concentrations in brain and plasma after 3 days of daily Aldara. N=8 per group (B) Imiquimod concentrations in brain and plasma 4, 12 and 24 hours after a single Aldara treatment. N=4 per group (C) Linear regression of brain and plasma imiquimod levels in all treated animals. (D) Residual plot of linear regression analysis. Student's T-test with Bonferroni multiple testing correction (where required) was used to determine statistical significance between groups. Linear regression analysis was performed to look at relationship between brain and plasma imiquimod *= $P<0.05$; **= $P<0.01$. Bars represent mean \pm SD.

6.3 Discussion

6.3.1 Overview of results

In this chapter, control levels of chemokine and cytokine expression in peripheral tissues were initially reported. This revealed that absolute expression of measured chemokines and cytokines normalised to *Tbp* was generally lower in the brain than other tissues investigated. The primary finding when examining the response to a single cutaneous Aldara treatment was that the brain chemokine and cytokine transcriptional response was at its peak after 1 day when compared to 3 and 5 days after treatment. This is in contrast to the repeated treatment model where the peak was after 3 days of daily treatments. Despite this, similar to the time-course experiment, 1 day after treatment the majority of examined transcripts were upregulated in the brain and lungs, and a summary heat-map of the transcriptional data is provided in Figure 4.31.

In addition to the single treatment model, IMQ entry into both the circulation and the brain was investigated, to assess whether direct TLR7 agonism within tissues may contribute to observed inflammatory responses. Mass spectrometry analysis provided two main findings; (i) IMQ can enter both the circulation and the brain within 4 hours of cutaneous treatment; (ii) Plasma levels of IMQ correlate strongly with brain levels of IMQ;

6.3.2 Control gene expression between tissues

How control levels of genes varied between tissues was initially examined, to investigate whether large fold changes in the brain are due to an increased induction of transcriptional responses compared to other tissues or lower baseline levels. As mentioned, the brain generally had much lower absolute levels of expression of measured transcripts than many of the other tissues. The findings presented here suggest that, at least in part, the magnitude of fold change observed in the brain is due to lower baseline levels compared to other peripheral tissues.

	Brain			Skin			PBLs			Liver			Lungs			Spleen			Colon		
	1d	3d	5d	1d	3d	5d	1d	3d	5d	1d	3d	5d	1d	3d	5d	1d	3d	5d	1d	3d	5d
Ccl2	7.39	3.82	1.07	3.65	-0.44	0.70	5.75	6.96	-	3.08	-0.96	-0.24	4.04	1.94	-0.25	4.07	-0.35	-0.51	2.71	-0.01	-0.98
Ccl3	4.06	1.77	0.79	2.88	3.13	-0.36	1.86	1.32	-0.57	2.93	0.17	-0.97	1.83	1.77	0.43	3.96	0.81	0.45	2.65	0.75	-1.37
Ccl5	4.57	7.24	5.13	1.74	-0.25	-0.54	0.79	1.13	-0.17	1.73	1.30	0.71	0.17	2.56	1.15	1.28	0.37	0.54	-0.64	0.12	-1.45
Cxcl10	7.02	2.91	1.08	1.48	-0.02	0.46	4.82	1.18	-1.19	2.00	-1.45	-0.77	5.55	1.50	0.24	1.03	-0.33	-0.59	0.28	-0.87	-2.05
Ccr5	0.45	0.68	0.47	0.61	-0.50	0.25	2.19	1.43	0.56	-0.97	-0.39	0.23	1.90	1.61	0.79	0.34	0.18	-0.04	0.85	1.58	-0.23
Il-1b	3.45	0.84	-0.42	2.75	2.50	-0.75	-0.28	-0.35	-0.56	0.32	-2.28	-0.30	1.77	-0.21	0.22	0.37	-2.18	-1.36	0.35	-1.05	-0.59
Tnfa	4.96	2.72	0.75	1.35	-0.14	0.02	0.32	-0.39	-0.42	1.79	-1.16	0.52	0.34	0.41	-0.30	1.19	-0.95	-1.35	1.48	0.04	-0.34
Il-6	2.53	-0.93	0.81	6.33	0.35	1.10	1.49	-0.11	0.54	-	-	-	2.68	1.67	0.68	6.33	-0.16	-1.00	3.80	0.64	-0.59
Il-10	0.40	2.20	-0.70	1.93	-0.91	-0.78	2.72	3.63	0.97	4.15	-0.97	-0.36	6.57	1.95	0.09	4.52	1.34	0.17	6.02	2.03	-0.02

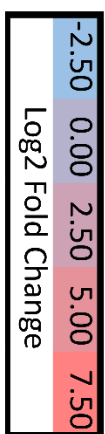


Figure 6.18: Heatmap of chemokine and cytokine gene expression after a single cutaneous treatment of Aldara cream.

Animals were treated once at day 0 with 62.5mg of Aldara cream (5% imiquimod) or control cream. At 1 day, 3 days and 5 days after treatment tissues were collected and analysed by qRT-PCR. Log2 fold changes compared to control levels of gene expression were calculated. Grey squares indicate samples where expression levels could not be determined. Student's T-test with Bonferroni multiple testing correction was used to determine significance. Results in bold demonstrate significant results $P < 0.05$

6.3.3 Relevance of findings from single treatment model

To investigate whether or not the 3 day peak in chemokine and cytokine transcriptional responses observed in the brain was a natural feature of the brain immune response, or a consequence of repeated treatments augmenting the brain response over time, a single cutaneous treatment model examining 1, 3 and 5-day time points was performed. This showed that after a single treatment the peak brain response point shifted from 3 days to 1 day, strongly supporting the idea that sustained peripheral insults result in more sustained central responses. This suggests that the brain takes longer to induce immune-regulatory responses and/or to tolerise itself to immune stimuli. The idea of the brain taking longer to induce immune-regulatory responses is supported by data showing that after 1 day of treatment, unlike in other organs, *Il10* was not significantly upregulated in the brain.

There is reasonable evidence that pre-treatment with TLR7 agonists can diminish subsequent TLR7 responses. This has been demonstrated *in vivo* using models of experimental autoimmune encephalitis (487, 488) and *in vitro* in both macrophages(489) and microglia(488). Suggested mechanisms for this change include reductions in *Tlr7*(490) and reductions in phospho-interleukin-1 receptor associated kinase 1(489) that can activate NF- κ B. These data support the idea that the lack of peripheral responses at later time-points in the repeated treatments model may be due to tolerisation. One unanswered point is still the question of why the brain does not appear to tolerise as quickly. A parallel hypothesis is that the slower rise in *Il10* is what results in a more prolonged response, *Il10* appears to be critical to suppression of LPS responses but not the tolerisation process itself (491, 492). Due to the complex nature of inflammatory responses it is entirely plausible that both reduced tolerisation and slower up regulation of anti-inflammatory mediators contribute to this response, particularly as the two may be linked.

6.3.4 Importance of the mass spectrometry results

As discussed, there was concern that the effects of Aldara treatment may be mediated by direct entry of the TLR7 agonist IMQ to the CNS. To this end, mass spectrometry identified IMQ in both the plasma and the brain of treated animals

from 4 hours after treatment. Microglia, astrocytes and neurons have all been shown to express TLR7 (238, 493), highlighting that direct IMQ agonism of TLR7 within the CNS is a plausible mechanism for immune activation. This strongly suggests that, at least for the brain, if not the other peripheral organs, many of the observed effects are mediated by entry of IMQ to the brain parenchyma itself. This pathway of immune activation characterised by direct activation of resident immune cells of the brain suggests that the Aldara model is more akin to a model of systemic viral infection, particularly ssRNA viruses, (e.g. VSV and WNV) where the initial site of inoculation is the skin. This is in contrast to our previous conceptual model where Aldara was a peripherally restricted insult, and the resultant changes observed within the CNS were due to either humoral or neural routes of immune communication. Therefore, the responses observed in the brain are more likely to reflect changes expected in viral encephalitis. Examining chemokine and cytokine responses in models of ssRNA viral encephalitis, identifies upregulation of CCL2, CCL5, CXCL10, Il-1 β and TNF α demonstrating considerable overlap with our own findings (209, 213, 494-497). In addition, reactive changes in microglia and astrocytes, alongside T cell infiltration are consistent findings in these models (216, 496, 498). These data highlight that the Aldara model is likely a useful tool for studying TLR7-mediated brain inflammation using a non-infectious and non-invasive model. However, it is not an appropriate tool for the study of neuroinflammatory responses to a localized peripheral inflammatory stimulus.

Briefly, the fact that plasma levels of IMQ have strong linear associations with brain levels of IMQ suggests that IMQ is either transported rapidly across the BBB in a non-saturable manner across the range of concentrations observed, or, that it is able to freely diffuse across the BBB. Based on its low molecular weight and high lipophilicity, it is probably that it is the latter.

6.3.5 Summary and conclusions

In this chapter it was demonstrated that a single treatment with Aldara generates a distinct response in the brain when compared to repeated treatments over a similar time-course. The finding that the peak response point is earlier in this model suggests that prolonged responses in the context of repeated treatments are due to delayed inflammatory dampening when

compared to peripheral tissues. While limited data are available on the mechanisms through which this occurs, the slower upregulation of anti-inflammatory mediators, particularly *Il10* examined here, is a compelling explanatory factor. Alongside this work, brief examination of control gene expression suggests that many of the inflammatory mediators examined in this thesis are expressed at lower constitutive levels in the brain than in other organs. This suggests that increased magnitude of fold changes in chemokine and cytokine expression observed in the brain are at least partly due to lower levels of baseline expression rather than increased absolute expression following cutaneous Aldara treatment.

In addition to data from a single treatment model, IMQ entry into the circulation and brain, that may be responsible for observed changes, was examined. Mass spectrometry data provide strong evidence for entry of IMQ into the brain. It is therefore likely that many of the results obtained for brain responses reported in this Thesis are not driven by peripheral inflammatory responses but through central TLR7 agonism. While this does not prevent the Aldara model being used as a tool for studying neuroinflammatory responses, it strongly suggests that it is not an appropriate model for the study of peripheral-central crosstalk.

Chapter 7

Discussion

Chapter 7 Discussion

7.1 Summary of Findings

This thesis initially introduced the overlapping interactions between the immune system and the CNS (4, 5, 8, 499), and the subsequent effects on behavioural phenotypes (103, 295, 500). Research into these interactions identified associative links and had begun to point to putative mechanisms. However a number of gaps in the current literature were identified as areas for further research. As chemokines appeared to be a point of overlap between the immune system and CNS (32, 101, 501-504), and are a particular focus of our laboratory's work, they were chosen as candidate molecules for further investigation.

Chemokine molecules are increasingly being associated with immune-CNS interactions in the pre-clinical literature. However the role that these molecules play in psychiatric disease, specifically in depression, is somewhat unclear. To address this, a comprehensive systematic review and meta-analysis of the role of chemokines in human depressive disorder was undertaken. This work showed that, despite limitations of the human biomarker literature, alterations in a number of chemokines (CCL2, CCL3, CCL4, CCL11, CXCL4, CXCL7 and CXCL8) appeared to be associated with human depressive disorder.

Previous work within our laboratory had identified the Aldara model of psoriasis-like inflammation, which utilises the TLR7 agonist IMQ, as a compelling tool for studying peripherally induced CNS inflammation (24, 25). Cutaneous Aldara treatment was shown to induce inflammatory changes within the CNS that were associated with alterations of behavioural phenotypes. However, there were a number of gaps regarding the cytokine and chemokine response, CNS cellular responses, early time-points and the mechanisms of inflammatory induction. To this end we aimed to perform a more comprehensive examination of the inflammatory response in the Aldara model and to begin to investigate mechanisms of inflammatory induction.

Work to further characterise the Aldara model showed that, in keeping with the initial hypotheses, a broad array of previously unexamined chemokines and

cytokines were induced in the brains of treated animals. These transcriptional changes were associated with alterations in cellular populations of the CNS. Reassuringly, these findings appeared to be consistent across a number of experiments and mouse genotypes. In addition, it was shown that the CNS response was temporally distinct from the periphery, taking longer to be fully induced and to resolve in response to repeated treatments.

Subsequently, work was performed to examine potential mechanisms through which this response might occur. Using iCCRKO mice it was shown that absence of the iCCRs (CCR1, CCR2, CCR3 and CCR5) does not appear to result in significant deficits of transcriptional response or microglial reactivity. However, these receptors may play a role in the recruitment of CD3⁺ cells. In contrast, using IFNARKO mice, demonstrated that type I IFN signalling appears to be important to the induction of the CNS response to cutaneous Aldara treatment. This was shown through the identification of reduced transcriptional responses, alongside alterations in cellular reactivity and recruitment in Aldara treated IFNARKO mice. Use of a single treatment model helped to show that the prolonged response identified within the CNS requires repeated stimulation.

Finally, through the use of mass spectrometry, it was shown that IMQ can enter into the circulation and CNS. As such, systemic effects of cutaneous Aldara treatment are likely driven through IMQ-mediated TLR7 agonism within tissues, although there may be a contributory role for inflammatory mediators produced at the site of stimulation.

7.2 Discussion

7.2.1 Human biomarker data

Having initially identified evidence of raised chemokines in human biomarker studies of depression, it is important to explore possible links with the animal data presented in this thesis. Of note, CCL2, CCL3 and CXCL8 (mouse homolog CXCL1) that were raised in depressive disorder, were all raised following cutaneous Aldara treatment. While direct correlates are impossible to draw, particularly as IMQ appears to enter the brain and this is not a model of depression. It is interesting that, at least for *Ccl2* and *Ccl3*, there was a

significant reduction in expression in IFNARKO mice. This links with human data suggesting that IFN responses can drive depressive disorders (14) and suggests that induction of these molecules in humans may be secondary to type I IFN signalling.

Another finding of interest, is that although in the mouse in response to Aldara treatment there is a rise in *Ccl4*, in the human literature the opposite is found. This rise in CCL2 and CCL3 that is accompanied by decreases in CCL4 in humans appears paradoxical, yet, both Ho et al. and Lu et al. studied all three of these molecules in physically healthy depressed patients and found these paradoxical findings within the same groups of individuals (360, 379). Considering that CCL4 is thought to be important for regulatory T-cell recruitment (418) and reductions in regulatory T-cells are associated with depressive disorder(419), this may have mechanistic significance.

If these findings are robust and represent a true immunological alteration in the depressed population it would be interesting to compare the expression of these chemokines in individual patients. If within individual patients CCL2 and CCL3 were raised, but, CCL4 was decreased this would suggest that dysregulation of CCL4 specifically may be important and warrant further investigation, possibly at a genetic or epigenetic level.

7.2.2 IMQ in the brain

Given the finding of IMQ in the brain it is difficult to draw any conclusions on the mechanisms through which peripheral immune alterations drive changes in the CNS using the Aldara model. In addition, this finding highlights how important it is to ensure that the models we use to study human disease are appropriately characterised and understood, so as to not draw false conclusions.

Although the fact that IMQ enters the brain makes the model inappropriate for investigation of peripheral-central immune crosstalk, it does highlight a potentially novel use for this model. This work identifies the Aldara model as a tool for introducing a TLR7-specific non-infectious immune stimulus into the CNS in a non-invasive manner. This is particularly useful for a number of reasons; (i) it allows one to avoid the invasive nature of i.c.v injection that is at least mildly

traumatic to brain parenchyma(505); (ii) the fact that it is introduced through a peripheral route means it is probably closer to normal physiology; (iii) as a non-infectious tool for studying neuro-inflammation it allows for investigation of more specific aspects of immune function, in this case TLR7 signalling. In addition, viral encephalitis in KO mice can result in raised and more rapid-onset mortality making study of later time-points challenging, whereas this does not appear to be the case for the Aldara model (216, 506). Work in our laboratory has shown that mice treated with Aldara for 4 days and left for an additional 7 days do not develop any signs of terminal illness [personal communication] and data in this thesis has shown that recovery appears to begin around day 3.

Alongside enhancing our understanding of the model, this finding of IMQ within the brain parenchyma helps to provide answers to a question raised in the iCCR and IFNARKO chapter. This was whether or not the effect of KO on peripheral responses was the critical mechanism that changed the brain response. The fact that IMQ can enter the brain and probably bind to TLR7 receptors that are known to be expressed by microglia, astrocytes, and neurons (487, 488), suggests that observed findings are due to the function of these receptors within the CNS. For IFNARKO this points to type I IFN signalling as being an important pathway within the brain for generating a chemokine and cytokine TLR7 response, whereas for iCCRKO it suggests that these receptors do not play a critical role. However, it is worth noting that diminished peripheral responses in KO mice may reduce the CNS inflammatory response and this would be an interesting area of investigation with the Aldara model.

7.2.3 Cellular responses to TLR7 Stimulus

Determining the relative contributions of the peripheral vs the central system requires assessment of the roles that exogenous cells play when compared to endogenous. Previous work within our laboratory has demonstrated an influx of a variety of cell types into the CNS in response to cutaneous Aldara treatment (24). The data in this thesis has demonstrated that CD3⁺ cells infiltrate into the hippocampus and cortex of Aldara treated mice and examination of endogenous CNS cells identified clear morphological changes in microglia, and evidence of astrogliosis in response to cutaneous Aldara treatment.

The role of microglia and astrocytes in CNS immune reactions is becoming increasingly clear and both cell types have been shown to produce chemokines and cytokines (182, 220, 231). Although clear morphological changes in Iba1+ cells that can be presumed to be predominantly microglia, and possible but not conclusive changes in the GFAP+ cell population presumed to be astrocytes were demonstrated, the effect on cellular function of these changes is not clear. As discussed, morphological changes in microglia do not necessarily correlate with specific changes in function (167, 469). However, based on the transcriptional and protein responses to cutaneous Aldara treatment reported in this thesis, alongside *in vitro* data from Butchi et al. demonstrating transcriptional alterations in astrocytes and microglia in response to IMQ (237), it can be hypothesised that, at least within the first 24 hours of cutaneous Aldara treatment when recruited immune cell populations appear to be sparse or absent (24), these endogenous cell types are the primary source of chemokines and cytokines within the CNS.

The mechanisms through which inflammation resolves is of particular interest given the temporal differences in chemokine and cytokine responses between the periphery and CNS. Examination of the literature suggests that TLR7 stimulation itself may be of particular importance for inflammatory resolution. *In vitro* work by Butchi et al. comparing TLR7, TLR9 and TLR7+TLR9 responses demonstrated that TLR7+TLR9 stimulation of microglia enhances *Il10* expression and diminishes the expression of the interferon stimulated gene *Cxcl10*, compared to TLR9 stimulation alone (237), suggesting that TLR7 signalling in microglia promotes an anti-inflammatory phenotype when compared to TLR9.

As discussed earlier in this thesis, the arrival of exogenous cell types within the CNS appears to coincide with the onset of inflammatory downregulation. *In vivo* work on TLR7KO mice infected with the neurotropic Langkat ssRNA virus found that the absence of TLR7 actually increased *Cd3ε* and *Cd8a* expression but did not influence *Cd4*, suggesting that in the absence of TLR7 there is an increased recruitment of CD8+ cytotoxic T-cells but not CD4+ helper T-cells. In addition, this study found that while IFN responses appear to be enhanced in TLR7KO mice, there were significant decreases in the expression of *Tnf*, *Ccl3*, *Ccl4* and *Cxcl13* (507). This deficiency in *Ccl4*, which is associated with enhanced

inflammatory responses, provides further support to the hypothesis that this chemokine may be important in promoting T-cell regulatory responses. CXCL13 is thought to attract B-cells, which have previously been shown to promote T_{reg} recruitment via CCL4 (418). Il10, found by Butchi et al. to be produced by microglia in response to TLR7, is also thought to be an important molecule for T_{reg} function, acting to promote suppressive functions (508, 509), further supporting the idea that TLR7 may act to restrain inflammatory reactions. Work in this thesis has shown that cutaneous Aldara treatment stimulates the upregulation of *Tnf*, *Ccl3*, *Ccl4*, *Cxcl13* and *Il10* within the brain, complementing these earlier findings by others. It is worth considering that these alterations may be peripherally driven, however Nazmi et al. demonstrated that even in the case of brain specific TLR7 knock-down, increases in the inflammatory response were still present (510) and alongside Butchi et al's. findings in *in vitro* microglia, this supports the suggestion that these changes are, at least in part, mediated by brain TLR7 and not just alterations in the peripheral immune response.

The findings of these studies and the work presented in this thesis are challenging to synthesise primarily due to differing time-points, *in vivo* and *in vitro* work and some slightly contradictory data, particularly considering our findings of robust IFN stimulation in response to TLR7 triggering. However, a potential model for this could be that at early time-points TLR7 promotes the expression of CCL4 and CXCL13 that in turn promote recruitment of T_{reg} cells and B cells. Concomitant induction of Il10 will also act to promote an anti-inflammatory environment and enhance the function of these recruited cells. Subsequently these cells enhance the recruitment of further regulatory cells, for example through B-cell derived increases in CCL4, and promote the resolution of the inflammatory response. This resolution then results in the reduction or termination of interferon and other immune responses at later time-points.

Alongside their immunological functions, recruited cells may act to influence behaviour. There is reasonable evidence that T-cells play important roles in modulating CNS function. Deficiency of T-cells results in cognitive impairment (506, 511), and a recent study by Filiano et al. demonstrated that T-cells appear to be important in modulating social behaviour through IFN- γ (500). This suggests

T-cell infiltration into the brain may play a role in the behavioural alterations observed in the Aldara model (24). However, even after a single day of treatment when T-cells appear to be largely absent from the CNS there are still decreases in burrowing behaviour in Aldara treated mice(24). This suggests that other factors may be responsible for this behavioural alteration. One possible cell type responsible for this effect are circulating monocytes that appear to be important mediators of behavioural and neuronal changes following peripheral inflammatory stimuli. This effect is thought to be mediated through their secretion of TNF α , as when signalling through TNFR, or when the production of TNF itself was knocked out these behavioural and neuronal responses to peripheral inflammation were absent (413, 512). Together these data suggest that signals from both innate and adaptive cells, present in both the periphery and brain parenchyma appear to be important for behavioural changes in response to immune stimulus and the relative contributions of each of these populations warrants further investigation.

7.3 Conclusions

The work in this thesis initially demonstrated that in a meta-analysis of human biomarker studies in depressive illness there was significant evidence of alterations in circulating chemokine levels. The primary caveats of these data were that: (i) the methodological quality of these studies was highly variable; (ii) there did not appear to be significant associations in depressed patients with comorbidities and; (iii) that due to the cross-sectional nature of the studies it is not possible to make inferences about directionality or mechanism.

Following this review of human literature, characterisation and investigation of an animal model of peripherally induced neuro-inflammation, the Aldara model of psoriasis-like inflammation, was performed. This study showed that cutaneous Aldara treatment induces significant increases in chemokine and cytokine expression within the brain that are temporally distinct from peripheral transcriptional changes. In addition there is consistent evidence of reactive microglial changes and T-cell recruitment in the brain, and, while more equivocal, there is also evidence of astrogliosis. Study into IFNAR and iCCR function showed that IFNAR was important for the induction of inflammatory transcripts, morphological changes in microglia and the recruitment of T cells to

the CNS. In contrast, iCCR appeared to not influence transcriptional or microglial response but did seem to affect the recruitment of CD3⁺ cells. Subsequent mass spectrometry investigations revealed that these changes appear to be primarily mediated by IMQ, a TLR-7 agonist in Aldara cream, gaining direct access to the brain parenchyma. Whilst a series of interesting findings have been presented in this thesis, the data suggest that the Aldara model is not an appropriate tool for the study of peripheral-central crosstalk but is a useful model for the study of viral responses.

Overall these data strongly support the investigation of chemokines as a molecular family in the context of both human psychiatric disease and neuro-inflammatory responses. The Aldara model appears to be a useful, and possibly unique, tool for the study of neuro-inflammatory responses *in vivo*, particularly if interested in TLR7 or IFN signalling which both appear to play important roles in observed immune changes.

7.4 Future directions

A number of possible future directions can be taken based on the work presented here: (i) longitudinal epidemiological studies of human immune status and psychiatric disease, or more methodologically rigorous cross-sectional studies that record and assess the effect of confounders; (ii) further investigation of temporal differences between the brain and periphery and the mechanisms through which immune resolution occurs at these sites; (iii) further investigation of the role specific cells play in the induction of CNS inflammation and; (iv) further studies on the roles of chemokines and IFN signalling in the induction of CNS inflammation and behavioural change.

While all are interesting this final section will focus on points (iii) and (iv). As discussed a number of questions remain to be answered with regards to the data presented here. These include, but are not limited to:

- Are microglia and/or astrocytes the source of transcriptional and protein changes within the brain?

- Are recruited cells, specifically T_{reg} cells, important for resolution of the inflammatory response?
- What are the outcomes of behavioural change in iCCRKO and IFNARKO mice, and if changes are present what are the mechanisms through which this occurs?

Experiments that can address each of these questions will be discussed in turn. Firstly to understand the role of microglia or astrocytes in the brain it is necessary to be able to isolate these cells either *ex vivo* or *in vivo*. It would be possible to isolate microglia or astrocytes *ex vivo* using cell sorting. Once isolated, cells could be rapidly fixed and then transcriptional and protein assays could be performed. Limitations of this approach would be the challenges of assessing the effect of isolation on these assays and, in addition, proteins that were rapidly secreted might not be identifiable in this manner. Other possible approaches would be to perform in-situ hybridization combined with immunohistochemistry to identify both cell types of interest and genes that were expressed by them. The major challenge of this approach is that with current techniques it would be challenging to identify more than one transcript and one cell type at the same time making this approach very low-throughput and perhaps more appropriate for the investigation of a specific molecule of interest. However, a major advantage over the use of cell sorting is that it would provide anatomical localisation within the CNS. A final approach would be to use specialised Cre/Lox mice that have cell-specific KO, for example, using TLR-7 floxed mice crossed to a GLAST-Cre/ERT2 background would abrogate TLR-7 signalling in astrocyte cells following treatment with tamoxifen (513) and provide insight into how they contribute to the neuro-inflammatory response to cutaneous Aldara treatment. In addition, due to this KO being tamoxifen inducible, it can provide temporal control over when this occurs.

In this discussion a potential role for the chemokine CCL4 and T_{reg} cells in the resolution of inflammatory response has been highlighted. It would be pertinent to initially confirm whether this subtype of T cells are present following cutaneous Aldara treatment and at what time-point they appear within the brain. Following this, depletion of T_{reg} cells would allow for an assessment of

their role in inflammatory resolution and the production of anti-inflammatory mediators such as *Il10*. It would also be interesting to assess the role of CCL4 in T_{reg} recruitment and, if possible, to assess the role of peripheral vs central T_{regs} in the modulation of the response to cutaneous Aldara treatment. Finally considering the tentative links to depressive disorder it would be worthwhile assessing the impact of T_{reg} depletion on burrowing behaviour or other cognitive tests.

Finally the behavioural response in either iCCRKO or IFNARKO mice could initially be investigated using the relatively simple burrowing task to look for gross deficits in wellbeing. Ideally more complex and controlled behavioural tasks would be performed such as the Morris water maze, to examine learning and memory, and the elevated plus maze to assess anxiety-based behaviours. In addition, use of controlling behavioural studies such as the open field test would help to confirm that these alterations were in fact psychologically based rather than mechanically. If behavioural deficits were observed it would then be interesting to use an approach similar to that used by Blank et al. to investigate this further(103). Use of cre/Lox mice, particularly those targeting neurons can begin to dissect if certain ligand-receptor relationships appear to mediate behavioural changes.

In conclusion there is a wide range of directions that work following on from this thesis can take. An increasing number of tools are available to psycho-neuro-immunologists to investigate the causes and mechanisms of behavioural alterations and the precise studies that people undertake will depend on their own specialist interests.

Appendices

Appendix 1: Companies referenced in methods

Agilent

(Agilent Technologies, Cheshire, UK)
 Agilent Technologies LDA UK Limited
 Life Sciences & Chemical Analysis
 Group
 Lakeside
 Cheadle Royal Business Park
 Stockport, Cheshire SK8 3GR

Alpha Laboratories

(Alpha Laboratories, Hampshire, UK)
 Alpha Laboratories
 40 Parham Drive
 Eastleigh
 Hampshire
 SO50 4NU
 United Kingdom

BD Biosciences

(BD Biosciences, CA, USA)
 BD Biosciences
 2350 Qume Drive
 San Jose
 CA 95131-1807
 USA

Biolegend

(Biolegend, CA, USA)
 Biolegend
 9727 Pacific Heights Blvd
 San Diego
 California
 92121

CellPath

(CellPath, Newtown, UK)
 Cellpath Ltd.
 Mochdre Industrial Estate
 Mochdre
 Newtown
 SY16 4LE

GraphPad Software, Inc

(GraphPad Software, CA, USA)
 GraphPad Software, Inc.
 7825 Fay Avenue, Suite 230
 La Jolla, CA 92037 USA

Greiner

(Greiner Bio-One, Stonehouse, UK)
 Greiner Bio-One Ltd
 Brunel Way
 Stroudwater Business Park
 Stonehouse
 UK

Leica Microsystems

(Leica Microsystems, Milton Keynes, UK)
 Larch House, Woodlands Business
 Park,
 Breckland,
 Linford Wood
 Milton Keynes
 MK14 6FG
 United Kingdom

Meda (Aldara)

(Meda AB, Solna, Sweden)
 Meda AB
 Box 906
 SE-170 09 Solna
 Sweden

Microsoft

(Microsoft, WA, USA)
 Microsoft Corporation
 Corporate Headquarters
 One Microsoft Way
 Redmond, WA 98052-6399
 UNITED STATES

Milestone SRL

(Milestone, Sorisole, IT)
Milestone Srl
Via Fatebenefratelli, 1/5
24010 Sorisole (Bergamo) - Italy

New England BioLabs

(New England BioLabs, MA, USA)
New England BioLabs
240 County Road
Ipswich
MA 019838-2723
USA

Quantabio

(Quantabio, MA, USA)
100 Cummings Center
Suite 407J
Beverly, MA 01915

Qiagen

(Qiagen, Hilden, GER)
Qiagen Str. 1
40724 Hilden
Germany

Roche

(Roche, West Sussex, UK)
Roche Diagnostics Ltd
Charles Avenue
Burgess Hill
West Sussex
RH15 9RY
United Kingdom

Sigma-Aldrich

(Sigma-Aldrich, Dorset, England)
Sigma-Aldrich Company Ltd.
The Old Brickyard, New Road
Gillingham, Dorset
SP8 4XT
United Kingdom

Starlab

(Starlab, Milton Keynes, UK)
STARLAB (UK), Ltd
5 Tanners Drive
Blakelands
Milton Keynes MK14 5BU
United Kingdom

STEMCELL Technologies

(STEMCELL Technologies, Cambridge, UK)
STEMCELL Technologies UK Ltd.
Building 7100 Cambridge Research
Park
Beach Drive
Waterbeach
Cambridge
UK
CB25 9TL

Tecan

(Tecan, Mannedorf, SWI)
Tecan Group Ltd.
Seestrasse 103
8708 Mannedorf
Switzerland

Thermo Fisher

(Thermo Fisher Scientific, MA, USA)
Thermo Fisher Scientific
168 Third Avenue
Waltham, MA USA 02451

Appendix 2: Example search strategy used for meta-analysis of chemokines

Search	Query
S1	chemokine*
S2	ccl1 or ccl2 or ccl3 or ccl4 or ccl5 or ccl6 or ccl7 or ccl8 or ccl9 or ccl10 or ccl11 or ccl12 or ccl13 or ccl14 or ccl15 or ccl16 or ccl17 or ccl18 or ccl19 or ccl20 or ccl21 or ccl22 or ccl23 or ccl24 or ccl25 or ccl26 or ccl27 or ccl28)
S3	(cxcl1 or cxcl2 or cxcl3 or cxcl4 or cxcl5 or cxcl6 or cxcl7 or cxcl8 or cxcl9 or cxcl10 or cxcl11 or cxcl12 or cxcl13 or cxcl14 or cxcl15 or cxcl16 or cxcl17)
S4	(xcl1 or xcl2)
S5	cx3cl1
S6	(ccl or cxcl or xcl or cx3cl)
S7	(scya1 or scya2 or scya3 or scya4 or scya5 or scya6 or scya7 or scya8 or scya9 or scya10 or scya11 or scya12 or scya13 or scya14 or scya15 or scya16 or scya17 or scya18 or scya19 or scya20 or scya21 or scya22 or scya23 or scya24 or scya25 or scya26 or scya27 or scya28)
S8	(scyb1 or scyb2 or scyb3 or scyb4 or scyb5 or scyb6 or scyb7 or scyb8 or scyb9 or scyb10 or scyb11 or scyb12 or scyb13 or scyb14 or scyb15 or scyb16 or scyb17)
S9	(scyc1 or scyc2)
S10	synd1
S11	(scya or scyb or scyc or synd)
S12	chemokine receptor*
S13	(ccr1 or ccr2 or ccr2b or ccr3 or ccr4 or ccr5 or ccr6 or ccr7 or ccr8 or ccr9 or ccr10)
S14	(cxcr1 or cxcr2 or cxcr3 or cxcr3b or cxcr4 or cxcr5 or cxcr6 or cxcr7)
S15	xcr1
S16	cx3cr1
S17	(ccr or cxcr or xcr or cx3cr)
S18	(chemotactic cytokine* or chemokine*)
S19	(i-309 or i309 or tca-3 or tca3 or sise)
S20	(monocyte chemotactic protein#1 or monocyte chemotactic protein-1 or mcp#1 or mcp-1 or small inducible cytokine a2 or gdcf#2 or gdcf-2 or hc11 or hsmcr30 or mcaf or cmc#cf or smc-cf)
S21	(macrophage inflammatory protein#1a or macrophage inflammatory protein-1a or mip#1a or mip-1a or g0s19#1 or g0s19-1 or ld78alpha or mip#1#alpha or mip#1-alpha or mip-1#alpha or mip-1-alpha or mip1a)
S22	(macrophage inflammatory protein#1# or macrophage inflammatory protein-1# or mip#1# or mip-1# or act2 or act-2 or at744#1 or g26 or g-26 or hc21 or lag-1 or lag1 or mip-1-beta or mip1b or mip1b1)
S23	((regulated on activation, normal t cell expressed and secreted) or rantes or d17s136e or sis-delta or sisd or tcp228 or eocp)
S24	(c10 or mrp#1 or mrp-1 or mrp#2 or mrp-2)
S25	(monocyte specific chemokine#3 or monocyte specific chemokine-3 or monocyte-specific chemokine#3 or monocyte-specific chemokine-3 or mcp#3 or fic or marc or mcp-3 or nc28)
S26	(monocyte chemotactic protein#2 or monocyte chemotactic protein-2 or mcp-2 or mcp#2 or hc14)

Search	Query
S27	(macrophage inflammatory protein#1#gamma or macrophage inflammatory protein-1#gamma or macrophage inflammatory protein#1-gamma or macrophage inflammatory protein-1-gamma or mip#1#gamma or mip#1-gamma or mip-1#gamma or mip-1-gamma or macrophage inflammatory protein#1* or macrophage inflammatory protein-1* or macrophage inflammatory protein-related protein-2 or mrp#2 or mrp-2 or ccf18)
S28	(eosinophil chemotactic protein or eotaxin-1 or eotaxin#1)
S29	(monocyte chemotactic protein 5 or mcp#5 or mcp-5 or mcp#1-related chemokine or mcp-1#related chemokine or mcp#1#related chemokine or mcp-1-related chemokine)
S30	(mcp#4 or mcp-4 or ncc#1 or ncc-1 or ckbeta10 or scyl1 or ckb10)
S31	(hcc#1 or hcc-1 or mcif or ckb1 or ckbeta1 or ncc#2 or ncc-2 or hcc#3 or hcc-3 or scyl2)
S32	(leukotactin#1 or leukotactin-1 or mip#5 or mip-5 or hcc#2 or hcc-2 or ncc#3 or ncc-3 or scyl3 or lkn#1 or lkn-1 or mip#1d or mip-1d or hmrp#2b or hmrp-2b)
S33	(lec or ncc#4 or ncc-4 or lmc or ckb12 or ckbeta12 or liver#expressed chemokine or liver-expressed chemokine or monotactin#1 or monotactin-1 or mtn#1 or mtn-1 or scyl4 or hcc#4 or hcc-4 or lcc#1 or lcc-1)
S34	(tarc or dendrokinine or abcd#2 or abcd-2 or (thymus and activation regulated chemokine) or a#152e5#3 or a-152e5#3)
S35	(parc or dc-ck1 or dc#ck1 or amac-1 or amac#1 or ckb7 or ckbeta7 or mip#4 or mip-4 or (pulmonary and activation-regulated chemokine) or (pulmonary and activation#regulated chemokine) or dendritic cell-chemokine 1 or dendritic cell#chemokine 1 or alternative macrophage activation-associated cc chemokine-1 or alternative macrophage activation#associated cc chemokine-1 or alternative macrophage activation-associated cc chemokine#1 or alternative macrophage activation#associated cc chemokine#1 or macrophage inflammatory protein-4)
S36	(elc or exodus#3 or exodus-3 or ckb11 or ckbeta11 or ebi1#ligand chemokine or ebi1-ligand chemokine or macrophage inflammatory protein-3-beta or macrophage inflammatory protein#3#beta or mip-3-beta or mip-3b or mip#3b)
S37	(larc or exodus#1 or exodus-1 or ckb4 or ckbeta4 or liver activation regulated chemokine or macrophage inflammatory protein#3 or macrophage inflammatory protein-3 or mip#3#alpha or mip-3#alpha or mip#3-alpha or mip-3-alpha or mip-3a or mip#3a or st38)
S38	(slc or 6ckine or exodus#2 or exodus-2 or ckb9 or ckbeta9 or tca-4 or tca#4 or lymphoid-tissue chemokine* or lymphoid#tissue chemokine*)
S39	(mdc or dc#b-ck or dc#beta-ck or dc-b-ck or abcd#1 or abcd-1 or stcp#1 or stcp-1)
S40	(mpif#1 or mpif-1 or ckb8 or ckbeta8 or mip#3 or mip-3 or macrophage inflammatory protein 3 or myeloid progenitor inhibitory factor 1)
S41	(eotaxin#2 or eotaxin-2 or mpif#2 or mpif-2 or ckb6 or ckbeta6 or myeloid progenitor inhibitory factor 2 or eosinophil chemotactic protein 2)
S42	(teck or ckb15 or ckbeta15 or thymus#expressed chemokine or thymus-expressed chemokine)
S43	(eotaxin#3 or eotaxin-3 or mip#4a or mip-4a or imac or tsc#1 or tsc-1 or thymic stroma chemokine#1 or thymic stroma chemokine-1 or macrophage inflammatory protein 4#alpha or macrophage inflammatory protein 4-alpha or mip#4#alpha or mip-4-alpha or mip-4#alpha)
S44	(ctack or ilc or eskine or pesky or skinkine or eskine or il#11 r#alpha#locus chemokine or il-11 r-alpha-locus chemokine or cutaneous t#cell#attracting chemokine or cutaneous t-cell-attracting chemokine)
S45	(mec or mucosae#associated epithelial chemokine mucosae-associated epithelial chemokine or cck1)

Search	Query
S46	(gro#a or gro-a or gro#alpha or gro-alpha or gro1 or nap#3 or nap-3 or kc or neutrophil#activating protein 3 or neutrophil-activating protein 3 or melanoma growth stimulating activity alpha or msga#alpha or msga-alpha or msga#a or msga-a)
S47	(gro#b or gro-b or gro#beta or gro-beta or gro#2 or mip#2a or mip-2a or macrophage inflammatory protein 2#alpha or macrophage inflammatory protein 2-alpha or mip2#alpha or mip2-alpha or growth#regulated protein beta or growth-regulated protein beta or gro oncogene#2 or gro oncogene-2 or gro-2 or msga#beta or msga-beta or msga#b or msga-b or cinc#2a or cinc-2a)
S48	(gro#gamma or gro-gamma or gro#3 or gro-3 or mip#2b or mip-2b or mip#2beta or mip2-beta or gro3 oncogene or gro protein gamma or grog or macrophage inflammatory protein#2#beta or macrophage inflammatory protein#2-beta or macrophage inflammatory protein-2#beta or macrophage inflammatory protein-2-beta or cinc#2b or cinc-2b)
S49	(pf-4 or platelet factor#4 or pf#4 or platelet factor-4)
S50	(ena#78 or ena-78 or epithelial-derived neutrophil-activating peptide 78 or epithelial#derived neutrophil#activating peptide 78)
S51	(gcp#2 or gcp-2 or granulocyte chemotactic protein#2 or granulocyte chemotactic protein-2 or cka#3 or cka-3)
S52	(nap#2 or nap-2 or ctapiii or b-tg or beta-tg or b#tg or beta#tg or pep or beta-thromboglobulin or beta#thromboglobulin or pro#platelet basic protein or pro-platelet basic protein or pbbp or b#tg1 or b-tg1 or ctap#iii or ctap-iii or ctap#3 or ctap-3 or la#pf4 or la-pf4 or ldgf or mdgf or pbp or tc#1 or tc-1 or tc#2 or tc-2 or tgb or tgb#1 or tgb-1 or thbgb or thbgb#1 or thbgb-1)
S53	(il-8 or nap-1 or mdnfc or gcp-1 or gcp#1 or il#8 or interleukin 8 or neutrophil chemotactic factor or lect or luct or lynap or mdnfc or monap or naf or nap#1)
S54	(mig or crg-10 or monokine induced by gamma interferon or cmk or humig or crg#10)
S55	(ip-10 or ip#10 or crg#2 or crg-2 or interferon gamma-induced protein 10 or interferon gamma induced protein 10 or small-inducible cytokine b10 or small inducible cytokine b10 or c7 or ifi10 or inp10 or gip#10 or gip-10 or mob#1 or mob-1)
S56	(i#tac or i-tac or h#174 or h-174 or ip#9 or ip-9 or scyb9b or b#r1 or b-r1 or beta#r1 or beta-r1 or interferon inducible t cell alpha chemoattractant or interferon-inducible t-cell alpha chemoattractant or interferon-gamma-inducible protein 9 or intergeron gamma inducible protein 9)
S57	(sdf-1 or sdf#1 or tlsx or tpar1 or pbsf or stromal cell-derived factor 1 or stromal cell#derived factor 1 or irh)
S58	(b lymphocyte chemoattractant or bca-1 or bca#1 or blr1l or blc or angie#)
S59	((breast and kidney-expressed chemokine) or brak or njac or bolekin or kec or mip-2g or mip#2g or bmac or ks1)
S60	(lungkine or weche)
S61	(sr#psox or sr-psox or cxclg16)
S62	(dmc or vcc#1 or vcc-1 or vegf co#regulated chemokine 1 or vegf co-regulated chemokine 1 or (dendritic cell- and monocyte-attracting chemokine-like protein) or (dendritic cell and monocyte attracting chemokine-like protein) or (dendritic cell and monocyte attracting chemokine like protein))
S63	(lymphotactin or atac or ltn or lptn or scm#1# or scm-1#)
S64	lymphotactin
S65	(fractalkine or neurotactin or abcd#3 or abcd-3 or c3xkine or cxc3 or cxc3c or ntn or ntt)
S66	(cluster of differentiation 191 or cd191 or ckr-1 or ckr#1 or cmkbr1 or hm145 or mip1ar or scyar1)

Search	Query
S67	(ccr2# or cd192 or cluster of differentiation 192 or cc#ckr#2 or cc#ckr-2 or cc-ckr#2 or cc-ckr-2 or ccr#2 or ccr-2 or ckr-2# or ckr#2# or cmkbr2 or mcp#1#r or mcp-1#r or mcp#1-r or mcp-1-r)
S68	(cd193 or cluster of differentiation 193 or cc#ckr#3 or cc-ckr#3 or cc#ckr-3 or cc-ckr-3 or ckr-3 or ckr#3 or cmkbr3)
S69	(cd194 or cluster of differentiation 194 or cc#ckr#4 or cc#ckr-4 or cc-ckr#4 or cc-ckr-4 or ckr-4 or ckr#4 or cmkbr4 or chemr13 or hgcn:14099 or k5-5)
S70	(cd195 or cluster of differentiation 195 or cc#ckr#5 or cc#ckr-5 or cc-ckr#5 or cc-ckr-5 or ccr#5 or ccr-5 or ckr-5 or ckr#5 or cmkbr5 or iddm22)
S71	(cd196 or cluster of differentiation 196 or bn#1 or bn-1 or cc#ckr#6 or cc#ckr-6 or cc-ckr#6 or cc-ckr-6 or ccr#6 or ccr-6 or ckr-l3 or ckr#l3 or cmkbr6 or dcr2 or dry6 or g protein-coupled receptor 29 or g protein-coupled receptor cy4 or gpr29 or gprcy4 or strl22)
S72	(cd197 or cluster of differentiation 197 or blr2 or cdw197 or cmkbr7 or ebi1)
S73	(cdw198 or cluster of differentiation w198 or cc#ckr#8 or cc#ckr-8 or cc-ckr#8 or cc-ckr-8 or ccr#8 or ccr-8 or ckr1 or cmkbr8 or cmkbrl2 or cy6 or g protein-coupled receptor cy6 or gprcy6 or ter1)
S74	(cdw199 or cluster of differentiation w199 or cc#ckr#9 or cc#ckr-9 or cc-ckr#9 or cc-ckr-9 or g protein-coupled receptor 9-6 or gpr#9-6 or gpr-9-6 or g protein-coupled receptor 28 or gpr28)
S75	(gpr2 or g protein-coupled receptor 2 or g protein coupled receptor 2)
S76	(interleukin 8 receptor or il-8ra or cd181 or cluster of differentiation 181 or cc#ckr#1 or cc#ckr-1 or cc-ckr#1 or cc-ckr-1 or cd128 or cdw128a or ckr#1 or ckr-1 or cmkar1 or il8r1 or il8ra or il8ra)
S77	(il8rb or cluster of differentiation 182 or cd182 or cdw128b or cmkar2 or il#8r2 or il-8r2 or il#8ra or il-8ra or il#8rb or il-8rb)
S78	(g protein-coupled receptor 9 or cd183 or cluster of differentiation 182 or cxcr3#a or cxcr3-a or cxcr3#b or cxcr3-b or cd182 or cd183 or ckr#l2 or ckr-l2 or cmkar3 or gpr9 or ip10#r or ip10-r or mig-r or mig#r)
S79	(fusin or cd184 or cluster of differentiation 184 or d2s201e or fb22 or hm89 or hsy3rr or lap-3 or lap#3 or lcr#1 or lcr-1 or lestr or npy3r or npyr# or nppy3r or whim)
S80	(cd185 or cluster of differentiation 185 or burkitt lymphoma receptor 1 or blr#1 or blr-1 or mdr#15 or mdr-15)
S81	(cd186 or cluster of differentiation 186 or bonzo or strl33 or tymstr)
S82	(ackr#3 or ackr-3 or cmkor#1 or cmkor-1 or cxc-r7 or cxcr-7 or cxcr#7 or g protein-coupled receptor 159 or g protein coupled receptor 159 or gpr159 or rdc-1 or rdc#1)
S83	(g protein-coupled receptor 5 or g protein coupled receptor 5 or gpr5 or cc#xcr#1 or cc-xcr#1 or cc#xcr-1 or cc-xcr-1)
S84	(fractalkine receptor or g protein-coupled receptor 13 or g protein coupled receptor 13 or gpr13 or ccr1 or cmkbrl1 or cmkdr1 or g protein-coupled receptor v28 or g protein coupled receptor v28 or gprv28 or v28)
S85	S1 OR S2 OR S3 OR S4 OR S5 OR S6 OR S7 OR S8 OR S9 OR S10 OR S11 OR S12 OR S13 OR S14 OR S15 OR S16 OR S17 OR S18 OR S19 OR S20 OR S21 OR S22 OR S23 OR S24 OR S25 OR S26 OR S27 OR S28 OR S29 OR S30 OR S31 OR S32 OR S33 OR S34 OR S35 OR S36 OR S37 OR S38 OR S39 OR S40 OR S41 OR S42 OR S43 OR S44 OR S45 OR S46 OR S47 OR S48 OR S49 OR S50 OR S51 OR S52 OR S53 OR S54 OR S55 OR S56 OR S57 OR S58 OR S59 OR S60 OR S61 OR S62 OR S63 OR S64 OR S65 OR S66 OR S67 OR S68 OR S69 OR S70 OR S71 OR S72 OR S73 OR S74 OR S75 OR S76 OR S77 OR S78 OR S79 OR S80 OR S81 OR S82 OR S83 OR S84
S86	DE "Major Depression" OR DE "Anaclitic Depression" OR DE "Dysthymic Disorder" OR DE "Endogenous Depression" OR DE "Postpartum Depression" OR DE "Reactive Depression" OR DE "Recurrent Depression" OR DE "Treatment Resistant Depression"

Search	Query
S87	depress*
S88	(beck depression or bdi or bdi#1a or bdi-1a or bdi#ii or bdi-ii)
S89	(burns depression or bdc)
S90	(center for epidemiologic studies depression or ces-d or ces#d)
S91	(cornell scale for depression in dementia or csdd)
S92	(edinburgh post#natal depression or edinburgh post-natal depression or epds)
S93	(geriatric depression or gds)
S94	(hamilton rating scale for depression or hamilton depression rating scale or hrsd or hdrs or ham-d or ham#d)
S95	(hospital anxiety and depression scale)
S96	(inventory of depressive symptomatology or ids)
S97	(inventory to diagnose depression or idd)
S98	(kutcher adolescent depression or kads)
S99	(major depress* or mdd or mdi)
S100	(montgomery-asberg depression rating scale or montgomery asberg depression rating scale or madrs)
S101	(patient health questionnaire-9 or phq-9 or patient health questionnaire#9 or phq#9)
S102	(quick inventory of depressive symptomatology or qids)
S103	(raskin depression rating scale or three-area severity of depression scale or three area severity of depression scale or rdrs)
S104	(rads-2 or reynolds adolescent depression scale or rads#2 or rads or rcds-2 or rcds or rcds#2 or reynolds child depression scale)
S105	(wechsler depression rating scale or wdrs)
S106	(zung self-rating depression scale or zung self rating depression scale or sds or zsrds)
S107	S86 OR S87 OR S88 OR S89 OR S90 OR S91 OR S92 OR S93 OR S94 OR S95 OR S96 OR S97 OR S98 OR S99 OR S100 OR S101 OR S102 OR S103 OR S104 OR S105 OR S106
S108	S85 AND S107

Appendix 3: Custom data extraction template used for assessment of studies in meta-analysis

Systematic Review Data Collection Tool

Adapted from handbook.cochrane.org

*Required

Our Review Questions

1 - Is depression as a state (presence of depressive symptoms) associated with altered levels of specific chemokines?

2a - Is there a subtype of people with depressive symptoms which are associated with altered levels of specific chemokines vs a subtype who are not? (e.g. based on severity, based on the symptoms being part of a primary depressive illness or in the context of another syndrome/ disease)

2b - Is depression as a trait associated with altered levels of specific chemokines?

Review Author Notes

Any comments, notes, questions or reminders for this study not covered below?

E.g.

conclusions drawn to not tie up with results etc.

Source

Study ID *

A unique ID code given to an included or excluded study by the review author (e.g. first author's name and year of publication from the main report of the study). Although a study may have multiple reports or references, it should have one single Study ID to help review authors keep track of all the different sources of information for a study.

Report ID *

A unique ID code given to a publication or other report of a study by the review author (e.g. first author's name and year of publication). If a study has more than one report (e.g. multiple publications or additional unpublished data) a separate Report ID can be allocated to each to help review authors keep track of the source of extracted data.

Review Author ID *

- SL
- LN

Citation & contact details*

Eligibility

Confirm Eligibility *

- Eligible
- Not Eligible
- Unsure

Reason for exclusion
(if not eligible)

Methods

Study Design

(Presumably all observational)

- Case-Control Study
- Cohort Study
- Randomised Controlled Trial
- Controlled Clinical Trail (no randomisation)
- Cross-Sectional Study
- Other:

Total Study Duration

in days to allow comparison

Bias

See:

handbook.cochrane.org/chapter_8/table_8_5_a_the_cochrane_collaborations_to_ol_for_assessing.htm

N.B. Some of these biases may not be applicable for many studies because our intervention is the presence or absence of depression which is not really allocated and can't be blinded to the participants. It can be to the investigators etc.

Random Sequence Generation

Describe the method used to generate the allocation sequence in sufficient detail to allow an assessment of whether it should produce comparable groups.

Is there evidence selection bias (biased allocation to interventions) due to inadequate generation of a randomised sequence? *

- Yes
- No
- Other:

Allocation Concealment

Describe the method used to conceal the allocation sequence in sufficient detail to determine whether intervention allocations could have been foreseen in advance of, or during, enrolment.

Is there evidence of selection bias (biased allocation to interventions) due to inadequate concealment of allocations prior to assignment? *

- Yes
- No
- Other:

Blinding of Participants

Describe all measures used, if any, to blind study participants and personnel from knowledge of which intervention a participant received. Provide any information relating to whether the intended blinding was effective. Assessments should be made for each main outcome (or class of outcomes).

Is there evidence of performance bias due to knowledge of the allocated interventions by participants and personnel during the study? *

- Yes
- No
- Other:

Blinding of Outcome Assessment

Describe all measures used, if any, to blind outcome assessors from knowledge of which intervention a participant received. Provide any information relating to whether the intended blinding was effective. Assessments should be made for each main outcome (or class of outcomes).

Is there evidence of detection bias due to knowledge of the allocated interventions by outcome assessors? *

- Yes
- No
- Other:

Completeness of Outcome Data

Describe the completeness of outcome data for each main outcome, including attrition and exclusions from the analysis. State whether attrition and exclusions were reported, the numbers in each intervention group (compared with total randomized participants), reasons for attrition/exclusions where reported, and any reinclusions in analyses performed by the review authors. Assessments should be made for each main outcome (or class of outcomes).

Is there evidence of attrition bias due to amount, nature or handling of incomplete outcome data? *

- Yes
- No
- Other:

Outcome Reporting

State how the possibility of selective outcome reporting was examined by the review authors, and what was found.

Is there evidence of reporting bias due to selective outcome reporting? *

- Yes
- No
- Other:

Is there evidence of bias due to problems not covered above? *

- Yes
- No
- Other:

Other Sources of Bias

Participants

Where applicable indicate if information is for the whole study or for each intervention group separately

Total Number

Power Calculation Used?

- No
- Yes & Reached
- Yes But Not Reached
- Other:

Setting of Study

- Psychiatric Inpatient
- Psychiatric Outpatient
- Medical Inpatient
- Medical Outpatient
- Primary Care
- Other:

Setting of Study Included in Analysis as Confounder?

- Yes
- No
- Other:

Diagnostic Criteria Used

DSM, ICD, other - indicate code (e.g. ICD10 F32.2 Severe depressive episode without psychotic symptoms); Scale - indicate cut off used

Diagnostic Criteria Used Included in Analysis as Confounder?

- Yes
- No
- Other:

Age

e.g. as means or medians, with SDs or ranges

Age Included in Analysis as Confounder?

- Yes
- No
- Other:

Sex

e.g. as percentages or counts

Sex Included in Analysis as Confounder?

- Yes
- No
- Other:

Country

Indicate which one(s) and if important cultural characteristics that could affect delivery of an intervention and its outcomes?

Country Included in Analysis as Confounder?

- Yes
- No
- Other:

Comorbidity

- What information is provided?
- Physical Illness (especially inflammatory)
- Psychiatric Illness (including addictions)
- Concomitant Medications
- BMI / Other Measure of Adiposity
- Smoking
- Measures of Autonomic Function (e.g. HR, BP, etc)
- Physical Activity
- Genetic / Epigenetic factors
- Other:

Additional Info on Comorbidities?

All Recorded Comorbidities Included in Analysis as Confounders?
If only certain ones indicate which in answer

- Yes
- No
- Other:

Sociodemographics

Qualitative or quantitative measures?

Sociodemographics

Included in Analysis as Confounder?

- Yes
- No
- Other:

Ethnicity

Ethnicity Included in Analysis as Confounder?

- Yes
- No
- Other:

Start Date of Study

dd/mm/yyyy

Intervention / Exposure

Total Number of Intervention/ Exposure Groups? *

(e.g. in our case would normally be 2 - depressed versus not depressed, where the intervention is the presence of depression)

What is the Intervention / Exposure? *

Provide details (enough for replication if possible). Comment on integrity of intervention - see

http://handbook.cochrane.org/chapter_7/7_3_4_interventions.htm. In our case the intervention would normally be presence or absence of depression. However, could be a single group of depressed individuals where the intervention is a drug. If so, we may need to do some data conversion to answer our primary question. It may be helpful to indicate here if this is likely to be possible - e.g. if can differentiate by depression score of those treated and compare this with levels of chemokines.

Outcomes

Number of Outcomes & Time Points Collected? *

e.g. 4 outcomes at 2 time point

Number of Outcomes & Time Points Reported? *

e.g. 2 outcomes at 1 time point

For Each Outcome... *

Give definition (e.g. serum chemokine level); unit of measurement; if scale - upper & lower limits; whether high or low is good

How Was Outcome Measured?

Time of day, season, fasting etc

What Chemokines Are Included In This Study?

Use international naming convention

Results

Number of Participants Allocated to Each Intervention Group *

In our case the intervention would normally be the presence or absence of depression.

Each Outcome of Interest *

In our case continuous data so detail the sample size, the mean and the standard deviation for the outcome for each intervention group. These are often not available directly, especially the standard deviation, and alternative statistics enable calculation or estimation of the missing standard deviation (such as a standard error, a confidence interval, a test statistic (e.g. from a t-test or F-test) or a P value). Finally, for each outcome detail any subgroup analysis and if this was pre-specified in the study methods or post-hoc.

Miscellaneous**Ethical Approval Obtained?**

- Yes
- No
- Other:

Any Potential Conflicts of Interest?

For study authors.

Key Conclusions From Study ***Miscellaneous Comments from the Study Authors****References to Other Relevant Studies**

Be aware of the possibility of citation bias

Correspondence Required? *

E.g. if we need more information or there is missing data.

- Yes
- No
- Other:

Appendix 4: RIN Values determined by agilent bioanalyzer at Glasgow Polyomics

Tissue	Group	Time-point	RIN
Brain	Control	4h	7.8
Brain	Control	4h	8.2
Brain	Control	4h	8.2
Brain	Control	4h	8.2
Brain	Treated	4h	8.1
Brain	Treated	4h	8.2
Brain	Treated	4h	8.2
Brain	Treated	4h	8.2
Brain	Control	12h	8.3
Brain	Control	12h	8.2
Brain	Control	12h	8.1
Brain	Control	12h	8.4
Brain	Treated	12h	8.3
Brain	Treated	12h	8.2
Brain	Treated	12h	7.9
Brain	Treated	12h	7.9
Brain	Control	24h	8.1
Brain	Control	24h	8.1
Brain	Control	24h	8.1
Brain	Control	24h	8.3
Brain	Treated	24h	8.5
Brain	Treated	24h	8.3
Brain	Treated	24h	8.4
Brain	Treated	24h	8.3
Brain	Control	3d	8
Brain	Control	3d	8.1
Brain	Control	3d	8.1
Brain	Control	3d	8.2
Brain	Treated	3d	8.2
Brain	Treated	3d	8.1
Brain	Treated	3d	8.2
Brain	Treated	3d	8.2
Brain	Control	5d	8.1
Brain	Control	5d	7.8
Brain	Control	5d	8
Brain	Control	5d	8.3
Brain	Treated	5d	8.3
Brain	Treated	5d	8
Brain	Treated	5d	7.9
Brain	Treated	5d	8.3

Brain time-course RIN Values

Samples were analysed by Glasgow Polyomics at the University of Glasgow using Agilent Bioanalyzer to generate RIN values. Refers to Figure 4.6, Figure 4.7, Figure 4.8

Tissue	Group	Time-point	RIN
Skin	Control	4h	EXCLUDED
Skin	Control	4h	6.7
Skin	Control	4h	6.7
Skin	Control	4h	7.1
Skin	Treated	4h	EXCLUDED
Skin	Treated	4h	7.2
Skin	Treated	4h	6.6
Skin	Treated	4h	6.9
Skin	Control	12h	4.9
Skin	Control	12h	4.7
Skin	Control	12h	7.3
Skin	Control	12h	6.7
Skin	Treated	12h	5
Skin	Treated	12h	6.3
Skin	Treated	12h	7.1
Skin	Treated	12h	7.3
Skin	Control	24h	7.6
Skin	Control	24h	EXCLUDED
Skin	Control	24h	6
Skin	Control	24h	6.9
Skin	Treated	24h	6.5
Skin	Treated	24h	6.2
Skin	Treated	24h	6
Skin	Treated	24h	6
Skin	Control	3d	5.5
Skin	Control	3d	6.7
Skin	Control	3d	8.7
Skin	Control	3d	8.2
Skin	Treated	3d	6.6
Skin	Treated	3d	6.7
Skin	Treated	3d	7.2
Skin	Treated	3d	6
Skin	Control	5d	7.3
Skin	Control	5d	6.9
Skin	Control	5d	6.6
Skin	Control	5d	6.7
Skin	Treated	5d	7.3
Skin	Treated	5d	7.6
Skin	Treated	5d	7.3
Skin	Treated	5d	7.6

Skin time-course RIN values

Samples were analysed by Glasgow Polyomics at the University of Glasgow using Agilent Bioanalyzer to generate RIN values. Refers to Figure 4.9, Figure 4.10, Figure 4.11

Tissue	Group	Time-point	RIN
PBL	Control	4h	8.9
PBL	Control	4h	9.4
PBL	Control	4h	9
PBL	Control	4h	8.9
PBL	Treated	4h	9.2
PBL	Treated	4h	8.6
PBL	Treated	4h	8
PBL	Treated	4h	8.3
PBL	Control	12h	8.6
PBL	Control	12h	8.6
PBL	Control	12h	8
PBL	Control	12h	8.8
PBL	Treated	12h	9
PBL	Treated	12h	8.8
PBL	Treated	12h	8.7
PBL	Treated	12h	9.2
PBL	Control	24h	7.7
PBL	Control	24h	8.5
PBL	Control	24h	8.6
PBL	Control	24h	7.8
PBL	Treated	24h	7.9
PBL	Treated	24h	8.1
PBL	Treated	24h	7.9
PBL	Treated	24h	8.3
PBL	Control	3d	6.6
PBL	Control	3d	8.5
PBL	Control	3d	EXCLUDED
PBL	Control	3d	7.8
PBL	Treated	3d	8.5
PBL	Treated	3d	7.6
PBL	Treated	3d	8.3
PBL	Treated	3d	EXCLUDED
PBL	Control	5d	8.7
PBL	Control	5d	8.3
PBL	Control	5d	8.5
PBL	Control	5d	8.2
PBL	Treated	5d	9.1
PBL	Treated	5d	9.2
PBL	Treated	5d	9.2
PBL	Treated	5d	9.2

PBL time-course RIN values

Samples were analysed by Glasgow Polyomics at the University of Glasgow using Agilent Bioanalyzer to generate RIN values. Refers to Figure 4.12, Figure 4.13, Figure 4.14

Tissue	Group	Time-point	RIN
Liver	Control	4h	7.4
Liver	Control	4h	7.5
Liver	Control	4h	7.1
Liver	Control	4h	6.5
Liver	Treated	4h	7.1
Liver	Treated	4h	7.9
Liver	Treated	4h	7.6
Liver	Treated	4h	7.9
Liver	Control	12h	7.8
Liver	Control	12h	7.6
Liver	Control	12h	6.3
Liver	Control	12h	7.2
Liver	Treated	12h	7
Liver	Treated	12h	7.3
Liver	Treated	12h	7.5
Liver	Treated	12h	7.3
Liver	Control	24h	8.2
Liver	Control	24h	8.2
Liver	Control	24h	7.9
Liver	Control	24h	8.1
Liver	Treated	24h	8.1
Liver	Treated	24h	8.3
Liver	Treated	24h	8.5
Liver	Treated	24h	8.4
Liver	Control	3d	8.2
Liver	Control	3d	7.8
Liver	Control	3d	7.8
Liver	Control	3d	8.1
Liver	Treated	3d	8.1
Liver	Treated	3d	8.2
Liver	Treated	3d	8.3
Liver	Treated	3d	8.2
Liver	Control	5d	8.1
Liver	Control	5d	8.2
Liver	Control	5d	7.8
Liver	Control	5d	8.2
Liver	Treated	5d	8.8
Liver	Treated	5d	8.2
Liver	Treated	5d	8.5
Liver	Treated	5d	8.4

Liver time-course RIN values

Samples were analysed by Glasgow Polyomics at the University of Glasgow using Agilent Bioanalyzer to generate RIN values. Refers to Figure 4.15, Figure 4.16, Figure 4.17

Tissue	Group	Time-point	RIN
Lung	Control	4h	7.4
Lung	Control	4h	6
Lung	Control	4h	6.7
Lung	Control	4h	6.8
Lung	Treated	4h	7.7
Lung	Treated	4h	7.6
Lung	Treated	4h	8.2
Lung	Treated	4h	7.9
Lung	Control	12h	6.5
Lung	Control	12h	7.2
Lung	Control	12h	8
Lung	Control	12h	7.2
Lung	Treated	12h	6.8
Lung	Treated	12h	8.1
Lung	Treated	12h	8
Lung	Treated	12h	8.3
Lung	Control	24h	7.6
Lung	Control	24h	7.9
Lung	Control	24h	7.2
Lung	Control	24h	7.8
Lung	Treated	24h	8.5
Lung	Treated	24h	8
Lung	Treated	24h	8.6
Lung	Treated	24h	8.4
Lung	Control	3d	7.2
Lung	Control	3d	8
Lung	Control	3d	7.9
Lung	Control	3d	7.5
Lung	Treated	3d	8
Lung	Treated	3d	8.2
Lung	Treated	3d	8.1
Lung	Treated	3d	8.3
Lung	Control	5d	7.1
Lung	Control	5d	6.9
Lung	Control	5d	7
Lung	Control	5d	6.7
Lung	Treated	5d	8.1
Lung	Treated	5d	8
Lung	Treated	5d	8.2
Lung	Treated	5d	8.3

Lung time-course RIN values

Samples were analysed by Glasgow Polyomics at the University of Glasgow using Agilent Bioanalyzer to generate RIN values. Refers to Figure 4.18, Figure 4.19, Figure 4.20

Tissue	Group	Genotype	RIN
Brain	Treated	WT	8
Brain	Treated	WT	8.2
Brain	Treated	WT	8
Brain	Treated	WT	8
Brain	Treated	HET	8.8
Brain	Treated	HET	8
Brain	Treated	HET	7.9
Brain	Treated	HET	8
Brain	Treated	HET	7.7
Brain	Treated	HET	7.9
Brain	Treated	KO	7.8
Brain	Treated	KO	7.9
Brain	Treated	KO	8.2
Brain	Treated	KO	8.5
Brain	Treated	KO	8.2
Brain	Treated	KO	8.1

Brain iCCRKO experiment 1 RIN values

Samples were analysed by Glasgow Polyomics at the University of Glasgow using Agilent Bioanalyzer to generate RIN values. Refers to Figure 5.2, Figure 5.3

Tissue	Group	Genotype	RIN
Brain	Control	WT	5
Brain	Control	WT	7.4
Brain	Control	WT	7.8
Brain	Control	WT	7.8
Brain	Control	WT	7.7
Brain	Treated	WT	8
Brain	Treated	WT	8
Brain	Treated	WT	8
Brain	Treated	WT	8
Brain	Treated	WT	8
Brain	Control	KO	7.8
Brain	Control	KO	7.7
Brain	Control	KO	7.1
Brain	Control	KO	7.4
Brain	Control	KO	7.8
Brain	Control	KO	7.5
Brain	Treated	KO	7.8
Brain	Treated	KO	7.9
Brain	Treated	KO	7.3
Brain	Treated	KO	7.6
Brain	Treated	KO	7.9

Brain iCCRKO experiment 2 RIN values

Samples were analysed by Glasgow Polyomics at the University of Glasgow using Agilent Bioanalyzer to generate RIN values. Refers to Figure 5.4, Figure 5.5

Tissue	Group	Genotype	RIN
Brain	Treated	WT	8.4
Brain	Treated	WT	8.4
Brain	Treated	WT	8.2
Brain	Treated	WT	8.3
Brain	Treated	KO	7.9
Brain	Treated	KO	8.2
Brain	Treated	KO	8.3
Brain	Treated	KO	8

Brain IFNARKO1 RIN values

Samples were analysed by Glasgow Polyomics at the University of Glasgow using Agilent Bioanalyzer to generate RIN values. Refers to Figure 5.9

Tissue	Group	Genotype	RIN
Skin	Treated	WT	7.4
Skin	Treated	WT	5.9
Skin	Treated	WT	7.4
Skin	Treated	WT	7.6
Skin	Treated	KO	7.7
Skin	Treated	KO	8
Skin	Treated	KO	8.2
Skin	Treated	KO	7.5

Skin IFNARKO1 RIN values

Samples were analysed by Glasgow Polyomics at the University of Glasgow using Agilent Bioanalyzer to generate RIN values. Refers to Figure 5.12

Tissue	Group	Genotype	RIN
PBL	Treated	WT	6.9
PBL	Treated	WT	8.3
PBL	Treated	WT	8.7
PBL	Treated	WT	8.5
PBL	Treated	KO	8
PBL	Treated	KO	8.7
PBL	Treated	KO	7.6
PBL	Treated	KO	8.9

PBL IFNARKO1 RIN values

Samples were analysed by Glasgow Polyomics at the University of Glasgow using Agilent Bioanalyzer to generate RIN values. Refers to Figure 5.13

Tissue	Group	Genotype	RIN
Brain	Control	WT	8.0
Brain	Control	WT	8.0
Brain	Control	WT	8.0
Brain	Control	WT	7.8
Brain	Treated	WT	8.0
Brain	Treated	WT	7.9
Brain	Treated	WT	8.0
Brain	Treated	WT	7.6
Brain	Control	KO	7.3
Brain	Control	KO	7.9
Brain	Control	KO	7.8
Brain	Control	KO	7.8
Brain	Treated	KO	8.2
Brain	Treated	KO	7.8
Brain	Treated	KO	8.0
Brain	Treated	KO	7.9

Brain IFNARKO2 RIN values

Samples were analysed by Glasgow Polyomics at the University of Glasgow using Agilent Bioanalyzer to generate RIN values. Refers to Figure 5.10, Figure 5.11

Tissue	Group	Time-point	RIN
Brain	Control	1d	7.4
Brain	Control	1d	7.7
Brain	Control	1d	7.3
Brain	Control	1d	7.5
Brain	Treated	1d	7.5
Brain	Treated	1d	7.5
Brain	Treated	1d	7.6
Brain	Treated	1d	7.5
Brain	Control	3d	7.6
Brain	Control	3d	7.5
Brain	Control	3d	7.5
Brain	Control	3d	7.6
Brain	Treated	3d	7.5
Brain	Treated	3d	7.7
Brain	Treated	3d	7.6
Brain	Treated	3d	7.4
Brain	Control	5d	7.7
Brain	Control	5d	7.7
Brain	Control	5d	7.7
Brain	Control	5d	7.8
Brain	Treated	5d	7.6
Brain	Treated	5d	7.6
Brain	Treated	5d	7.9
Brain	Treated	5d	7.8

Brain single treatment RIN values

Samples were analysed by Glasgow Polyomics at the University of Glasgow using Agilent Bioanalyzer to generate RIN values. Refers to Figure 6.3, Figure 6.4

Tissue	Group	Time-point	RIN
Skin	Control	1d	7.7
Skin	Control	1d	7.6
Skin	Control	1d	7.7
Skin	Control	1d	7.7
Skin	Treated	1d	7.6
Skin	Treated	1d	8.1
Skin	Treated	1d	8.3
Skin	Treated	1d	7.5
Skin	Control	3d	8.1
Skin	Control	3d	7.5
Skin	Control	3d	7.8
Skin	Control	3d	7.6
Skin	Treated	3d	7.9
Skin	Treated	3d	9
Skin	Treated	3d	8
Skin	Treated	3d	8
Skin	Control	5d	7.3
Skin	Control	5d	7.1
Skin	Control	5d	7.7
Skin	Control	5d	7.9
Skin	Treated	5d	7.7
Skin	Treated	5d	7.9
Skin	Treated	5d	8.2
Skin	Treated	5d	7.6

Skin single treatment RIN values

Samples were analysed by Glasgow Polyomics at the University of Glasgow using Agilent Bioanalyzer to generate RIN values. Refers to Figure 6.5, Figure 6.6

Tissue	Group	Time-point	RIN
PBL	Control	1d	8.7
PBL	Control	1d	8.9
PBL	Control	1d	8.1
PBL	Control	1d	9.1
PBL	Treated	1d	7.3
PBL	Treated	1d	8.5
PBL	Treated	1d	7.3
PBL	Treated	1d	8
PBL	Control	3d	8.6
PBL	Control	3d	8.9
PBL	Control	3d	8.4
PBL	Control	3d	9.1
PBL	Treated	3d	7.9
PBL	Treated	3d	8.6
PBL	Treated	3d	6.5
PBL	Treated	3d	No reading
PBL	Control	5d	8.4
PBL	Control	5d	8.5
PBL	Control	5d	8.5
PBL	Control	5d	8.4
PBL	Treated	5d	7.6
PBL	Treated	5d	9
PBL	Treated	5d	8.7
PBL	Treated	5d	9.2

PBL single treatment RIN values

Samples were analysed by Glasgow Polyomics at the University of Glasgow using Agilent Bioanalyzer to generate RIN values. Refers to Figure 6.7, Figure 6.8

Tissue	Group	Time-point	RIN
Liver	Control	1d	7.9
Liver	Control	1d	7.9
Liver	Control	1d	7.4
Liver	Control	1d	7.6
Liver	Treated	1d	7.3
Liver	Treated	1d	7.7
Liver	Treated	1d	8
Liver	Treated	1d	7.3
Liver	Control	3d	8
Liver	Control	3d	7.6
Liver	Control	3d	8.1
Liver	Control	3d	7.6
Liver	Treated	3d	7.7
Liver	Treated	3d	7.9
Liver	Treated	3d	8
Liver	Treated	3d	7.5
Liver	Control	5d	8.1
Liver	Control	5d	7.6
Liver	Control	5d	7.8
Liver	Control	5d	8
Liver	Treated	5d	7.9
Liver	Treated	5d	8
Liver	Treated	5d	8.1
Liver	Treated	5d	7.9

Liver single treatment RIN values

Samples were analysed by Glasgow Polyomics at the University of Glasgow using Agilent Bioanalyzer to generate RIN values. Refers to Figure 6.9, Figure 6.10

Tissue	Group	Time-point	RIN
Lung	Control	1d	7
Lung	Control	1d	7
Lung	Control	1d	6.7
Lung	Control	1d	7.8
Lung	Treated	1d	7.4
Lung	Treated	1d	8
Lung	Treated	1d	7.2
Lung	Treated	1d	7.2
Lung	Control	3d	6.6
Lung	Control	3d	7.4
Lung	Control	3d	7.5
Lung	Control	3d	7.8
Lung	Treated	3d	7.8
Lung	Treated	3d	7.6
Lung	Treated	3d	8
Lung	Treated	3d	7.8
Lung	Control	5d	7.2
Lung	Control	5d	7.5
Lung	Control	5d	7.3
Lung	Control	5d	7.6
Lung	Treated	5d	7.8
Lung	Treated	5d	7.9
Lung	Treated	5d	8.1
Lung	Treated	5d	7.8

Lung single treatment RIN values

Samples were analysed by Glasgow Polyomics at the University of Glasgow using Agilent Bioanalyzer to generate RIN values. Refers to Figure 6.11, Figure 6.12

Tissue	Group	Timepoint	RIN
Spleen	Control	1d	7.6
Spleen	Control	1d	7.7
Spleen	Control	1d	8.1
Spleen	Control	1d	7.8
Spleen	Treated	1d	8.4
Spleen	Treated	1d	7.8
Spleen	Treated	1d	8.4
Spleen	Treated	1d	9.1
Spleen	Control	3d	8.3
Spleen	Control	3d	7.6
Spleen	Control	3d	8.1
Spleen	Control	3d	8
Spleen	Treated	3d	8.1
Spleen	Treated	3d	8.4
Spleen	Treated	3d	8
Spleen	Treated	3d	8.1
Spleen	Control	5d	7.9
Spleen	Control	5d	7.8
Spleen	Control	5d	7.8
Spleen	Control	5d	8
Spleen	Treated	5d	8.2
Spleen	Treated	5d	8.1
Spleen	Treated	5d	7.5
Spleen	Treated	5d	8.4

Spleen single treatment RIN values

Samples were analysed by Glasgow Polyomics at the University of Glasgow using Agilent Bioanalyzer to generate RIN values. Refers to Figure 6.13, Figure 6.14

Tissue	Group	Timepoint	RIN
Gut	Control	1d	7.5
Gut	Control	1d	8.5
Gut	Control	1d	6.1
Gut	Control	1d	8
Gut	Treated	1d	8.6
Gut	Treated	1d	8.8
Gut	Treated	1d	7.1
Gut	Treated	1d	5.2
Gut	Control	3d	7.7
Gut	Control	3d	8
Gut	Control	3d	7.2
Gut	Control	3d	7.4
Gut	Treated	3d	6.5
Gut	Treated	3d	7.2
Gut	Treated	3d	6.5
Gut	Treated	3d	8.6
Gut	Control	5d	6.9
Gut	Control	5d	7.4
Gut	Control	5d	5.6
Gut	Control	5d	7.4
Gut	Treated	5d	6.6
Gut	Treated	5d	8
Gut	Treated	5d	8.2
Gut	Treated	5d	8.3

Gut single treatment RIN values

Samples were analysed by Glasgow Polyomics at the University of Glasgow using Agilent Bioanalyzer to generate RIN values. Refers to Figure 6.15, Figure 6.16

List of References

1. Kassebaum NJ, Arora M, Barber RM, Bhutta ZA, Brown J, Carter A, et al. Global, regional, and national disability-adjusted life-years (DALYs) for 315 diseases and injuries and healthy life expectancy (HALE), 1990-2015: a systematic analysis for the Global Burden of Disease Study 2015. *The Lancet*. 2016;388(10053):1603-58.
2. Hasler G. PATHOPHYSIOLOGY OF DEPRESSION: DO WE HAVE ANY SOLID EVIDENCE. *World Psychiatry*. 2010;9(3):155-61.
3. Fava M. Diagnosis and definition of treatment-resistant depression. *Biological Psychiatry*. 2003;53(8):649-59.
4. Dantzer R. Cytokine, Sickness Behavior, and Depression. *Immunology and Allergy Clinics of North America*. 2009;29(2):247-+.
5. Dantzer R, O'Connor JC, Freund GG, Johnson RW, Kelley KW. From inflammation to sickness and depression: when the immune system subjugates the brain. *Nature Reviews Neuroscience*. 2008;9(1):46-57.
6. Eyre HA, Stuart MJ, Baune BT. A phase-specific neuroimmune model of clinical depression. *Progress in Neuro-Psychopharmacology & Biological Psychiatry*. 2014;54:265-74.
7. Maes M. Depression is an inflammatory disease, but cell-mediated immune activation is the key component of depression. *Progress in Neuro-Psychopharmacology and Biological Psychiatry*. 2011;35(3):664-75.
8. Miller AH, Raison CL. The role of inflammation in depression: from evolutionary imperative to modern treatment target. *Nature reviews Immunology*. 2016;16(1):22-34.
9. Dantzer R. Cytokine-induced sickness behaviour: a neuroimmune response to activation of innate immunity. *European Journal of Pharmacology*. 2004;500(1-3):399-411.
10. Dantzer R, Kelley KW. Twenty years of research on cytokine-induced sickness behavior. *Brain, Behavior, and Immunity*. 2007;21(2):153-60.
11. Raison CL, Capuron L, Miller AH. Cytokines sing the blues: inflammation and the pathogenesis of depression. *Trends in Immunology*. 2006;27(1):24-31.
12. Kubera M, Obuchowicz E, Goehler L, Brzeszcz J, Maes M. In animal models, psychosocial stress-induced (neuro)inflammation, apoptosis and reduced neurogenesis are associated to the onset of depression. *Prog Neuropsychopharmacol Biol Psychiatry*. 2011;35(3):744-59.
13. Zdilar D, Franco-Bronson K, Buchler N, Locala JA, Younossi ZM. Hepatitis C, interferon alfa, and depression. *Hepatology*. 2000;31(6):1207-11.
14. Udina M, Castellvi P, Moreno-Espana J, Navines R, Valdes M, Fornis X, et al. Interferon-induced depression in chronic hepatitis C: a systematic review and meta-analysis. *The Journal of clinical psychiatry*. 2012;73(8):1128-38.
15. Köhler CA, Freitas TH, Maes M, de Andrade NQ, Liu CS, Fernandes BS, et al. Peripheral cytokine and chemokine alterations in depression: a meta-analysis of 82 studies. *Acta Psychiatrica Scandinavica*. 2017:n/a-n/a.
16. Goldsmith DR, Rapaport MH, Miller BJ. A meta-analysis of blood cytokine network alterations in psychiatric patients: comparisons between schizophrenia, bipolar disorder and depression. *Mol Psychiatry*. 2016;21(12):1696-709.
17. Dowlati Y, Herrmann N, Swardfager W, Liu H, Sham L, Reim EK, et al. A meta-analysis of cytokines in major depression. *Biol Psychiatry*. 2010;67(5):446-57.

18. Kohler O, Sylvia LG, Bowden CL, Calabrese JR, Thase M, Shelton RC, et al. White blood cell count correlates with mood symptom severity and specific mood symptoms in bipolar disorder. *The Australian and New Zealand journal of psychiatry*. 2016.
19. Duivis HE, Kupper N, Penninx BW, Na B, de Jonge P, Whooley MA. Depressive symptoms and white blood cell count in coronary heart disease patients: prospective findings from the Heart and Soul Study. *Psychoneuroendocrinology*. 2013;38(4):479-87.
20. Brown SL, Salive ME, Guralnik JM, Wallace RB, Ostfeld AM, Blazer D. Depressive symptoms in the elderly: association with total white blood cell count. *Prog Neuropsychopharmacol Biol Psychiatry*. 1995;19(5):849-60.
21. Kappelmann N, Lewis G, Dantzer R, Jones PB, Khandaker GM. Antidepressant activity of anti-cytokine treatment: a systematic review and meta-analysis of clinical trials of chronic inflammatory conditions. *Mol Psychiatry*. 2016.
22. Kohler O, Benros ME, Nordentoft M, Farkouh ME, Iyengar RL, Mors O, et al. Effect of anti-inflammatory treatment on depression, depressive symptoms, and adverse effects: a systematic review and meta-analysis of randomized clinical trials. *JAMA Psychiatry*. 2014;71(12):1381-91.
23. Hannestad J, DellaGioia N, Bloch M. The Effect of Antidepressant Medication Treatment on Serum Levels of Inflammatory Cytokines: A Meta-Analysis. *Neuropsychopharmacology*. 2011;36(12):2452-9.
24. McColl A, Thomson CA, Nerurkar L, Graham GJ, Cavanagh J. TLR7-mediated skin inflammation remotely triggers chemokine expression and leukocyte accumulation in the brain. *Journal of Neuroinflammation*. 2016;13(1):1-16.
25. Thomson CA, McColl A, Cavanagh J, Graham GJ. Peripheral inflammation is associated with remote global gene expression changes in the brain. *Journal of Neuroinflammation*. 2014;11:16.
26. Kunkel EJ, Butcher EC. Chemokines and the Tissue-Specific Migration of Lymphocytes. *Immunity*. 2002;16(1):1-4.
27. Griffith JW, Sokol CL, Luster AD. Chemokines and Chemokine Receptors: Positioning Cells for Host Defense and Immunity. *Annual Review of Immunology*, Vol 32. 2014;32:659-702.
28. Tran PB, Miller RJ. Chemokine receptors: signposts to brain development and disease. *Nat Rev Neurosci*. 2003;4(6):444-55.
29. Zlotnik A, Yoshie O. The Chemokine Superfamily Revisited. *Immunity*. 2012;36(5):705-16.
30. Miller RJ, Rostene W, Apartis E, Banisadr G, Biber K, Milligan ED, et al. Chemokine Action in the Nervous System. *Journal of Neuroscience*. 2008;28(46):11792-5.
31. Li M, Ransohoff RA. Multiple roles of chemokine CXCL12 in the central nervous system: A migration from immunology to neurobiology. *Progress in Neurobiology*. 2008;84(2):116-31.
32. Rostene W, Kitabgi P, Parsadaniantz SM. Chemokines: a new class of neuromodulator? *Nat Rev Neurosci*. 2007;8(11):895-903.
33. Murphy K, Travers P, Walport M, Janeway C. *Janeway's immunobiology*. 8th ed. New York: Garland Science; 2012.
34. Ransohoff RM, Trettel F. Editorial Research Topic "Chemokines and chemokine receptors in brain homeostasis". *Frontiers in Cellular Neuroscience*. 2015;9(132).

35. Deverman BE, Patterson PH. Cytokines and CNS development. *Neuron*. 2009;64(1):61-78.
36. NIH. CBC blood test: MedlinePlus Medical Encyclopedia. 2017.
37. Shi F-D, Ljunggren H-G, Sarvetnick N. Innate immunity and autoimmunity: from self-protection to self-destruction. *Trends in Immunology*. 2001;22(2):97-101.
38. Doria A, Zen M, Bettio S, Gatto M, Bassi N, Nalotto L, et al. Autoinflammation and autoimmunity: Bridging the divide. *Autoimmunity Reviews*. 2012;12(1):22-30.
39. Parkin J, Cohen B. An overview of the immune system. *The Lancet*. 2001;357(9270):1777-89.
40. Serhan CN, Brain SD, Buckley CD, Gilroy DW, Haslett C, O'Neill LAJ, et al. Resolution of inflammation: state of the art, definitions and terms. *FASEB journal : official publication of the Federation of American Societies for Experimental Biology*. 2007;21(2):325-32.
41. Ortega-Gómez A, Perretti M, Soehnlein O. Resolution of inflammation: an integrated view. *EMBO Molecular Medicine*. 2013;5(5):661-74.
42. Takeuchi O, Akira S. Pattern Recognition Receptors and Inflammation. *Cell*.140(6):805-20.
43. Moynagh PN. TLR signalling and activation of IRFs: revisiting old friends from the NF- κ B pathway. *Trends in Immunology*. 2005;26(9):469-76.
44. O'Neill LAJ, Golenbock D, Bowie AG. The history of Toll-like receptors - redefining innate immunity. *Nature reviews Immunology*. 2013;13(6):453-60.
45. Toll-like Receptors (TLRs) Pathway | Cell Signaling Technology Danvers, MA: Cell Signaling Technology; 2017 [Available from: [https://www.cellsignal.com/contents/science-pathway-research-immunology-and-inflammation/toll-like-receptors-\(tlrs\)-pathway/pathways-tlr](https://www.cellsignal.com/contents/science-pathway-research-immunology-and-inflammation/toll-like-receptors-(tlrs)-pathway/pathways-tlr).
46. Honda K, Taniguchi T. IRFs: master regulators of signalling by Toll-like receptors and cytosolic pattern-recognition receptors. *Nature reviews Immunology*. 2006;6(9):644-58.
47. Dwinell MB, Luger N, Eckmann L, Kagnoff MF. Regulated production of interferon-inducible T-cell chemoattractants by human intestinal epithelial cells. *Gastroenterology*. 2001;120(1):49-59.
48. McNab F, Mayer-Barber K, Sher A, Wack A, O'Garra A. Type I interferons in infectious disease. *Nature reviews Immunology*. 2015;15(2):87-103.
49. Lawrence T. The Nuclear Factor NF- κ B Pathway in Inflammation. *Cold Spring Harbor Perspectives in Biology*. 2009;1(6):a001651.
50. Bauernfeind F, Horvath G, Stutz A, Alnemri ES, MacDonald K, Speert D, et al. NF- κ B activating pattern recognition and cytokine receptors license NLRP3 inflammasome activation by regulating NLRP3 expression. *Journal of immunology (Baltimore, Md : 1950)*. 2009;183(2):787-91.
51. Guo H, Callaway JB, Ting JPY. Inflammasomes: mechanism of action, role in disease, and therapeutics. *Nat Med*. 2015;21(7):677-87.
52. Latz E, Xiao TS, Stutz A. Activation and regulation of the inflammasomes. *Nature reviews Immunology*. 2013;13(6):397-411.
53. Etzioni A. Adhesion Molecules-Their Role in Health and Disease. *Pediatr Res*. 1996;39(2):191-8.
54. Bhagat K, Hingorani AD, Palacios M, Charles IG, Vallance P. Cytokine-induced venodilatation in humans in vivo: eNOS masquerading as iNOS. *Cardiovascular research*. 1999;41(3):754-64.

55. Sabroe I, Dower SK, Whyte MKB. The Role of Toll-Like Receptors in the Regulation of Neutrophil Migration, Activation, and Apoptosis. *Clinical Infectious Diseases*. 2005;41(Supplement_7):S421-S6.
56. Kolaczkowska E, Kubes P. Neutrophil recruitment and function in health and inflammation. *Nature reviews Immunology*. 2013;13(3):159-75.
57. Seth S, Oberdörfer L, Hyde R, Hoff K, Thies V, Worbs T, et al. CCR7 Essentially Contributes to the Homing of Plasmacytoid Dendritic Cells to Lymph Nodes under Steady-State As Well As Inflammatory Conditions. *The Journal of Immunology*. 2011;186(6):3364-72.
58. Weber M, Hauschild R, Schwarz J, Moussion C, de Vries I, Legler DF, et al. Interstitial Dendritic Cell Guidance by Haptotactic Chemokine Gradients. *Science*. 2013;339(6117):328-32.
59. Cerwenka A, Lanier LL. Natural killer cells, viruses and cancer. *Nature reviews Immunology*. 2001;1(1):41-9.
60. Jost S, Altfeld M. Control of human viral infections by natural killer cells. *Annu Rev Immunol*. 2013;31:163-94.
61. Hart OM, Athie-Morales V, O'Connor GM, Gardiner CM. TLR7/8-Mediated Activation of Human NK Cells Results in Accessory Cell-Dependent IFN- γ Production. *The Journal of Immunology*. 2005;175(3):1636-42.
62. Adib-Conquy M, Scott-Algara D, Cavaillon J-M, Souza-Fonseca-Guimaraes F. TLR-mediated activation of NK cells and their role in bacterial/viral immune responses in mammals. *Immunol Cell Biol*. 2014;92(3):256-62.
63. Sawaki J, Tsutsui H, Hayashi N, Yasuda K, Akira S, Tanizawa T, et al. Type 1 cytokine/chemokine production by mouse NK cells following activation of their TLR/MyD88-mediated pathways. *International Immunology*. 2007;19(3):311-20.
64. Netea MG, Latz E, Mills KHG, O'Neill LAJ. Innate immune memory: a paradigm shift in understanding host defense. *Nat Immunol*. 2015;16(7):675-9.
65. Koga-Yamakawa E, Murata M, Dovedi SJ, Wilkinson RW, Ota Y, Umehara H, et al. TLR7 tolerance is independent of the type I IFN pathway and leads to loss of anti-tumor efficacy in mice. *Cancer immunology, immunotherapy : CII*. 2015;64(10):1229-39.
66. Dobrovolskaia MA, Medvedev AE, Thomas KE, Cuesta N, Toshchakov V, Ren T, et al. Induction of In Vitro Reprogramming by Toll-Like Receptor (TLR)2 and TLR4 Agonists in Murine Macrophages: Effects of TLR "Homotolerance" Versus "Heterotolerance" on NF- κ B Signaling Pathway Components. *The Journal of Immunology*. 2003;170(1):508-19.
67. Nair-Gupta P, Baccarini A, Tung N, Seyffer F, Florey O, Huang Y, et al. TLR signals induce phagosomal MHC-I delivery from the endosomal recycling compartment to allow cross-presentation. *Cell*. 2014;158(3):506-21.
68. Takeda K, Akira S. Toll-like receptors in innate immunity. *International Immunology*. 2005;17(1):1-14.
69. Boeglin E, Smulski CR, Brun S, Milosevic S, Schneider P, Fournel S. Toll-Like Receptor Agonists Synergize with CD40L to Induce Either Proliferation or Plasma Cell Differentiation of Mouse B Cells. *PLOS ONE*. 2011;6(10):e25542.
70. Chang J, Kunkel SL, Chang C-H. Negative regulation of MyD88-dependent signaling by IL-10 in dendritic cells. *Proceedings of the National Academy of Sciences*. 2009;106(43):18327-32.
71. Couper KN, Blount DG, Riley EM. IL-10: The master regulator of immunity to infection. *Journal of Immunology*. 2008;180(9):5771-7.
72. Serhan CN, Chiang N, Van Dyke TE. Resolving inflammation: dual anti-inflammatory and pro-resolution lipid mediators. *Nature reviews Immunology*. 2008;8(5):349-61.

73. deCathelineau AM, Henson PM. The final step in programmed cell death: phagocytes carry apoptotic cells to the grave. *Essays In Biochemistry*. 2003;39:105-17.
74. Dyer DP, Pallas K, Ruiz LM, Schuette F, Wilson GJ, Graham GJ. CXCR2 deficient mice display macrophage-dependent exaggerated acute inflammatory responses. *Scientific Reports*. 2017;7:42681.
75. Bystrom J, Evans I, Newson J, Stables M, Toor I, van Rooijen N, et al. Resolution-phase macrophages possess a unique inflammatory phenotype that is controlled by cAMP. *Blood*. 2008;112(10):4117-27.
76. Jamieson T, Cook DN, Nibbs RJB, Rot A, Nixon C, McLean P, et al. The chemokine receptor D6 limits the inflammatory response in vivo. *Nat Immunol*. 2005;6(4):403-11.
77. Nibbs RJB, Graham GJ. Immune regulation by atypical chemokine receptors. *Nature reviews Immunology*. 2013;13(11):815-29.
78. Heppner FL, Ransohoff RM, Becher B. Immune attack: the role of inflammation in Alzheimer disease. *Nat Rev Neurosci*. 2015;16(6):358-72.
79. Heneka MT, Carson MJ, Khoury JE, Landreth GE, Brosseron F, Feinstein DL, et al. Neuroinflammation in Alzheimer's disease. *The Lancet Neurology*. 2015;14(4):388-405.
80. Hay J, Johnson VE, Smith DH, Stewart W. Chronic Traumatic Encephalopathy: The Neuropathological Legacy of Traumatic Brain Injury. *Annual review of pathology*. 2016;11:21-45.
81. Qin LY, Wu XF, Block ML, Liu YX, Bresse GR, Hong JS, et al. Systemic LPS causes chronic neuroinflammation and progressive neurodegeneration. *Glia*. 2007;55(5):453-62.
82. Honda K, Yanai H, Negishi H, Asagiri M, Sato M, Mizutani T, et al. IRF-7 is the master regulator of type-I interferon-dependent immune responses. *Nature*. 2005;434(7034):772-7.
83. Theofilopoulos AN, Baccala R, Beutler B, Kono DH. Type I interferons (alpha/beta) in immunity and autoimmunity. *Annu Rev Immunol*. 2005;23:307-36.
84. Samarajiva SA, Forster S, Auchetl K, Hertzog PJ. INTERFEROME: the database of interferon regulated genes. *Nucleic Acids Research*. 2009;37(suppl_1):D852-D7.
85. de Veer MJ, Holko M, Frevel M, Walker E, Der S, Paranjape JM, et al. Functional classification of interferon-stimulated genes identified using microarrays. *J Leukoc Biol*. 2001;69(6):912-20.
86. Sheikh F, Dickensheets H, Gamero AM, Vogel SN, Donnelly RP. An essential role for IFN- β in the induction of IFN-stimulated gene expression by LPS in macrophages. *Journal of Leukocyte Biology*. 2014;96(4):591-600.
87. Gorski KS, Waller EL, Bjornton-Severson J, Hanten JA, Riter CL, Kieper WC, et al. Distinct indirect pathways govern human NK-cell activation by TLR-7 and TLR-8 agonists. *International Immunology*. 2006;18(7):1115-26.
88. Hu X, Chakravarty SD, Ivashkiv LB. Regulation of IFN and TLR Signaling During Macrophage Activation by Opposing Feedforward and Feedback Inhibition Mechanisms. *Immunological reviews*. 2008;226:41-56.
89. Schroder K, Hertzog PJ, Ravasi T, Hume DA. Interferon- γ : an overview of signals, mechanisms and functions. *Journal of Leukocyte Biology*. 2004;75(2):163-89.
90. Hunter CA, Jones SA. IL-6 as a keystone cytokine in health and disease. *Nat Immunol*. 2015;16(5):448-57.

91. Kalliolias GD, Ivashkiv LB. TNF biology, pathogenic mechanisms and emerging therapeutic strategies. *Nat Rev Rheumatol*. 2016;12(1):49-62.
92. Higuchi M, Aggarwal BB. TNF induces internalization of the p60 receptor and shedding of the p80 receptor. *The Journal of Immunology*. 1994;152(7):3550-8.
93. Ilyin SE, Plata-Salamán CR. In Vivo Regulation of the IL-1 β System (Ligand, Receptors I and II, Receptor Accessory Protein, and Receptor Antagonist) and TNF- α mRNAs in Specific Brain Regions. *Biochemical and Biophysical Research Communications*. 1996;227(3):861-7.
94. Benveniste EN, Tang LP, Law RM. Differential regulation of astrocyte TNF- α expression by the cytokines TGF- β , IL-6 and IL-10. *International journal of developmental neuroscience : the official journal of the International Society for Developmental Neuroscience*. 1995;13(3-4):341-9.
95. Saraiva M, O'Garra A. The regulation of IL-10 production by immune cells. *Nature reviews Immunology*. 2010;10(3):170-81.
96. Iyer SS, Cheng G. Role of Interleukin 10 Transcriptional Regulation in Inflammation and Autoimmune Disease. *Critical reviews in immunology*. 2012;32(1):23-63.
97. Mehrad B, Keane MP, Strieter RM. Chemokines as mediators of angiogenesis. *Thrombosis and Haemostasis*. 2007;97(5):755-62.
98. Dimberg A. Chemokines in angiogenesis. *Current topics in microbiology and immunology*. 2010;341:59-80.
99. Callewaere C, Banisadr G, Rostene W, Melik-Parsadaniantz S. Chemokines and chemokine receptors in the brain: implication in neuroendocrine regulation. *Journal of Molecular Endocrinology*. 2007;38(3-4):355-63.
100. Rostene W, Guyon A, Kular L, Godefroy D, Barbieri F, Bajetto A, et al. Chemokines and chemokine receptors: New actors in neuroendocrine regulations. *Frontiers in Neuroendocrinology*. 2011;32(1):10-24.
101. Melik-Parsadaniantz S, Rostene W. Chemokines and neuromodulation. *Journal of Neuroimmunology*. 2008;198(1-2):62-8.
102. Cazareth J, Guyon A, Heurteaux C, Chabry J, Petit-Paitel A. Molecular and cellular neuroinflammatory status of mouse brain after systemic lipopolysaccharide challenge: importance of CCR2/CCL2 signaling. *Journal of Neuroinflammation*. 2014;11:132-.
103. Blank T, Detje Claudia N, Spieß A, Hagemeyer N, Brendecke Stefanie M, Wolfart J, et al. Brain Endothelial- and Epithelial-Specific Interferon Receptor Chain 1 Drives Virus-Induced Sickness Behavior and Cognitive Impairment. *Immunity*. 2016;44(4):901-12.
104. Li M, Ransohoff RM. Multiple roles of chemokine CXCL12 in the central nervous system: a migration from immunology to neurobiology. *Prog Neurobiol*. 2008;84(2):116-31.
105. Williams JL, Holman DW, Klein RS. Chemokines in the balance: maintenance of homeostasis and protection at CNS barriers. *Frontiers in Cellular Neuroscience*. 2014;8.
106. Kakinuma T, Hwang ST. Chemokines, chemokine receptors, and cancer metastasis. *J Leukoc Biol*. 2006;79(4):639-51.
107. Sarvaiya PJ, Guo D, Ulasov I, Gabikian P, Lesniak MS. Chemokines in tumor progression and metastasis. *Oncotarget*. 2013;4(12):2171-85.
108. Cardona AE, Pioro EP, Sasse ME, Kostenko V, Cardona SM, Dijkstra IM, et al. Control of microglial neurotoxicity by the fractalkine receptor. *Nat Neurosci*. 2006;9(7):917-24.

109. Matloubian M, David A, Engel S, Ryan JE, Cyster JG. A transmembrane CXC chemokine is a ligand for HIV-coreceptor Bonzo. *Nature Immunology*. 2000;1(4):298-304.
110. Bazan JF, Bacon KB, Hardiman G, Wang W, Soo K, Rossi D, et al. A new class of membrane-bound chemokine with a CX3C motif. *Nature*. 1997;385(6617):640-4.
111. Haessler U, Pisano M, Wu M, Swartz MA. Dendritic cell chemotaxis in 3D under defined chemokine gradients reveals differential response to ligands CCL21 and CCL19. *Proc Natl Acad Sci U S A*. 2011;108(14):5614-9.
112. Forster R, Davalos-Miszlitz AC, Rot A. CCR7 and its ligands: balancing immunity and tolerance. *Nature reviews Immunology*. 2008;8(5):362-71.
113. Fantuzzi L, Canini I, Belardelli F, Gessani S. IFN-beta stimulates the production of beta-chemokines in human peripheral blood monocytes. Importance of macrophage differentiation. *European cytokine network*. 2001;12(4):597-603.
114. Luster AD, Unkeless JC, Ravetch JV. Gamma-interferon transcriptionally regulates an early-response gene containing homology to platelet proteins. *Nature*. 1985;315(6021):672-6.
115. Kim JM, Lee JY, Yoon YM, Oh YK, Youn J, Kim YJ. NF- κ B Activation Pathway is Essential for the Chemokine Expression in Intestinal Epithelial Cells Stimulated with *Clostridium difficile* Toxin A. *Scandinavian Journal of Immunology*. 2006;63(6):453-60.
116. Wong CK, Wang CB, Ip WK, Tian YP, Lam CWK. Role of p38 MAPK and NF- κ B for chemokine release in coculture of human eosinophils and bronchial epithelial cells. *Clinical and Experimental Immunology*. 2005;139(1):90-100.
117. del Pozo MA, Sánchez-Mateos P, Sánchez-Madrid F. Cellular polarization induced by chemokines: a mechanism for leukocyte recruitment? *Immunology Today*. 1996;17(3):127-31.
118. Kijima T, Maulik G, Ma PC, Tibaldi EV, Turner RE, Rollins B, et al. Regulation of Cellular Proliferation, Cytoskeletal Function, and Signal Transduction through CXCR4 and c-Kit in Small Cell Lung Cancer Cells. *Cancer Research*. 2002;62(21):6304-11.
119. Serrador JM, Nieto M, Sánchez-Madrid F. Cytoskeletal rearrangement during migration and activation of T lymphocytes. *Trends in Cell Biology*. 1999;9(6):228-33.
120. Balkwill F. Cancer and the chemokine network. *Nat Rev Cancer*. 2004;4(7):540-50.
121. Lim K, Hyun YM, Lambert-Emo K, Capece T, Bae S, Miller R, et al. Neutrophil trails guide influenza-specific CD8(+) T cells in the airways. *Science*. 2015;349(6252):aaa4352.
122. Groom JR, Luster AD. CXCR3 in T cell function. *Experimental cell research*. 2011;317(5):620-31.
123. Schall TJ, Bacon K, Toy KJ, Goeddel DV. Selective attraction of monocytes and T lymphocytes of the memory phenotype by cytokine RANTES. *Nature*. 1990;347(6294):669-71.
124. Serbina NV, Pamer EG. Monocyte emigration from bone marrow during bacterial infection requires signals mediated by chemokine receptor CCR2. *Nat Immunol*. 2006;7(3):311-7.
125. Shi C, Pamer EG. Monocyte recruitment during infection and inflammation. *Nature reviews Immunology*. 2011;11(11):762-74.

126. Sugiyama T, Kohara H, Noda M, Nagasawa T. Maintenance of the hematopoietic stem cell pool by CXCL12-CXCR4 chemokine signaling in bone marrow stromal cell niches. *Immunity*. 2006;25(6):977-88.
127. Liu Q, Li Z, Gao J-L, Wan W, Ganesan S, McDermott DH, et al. The CXCR4 antagonist AMD3100 redistributes leukocytes from primary immune organs to secondary immune organs, lung and blood in mice. *European journal of immunology*. 2015;45(6):1855-67.
128. Eash KJ, Means JM, White DW, Link DC. CXCR4 is a key regulator of neutrophil release from the bone marrow under basal and stress granulopoiesis conditions. *Blood*. 2009;113(19):4711-9.
129. Furze RC, Rankin SM. Neutrophil mobilization and clearance in the bone marrow. *Immunology*. 2008;125(3):281-8.
130. Ma Q, Jones D, Borghesani PR, Segal RA, Nagasawa T, Kishimoto T, et al. Impaired B-lymphopoiesis, myelopoiesis, and derailed cerebellar neuron migration in CXCR4- and SDF-1-deficient mice. *Proc Natl Acad Sci U S A*. 1998;95(16):9448-53.
131. Zou YR, Kottmann AH, Kuroda M, Taniuchi I, Littman DR. Function of the chemokine receptor CXCR4 in haematopoiesis and in cerebellar development. *Nature*. 1998;393(6685):595-9.
132. Jang MH, Sougawa N, Tanaka T, Hirata T, Hiroi T, Tohya K, et al. CCR7 is critically important for migration of dendritic cells in intestinal lamina propria to mesenteric lymph nodes. *Journal of immunology (Baltimore, Md : 1950)*. 2006;176(2):803-10.
133. Soler D, Humphreys TL, Spinola SM, Campbell JJ. CCR4 versus CCR10 in human cutaneous TH lymphocyte trafficking. *Blood*. 2003;101(5):1677-82.
134. Homey B, Alenius H, Muller A, Soto H, Bowman EP, Yuan W, et al. CCL27-CCR10 interactions regulate T cell-mediated skin inflammation. *Nat Med*. 2002;8(2):157-65.
135. Svensson M, Marsal J, Ericsson A, Carramolino L, Brodén T, Márquez G, et al. CCL25 mediates the localization of recently activated CD8 α β ⁺ lymphocytes to the small-intestinal mucosa. *The Journal of Clinical Investigation*. 2002;110(8):1113-21.
136. Kunkel EJ, Campbell JJ, Haraldsen G, Pan J, Boisvert J, Roberts AI, et al. Lymphocyte Cc Chemokine Receptor 9 and Epithelial Thymus-Expressed Chemokine (Teck) Expression Distinguish the Small Intestinal Immune Compartment. Epithelial Expression of Tissue-Specific Chemokines as an Organizing Principle in Regional Immunity. 2000;192(5):761-8.
137. Klein M, Brouwer MC, Angele B, Geldhoff M, Marquez G, Varona R, et al. Leukocyte Attraction by CCL20 and Its Receptor CCR6 in Humans and Mice with Pneumococcal Meningitis. *PLOS ONE*. 2014;9(4):e93057.
138. Reboldi A, Coisne C, Baumjohann D, Benvenuto F, Bottinelli D, Lira S, et al. C-C chemokine receptor 6-regulated entry of TH-17 cells into the CNS through the choroid plexus is required for the initiation of EAE. *Nat Immunol*. 2009;10(5):514-23.
139. Coursey TG, Gandhi NB, Volpe EA, Pflugfelder SC, de Paiva CS. Chemokine Receptors CCR6 and CXCR3 Are Necessary for CD4⁺ T Cell Mediated Ocular Surface Disease in Experimental Dry Eye Disease. *PLOS ONE*. 2013;8(11):e78508.
140. Durrant DM, Williams JL, Daniels BP, Klein RS. Chemokines Referee Inflammation within the Central Nervous System during Infection and Disease. *Advances in Medicine*. 2014;2014:10.
141. Waring P, Mullbacher A. Cell death induced by the Fas/Fas ligand pathway and its role in pathology. *Immunol Cell Biol*. 1999;77(4):312-7.

142. Bouillet P, O'Reilly LA. CD95, BIM and T cell homeostasis. *Nature reviews Immunology*. 2009;9(7):514-9.
143. Re F, Strominger JL. Toll-like Receptor 2 (TLR2) and TLR4 Differentially Activate Human Dendritic Cells. *Journal of Biological Chemistry*. 2001;276(40):37692-9.
144. Netea MG, Van der Meer JWM, Suttmuller RP, Adema GJ, Kullberg B-J. From the Th1/Th2 Paradigm towards a Toll-Like Receptor/T-Helper Bias. *Antimicrobial Agents and Chemotherapy*. 2005;49(10):3991-6.
145. Zanoni I, Foti M, Ricciardi-Castagnoli P, Granucci F. TLR-Dependent Activation Stimuli Associated with Th1 Responses Confer NK Cell Stimulatory Capacity to Mouse Dendritic Cells. *The Journal of Immunology*. 2005;175(1):286-92.
146. Vyas JM, Van der Veen AG, Ploegh HL. The known unknowns of antigen processing and presentation. *Nature reviews Immunology*. 2008;8(8):607-18.
147. Watts C. Capture and processing of exogenous antigens for presentation on MHC molecules. *Annu Rev Immunol*. 1997;15:821-50.
148. Flannagan RS, Cosio G, Grinstein S. Antimicrobial mechanisms of phagocytes and bacterial evasion strategies. *Nat Rev Micro*. 2009;7(5):355-66.
149. Shepherd VL. The role of the respiratory burst of phagocytes in host defense. *Seminars in respiratory infections*. 1986;1(2):99-106.
150. Voskoboinik I, Whisstock JC, Trapani JA. Perforin and granzymes: function, dysfunction and human pathology. *Nature reviews Immunology*. 2015;15(6):388-400.
151. Leffell MS, Spitznagel JK. Intracellular and Extracellular Degranulation of Human Polymorphonuclear Azurophil and Specific Granules Induced by Immune Complexes. *Infection and Immunity*. 1974;10(6):1241-9.
152. Brinker T, Stopa E, Morrison J, Klinge P. A new look at cerebrospinal fluid circulation. *Fluids and Barriers of the CNS*. 2014;11:10-.
153. Kandel E. *Principles of Neural Science, Fifth Edition*: McGraw-Hill Education; 2013.
154. Xie L, Kang H, Xu Q, Chen MJ, Liao Y, Thiyagarajan M, et al. Sleep Drives Metabolite Clearance from the Adult Brain. *Science (New York, NY)*. 2013;342(6156):10.1126/science.1241224.
155. Iliff JJ, Wang M, Liao Y, Plogg BA, Peng W, Gundersen GA, et al. A Paravascular Pathway Facilitates CSF Flow Through the Brain Parenchyma and the Clearance of Interstitial Solutes, Including Amyloid β . *Science translational medicine*. 2012;4(147):147ra11-ra11.
156. *Neurocytology: Cells of the CNS. Neuroanatomy for the Neuroscientist*. Boston, MA: Springer US; 2008. p. 23-54.
157. Stevens A, Lowe JS. *Human Histology*: Elsevier/Mosby; 2005.
158. Abbott NJ, Ronnback L, Hansson E. Astrocyte-endothelial interactions at the blood-brain barrier. *Nat Rev Neurosci*. 2006;7(1):41-53.
159. Prinz M, Priller J. The role of peripheral immune cells in the CNS in steady state and disease. *Nat Neurosci*. 2017;20(2):136-44.
160. Obermeier B, Daneman R, Ransohoff RM. Development, maintenance and disruption of the blood-brain barrier. *Nat Med*. 2013;19(12):1584-96.
161. Farina C, Aloisi F, Meinl E. Astrocytes are active players in cerebral innate immunity. *Trends Immunol*. 2007;28(3):138-45.
162. Dong Y, Benveniste EN. Immune function of astrocytes. *Glia*. 2001;36(2):180-90.

163. Ginhoux F, Greter M, Leboeuf M, Nandi S, See P, Gokhan S, et al. Fate Mapping Analysis Reveals That Adult Microglia Derive from Primitive Macrophages. *Science*. 2010;330(6005):841-5.
164. Saijo K, Glass CK. Microglial cell origin and phenotypes in health and disease. *Nature reviews Immunology*. 2011;11(11):775-87.
165. Nakagawa Y, Chiba K. Diversity and plasticity of microglial cells in psychiatric and neurological disorders. *Pharmacology & Therapeutics*. 2015;154:21-35.
166. Ransohoff RM. A polarizing question: do M1 and M2 microglia exist? *Nat Neurosci*. 2016;19(8):987-91.
167. Perry VH, Cunningham C, Holmes C. Systemic infections and inflammation affect chronic neurodegeneration. *Nature reviews Immunology*. 2007;7(2):161-7.
168. Lee SC, Liu W, Dickson DW, Brosnan CF, Berman JW. Cytokine production by human fetal microglia and astrocytes. Differential induction by lipopolysaccharide and IL-1 beta. *Journal of immunology (Baltimore, Md : 1950)*. 1993;150(7):2659-67.
169. Wang H, Liu C, Han M, Cheng C, Zhang D. TRAM1 Promotes Microglia M1 Polarization. *Journal of Molecular Neuroscience*. 2016;58(2):287-96.
170. Olson JK, Miller SD. Microglia Initiate Central Nervous System Innate and Adaptive Immune Responses through Multiple TLRs. *The Journal of Immunology*. 2004;173(6):3916-24.
171. Kloss CUA, Bohatschek M, Kreutzberg GW, Raivich G. Effect of Lipopolysaccharide on the Morphology and Integrin Immunoreactivity of Ramified Microglia in the Mouse Brain and in Cell Culture. *Experimental neurology*. 2001;168(1):32-46.
172. Kreutzberg GW. Microglia: a sensor for pathological events in the CNS. *Trends in Neurosciences*. 1996;19(8):312-8.
173. Stevens B, Allen NJ, Vazquez LE, Howell GR, Christopherson KS, Nouri N, et al. The classical complement cascade mediates CNS synapse elimination. *Cell*. 2007;131(6):1164-78.
174. Schafer DP, Lehrman EK, Kautzman AG, Koyama R, Mardinly AR, Yamasaki R, et al. Microglia sculpt postnatal neural circuits in an activity and complement-dependent manner. *Neuron*. 2012;74(4):691-705.
175. Araque A, Parpura V, Sanzgiri RP, Haydon PG. Tripartite synapses: glia, the unacknowledged partner. *Trends Neurosci*. 1999;22(5):208-15.
176. Rothstein JD, Dykes-Hoberg M, Pardo CA, Bristol LA, Jin L, Kuncl RW, et al. Knockout of glutamate transporters reveals a major role for astroglial transport in excitotoxicity and clearance of glutamate. *Neuron*. 1996;16(3):675-86.
177. Flynn G, Maru S, Loughlin J, Romero IA, Male D. Regulation of chemokine receptor expression in human microglia and astrocytes. *J Neuroimmunol*. 2003;136(1-2):84-93.
178. Prinz M, Schmidt H, Mildner A, Knobeloch K-P, Hanisch U-K, Raasch J, et al. Distinct and Nonredundant In Vivo Functions of IFNAR on Myeloid Cells Limit Autoimmunity in the Central Nervous System. *Immunity*. 2005;22(5):675-86.
179. Carpentier PA, Begolka WS, Olson JK, Elhofy A, Karpus WJ, Miller SD. Differential activation of astrocytes by innate and adaptive immune stimuli. *Glia*. 2005;49(3):360-74.
180. Tada M, Diserens AC, Desbaillets I, de Tribolet N. Analysis of cytokine receptor messenger RNA expression in human glioblastoma cells and normal astrocytes by reverse-transcription polymerase chain reaction. *Journal of neurosurgery*. 1994;80(6):1063-73.

181. Hasegawa-Ishii S, Inaba M, Umegaki H, Unno K, Wakabayashi K, Shimada A. Endotoxemia-induced cytokine-mediated responses of hippocampal astrocytes transmitted by cells of the brain-immune interface. *Scientific Reports*. 2016;6:25457.
182. Choi SS, Lee HJ, Lim I, Satoh J-i, Kim SU. Human Astrocytes: Secretome Profiles of Cytokines and Chemokines. *PLOS ONE*. 2014;9(4):e92325.
183. Brahmachari S, Fung YK, Pahan K. Induction of Glial Fibrillary Acidic Protein Expression in Astrocytes by Nitric Oxide. *The Journal of neuroscience : the official journal of the Society for Neuroscience*. 2006;26(18):4930-9.
184. Jang E, Kim J-H, Lee S, Kim J-H, Seo J-W, Jin M, et al. Phenotypic Polarization of Activated Astrocytes: The Critical Role of Lipocalin-2 in the Classical Inflammatory Activation of Astrocytes. *The Journal of Immunology*. 2013;191(10):5204-19.
185. Imayoshi I, Sakamoto M, Ohtsuka T, Takao K, Miyakawa T, Yamaguchi M, et al. Roles of continuous neurogenesis in the structural and functional integrity of the adult forebrain. *Nat Neurosci*. 2008;11(10):1153-61.
186. Nunes MC, Roy NS, Keyoung HM, Goodman RR, McKhann G, 2nd, Jiang L, et al. Identification and isolation of multipotential neural progenitor cells from the subcortical white matter of the adult human brain. *Nat Med*. 2003;9(4):439-47.
187. Kukekov VG, Laywell ED, Suslov O, Davies K, Scheffler B, Thomas LB, et al. Multipotent stem/progenitor cells with similar properties arise from two neurogenic regions of adult human brain. *Experimental neurology*. 1999;156(2):333-44.
188. Schmaal L, Veltman DJ, van Erp TGM, Samann PG, Frodl T, Jahanshad N, et al. Subcortical brain alterations in major depressive disorder: findings from the ENIGMA Major Depressive Disorder working group. *Mol Psychiatry*. 2016;21(6):806-12.
189. Campbell S, Marriott M, Nahmias C, MacQueen GM. Lower hippocampal volume in patients suffering from depression: a meta-analysis. *Am J Psychiatry*. 2004;161(4):598-607.
190. Videbech P, Ravnkilde B. Hippocampal volume and depression: a meta-analysis of MRI studies. *Am J Psychiatry*. 2004;161(11):1957-66.
191. Malberg JE, Eisch AJ, Nestler EJ, Duman RS. Chronic Antidepressant Treatment Increases Neurogenesis in Adult Rat Hippocampus. *The Journal of Neuroscience*. 2000;20(24):9104-10.
192. Marcussen AB, Flagstad P, Kristjansen PE, Johansen FF, Englund U. Increase in neurogenesis and behavioural benefit after chronic fluoxetine treatment in Wistar rats. *Acta Neurol Scand*. 2008;117(2):94-100.
193. Anacker C, Zunszain PA, Cattaneo A, Carvalho LA, Garabedian MJ, Thuret S, et al. Antidepressants increase human hippocampal neurogenesis by activating the glucocorticoid receptor. *Molecular Psychiatry*. 2011;16(7):738-50.
194. Klein RS, Rubin JB, Gibson HD, DeHaan EN, Alvarez-Hernandez X, Segal RA, et al. SDF-1 alpha induces chemotaxis and enhances Sonic hedgehog-induced proliferation of cerebellar granule cells. *Development (Cambridge, England)*. 2001;128(11):1971-81.
195. Imitola J, Raddassi K, Park KI, Mueller FJ, Nieto M, Teng YD, et al. Directed migration of neural stem cells to sites of CNS injury by the stromal cell-derived factor 1alpha/CXC chemokine receptor 4 pathway. *Proc Natl Acad Sci U S A*. 2004;101(52):18117-22.

196. Thacker MA, Clark AK, Bishop T, Grist J, Yip PK, Moon LDF, et al. CCL2 is a key mediator of microglia activation in neuropathic pain states. *European Journal of Pain*. 2009;13(3):263-72.
197. Van Steenwinckel J, Auvynet C, Sapienza A, Reaux-Le Goazigo A, Combadière C, Melik Parsadaniantz S. Stromal cell-derived CCL2 drives neuropathic pain states through myeloid cell infiltration in injured nerve. *Brain, Behavior, and Immunity*. 2015;45:198-210.
198. Carson MJ, Doose JM, Melchior B, Schmid CD, Ploix CC. CNS immune privilege: hiding in plain sight. *Immunological reviews*. 2006;213:48-65.
199. Engelhardt B, Vajkoczy P, Weller RO. The movers and shapers in immune privilege of the CNS. *Nat Immunol*. 2017;18(2):123-31.
200. Louveau A, Harris TH, Kipnis J. Revisiting the concept of CNS immune privilege. *Trends in immunology*. 2015;36(10):569-77.
201. Engelhardt B, Sorokin L. The blood-brain and the blood-cerebrospinal fluid barriers: function and dysfunction. *Seminars in Immunopathology*. 2009;31(4):497-511.
202. Medawar PB. Immunity to homologous grafted skin; the fate of skin homografts transplanted to the brain, to subcutaneous tissue, and to the anterior chamber of the eye. *British journal of experimental pathology*. 1948;29(1):58-69.
203. Matyszak MK, Perry VH. Bacillus Calmette-Guérin sequestered in the brain parenchyma escapes immune recognition. *Journal of Neuroimmunology*. 1998;82(1):73-80.
204. Brabb T, Goldrath AW, von Dassow P, Paez A, Liggitt HD, Goverman J. Triggers of autoimmune disease in a murine TCR-transgenic model for multiple sclerosis. *Journal of immunology (Baltimore, Md : 1950)*. 1997;159(1):497-507.
205. Derecki NC, Cardani AN, Yang CH, Quinnes KM, Carihfield A, Lynch KR, et al. Regulation of learning and memory by meningeal immunity: a key role for IL-4. *The Journal of experimental medicine*. 2010;207(5):1067-80.
206. Ransohoff RM, Engelhardt B. The anatomical and cellular basis of immune surveillance in the central nervous system. *Nature reviews Immunology*. 2012;12(9):623-35.
207. Louveau A, Smirnov I, Keyes TJ, Eccles JD, Rouhani SJ, Peske JD, et al. Structural and functional features of central nervous system lymphatic vessels. *Nature*. 2015;523(7560):337-41.
208. Korn T, Kallies A. T cell responses in the central nervous system. *Nature reviews Immunology*. 2017;17(3):179-94.
209. Kumar M, Belcaid M, Nerurkar VR. Identification of host genes leading to West Nile virus encephalitis in mice brain using RNA-seq analysis. *Scientific Reports*. 2016;6:26350.
210. Dvorak F, Martinez-Torres F, Sellner J, Haas J, Schellinger PD, Schwaninger M, et al. Experimental herpes simplex virus encephalitis: a long-term study of interleukin-6 expression in mouse brain tissue. *Neuroscience Letters*. 2004;367(3):289-92.
211. Roos KL, Tunkel AR. *Bacterial Infections of the Central Nervous System*: Elsevier Science; 2010.
212. Kielian T, Hickey WF. Proinflammatory Cytokine, Chemokine, and Cellular Adhesion Molecule Expression during the Acute Phase of Experimental Brain Abscess Development. *The American Journal of Pathology*. 2000;157(2):647-58.
213. Pajek D. Identifying chemokine receptors as plausible therapeutic targets in viral encephalitis [PhD]: University of Glasgow; 2013.

214. Klein RS, Lin E, Zhang B, Luster AD, Tollett J, Samuel MA, et al. Neuronal CXCL10 directs CD8⁺ T-cell recruitment and control of West Nile virus encephalitis. *J Virol.* 2005;79(17):11457-66.
215. Zhang B, Chan YK, Lu B, Diamond MS, Klein RS. CXCR3 Mediates Region-Specific Antiviral T Cell Trafficking within the Central Nervous System during West Nile Virus Encephalitis. *The Journal of Immunology.* 2008;180(4):2641-9.
216. Glass WG, Lim JK, Cholera R, Pletnev AG, Gao JL, Murphy PM. Chemokine receptor CCR5 promotes leukocyte trafficking to the brain and survival in West Nile virus infection. *The Journal of experimental medicine.* 2005;202(8):1087-98.
217. Bréhin A-C, Mouriès J, Frenkiel M-P, Dadaglio G, Desprès P, Lafon M, et al. Dynamics of Immune Cell Recruitment during West Nile Encephalitis and Identification of a New CD19⁺B220⁻BST-2⁺ Leukocyte Population. *The Journal of Immunology.* 2008;180(10):6760-7.
218. van Marle G, Antony J, Ostermann H, Dunham C, Hunt T, Halliday W, et al. West Nile Virus-Induced Neuroinflammation: Glial Infection and Capsid Protein-Mediated Neurovirulence. *Journal of Virology.* 2007;81(20):10933-49.
219. Lim SM, Koraka P, van Boheemen S, Roose JM, Jaarsma D, van de Vijver DAMC, et al. Characterization of the Mouse Neuroinvasiveness of Selected European Strains of West Nile Virus. *PLOS ONE.* 2013;8(9):e74575.
220. Phares TW, Stohlman SA, Hinton DR, Bergmann CC. Astrocyte-Derived CXCL10 Drives Accumulation of Antibody-Secreting Cells in the Central Nervous System during Viral Encephalomyelitis. *Journal of Virology.* 2013;87(6):3382-92.
221. Glass WG, McDermott DH, Lim JK, Lekhong S, Yu SF, Frank WA, et al. CCR5 deficiency increases risk of symptomatic West Nile virus infection. *The Journal of experimental medicine.* 2006;203(1):35-40.
222. Bardina SV, Michlmayr D, Hoffman KW, Obara CJ, Sum J, Charo IF, et al. Differential Roles of Chemokines CCL2 and CCL7 in Monocytosis and Leukocyte Migration during West Nile Virus Infection. *The Journal of Immunology.* 2015;195(9):4306-18.
223. Dufour JH, Dziejman M, Liu MT, Leung JH, Lane TE, Luster AD. IFN- γ -Inducible Protein 10 (IP-10; CXCL10)-Deficient Mice Reveal a Role for IP-10 in Effector T Cell Generation and Trafficking. *The Journal of Immunology.* 2002;168(7):3195-204.
224. McCandless EE, Wang Q, Woerner BM, Harper JM, Klein RS. CXCL12 limits inflammation by localizing mononuclear infiltrates to the perivascular space during experimental autoimmune encephalomyelitis. *Journal of immunology (Baltimore, Md : 1950).* 2006;177(11):8053-64.
225. Leow-Dyke S, Allen C, Denes A, Nilsson O, Maysami S, Bowie AG, et al. Neuronal toll-like receptor 4 signaling induces brain endothelial activation and neutrophil transmigration in vitro. *Journal of Neuroinflammation.* 2012;9(1):230.
226. Cai Z, Pang Y, Lin S, Rhodes PG. Differential roles of tumor necrosis factor-alpha and interleukin-1 beta in lipopolysaccharide-induced brain injury in the neonatal rat. *Brain Res.* 2003;975(1-2):37-47.
227. Lawson MA, Parrott JM, McCusker RH, Dantzer R, Kelley KW, O'Connor JC. Intracerebroventricular administration of lipopolysaccharide induces indoleamine-2,3-dioxygenase-dependent depression-like behaviors. *Journal of Neuroinflammation.* 2013;10:87-.
228. Rankine EL, Hughes PM, Botham MS, Perry VH, Felton LM. Brain cytokine synthesis induced by an intraparenchymal injection of LPS is reduced in MCP-1-deficient mice prior to leucocyte recruitment. *European Journal of Neuroscience.* 2006;24(1):77-86.

229. Huang Y, Henry CJ, Dantzer R, Johnson RW, Godbout JP. Exaggerated sickness behavior and brain proinflammatory cytokine expression in aged mice in response to intracerebroventricular lipopolysaccharide. *Neurobiology of aging*. 2008;29(11):1744-53.
230. Wang P, You S-W, Yang Y-J, Wei X-Y, Wang Y-Z, Wang X, et al. Systemic Injection of Low-Dose Lipopolysaccharide Fails to Break down the Blood-Brain Barrier or Activate the TLR4-MyD88 Pathway in Neonatal Rat Brain. *International Journal of Molecular Sciences*. 2014;15(6):10101-15.
231. Lund S, Christensen KV, Hedtjörn M, Mortensen AL, Hagberg H, Falsig J, et al. The dynamics of the LPS triggered inflammatory response of murine microglia under different culture and in vivo conditions. *Journal of Neuroimmunology*. 2006;180(1-2):71-87.
232. Lo U, Selvaraj V, Plane JM, Chechneva OV, Otsu K, Deng W. p38 α (MAPK14) critically regulates the immunological response and the production of specific cytokines and chemokines in astrocytes. *Scientific Reports*. 2014;4:7405.
233. McKimmie CS, Graham GJ. Astrocytes modulate the chemokine network in a pathogen-specific manner. *Biochemical and Biophysical Research Communications*. 2010;394(4):1006-11.
234. Van Neerven S, Regen T, Wolf D, Nemes A, Johann S, Beyer C, et al. Inflammatory chemokine release of astrocytes in vitro is reduced by all-trans retinoic acid. *Journal of Neurochemistry*. 2010;114(5):1511-26.
235. Butchi NB, Pourciau S, Du M, Morgan TW, Peterson KE. Analysis of the neuroinflammatory response to TLR7 stimulation in the brain: comparison of multiple TLR7 and/or TLR8 agonists. *Journal of immunology (Baltimore, Md : 1950)*. 2008;180(11):7604-12.
236. Butchi NB, Woods T, Du M, Morgan TW, Peterson KE. TLR7 and TLR9 Trigger Distinct Neuroinflammatory Responses in the CNS. *American Journal of Pathology*. 2011;179(2):783-94.
237. Butchi NB, Du M, Peterson KE. Interactions between TLR7 and TLR9 agonists and receptors regulate innate immune responses by astrocytes and microglia. *Glia*. 2010;58(6):650-64.
238. Lehmann SM, Kruger C, Park B, Derkow K, Rosenberger K, Baumgart J, et al. An unconventional role for miRNA: let-7 activates Toll-like receptor 7 and causes neurodegeneration. *Nat Neurosci*. 2012;15(6):827-35.
239. Layé S, Parnet P, Goujon E, Dantzer R. Peripheral administration of lipopolysaccharide induces the expression of cytokine transcripts in the brain and pituitary of mice. *Molecular Brain Research*. 1994;27(1):157-62.
240. Noh H, Jeon J, Seo H. Systemic injection of LPS induces region-specific neuroinflammation and mitochondrial dysfunction in normal mouse brain. *Neurochemistry international*. 2014;69:35-40.
241. Skelly DT, Hennessy E, Dansereau MA, Cunningham C. A Systematic Analysis of the Peripheral and CNS Effects of Systemic LPS, IL-1B, TNF-alpha and IL-6 Challenges in C57BL/6 Mice. *Plos One*. 2013;8(7).
242. Erickson MA, Banks WA. Cytokine and chemokine responses in serum and brain after single and repeated injections of lipopolysaccharide: Multiplex quantification with path analysis. *Brain Behavior and Immunity*. 2011;25(8):1637-48.
243. Bian YQ, Zhao XJ, Li MH, Zeng SH, Zhao BH. Various roles of astrocytes during recovery from repeated exposure to different doses of lipopolysaccharide. *Behavioural Brain Research*. 2013;253:253-61.
244. Banks WA, Robinson SM. Minimal penetration of lipopolysaccharide across the murine blood-brain barrier. *Brain Behavior and Immunity*. 2010;24(1):102-9.

245. Fil D, Borysiewicz E, Konat GW. A broad upregulation of cerebral chemokine genes by peripherally-generated inflammatory mediators. *Metabolic Brain Disease*. 2011;26(1):49-59.
246. Konat GW, Borysiewicz E, Fil D, James I. Peripheral Challenge With Double-Stranded RNA Elicits Global Up-Regulation of Cytokine Gene Expression in the Brain. *Journal of Neuroscience Research*. 2009;87(6):1381-8.
247. Michalovicz LT, Konat GW. Peripherally restricted acute phase response to a viral mimic alters hippocampal gene expression. *Metabolic Brain Disease*. 2014;29(1):75-86.
248. Thibeault I, Laflamme N, Rivest S. Regulation of the gene encoding MCP-1 in the mouse and rat brain in response to circulating LPS and proinflammatory cytokines. *Society for Neuroscience Abstracts*. 2001;27(2):2240-.
249. Semmler A, Okulla T, Sastre M, Dumitrescu-Ozimek L, Heneka MT. Systemic inflammation induces apoptosis with variable vulnerability of different brain regions. *Journal of Chemical Neuroanatomy*. 2005;30(2-3):144-57.
250. Hannestad J, Gallezot J-D, Schafbauer T, Lim K, Kloczynski T, Morris ED, et al. Endotoxin-induced systemic inflammation activates microglia: [¹¹C]PBR28 positron emission tomography in nonhuman primates. *Neuroimage*. 2012;63(1):232-9.
251. He H, Geng T, Chen P, Wang M, Hu J, Kang L, et al. NK cells promote neutrophil recruitment in the brain during sepsis-induced neuroinflammation. *Scientific Reports*. 2016;6:27711.
252. Schiltz JC, Sawchenko PE. Distinct brain vascular cell types manifest inducible cyclooxygenase expression as a function of the strength and nature of immune insults. *J Neurosci*. 2002;22(13):5606-18.
253. Pan W, Stone KP, Hsueh H, Manda VK, Zhang Y, Kastin AJ. Cytokine Signaling Modulates Blood-Brain Barrier Function. *Current pharmaceutical design*. 2011;17(33):3729-40.
254. Banks WA, Kastin AJ, Broadwell RD. Passage of cytokines across the blood-brain barrier. *Neuroimmunomodulation*. 1995;2(4):241-8.
255. Banks WA, Moinuddin A, Morley JE. Regional transport of TNF-alpha across the blood-brain barrier in young ICR and young and aged SAMP8 mice. *Neurobiology of aging*. 2001;22(4):671-6.
256. Banks WA. Blood-brain barrier transport of cytokines: a mechanism for neuropathology. *Curr Pharm Des*. 2005;11(8):973-84.
257. Quan N, Whiteside M, Herkenham M. Time course and localization patterns of interleukin-1beta messenger RNA expression in brain and pituitary after peripheral administration of lipopolysaccharide. *Neuroscience*. 1998;83(1):281-93.
258. Buller KM. Circumventricular Organs: Gateways to the Brain Role Of Circumventricular Organs In Pro-Inflammatory Cytokine-Induced Activation Of The Hypothalamic- Pituitary-Adrenal Axis. *Clinical and Experimental Pharmacology and Physiology*. 2001;28(7):581-9.
259. Bohatschek M, Werner A, Raivich G. Systemic LPS Injection Leads to Granulocyte Influx into Normal and Injured Brain: Effects of ICAM-1 Deficiency. *Experimental neurology*. 2001;172(1):137-52.
260. Verma S, Nakaoke R, Dohgu S, Banks WA. Release of cytokines by brain endothelial cells: A polarized response to lipopolysaccharide. *Brain, Behavior, and Immunity*. 2006;20(5):449-55.
261. Chui R, Dorovini-Zis K. Regulation of CCL2 and CCL3 expression in human brain endothelial cells by cytokines and lipopolysaccharide. *Journal of Neuroinflammation*. 2010;7(1):1.

262. Pugin J, Schürer-Maly CC, Leturcq D, Moriarty A, Ulevitch RJ, Tobias PS. Lipopolysaccharide activation of human endothelial and epithelial cells is mediated by lipopolysaccharide-binding protein and soluble CD14. *Proceedings of the National Academy of Sciences of the United States of America*. 1993;90(7):2744-8.
263. Li S, Wang Y, Matsumura K, Ballou LR, Morham SG, Blatteis CM. The febrile response to lipopolysaccharide is blocked in cyclooxygenase-2^{-/-}, but not in cyclooxygenase-1^{-/-} mice. *Brain Research*. 1999;825(1-2):86-94.
264. Vitkovic L, Konsman JP, Bockaert J, Dantzer R, Homburger V, Jacque C. Cytokine signals propagate through the brain. *Mol Psychiatry*. 2000;5(6):604-15.
265. Morita S, Furube E, Mannari T, Okuda H, Tatsumi K, Wanaka A, et al. Heterogeneous vascular permeability and alternative diffusion barrier in sensory circumventricular organs of adult mouse brain. *Cell and Tissue Research*. 2016;363(2):497-511.
266. Morita S, Miyata S. Different vascular permeability between the sensory and secretory circumventricular organs of adult mouse brain. *Cell and Tissue Research*. 2012;349(2):589-603.
267. Willis CL, Garwood CJ, Ray DE. A size selective vascular barrier in the rat area postrema formed by perivascular macrophages and the extracellular matrix. *Neuroscience*. 2007;150(2):498-509.
268. Willis WD, Westlund KN. Neuroanatomy of the pain system and of the pathways that modulate pain. *Journal of clinical neurophysiology : official publication of the American Electroencephalographic Society*. 1997;14(1):2-31.
269. Rosas-Ballina M, Tracey KJ. The Neurology of the Immune System: Neural Reflexes Regulate Immunity. *Neuron*. 64(1):28-32.
270. Tracey KJ. The inflammatory reflex. *Nature*. 2002;420(6917):853-9.
271. Andersson U, Tracey KJ. Neural reflexes in inflammation and immunity. *Journal of Experimental Medicine*. 2012;209(6):1057-68.
272. Tracey KJ. Reflex control of immunity. *Nature Reviews Immunology*. 2009;9(6):418-28.
273. Meneses G, Bautista M, Florentino A, Díaz G, Acero G, Besedovsky H, et al. Electric stimulation of the vagus nerve reduced mouse neuroinflammation induced by lipopolysaccharide. *Journal of Inflammation*. 2016;13(1):33.
274. Bratton BO, Martelli D, McKinley MJ, Trevaks D, Anderson CR, McAllen RM. Neural regulation of inflammation: no neural connection from the vagus to splenic sympathetic neurons. *Experimental Physiology*. 2012;97(11):1180-5.
275. Romanovsky AA. The inflammatory reflex: the current model should be revised. *Experimental Physiology*. 2012;97(11):1178-9.
276. Hinojosa AE, Caso JR, García-Bueno B, Leza JC, Madrigal JLM. Dual effects of noradrenaline on astroglial production of chemokines and pro-inflammatory mediators. *Journal of Neuroinflammation*. 2013;10(1):852.
277. Scanzano A, Cosentino M. Adrenergic regulation of innate immunity: a review. *Frontiers in Pharmacology*. 2015;6:171.
278. Pongratz G, Straub RH. The sympathetic nervous response in inflammation. *Arthritis Research & Therapy*. 2014;16:504.
279. Gold MS, Gebhart GF. Nociceptor sensitization in pain pathogenesis. *Nat Med*. 2010;16(11):1248-57.
280. Ji R-R, Xu Z-Z, Gao Y-J. Emerging targets in neuroinflammation-driven chronic pain. *Nat Rev Drug Discov*. 2014;13(7):533-48.
281. Biber K, Boddeke E. Neuronal CC chemokines: the distinct roles of CCL21 and CCL2 in neuropathic pain. *Frontiers in Cellular Neuroscience*. 2014;8:210.

282. Clark AK, Old EA, Malcangio M. Neuropathic pain and cytokines: current perspectives. *Journal of Pain Research*. 2013;6:803-14.
283. Saperstein A, Brand H, Audhya T, Nabriski D, Hutchinson B, Rosenzweig S, et al. Interleukin 1 beta mediates stress-induced immunosuppression via corticotropin-releasing factor. *Endocrinology*. 1992;130(1):152-8.
284. Berkenbosch F, van Oers J, del Rey A, Tilders F, Besedovsky H. Corticotropin-releasing factor-producing neurons in the rat activated by interleukin-1. *Science*. 1987;238(4826):524-6.
285. van der Fits L, Mourits S, Voerman JSA, Kant M, Boon L, Laman JD, et al. Imiquimod-Induced Psoriasis-Like Skin Inflammation in Mice Is Mediated via the IL-23/IL-17 Axis. *The Journal of Immunology*. 2009;182(9):5836-45.
286. Wang Y, Abel K, Lantz K, Krieg AM, McChesney MB, Miller CJ. The Toll-Like Receptor 7 (TLR7) Agonist, Imiquimod, and the TLR9 Agonist, CpG ODN, Induce Antiviral Cytokines and Chemokines but Do Not Prevent Vaginal Transmission of Simian Immunodeficiency Virus When Applied Intravaginally to Rhesus Macaques. *Journal of Virology*. 2005;79(22):14355-70.
287. Walter A, Schäfer M, Cecconi V, Matter C, Urosevic-Maiwald M, Belloni B, et al. Aldara activates TLR7-independent immune defence. *Nature Communications*. 2013;4:1560.
288. Grine L, Steeland S, Van Ryckeghem S, Ballegeer M, Lienenklaus S, Weiss S, et al. Topical imiquimod yields systemic effects due to unintended oral uptake. *Scientific Reports*. 2016;6:20134.
289. Constantinescu CS, Farooqi N, O'Brien K, Gran B. Experimental autoimmune encephalomyelitis (EAE) as a model for multiple sclerosis (MS). *British Journal of Pharmacology*. 2011;164(4):1079-106.
290. Baxter AG. The origin and application of experimental autoimmune encephalomyelitis. *Nature reviews Immunology*. 2007;7(11):904-12.
291. Biesmans S, Meert TF, Bouwknecht JA, Acton PD, Davoodi N, De Haes P, et al. Systemic Immune Activation Leads to Neuroinflammation and Sickness Behavior in Mice. *Mediators of Inflammation*. 2013:14.
292. Painsipp E, Köfer MJ, Sinner F, Holzer P. Prolonged Depression-Like Behavior Caused by Immune Challenge: Influence of Mouse Strain and Social Environment. *PLoS ONE*. 2011;6(6):e20719.
293. Konsman JP, Parnet P, Dantzer R. Cytokine-induced sickness behaviour: mechanisms and implications. *Trends in Neurosciences*. 2002;25(3):154-9.
294. O'Connor JC, Lawson MA, Andre C, Moreau M, Lestage J, Castanon N, et al. Lipopolysaccharide-induced depressive-like behavior is mediated by indoleamine 2,3-dioxygenase activation in mice. *Mol Psychiatry*. 2008;14(5):511-22.
295. Goshen I, Kreisel T, Ben-Menachem-Zidon O, Licht T, Weidenfeld J, Ben-Hur T, et al. Brain interleukin-1 mediates chronic stress-induced depression in mice via adrenocortical activation and hippocampal neurogenesis suppression. *Mol Psychiatry*. 2007;13(7):717-28.
296. Hayes PE, Ettigi P. Dexamethasone suppression test in diagnosis of depressive illness. *Clinical pharmacy*. 1983;2(6):538-45.
297. Delgado PL. Depression: The case for a monoamine deficiency. *Journal of Clinical Psychiatry*. 2000;61:7-11.
298. Hirschfeld RMA. History and evolution of the monoamine hypothesis of depression. *Journal of Clinical Psychiatry*. 2000;61:4-6.
299. Caraci F, Copani A, Nicoletti F, Drago F. Depression and Alzheimer's disease: neurobiological links and common pharmacological targets. *Eur J Pharmacol*. 2010;626(1):64-71.

300. Eyre HA, Air T, Pradhan A, Johnston J, Lavretsky H, Stuart MJ, et al. A meta-analysis of chemokines in major depression. *Prog Neuropsychopharmacol Biol Psychiatry*. 2016;68:1-8.
301. Haapakoski R, Mathieu J, Ebmeier KP, Alenius H, Kivimaki M. Cumulative meta-analysis of interleukins 6 and 1beta, tumour necrosis factor alpha and C-reactive protein in patients with major depressive disorder. *Brain Behav Immun*. 2015;49:206-15.
302. Howren MB, Lamkin DM, Suls J. Associations of depression with C-reactive protein, IL-1, and IL-6: a meta-analysis. *Psychosom Med*. 2009;71(2):171-86.
303. Valkanova V, Ebmeier KP, Allan CL. CRP, IL-6 and depression: a systematic review and meta-analysis of longitudinal studies. *J Affect Disord*. 2013;150(3):736-44.
304. Capuron L, Ravaud A, Dantzer R. Early depressive symptoms in cancer patients receiving interleukin 2 and/or interferon alfa-2b therapy. *Journal of clinical oncology : official journal of the American Society of Clinical Oncology*. 2000;18(10):2143-51.
305. Denicoff KD, Rubinow DR, Papa MZ, Simpson C, Seipp CA, Lotze MT, et al. The neuropsychiatric effects of treatment with interleukin-2 and lymphokine-activated killer cells. *Annals of internal medicine*. 1987;107(3):293-300.
306. Mesquita AR, Correia-Neves M, Roque S, Castro AG, Vieira P, Pedrosa J, et al. IL-10 modulates depressive-like behavior. *J Psychiatr Res*. 2008;43(2):89-97.
307. Munzer A, Sack U, Mergl R, Schonherr J, Petersein C, Bartsch S, et al. Impact of antidepressants on cytokine production of depressed patients in vitro. *Toxins*. 2013;5(11):2227-40.
308. Yirmiya R, Rimmerman N, Reshef R. Depression as a Microglial Disease. *Trends in Neurosciences*. 38(10):637-58.
309. Miller AH. Depression and immunity: a role for T cells? *Brain Behav Immun*. 2010;24(1):1-8.
310. Major Depressive Disorder Working Group of the Psychiatric GC. A mega-analysis of genome-wide association studies for major depressive disorder. *Mol Psychiatry*. 2013;18(4):497-511.
311. Power RA, Tansey KE, Buttenschøn HN, Cohen-Woods S, Bigdeli T, Hall LS, et al. Genome-wide Association for Major Depression Through Age at Onset Stratification: Major Depressive Disorder Working Group of the Psychiatric Genomics Consortium. *Biological Psychiatry*. 2017;81(4):325-35.
312. Masaki M, Ikeda A, Shiraki E, Oka S, Kawasaki T. Mixed lineage kinase LZK and antioxidant protein-1 activate NF-kappaB synergistically. *European journal of biochemistry*. 2003;270(1):76-83.
313. consortium C. Sparse whole-genome sequencing identifies two loci for major depressive disorder. *Nature*. 2015;523(7562):588-91.
314. Kauppinen A, Suuronen T, Ojala J, Kaarniranta K, Salminen A. Antagonistic crosstalk between NF-kappaB and SIRT1 in the regulation of inflammation and metabolic disorders. *Cellular signalling*. 2013;25(10):1939-48.
315. Yeung F, Hoberg JE, Ramsey CS, Keller MD, Jones DR, Frye RA, et al. Modulation of NF-kB-dependent transcription and cell survival by the SIRT1 deacetylase. *The EMBO Journal*. 2004;23(12):2369-80.
316. Ware EB, Mukherjee B, Sun YV, Diez-Roux AV, Kardia SLR, Smith JA. Comparative genome-wide association studies of a depressive symptom phenotype in a repeated measures setting by race/ethnicity in the multi-ethnic study of atherosclerosis. *BMC Genetics*. 2015;16(1):118.

317. Hyde CL, Nagle MW, Tian C, Chen X, Paciga SA, Wendland JR, et al. Identification of 15 genetic loci associated with risk of major depression in individuals of European descent. *Nat Genet.* 2016;48(9):1031-6.
318. Krishnadas R, Nicol A, Sassarini J, Puri N, Burden AD, Leman J, et al. Circulating tumour necrosis factor is highly correlated with brainstem serotonin transporter availability in humans. *Brain Behav Immun.* 2016;51:29-38.
319. Mora F, Segovia G, del Arco A, de Blas M, Garrido P. Stress, neurotransmitters, corticosterone and body-brain integration. *Brain Research.* 2012;1476:71-85.
320. Ulrich-Lai YM, Herman JP. Neural regulation of endocrine and autonomic stress responses. *Nat Rev Neurosci.* 2009;10(6):397-409.
321. Kullmann JS, Grigoleit JS, Lichte P, Kobbe P, Rosenberger C, Banner C, et al. Neural response to emotional stimuli during experimental human endotoxemia. *Human brain mapping.* 2013;34(9):2217-27.
322. van den Boogaard M, Ramakers BP, van Alfen N, van der Werf SP, Fick WF, Hoedemaekers CW, et al. Endotoxemia-induced inflammation and the effect on the human brain. *Critical Care.* 2010;14(3):R81-R.
323. Grigoleit J-S, Kullmann JS, Wolf OT, Hammes F, Wegner A, Jablonowski S, et al. Dose-Dependent Effects of Endotoxin on Neurobehavioral Functions in Humans. *PLOS ONE.* 2011;6(12):e28330.
324. Eisenberger NI, Inagaki TK, Rameson LT, Mashal NM, Irwin MR. An fMRI study of cytokine-induced depressed mood and social pain: The role of sex differences. *Neuroimage.* 2009;47(3):881-90.
325. Kullmann JS, Grigoleit J-S, Lichte P, Kobbe P, Rosenberger C, Banner C, et al. Neural response to emotional stimuli during experimental human endotoxemia. *Human brain mapping.* 2013;34(9):2217-27.
326. Mitchell M. Engauge Digitizer Version 7.2. Torrance, California: GNU General Public License Version 2; 2014.
327. Wan X, Wang W, Liu J, Tong T. Estimating the sample mean and standard deviation from the sample size, median, range and/or interquartile range. *BMC Medical Research Methodology.* 2014;14(1):135.
328. Higgins JP, Green S. *Cochrane Handbook for Systematic Reviews of Interventions.* Version 5.1.0 ed. Oxford: The Cochrane Collaboration; 2011.
329. Wells G, Shea B, O'Connell D, Peterson J, Welch V, Losos M, et al. The Newcastle-Ottawa Scale (NOS) for assessing the quality of nonrandomised studies in meta-analyses.
330. Review Manager. Version 5.3. Copenhagen: The Nordic Cochrane Centre: The Cochrane Collaboration; 2014.
331. R version 3.2.3. Vienna, Austria: The R Foundation for Statistical Computing; 2015.
332. Viechtbauer W. Conducting Meta-Analyses in R with the metafor Package. 2010. 2010;36(3):48.
333. Untergasser A, Cutcutache I, Koressaar T, Ye J, Faircloth BC, Remm M, et al. Primer3—new capabilities and interfaces. *Nucleic acids research.* 2012;40(15):e115-e.
334. Koressaar T, Remm M. Enhancements and modifications of primer design program Primer3. *Bioinformatics (Oxford, England).* 2007;23(10):1289-91.
335. Ye J, Coulouris G, Zaretskaya I, Cutcutache I, Rozen S, Madden TL. Primer-BLAST: A tool to design target-specific primers for polymerase chain reaction. *BMC Bioinformatics.* 2012;13(1):134.
336. Kibbe WA. OligoCalc: an online oligonucleotide properties calculator. *Nucleic Acids Res.* 2007;35(Web Server issue):W43-6.

337. Rostene W, Guyon A, Kular L, Godefroy D, Barbieri F, Bajetto A, et al. Chemokines and chemokine receptors: new actors in neuroendocrine regulations. *Front Neuroendocrinol.* 2011;32(1):10-24.
338. Nomenclature IWSoc. Chemokine/chemokine receptor nomenclature. *Cytokine.* 2003;21(1):48-9.
339. Bai Y-M, Chiou W-F, Su T-P, Li C-T, Chen M-H. Pro-inflammatory cytokine associated with somatic and pain symptoms in depression. *Journal of Affective Disorders.* 2014;155:28-34.
340. Bai Y-M, Su T-P, Li C-T, Tsai S-J, Chen M-H, Tu P-C, et al. Comparison of pro-inflammatory cytokines among patients with bipolar disorder and unipolar depression and normal controls. *Bipolar Disorders.* 2015;17(3):269-77.
341. Bazzichi L, Rossi A, Massimetti G, Giannaccini G, Giuliano T, De Feo F, et al. Cytokine patterns in fibromyalgia and their correlation with clinical manifestations. *Clinical and experimental rheumatology.* 2007;25(2):225-30.
342. Blasko I, Lederer W, Oberbauer H, Walch T, Kemmler G, Hinterhuber H, et al. Measurement of Thirteen Biological Markers in CSF of Patients with Alzheimer's Disease and Other Dementias. *Dementia and Geriatric Cognitive Disorders.* 2006;21(1):9-15.
343. Byrne ML, O'Brien-Simpson NM, Reynolds EC, Walsh KA, Laughton K, Waloszek JM, et al. Acute phase protein and cytokine levels in serum and saliva: A comparison of detectable levels and correlations in a depressed and healthy adolescent sample. *Brain, Behavior, and Immunity.* 2013;34:164-75.
344. Cizza G, Marques AH, Eskandari F, Christie IC, Torvik S, Silverman MN, et al. Elevated Neuroimmune Biomarkers in Sweat Patches and Plasma of Premenopausal Women with Major Depressive Disorder in Remission: The POWER Study. *Biological Psychiatry.* 2008;64(10):907-11.
345. Corwin EJ, Pajer K, Paul S, Lowe N, Weber M, McCarthy DO. Bidirectional psychoneuroimmune interactions in the early postpartum period influence risk of postpartum depression. *Brain, Behavior, and Immunity.* 2015;49:86-93.
346. Dahl J, Ormstad H, Aass HCD, Malt UF, Bendz LT, Sandvik L, et al. The plasma levels of various cytokines are increased during ongoing depression and are reduced to normal levels after recovery. *Psychoneuroendocrinology.* 2014;45:77-86.
347. Daniele A, Divella R, Abbate I, Giotta F, Trerotoli P, Mautino A, et al. Coexistence of an imbalance of cytokines, chemokines and growth factors serum levels and symptoms of fatigue and pain in long-term breast cancer survivors. *Journal of Clinical Oncology Conference.* 2015;33.
348. Dantoft TM, Elberling J, Brix S, Szecsi PB, Vesterhauge S, Skovbjerg S. An elevated pro-inflammatory cytokine profile in multiple chemical sensitivity. *Psychoneuroendocrinology.* 2014;40:140-50.
349. Dekker RL, Moser DK, Tovar EG, Chung ML, Heo S, Wu JR, et al. Depressive symptoms and inflammatory biomarkers in patients with heart failure. *European journal of cardiovascular nursing : journal of the Working Group on Cardiovascular Nursing of the European Society of Cardiology.* 2014;13(5):444-50.
350. Dong T, Zhao X, Yang Z, editors. Concept and approach of human signal-molecular-profiling database: A pilot study on depression using Lab-on-chips. 2013 35th Annual International Conference of the IEEE Engineering in Medicine and Biology Society (EMBC); 2013 3-7 July 2013.
351. Einvik G, Vistnes M, Hrubos-Strøm H, Randby A, Namtvedt SK, Nordhus IH, et al. Circulating cytokine concentrations are not associated with major

- depressive disorder in a community-based cohort. *General Hospital Psychiatry*. 2012;34(3):262-7.
352. Eller T, Vasar V, Shlik J, Maron E. Pro-inflammatory cytokines and treatment response to escitalopram in major depressive disorder. *Progress in Neuro-Psychopharmacology and Biological Psychiatry*. 2008;32(2):445-50.
353. Fontenelle LF, Barbosa IG, Luna JV, de Sousa LP, Abreu MNS, Teixeira AL. A cytokine study of adult patients with obsessive-compulsive disorder. *Comprehensive Psychiatry*. 2012;53(6):797-804.
354. García-Lozano J-R, Capilla-Sevilla C, García-López O, Moreno-Gallego I. Correlation Between Cytokines and Anxious-Depressive Symptoms in Patients With Fibromyalgia. *Reumatología Clínica*. 2008;4(4):136-9.
355. Gehi A, Musselman D, Otte C, Bruce Royster E, Ali S, Whooley MA. Depression and platelet activation in outpatients with stable coronary heart disease: Findings from the Heart and Soul Study. *Psychiatry Research*. 2010;175(3):200-4.
356. Grassi-Oliveira R, Brieztke E, Teixeira A, Pezzi JC, Zanini M, Lopes RP, et al. Peripheral chemokine levels in women with recurrent major depression with suicidal ideation. *Revista brasileira de psiquiatria (Sao Paulo, Brazil : 1999)*. 2012;34(1):71-5.
357. Gur A, Karakoc M, Nas K, Remzi, Cevik, Denli A, et al. Cytokines and depression in cases with fibromyalgia. *The Journal of rheumatology*. 2002;29(2):358-61.
358. Halaris A, Myint A-M, Savant V, Meresh E, Lim E, Guillemin G, et al. Does escitalopram reduce neurotoxicity in major depression? *Journal of Psychiatric Research*. 2015;66-67:118-26.
359. Hallberg L, Janelidze S, Engstrom G, Wisén AGM, Westrin Å, Brundin L. Exercise-induced release of cytokines in patients with major depressive disorder. *Journal of Affective Disorders*. 2010;126(1-2):262-7.
360. Ho P-S, Yeh Y-W, Huang S-Y, Liang C-S. A shift toward T helper 2 responses and an increase in modulators of innate immunity in depressed patients treated with escitalopram. *Psychoneuroendocrinology*. 2015;53:246-55.
361. Hocaoglu C, Kural B, Aliyazicioglu R, Deger O, Cengiz S. IL-1B, IL-6, IL-8, IL-10, IFN- γ , TNF- α and its relationship with lipid parameters in patients with major depression. *Metabolic Brain Disease*. 2012;27(4):425-30.
362. Hüfner K, Kandler C, Koudouovoh-Tripp P, Egeter J, Hochstrasser T, Stemer B, et al. Bioprofiling of platelets in medicated patients with depression. *Journal of Affective Disorders*. 2015;172:81-8.
363. Janelidze S, Suchankova P, Ekman A, Erhardt S, Sellgren C, Samuelsson M, et al. Low IL-8 is associated with anxiety in suicidal patients: genetic variation and decreased protein levels. *Acta Psychiatrica Scandinavica*. 2015;131(4):269-78.
364. Janelidze S, Ventorp F, Erhardt S, Hansson O, Minthon L, Flax J, et al. Altered chemokine levels in the cerebrospinal fluid and plasma of suicide attempters. *Psychoneuroendocrinology*. 2013;38(6):853-62.
365. Jonsdottir IH, Hägg DA, Glise K, Ekman R. Monocyte Chemotactic Protein-1 (MCP-1) and Growth Factors Called into Question as Markers of Prolonged Psychosocial Stress. *PLOS ONE*. 2009;4(11):e7659.
366. Juengst SB, Kumar RG, Failla MD, Goyal A, Wagner AK. Acute inflammatory biomarker profiles predict depression risk following moderate to severe traumatic brain injury. *The Journal of head trauma rehabilitation*. 2015;30(3):207-18.

367. Kahl KG, Bens S, Ziegler K, Rudolf S, Kordon A, Dibbelt L, et al. Angiogenic factors in patients with current major depressive disorder comorbid with borderline personality disorder. *Psychoneuroendocrinology*. 2009;34(3):353-7.
368. Karege F, Bondolfi G, Gervasoni N, Schwald M, Aubry J-M, Bertschy G. Low Brain-Derived Neurotrophic Factor (BDNF) levels in serum of depressed patients probably results from lowered platelet BDNF release unrelated to platelet reactivity. *Biological Psychiatry*. 2005;57(9):1068-72.
369. Kelly JR. Gut microbiome alterations in major depressive disorder: relevance to pathophysiology. *European Neuropsychopharmacology*. 2015;25, Supplement 2:S456.
370. Kern S, Skoog I, Börjesson-Hanson A, Blennow K, Zetterberg H, Östling S, et al. Higher CSF interleukin-6 and CSF interleukin-8 in current depression in older women. Results from a population-based sample. *Brain, Behavior, and Immunity*. 2014;41:55-8.
371. Kudoh A, Katagai H, Takazawa T. Plasma Inflammatory Cytokine Response To Surgical Trauma In Chronic Depressed Patients. *Cytokine*. 2001;13(2):104-8.
372. Laake J-PS, Stahl D, Amiel SA, Petrak F, Sherwood RA, Pickup JC, et al. The Association Between Depressive Symptoms and Systemic Inflammation in People With Type 2 Diabetes: Findings From the South London Diabetes Study. *Diabetes Care*. 2014;37(8):2186.
373. Laghrissi-Thode F, Wagner WR, Pollock BG, Johnson PC, Finkel MS. Elevated platelet factor 4 and B-thromboglobulin plasma levels in depressed patients with ischemic heart disease. *Biological Psychiatry*. 1997;42(4):290-5.
374. Lebedeva. N BOL, Ardashova. N. Role of inflammatory and sympathetic activation in anxiety and depression interaction with myocardial infarction. *European Heart Journal*. 2014;35(s1):488.
375. Lee KS, Chung JH, Lee KH, Shin M-J, Oh BH, Lee SH, et al. Simultaneous measurement of 23 plasma cytokines in late-life depression. *Neurological Sciences*. 2009;30(5):435-8.
376. Lehto SM, Niskanen L, Herzig K-H, Tolmunen T, Huotari A, Viinamäki H, et al. Serum chemokine levels in major depressive disorder. *Psychoneuroendocrinology*. 2010;35(2):226-32.
377. Lindqvist D, Janelidze S, Erhardt S, Träskman-Bendz L, Engström G, Brundin L. CSF biomarkers in suicide attempters - a principal component analysis. *Acta Psychiatrica Scandinavica*. 2011;124(1):52-61.
378. Lindqvist D, Janelidze S, Hagell P, Erhardt S, Samuelsson M, Minthon L, et al. Interleukin-6 Is Elevated in the Cerebrospinal Fluid of Suicide Attempters and Related to Symptom Severity. *Biological Psychiatry*. 2009;66(3):287-92.
379. Lu S, Peng H, Wang L, Vasish S, Zhang Y, Gao W, et al. Elevated specific peripheral cytokines found in major depressive disorder patients with childhood trauma exposure: A cytokine antibody array analysis. *Comprehensive Psychiatry*. 2013;54(7):953-61.
380. Mantur M, Tomczak AA, Chrzanowski W, Juchnowicz D, Borowiec M. SP-selectin and beta-TG as serum markers of platelet activation in menopausal women with depression. *Pol Merkur Lekarski*. 2006;20(120):682-4.
381. Marksteiner J, Kemmler G, Weiss EM, Knaus G, Ullrich C, Mechtcheriakov S, et al. Five out of 16 plasma signaling proteins are enhanced in plasma of patients with mild cognitive impairment and Alzheimer's disease. *Neurobiology of aging*. 2011;32(3):539-40.

382. Mikova O, Yakimova R, Bosmans E, Kenis G, Maes M. Increased serum tumor necrosis factor alpha concentrations in major depression and multiple sclerosis. *European Neuropsychopharmacology*. 2001;11(3):203-8.
383. Miller GE, Stetler CA, Carney RM, Freedland KE, Banks WA. Clinical depression and inflammatory risk markers for coronary heart disease. *The American Journal of Cardiology*. 2002;90(12):1279-83.
384. Motivala SJ, Sarfatti A, Olmos L, Irwin MR. Inflammatory markers and sleep disturbance in major depression. *Psychosom Med*. 2005;67(2):187-94.
385. Musselman DL, Marzec U, Davidoff M, Manatunga AK, Gao F, Reemsnyder A, et al. Platelet activation and secretion in patients with major depression, thoracic aortic atherosclerosis, or renal dialysis treatment. *Depression and Anxiety*. 2002;15(3):91-101.
386. Neupane SP, Lien L, Martinez P, Aukrust P, Ueland T, Mollnes TE, et al. Alteration of circulatory cytokine levels in alcohol-use disorder patients with or without comorbid major depression. *Drug and Alcohol Dependence*. 2015;146:e50.
387. O'Brien SM, Scully P, Fitzgerald P, Scott LV, Dinan TG. Plasma cytokine profiles in depressed patients who fail to respond to selective serotonin reuptake inhibitor therapy. *Journal of Psychiatric Research*. 2007;41(3-4):326-31.
388. Ogłodek EA, Szota A, Just MJ, Moś D, Araszkiwicz A. Comparison of chemokines (CCL-5 and SDF-1), chemokine receptors (CCR-5 and CXCR-4) and IL-6 levels in patients with different severities of depression. *Pharmacological Reports*. 2014;66(5):920-6.
389. Piletz JE, Halaris A, Iqbal O, Hoppensteadt D, Fareed J, Zhu H, et al. Pro-inflammatory biomarkers in depression: Treatment with venlafaxine. *The World Journal of Biological Psychiatry*. 2009;10(4):313-23.
390. Pisetsky DS, Trace SE, Brownley KA, Hamer RM, Zucker NL, Roux-Lombard P, et al. The expression of cytokines and chemokines in the blood of patients with severe weight loss from anorexia nervosa: An exploratory study. *Cytokine*. 2014;69(1):110-5.
391. Plourde A, Lavoie KL, Ring C, Carroll D, Bacon SL. The association between depression and psychological stress reactivity in coronary artery disease (CAD) patients. *Psychosomatic Medicine*. 2011;73 (3):A49-A.
392. Podlipny J, Hess Z, Vrzalova J, Rosolova H, Beran J, Petrlova B. Lower serum levels of interleukin-6 in a population sample with symptoms of depression than in a population sample without symptoms of depression. *Physiol Res*. 2010;59(1):121-6.
393. Pomara N, Bruno D, Reichert C, Nierenberg J, Sidtis JJ, Martiniuk FT, et al. Chemokine-specific relationships to ad biomarkers in CSF in healthy older adults. *Neuropsychopharmacology*. 2013;38:S164-S.
394. Pomara N, Nierenberg J, Sidtis J, Zetterberg H, Blennow K. Cerebrospinal fluid chemokine levels in healthy older adults: Relationship to beta-amyloid and tau indices. *Alzheimer's and Dementia*. 2013;1):P232-P.
395. Rajagopalan S, Brook R, Rubenfire M, Pitt E, Young E, Pitt B. Abnormal brachial artery flow-mediated vasodilation in young adults with major depression. *The American Journal of Cardiology*. 2001;88(2):196-8.
396. Rybka J, Czajkowska-Malinowska M, Nowak M, Kupczyk D, Kedziora-Kornatowska K, Piskunowicz M, et al. Inflammation as a hypothetic mechanisms underlying depression in patients with chronic obstructive pulmonary disease. *European Psychiatry*. 2012;27, Supplement 1:1.

397. Schins A, Hamulyák K, Scharpé S, Lousberg R, Van Melle J, Crijns H, et al. Whole blood serotonin and platelet activation in depressed post-myocardial infarction patients. *Life Sciences*. 2004;76(6):637-50.
398. Serebruany VL, Glassman AH, Malinin AI, Sane DC, Finkel MS, Krishnan RR, et al. Enhanced platelet/endothelial activation in depressed patients with acute coronary syndromes: evidence from recent clinical trials. *Blood Coagulation and Fibrinolysis*. 2003;14(6):563-7.
399. Shelton RC, Falola M, Li L, Zajecka J, Fava M, Papakostas GI. The pro-inflammatory profile of depressed patients is (partly) related to obesity. *Journal of Psychiatric Research*. 2015;70:91-7.
400. Simon NM, McNamara K, Chow CW, Maser RS, Papakostas GI, Pollack MH, et al. A detailed examination of cytokine abnormalities in Major Depressive Disorder. *European Neuropsychopharmacology*. 2008;18(3):230-3.
401. Song C, Lin A, Bonaccorso S, Heide C, Verkerk R, Kenis G, et al. The inflammatory response system and the availability of plasma tryptophan in patients with primary sleep disorders and major depression. *Journal of Affective Disorders*. 1998;49(3):211-9.
402. Sutçigil L, Oktenli C, Musabak U, Bozkurt A, Cansever A, Uzun O, et al. Pro- and Anti-Inflammatory Cytokine Balance in Major Depression: Effect of Sertraline Therapy. *Clinical and Developmental Immunology*. 2007;2007.
403. Tajfard M, Latiff LA, Rahimi HR, Mouhebati M, Esmaeily H, Taghipour A, et al. Serum Inflammatory Cytokines and Depression in Coronary Artery Disease. *Iran Red Crescent Med J*. 2014;16(7):e17111.
404. van Sloten TT, Schram MT, Adriaanse MC, Dekker JM, Nijpels G, Teerlink T, et al. Endothelial dysfunction is associated with a greater depressive symptom score in a general elderly population: the Hoorn Study. *Psychological Medicine*. 2014;44(7):1403-16.
405. Weng SH, Wang GH, Zhang L. Relationship between serotonin transporter linked polymorphic region and the plasma level of the platelet factor 4 in young patients with depression. [Chinese]. *Chinese Journal of Clinical Rehabilitation*. 2004;8:3518-9.
406. Whyte EM, Pollock BG, Wagner WR, Mulsant BH, Ferrell RE, Mazumdar S, et al. Influence of Serotonin-Transporter-Linked Promoter Region Polymorphism on Platelet Activation in Geriatric Depression. *American Journal of Psychiatry*. 2001;158(12):2074-6.
407. Wong ML, Dong C, Maestre-Mesa J, Licinio J. Polymorphisms in inflammation-related genes are associated with susceptibility to major depression and antidepressant response. *Mol Psychiatry*. 2008;13(8):800-12.
408. Xiong GL, Prybol K, Boyle SH, Hall R, Streilein RD, Steffens DC, et al. Inflammation Markers and Major Depressive Disorder in Patients With Chronic Heart Failure: Results From the Sertraline Against Depression and Heart Disease in Chronic Heart Failure Study. *Psychosom Med*. 2015;77(7):808-15.
409. Zahn D, Petrak F, Franke L, Hagele AK, Juckel G, Lederbogen F, et al. Cortisol, platelet serotonin content, and platelet activity in patients with major depression and type 2 diabetes: an exploratory investigation. *Psychosom Med*. 2015;77(2):145-55.
410. Zhen Y, Chu C, Zhou S, Qi M, Shu R. Imbalance of tumor necrosis factor- α , interleukin-8 and interleukin-10 production evokes barrier dysfunction, severe abdominal symptoms and psychological disorders in patients with irritable bowel syndrome-associated diarrhea. *Molecular medicine reports*. 2015;12(4):5239-45.

411. Shen Y, Lu P, Wei L, Cai L, Hu X, Chen W. Fluoxetine treatment for major depression decreases the plasma levels of cytokines. *African Journal of Biotechnology*. 2010;9:7346-51.
412. Pantazatos SP, Huang YY, Rosoklija GB, Dwork AJ, Arango V, Mann JJ. Whole-transcriptome brain expression and exon-usage profiling in major depression and suicide: evidence for altered glial, endothelial and ATPase activity. *Mol Psychiatry*. 2016.
413. D'Mello C, Le T, Swain MG. Cerebral Microglia Recruit Monocytes into the Brain in Response to Tumor Necrosis Factor alpha Signaling during Peripheral Organ Inflammation. *Journal of Neuroscience*. 2009;29(7):2089-102.
414. Selenica M-LB, Alvarez JA, Nash KR, Lee DC, Cao C, Lin X, et al. Diverse activation of microglia by chemokine (C-C motif) ligand 2 overexpression in brain. *Journal of Neuroinflammation*. 2013;10.
415. Marciniak E, Faivre E, Dutar P, Alves Pires C, Demeyer D, Caillierez R, et al. The Chemokine MIP-1 α /CCL3 impairs mouse hippocampal synaptic transmission, plasticity and memory. *Scientific Reports*. 2015;5:15862.
416. Gamo K, Kiryu-Seo S, Konishi H, Aoki S, Matsushima K, Wada K, et al. G-protein-coupled receptor screen reveals a role for chemokine receptor CCR5 in suppressing microglial neurotoxicity. *J Neurosci*. 2008;28(46):11980-8.
417. Stuart MJ, Singhal G, Baune BT. Systematic Review of the Neurobiological Relevance of Chemokines to Psychiatric Disorders. *Frontiers in Cellular Neuroscience*. 2015;9:357.
418. Bystry RS, Aluvihare V, Welch KA, Kallikourdis M, Betz AG. B cells and professional APCs recruit regulatory T cells via CCL4. *Nat Immunol*. 2001;2(12):1126-32.
419. Li Y, Xiao B, Qiu W, Yang L, Hu B, Tian X, et al. Altered expression of CD4(+)CD25(+) regulatory T cells and its 5-HT(1a) receptor in patients with major depression disorder. *J Affect Disord*. 2010;124(1-2):68-75.
420. Villeda SA, Luo J, Mosher KI, Zou B, Britschgi M, Bieri G, et al. The ageing systemic milieu negatively regulates neurogenesis and cognitive function. *Nature*. 2011;477(7362):90-4.
421. Flad H-D, Brandt E. Platelet-derived chemokines: pathophysiology and therapeutic aspects. *Cellular and Molecular Life Sciences*. 2010;67(14):2363-86.
422. Horstman LL, Jy W, Ahn YS, Zivadinov R, Maghzi AH, Etemadifar M, et al. Role of platelets in neuroinflammation: a wide-angle perspective. *Journal of Neuroinflammation*. 2010;7(1):10.
423. Morel-Kopp MC, McLean L, Chen Q, Tofler GH, Tennant C, Maddison V, et al. The association of depression with platelet activation: evidence for a treatment effect. *J Thromb Haemost*. 2009;7(4):573-81.
424. Parakh K, Sakhuja A, Bhat U, Ziegelstein RC. Platelet function in patients with depression. *Southern medical journal*. 2008;101(6):612-7.
425. De Jong EK, De Haas AH, Brouwer N, Van Weering HRJ, Hensens M, Bechmann I, et al. Expression of CXCL4 in microglia in vitro and in vivo and its possible signaling through CXCR3. *Journal of Neurochemistry*. 2008;105(5):1726-36.
426. Campbell SJ, Meier U, Mardiguian S, Jiang Y, Littleton ET, Bristow A, et al. Sickness behaviour is induced by a peripheral CXC-chemokine also expressed in Multiple Sclerosis and EAE. *Brain, Behavior, and Immunity*. 2010;24(5):738-46.
427. Aguliar-Valles A, Kim J, Jung S, Woodside B, Luheshi GN. Role of brain transmigrating neutrophils in depression-like behavior during systemic infection. *Mol Psychiatry*. 2014;19(5):599-606.

428. Guyon A. CXCL12 chemokine and its receptors as major players in the interactions between immune and nervous systems. *Front Cell Neurosci.* 2014;8:65.
429. Guyon A. CXCL12 chemokine and GABA neurotransmitter systems crosstalk and their putative roles. *Front Cell Neurosci.* 2014;5:115.
430. Liu Y, Carson-Walter E, Walter KA. Chemokine Receptor CXCR7 Is a Functional Receptor for CXCL12 in Brain Endothelial Cells. *PLOS ONE.* 2014;9(8):e103938.
431. Pariante CM, Lightman SL. The HPA axis in major depression: classical theories and new developments. *Trends Neurosci.* 2008;31(9):464-8.
432. Hill AS, Sahay A, Hen R. Increasing Adult Hippocampal Neurogenesis is Sufficient to Reduce Anxiety and Depression-Like Behaviors. *Neuropsychopharmacology.* 2015;40(10):2368-78.
433. Bruunsgaard H, Pedersen BK. Age-related inflammatory cytokines and disease. *Immunol Allergy Clin North Am.* 2003;23(1):15-39.
434. Aulock SV, Deininger S, Draing C, Gueinzius K, Dehus O, Hermann C. Gender Difference in Cytokine Secretion on Immune Stimulation with LPS and LTA. *Journal of Interferon & Cytokine Research.* 2006;26(12):887-92.
435. Fontana L, Eagon JC, Trujillo ME, Scherer PE, Klein S. Visceral fat adipokine secretion is associated with systemic inflammation in obese humans. *Diabetes.* 2007;56(4):1010-3.
436. Lee J, Taneja V, Vassallo R. Cigarette Smoking and Inflammation: Cellular and Molecular Mechanisms. *Journal of Dental Research.* 2012;91(2):142-9.
437. Haus E, Smolensky MH. Biologic rhythms in the immune system. *Chronobiology international.* 1999;16(5):581-622.
438. NIMH, Major Depression Among Adults Bethesda, MD, USA: NIMH; 2017 [Available from: <https://www.nimh.nih.gov/health/statistics/prevalence/major-depression-among-adults.shtml>].
439. Revah-Levy A, Speranza M, Barry C, Hassler C, Gasquet I, Moro M-R, et al. Association between Body Mass Index and depression: the "fat and jolly" hypothesis for adolescents girls. *BMC Public Health.* 2011;11(1):649.
440. de Wit LM, van Straten A, van Herten M, Penninx BWJH, Cuijpers P. Depression and body mass index, a u-shaped association. *BMC Public Health.* 2009;9:14-.
441. Chiwanda L, Cordiner M, Thompson AT, Shajahan P. Long-term antidepressant treatment in general practice: changes in body mass index. *BJPsych Bulletin.* 2016;40(6):310-4.
442. Anda RF, Williamson DF, Escobedo LG, Mast EE, Giovino GA, Remington PL. Depression and the dynamics of smoking: A national perspective. *Jama.* 1990;264(12):1541-5.
443. Glassman AH, Helzer JE, Covey LS, Cottler LB, Stetner F, Tipp JE, et al. Smoking, smoking cessation, and major depression. *Jama.* 1990;264(12):1546-9.
444. Germain A, Kupfer DJ. CIRCADIAN RHYTHM DISTURBANCES IN DEPRESSION. *Human psychopharmacology.* 2008;23(7):571-85.
445. Henry CJ, Huang Y, Wynne AM, Godbout JP. Peripheral lipopolysaccharide (LPS) challenge promotes microglial hyperactivity in aged mice that is associated with exaggerated induction of both pro-inflammatory IL-1 beta and anti-inflammatory IL-10 cytokines. *Brain Behavior and Immunity.* 2009;23(3):309-17.
446. McColl A. The brain response to peripheral inflammation: University of Glasgow; 2015.

447. Hackstein H, Hagel N, Knoche A, Kranz S, Lohmeyer J, von Wulffen W, et al. Skin TLR7 triggering promotes accumulation of respiratory dendritic cells and natural killer cells. *PLoS One*. 2012;7(8):e43320.
448. Al-Harbi NO, Nadeem A, Al-Harbi MM, Zoheir KMA, Ansari MA, El-Sherbeeney AM, et al. Psoriatic inflammation causes hepatic inflammation with concomitant dysregulation in hepatic metabolism via IL-17A/IL-17 receptor signaling in a murine model. *Immunobiology*. 2017;222(2):128-36.
449. Standiford TJ, Kunkel SL, Lukacs NW, Greenberger MJ, Danforth JM, Kunkel RG, et al. Macrophage inflammatory protein-1 alpha mediates lung leukocyte recruitment, lung capillary leak, and early mortality in murine endotoxemia. *The Journal of Immunology*. 1995;155(3):1515.
450. Rydström A, Wick MJ. Monocyte and neutrophil recruitment during oral *Salmonella* infection is driven by MyD88-derived chemokines. *European Journal of Immunology*. 2009;39(11):3019-30.
451. Scandella E, Men Y, Legler DF, Gillessen S, Prikler L, Ludewig B, et al. CCL19/CCL21-triggered signal transduction and migration of dendritic cells requires prostaglandin E2. *Blood*. 2004;103(5):1595-601.
452. Zhao X, Sato A, Dela Cruz CS, Linehan M, Luegering A, Kucharzik T, et al. CCL9 is secreted by the follicle-associated epithelium and recruits dome region Peyer's patch CD11b+ dendritic cells. *Journal of immunology (Baltimore, Md : 1950)*. 2003;171(6):2797-803.
453. Matloubian M, David A, Engel S, Ryan JE, Cyster JG. A transmembrane CXC chemokine is a ligand for HIV-coreceptor Bonzo. *Nat Immunol*. 2000;1(4):298-304.
454. Menzies-Gow A, Ying S, Sabroe I, Stubbs VL, Soler D, Williams TJ, et al. Eotaxin (CCL11) and eotaxin-2 (CCL24) induce recruitment of eosinophils, basophils, neutrophils, and macrophages as well as features of early- and late-phase allergic reactions following cutaneous injection in human atopic and nonatopic volunteers. *Journal of immunology (Baltimore, Md : 1950)*. 2002;169(5):2712-8.
455. Kowarik MC, Cepok S, Sellner J, Grummel V, Weber MS, Korn T, et al. CXCL13 is the major determinant for B cell recruitment to the CSF during neuroinflammation. *J Neuroinflammation*. 2012;9:93.
456. Robertson MJ. Role of chemokines in the biology of natural killer cells. *J Leukoc Biol*. 2002;71(2):173-83.
457. Davatelis G, Wolpe SD, Sherry B, Dayer JM, Chicheportiche R, Cerami A. Macrophage inflammatory protein-1: a prostaglandin-independent endogenous pyrogen. *Science*. 1989;243(4894):1066.
458. Ren K, Torres R. Role of interleukin-1beta during pain and inflammation. *Brain Res Rev*. 2009;60(1):57-64.
459. Hess A, Axmann R, Rech J, Finzel S, Heindl C, Kreitz S, et al. Blockade of TNF-alpha rapidly inhibits pain responses in the central nervous system. *Proc Natl Acad Sci U S A*. 2011;108(9):3731-6.
460. Probert L. TNF and its receptors in the CNS: The essential, the desirable and the deleterious effects. *Neuroscience*. 2015;302:2-22.
461. Erta M, Quintana A, Hidalgo J. Interleukin-6, a Major Cytokine in the Central Nervous System. *International Journal of Biological Sciences*. 2012;8(9):1254-66.
462. Gosselin D, Rivest S. Role of IL-1 and TNF in the brain: twenty years of progress on a Dr. Jekyll/Mr. Hyde duality of the innate immune system. *Brain Behav Immun*. 2007;21(3):281-9.

463. Shaftel SS, Griffin WST, O'Banion MK. The role of interleukin-1 in neuroinflammation and Alzheimer disease: an evolving perspective. *Journal of Neuroinflammation*. 2008;5(1):7.
464. Spooren A, Kolmus K, Laureys G, Clinckers R, De Keyser J, Haegeman G, et al. Interleukin-6, a mental cytokine. *Brain Res Rev*. 2011;67(1-2):157-83.
465. Durrant DM, Daniels BP, Klein RS. IL-1R1 signaling regulates CXCL12-mediated T cell localization and fate within the central nervous system during West Nile Virus encephalitis. *Journal of immunology (Baltimore, Md : 1950)*. 2014;193(8):4095-106.
466. Chen CJ, Ou YC, Chang CY, Pan HC, Liao SL, Raung SL, et al. TNF-alpha and IL-1beta mediate Japanese encephalitis virus-induced RANTES gene expression in astrocytes. *Neurochemistry international*. 2011;58(2):234-42.
467. Zhu CB, Blakely RD, Hewlett WA. The proinflammatory cytokines interleukin-1beta and tumor necrosis factor-alpha activate serotonin transporters. *Neuropsychopharmacology*. 2006;31(10):2121-31.
468. Moore KW, de Waal Malefyt R, Coffman RL, O'Garra A. Interleukin-10 and the interleukin-10 receptor. *Annu Rev Immunol*. 2001;19:683-765.
469. Boche D, Perry VH, Nicoll JAR. Review: Activation patterns of microglia and their identification in the human brain. *Neuropathology and Applied Neurobiology*. 2013;39(1):3-18.
470. Pekny M, Pekna M. Astrocyte Reactivity and Reactive Astrogliosis: Costs and Benefits. *Physiological Reviews*. 2014;94(4):1077-98.
471. Laidlaw BJ, Cui W, Amezcua RA, Gray SM, Guan T, Lu Y, et al. Production of IL-10 by CD4+ regulatory T cells during the resolution of infection promotes the maturation of memory CD8+ T cells. *Nat Immunol*. 2015;16(8):871-9.
472. McGeachy MJ, Stephens LA, Anderson SM. Natural recovery and protection from autoimmune encephalomyelitis: contribution of CD4+CD25+ regulatory cells within the central nervous system. *Journal of immunology (Baltimore, Md : 1950)*. 2005;175(5):3025-32.
473. van der Fits L, Mourits S, Voerman JS, Kant M, Boon L, Laman JD, et al. Imiquimod-induced psoriasis-like skin inflammation in mice is mediated via the IL-23/IL-17 axis. *Journal of immunology (Baltimore, Md : 1950)*. 2009;182(9):5836-45.
474. Dong J, Jimi E, Zeiss C, Hayden MS, Ghosh S. Constitutively active NF-kappaB triggers systemic TNFalpha-dependent inflammation and localized TNFalpha-independent inflammatory disease. *Genes & development*. 2010;24(16):1709-17.
475. Kohno H, Maeda T, Perusek L, Pearlman E, Maeda A. CCL3 production by microglial cells modulates disease severity in murine models of retinal degeneration. *Journal of immunology (Baltimore, Md : 1950)*. 2014;192(8):3816-27.
476. Hinojosa AE, Garcia-Bueno B, Leza JC, Madrigal JL. CCL2/MCP-1 modulation of microglial activation and proliferation. *J Neuroinflammation*. 2011;8:77.
477. Albright AV, Shieh JT, Itoh T, Lee B, Pleasure D, O'Connor MJ, et al. Microglia express CCR5, CXCR4, and CCR3, but of these, CCR5 is the principal coreceptor for human immunodeficiency virus type 1 dementia isolates. *J Virol*. 1999;73(1):205-13.
478. Louboutin JP, Strayer DS. Relationship between the chemokine receptor CCR5 and microglia in neurological disorders: consequences of targeting CCR5 on

- neuroinflammation, neuronal death and regeneration in a model of epilepsy. *CNS & neurological disorders drug targets*. 2013;12(6):815-29.
479. Fukada K, Sobao Y, Tomiyama H, Oka S, Takiguchi M. Functional expression of the chemokine receptor CCR5 on virus epitope-specific memory and effector CD8⁺ T cells. *Journal of immunology (Baltimore, Md : 1950)*. 2002;168(5):2225-32.
480. Campanella GS, Tager AM, El Khoury JK, Thomas SY, Abrazinski TA, Manice LA, et al. Chemokine receptor CXCR3 and its ligands CXCL9 and CXCL10 are required for the development of murine cerebral malaria. *Proc Natl Acad Sci U S A*. 2008;105(12):4814-9.
481. Stiles LN, Hosking MP, Edwards RA, Strieter RM, Lane TE. Differential roles for CXCR3 in CD4⁺ and CD8⁺ T cell trafficking following viral infection of the CNS. *Eur J Immunol*. 2006;36(3):613-22.
482. Xin L, Vargas-Inchaustegui DA, Raimer SS, Kelly BC, Hu J, Zhu L, et al. Type I IFN Receptor Regulates Neutrophil Functions and Innate Immunity to Leishmania Parasites. *The Journal of Immunology*. 2010;184(12):7047-56.
483. Ireland DDC, Stohlman SA, Hinton DR, Atkinson R, Bergmann CC. Type I Interferons Are Essential in Controlling Neurotropic Coronavirus Infection Irrespective of Functional CD8 T Cells. *Journal of Virology*. 2008;82(1):300-10.
484. Jeong H-K, Jou I, Joe E-h. Systemic LPS administration induces brain inflammation but not dopaminergic neuronal death in the substantia nigra. *Experimental & Molecular Medicine*. 2010;42(12):823-32.
485. Harrison LI, Skinner SL, Marbury TC, Owens ML, Kurup S, McKane S, et al. Pharmacokinetics and safety of imiquimod 5% cream in the treatment of actinic keratoses of the face, scalp, or hands and arms. *Archives of dermatological research*. 2004;296(1):6-11.
486. Canadian Institutes of Health Research. Imiquimod - DrugBank. 2017.
487. Hayashi T, Gray CS, Chan M, Tawatao RI, Ronacher L, McGargill MA, et al. Prevention of autoimmune disease by induction of tolerance to Toll-like receptor 7. *Proc Natl Acad Sci U S A*. 2009;106(8):2764-9.
488. Vuong L. Toll-like receptor 7 tolerance in anti-neuroinflammation in murine experimental autoimmune encephalomyelitis. 2010.
489. Tsukada K, Kitazawa T, Fukushima A, Okugawa S, Yanagimoto S, Tatsuno K, et al. Macrophage tolerance induced by stimulation with Toll-like receptor 7/8 ligands. *Immunology Letters*. 2007;111(1):51-6.
490. Koga-Yamakawa E, Murata M, Dovedi SJ, Wilkinson RW, Ota Y, Umehara H, et al. TLR7 tolerance is independent of the type I IFN pathway and leads to loss of anti-tumor efficacy in mice. *Cancer Immunology, Immunotherapy*. 2015;64(10):1229-39.
491. Berg DJ, Kühn R, Rajewsky K, Müller W, Menon S, Davidson N, et al. Interleukin-10 is a central regulator of the response to LPS in murine models of endotoxic shock and the Shwartzman reaction but not endotoxin tolerance. *Journal of Clinical Investigation*. 1995;96(5):2339-47.
492. Biswas SK, Lopez-Collazo E. Endotoxin tolerance: new mechanisms, molecules and clinical significance. *Trends in Immunology*. 2009;30(10):475-87.
493. McKimmie CS, Fazakerley JK. In response to pathogens, glial cells dynamically and differentially regulate Toll-like receptor gene expression. *Journal of Neuroimmunology*. 2005;169(1-2):116-25.
494. van Marle G, Antony J, Ostermann H, Dunham C, Hunt T, Halliday W, et al. West Nile virus-induced neuroinflammation: glial infection and capsid protein-mediated neurovirulence. *J Virol*. 2007;81(20):10933-49.

495. Asensio VC, Campbell IL. Chemokine gene expression in the brains of mice with lymphocytic choriomeningitis. *Journal of Virology*. 1997;71(10):7832-40.
496. Ireland DD, Reiss CS. Gene Expression Contributing to Recruitment of Circulating Cells in Response to Vesicular Stomatitis Virus Infection of the CNS. *Viral immunology*. 2006;19(3):536-45.
497. Nansen A, Marker O, Bartholdy C, Thomsen AR. CCR2+ and CCR5+ CD8+ T cells increase during viral infection and migrate to sites of infection. *European Journal of Immunology*. 2000;30(7):1797-806.
498. Garcia-Tapia D, Hassett DE, Mitchell WJ, Jr., Johnson GC, Kleiboeker SB. West Nile virus encephalitis: sequential histopathological and immunological events in a murine model of infection. *J Neurovirol*. 2007;13(2):130-8.
499. Kioussis D, Pachnis V. Immune and Nervous Systems: More Than Just a Superficial Similarity? *Immunity*. 2009;31(5):705-10.
500. Filiano AJ, Xu Y, Tustison NJ, Marsh RL, Baker W, Smirnov I, et al. Unexpected role of interferon-gamma in regulating neuronal connectivity and social behaviour. *Nature*. 2016;535(7612):425-9.
501. Adler MW, Rogers TJ. Are chemokines the third major system in the brain? *Journal of Leukocyte Biology*. 2005;78(6):1204-9.
502. Kirby LG, Heinisch S. Chemokines as Neuromodulators. *Journal of Neuroimmune Pharmacology*. 2011;6:S15-S.
503. Reaux-Le Goazigo A, Van Steenwinckel J, Rostene W, Parsadaniantz SM. Current status of chemokines in the adult CNS. *Progress in Neurobiology*. 2013;104:67-92.
504. Ransohoff RM. Chemokines and Chemokine Receptors: Standing at the Crossroads of Immunobiology and Neurobiology. *Immunity*. 2009;31(5):711-21.
505. Tejedor LS, Wostradowski T, Gingele S, Skripuletz T, Gudi V, Stangel M. The Effect of Stereotactic Injections on Demyelination and Remyelination: a Study in the Cuprizone Model. *Journal of molecular neuroscience : MN*. 2017;61(4):479-88.
506. Brynskikh A, Warren T, Zhu J, Kipnis J. Adaptive immunity affects learning behavior in mice. *Brain Behav Immun*. 2008;22(6):861-9.
507. Baker DG, Woods TA, Butchi NB, Morgan TM, Taylor RT, Sunyakumthorn P, et al. Toll-like receptor 7 suppresses virus replication in neurons but does not affect viral pathogenesis in a mouse model of Langkat virus infection. *The Journal of General Virology*. 2013;94(Pt 2):336-47.
508. Hsu P, Santner-Nanan B, Hu M, Skarratt K, Lee CH, Stormon M, et al. IL-10 Potentiates Differentiation of Human Induced Regulatory T Cells via STAT3 and Foxo1. *The Journal of Immunology*. 2015;195(8):3665-74.
509. Murai M, Turovskaya O, Kim G, Madan R, Karp CL, Cheroutre H, et al. Interleukin 10 acts on regulatory T cells to maintain expression of the transcription factor Foxp3 and suppressive function in mice with colitis. *Nat Immunol*. 2009;10(11):1178-84.
510. Nazmi A, Mukherjee S, Kundu K, Dutta K, Mahadevan A, Shankar SK, et al. TLR7 is a key regulator of innate immunity against Japanese encephalitis virus infection. *Neurobiology of Disease*. 2014;69:235-47.
511. Kipnis J, Cohen H, Cardon M, Ziv Y, Schwartz M. T cell deficiency leads to cognitive dysfunction: implications for therapeutic vaccination for schizophrenia and other psychiatric conditions. *Proc Natl Acad Sci U S A*. 2004;101(21):8180-5.
512. Garre JM, Silva HM, Lafaille JJ, Yang G. CX3CR1+ monocytes modulate learning and learning-dependent dendritic spine remodeling via TNF-[alpha]. *Nat Med*. 2017;23(6):714-22.

513. Mori T, Tanaka K, Buffo A, Wurst W, Kuhn R, Gotz M. Inducible gene deletion in astroglia and radial glia--a valuable tool for functional and lineage analysis. *Glia*. 2006;54(1):21-34.